# Improved Ultra Wideband Communication System through Adaptive Modulation and Spatial Diversity

*By*

**Musa Gayaunan Magani**

Submitted in partial fulfillment of the requirements of the Degree of

Doctor of Philosophy

School of Electronic Engineering and Computer Science
Queen Mary, University of London
United Kingdom

October 2013

# *ABSTRACT*

Advances in Multimedia communications have shown the need for high data rate wireless links over short distances. This is to enhance flexibility, accessibility, portability and mobility of devices in home and enterprise environment thereby making users more productive. In 2004, the WiMedia group proposed the Multiband Orthogonal Frequency Division Multiplex Ultra Wideband (MB-OFDM UWB) system with a target of delivering data rate of 480Mbps over 3 metres. However, by now no existing commercial UWB product can meet this proposed specification.

The project aims to investigate the reason why UWB technology has failed to realise its potential by carrying out detailed analysis and to seek ways of solving the technical problems. Detailed system analyses were carried out on the UWB technology using a commercial UWB product and a MB-OFDM UWB Evaluation kit.

UWB channel measurements of different scenarios were carried out in order to characterise both time varying and time invariant channels. The scenarios are the realistic environments where UWB devices are operating with human subjects in various movement patterns. It gives insight into the effects of human object blocking on the MB-OFDM system performance and estimates an acceptable feedback rate in a UWB time varying channel when implementing an adaptive modulation.

The adaptive modulation was proposed and implemented in the MB-OFDM system model to demonstrate the improved Bit Error Rate (BER) performance. Modulating bits are varied across the sub-channels depending on the signal to noise ratio (SNR). Sub-channels experiencing severe fading employ lower or no bit-loading while sub-channels with little or no fading utilise higher bit-loading to maintain a constant system data rate.

Spatial diversity was employed to exploit different properties of the radio channel to improve performance. Good diversity gain of two receiving diversity systems using maximal ratio combining and antenna selection techniques is demonstrated in the measurements with the different antenna orientations. An antenna selection circuit is designed and implemented working together with AT90CAP9 UWB Evaluation kit, verifying an improved performance of the UWB system in an indoor environment. The maximal ratio combining technique is also implemented and demonstrated to give a better system performance on a test bed after post-processing.

# *ACKNOWLEDGEMENTS*

First, I acknowledge the love of God, the grace of our lord Jesus Christ and the sweet fellowship of the Holy Spirit throughout my program. It is my pleasure to express my sincere appreciation and gratitude to my supervisor *Prof. Xiaodong Chen* for his beneficial discussions, encouragement, valuable advice and guidance throughout the course of this work. I will like to thank my second supervisor, *Dr Akram Alomainy*, for his beneficial discussions and advice.

I will like to thank *Dr Shuxian Chen, Dr Karl Liu, Dr Masood Rehman, Mr T. Aboufoul and Dr Lu Guo* for their constructive discussions and advises regarding this work. Finally, I am very grateful to my wife, parents and siblings who have done everything in their capacity to make me reach this point.

***Musa Gayaunan Magani***

**TABLE OF CONTENTS**

**Contents**

**LIST OF FIGURES**

**LIST OF TABLES**

**GLOSSARY**

| | |
|---|---|
| ADS | Advance Design System |
| BPSK | Bit Phase Shift Keying |
| CDF | Cumulative Distribution Function |
| CIR | Channel Impulse Response |
| CSI | Channel State Information |
| CPW | Coplanar Wave Guide |
| DAA | Detect and Avoid |
| EESS | Earth Exploration-Satellite Service |
| EIRP | Effective Isotropic Radiated Power |
| FCC | Federal Communication Commission |
| FFT | Fast Fourier Transform |
| IEEE | Institute of Electrical and Electronics Engineers |
| IFFT | Inverse Fast Fourier Transform |
| HDTV | High Definition Television |
| LMS | Least Mean Square |
| MAC | Medium Access Control |
| MISO | Multiple-Input-Single-Output |
| MIMO | Multiple-Input-Multiple-Output |
| MRC | Maximal Ratio Combining |
| OFDM | Orthogonal Frequency Division Multiplexing |
| QPSK | Quadrature Phase Shift Keying |
| OPSA | Optimal Power Spectrum Allocation |
| PCB | Printed Circuit Board |
| PSDU | PLCP Service Data Unit |
| PLCP | Physical Layer Convergence Protocol |
| RAS | Radio Astronomy Service |
| SIMO | Single-Input-Multiple-Output |
| RSSI | Received signal strength indicator |
| SISO | Single-Input-Single-Output |
| STC | Space Time Coding |
| UPSA | Uniform Power Spectrum Allocation |
| WBAN | Wireless Body Area Network |
| WiMax | World wide Interoperability for Microwave Access |
| WPAN | Wireless Personal Area Network |

# CHAPTER 1

**INRODUCTION**

## 1.1 Introduction

In today's world, wireless communication has enabled a new lifestyle filled with conveniences for users, which includes greater flexibility, mobility and increased efficiency. These benefits have resulted in demands for the same connectivity and convenience to other devices such as digital camcorder, digital camera, setup boxes, gaming console, digital video and audio player and Personal Digital Assistant (PDA). Consumers now want to be able to interconnect all their personal devices thereby having a wireless Personal Area Network (WPAN) in their office or home which is designed to provide connectivity between these devices over a short distance.

Wireless technologies are one of the most discussed subjects in the communication field due to its evolutional and revolutionary capacity. During the past two decades, wireless communication systems have substantially evolved to meet the data rate demand for wireless services. This growth is expected to continue as new applications and services are being introduced.

Current wireless technologies need improvement to meet the growing demand of wireless multimedia applications which require high data rate to deliver similar services like its wired counterpart. This opens up an opportunity for new technologies. One of the evolving wireless technologies is the Multiband Orthogonal Frequency Division Multiplexing Ultra wideband (MB-OFDM UWB). MB-OFDM UWB uses a huge frequency range of 3.1-10.6 GHz. The UWB spectrum is divided into 14 bands, each with a bandwidth of 528MHz. A total of 110 sub carriers are used per band to transmit information and 12 pilot cub carriers for coherent detection.

The data is spread using a time-frequency code (TFC) which specifies three types of time frequency codes: one where the coded information is interleaved over three bands, referred to as Time-Frequency Interleaving (TFI); one where the coded information is interleaved over two bands, referred to as two-band TFI or TFI2; and one where the coded information is transmitted on a single band, referred to as Fixed Frequency Interleaving (FFI). Individual OFDM sub carriers are allowed to be nulled. This together with the choice of frequency bands and the time frequency codes (TFI1, TFI2 and FFI) provides substantial control over the use of

spectrum by the transmitted signal. This allows the physical layer to be used in a range of regulatory and radio coexistence scenarios. Also, the capability of coping with Inter Symbol Interference (ISI) and reducing the transceiver complexity makes OFDM attractive. Ultra Wide Band technology has received great attention in both the industry and academia since it was approved by the Federal Communication Commission (FCC) in 2002 [1]. It offers large bandwidth while meeting cost, physical size and power consumption requirements of next generation devices.

Due to the challenges in wireless communication, researchers need to continually develop new technologies to satisfy current and future expectation of wireless services. The use of multiple antennas at the transmitter and the receiver increases the spectral efficiency through spatial multiplexing and improves the link reliability through diversity gain. Combining UWB and Multiple Input Multiple Output (MIMO) could provide data rate in excess of 1Gbps which will be suitable for High Definition Television (HDTV) real time streaming, wireless data bus for cable replacement and high speed internet access. Combining multiple antennas and UWB system could deliver very high data rate and link reliability, research is required to actualise the potential of combining the two technologies within limited power constrain.

### 1.2 UWB Applications

UWB technology applications can be broadly grouped into communication, sensor, and localisation. Demand for high data rate is on the increase, UWB has the potential to fulfil the demand and meet the needs of the market. Figure 1.1 shows the applications of UWB technology.

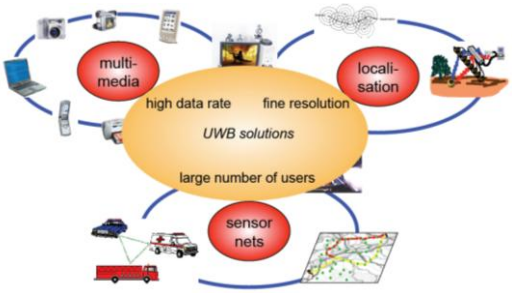


**Figure 1.1 Applications for UWB Technology [6]**

#### 1.2.1 High data rate Communications

High data rate applications such as internet services and multimedia services are offered via wired connections. UWB technology could be used to replace wired connection providing wider range of connectivity between devices. Considering Wireless PC peripheral connectivity [7], UWB technology can provide the performance users normally expect from the wired Universal Serial Bus (USB). A wireless USB will give users more conveniences when connecting peripherals to the PC. Bluetooth technology provides similar connectivity between PC and

peripherals but cannot offer high data rate compared to the UWB technology. Other high data rate application includes [7]

- Wireless Multimedia connectivity for Consumer devices for audio and video streaming
- Replacing cables between portable multimedia Consumer devices such as digital cameras , DVD/blue ray players , Camcorders
- Creating high bit rate ad hoc connections between UWB enabled devices
- Enabling high speed wireless USB (WUSB) connection for PC peripherals and PC
- Cable replacement and network access for mobile computing devices

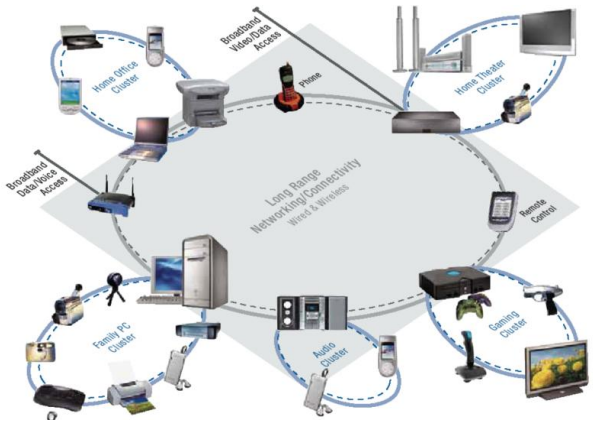


**Figure 1.2 Applications for Home Entertainment (Intel white paper on wireless USB) [8]**

### 1.2.2 Localisation

UWB technology is well suited for localisation and tracking as the large bandwidth results to fine delay resolution. Tracking and Position location have quite a number of benefits such as tracking items in the store/mall, locating patients, tracking cars and for military applications. UWB technology offers distinct advantages over other RF active tracking technologies. These advantages include multipath immunity for leading edge detection, precision time of flight measurement and lower power for extended operation. [9]

### 1.2.3 Sensors

UWB technology allows the operation of multiple devices without interference at the same time in the same space. This benefit can be utilised in wireless sensor network. Other benefit and advantages of using UWB sensors include:

a. Ranging accuracy- Ranging accuracy is determined by the bandwidth. The accuracy of the ranging could be under a centimetre.
b. Channel capacity- This increase linearly with bandwidth, whereas it only increases logarithmically with power.
c. Multipath resolution- The wide bandwidth leads to precise multipath resolution. Resilience to harmful multipath effects enables sensors to be placed in areas inhospitable to narrow system such as a factory packed with metallic objects.

d. Ultra wideband- The 7.5 GHz bandwidth allows opportunities for multiple access.
e. The wide bandwidth results in a low power spectral density, which in turn results in low probability of intercept and detection.

Wireless sensor networks (WSN) are spatially distributed autonomous sensors to monitor physical or environmental condition and to cooperatively pass their data through the network to a main location [10]. Although WSN solutions could be based on infra red, Zigbee, 802.11a/g , and Bluetooth technologies, the UWB technology offers more benefits and advantages. UWB technology is less affected by shadowing, allows transmission through objects, requires lower energy and offers a higher bandwidth. Application of UWB technology for sensors could be video surveillance [11], Inter vehicle [12], outdoor sports monitoring [13], localisation [14], perimeter intrusion detection [15], imaging of objects and environment [16], monitoring of highways, bridges and infrastructure [17].

**1.3 Motivation**

UWB is a wireless technology with a potential of high data rate over short distance. Although the technology is here for a decade now, not many UWB products can be found in the market. UWB technology promised to deliver 480Mbps over 3 metres but that promise has not been realised as current UWB products offer very low data rate. This low data rates cannot meet the demand of multimedia and high data rate communications. This necessitates more research to be done to further explore the potential of UWB technology. The aim of this research is to investigate, develop and evaluate novel solutions to enhance the performance of the UWB system by increasing the data rate and reducing its error rate.

UWB spectrum is a major issue in the commercialisation of UWB for both the government and communication industry. Generally, radio communications are subject to different regulations on power output at designated frequencies to minimise interference with other communication systems operating in the same or nearby frequency band. In order to maintain minimum interference from UWB, the FCC in the United States specified the spectral mask for UWB communication for both indoor and outdoor to be -41.3dBm/MHz and -63.5dBm/MHz respectively [1]. In Europe, a stricter spectral mask is specified than that of the USA with only the frequency range of 4.2GHz to 4.8GHz and 6 GHz to 8.5 GHz having the permitted EIRP emission of -41.3dBm/MHz [2]. The UK UWB regulation is the same as the European Union UWB regulation. In Japan, the ministry of POST and Telecommunications proposed its spectral mask for UWB in 2005 to be -41.3dBm/MHz for unlicensed UWB devices and the operating frequency range to be 3.4-4.8GHz and 7.25-10.25GHz for indoor applications [3]. The 3.1-3.4GHz is restricted to protect Radio Astronomy Service (RAS) which operates at 3.3GHz and 6-7.25GHz band is licensed to EESS (Earth Exploration Satellite Services) and TV [2]. In Korea, a

spectral mask of -41.3dBm/MHz is imposed for 3.1-4.2GHz and 7.2-10.2GHz. Both Japan and Korea have adopted a mitigation technique called Detect and Avoid (DAA) for UWB devices operating in 3.4-4.8GHz and 3.1-4.2GHz bands respectively. The band 6-7.2GHz is protected for licensed services. Figure 1.3 shows the UWB regulations for US, Europe, Japan and Korea.

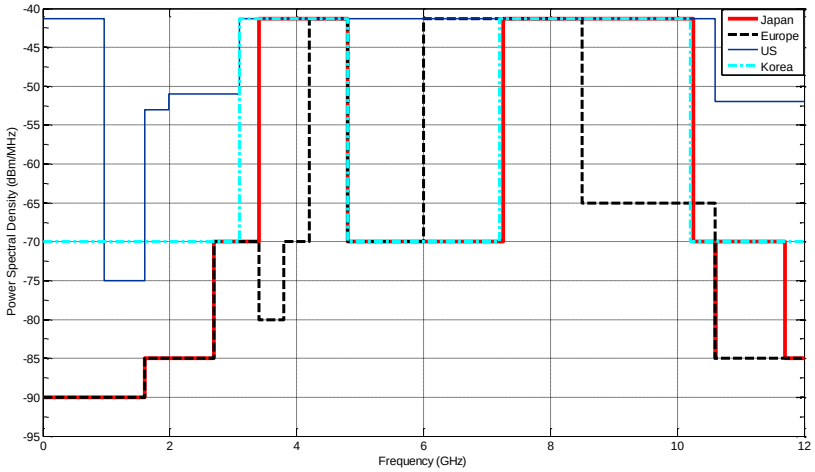


**Figure 1.3 UWB regulations in US, Europe, Japan and Korea**

The variation in spectrum allocation for UWB across different regions causes difficulties for the WiMedia Alliance in defining a common band group that enables a UWB product to be operable worldwide. This is because a minimum of 1.5GHz frequency bandwidth is required for such applications but only a common frequency bandwidth of 1.25GHz is available across all the regions between 7.25GHz and 8.5GHz. This requires the WiMedia group to modify their existing standard to enable devices be operable anywhere in the world.

The permissible EIRP for UWB is -41.3dBm. This shows on average that the EIRP of UWB is 60dB less than other wireless technologies. Figure 1.4 and Figure 1.5 show the frequency spectrum of UWB in comparison with other wireless technologies such as WLAN, Bluetooth and WiMax. The low EIRP is a bottleneck for UWB which greatly limits the performance of the system. This reduces the coverage distance and the data rate of the system.

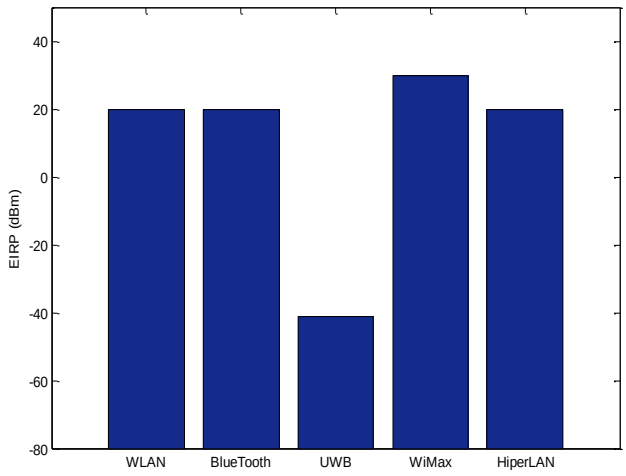


**Figure 1.4 EIRP of UWB compared with other wireless technologies**

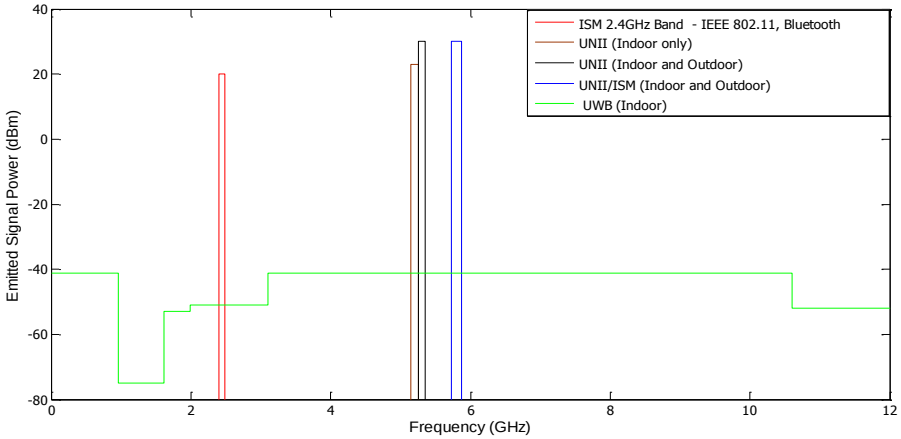


**Figure 1.5Frequency spectrum of UWB compared with IEEE 802.11, Bluetooth and HiperLAN**

Although UWB has a very wideband compared to the ISM bands, the power constraints limit its coverage distance and spectral efficiency. For example, comparing the EIRP of UWB and WLAN shows the magnitude of power restrictions on UWB. The maximum permissible EIRP spectral density is -41.3dBm (73nW) for UWB (FCC regulated) while it is 20dBm (100mW) for WLAN. Therefore UWB signals generally have low SNR, and based on Shannon's Law the low SNR will reduce the channel capacity.

$$Capacity = B\ Log\ (1 + \frac{Signal\ Power}{Noise\ power}) \qquad 1.1$$

One of the challenges in UWB system is to deal with the dense multipath channel. Indeed, each transmitted UWB signal arrives at the receiver as several replicas with different delays, amplitudes and phases. Wireless signals can take different path to arrive at the receiver. These paths could be through a straight route called Line of sight (LOS) or multiple reflected paths called multipath. However, due to the timing difference in their arrival, when the receiver combines the received signals, they could add up constructively to improve the signal or destructively to make the signal not to be decodeable. Figures 1.6 -1.7 show the UWB channel in a dense multipath with LOS and NLOS scenarios.

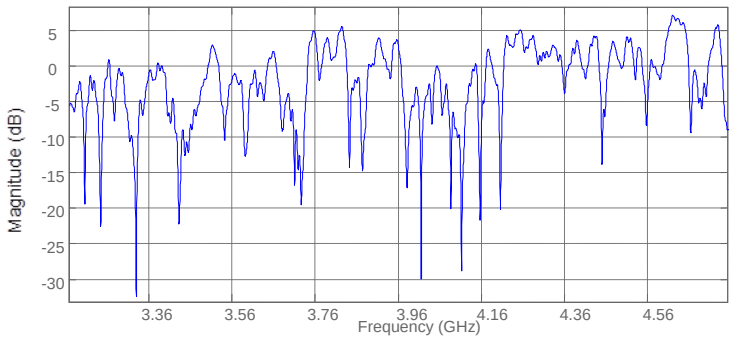


**Figure 1.6 UWB channel with non line of sight scenario**

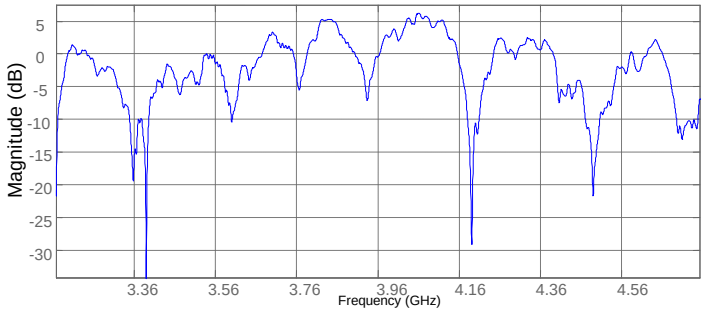


**Figure 1.7 UWB channel with line of sight scenario**

In a UWB channel which usually experiences selective fading, using non-adaptive modulation technique will not utilise the spectrum efficiently. This could result in high bit error rate (BER) as data are also sent through the sections of the spectrum that are experiencing deep fading. Figure 1.8 illustrates a QPSK modulated signal transmitted through a UWB channel experiencing selective fading. It could be seen that the signals sent through the faded region are lost while more information can be sent through section of the channel that is not experiencing any fading. It also shows the SNR of each of the data subchannel and the number of bits per symbol being modulated using QPSK. It is generated by overlaying the signal to noise ratio of each sub carrier over the number of bits modulated on the carrier. The stick is for the bits per symbol while the blue curve for the Signal to Noise Ratio (SNR).

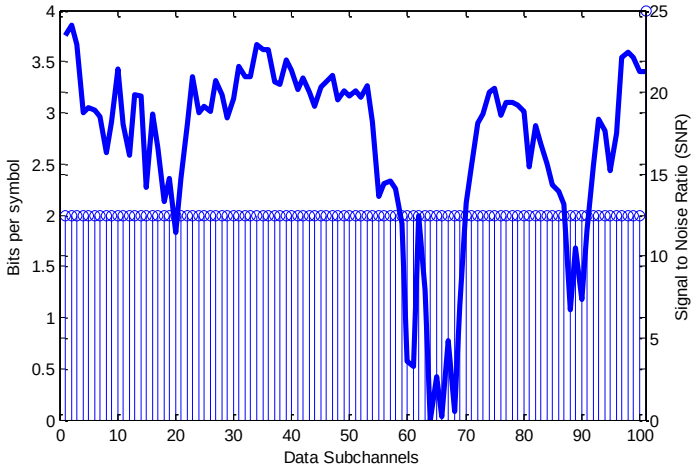


**Figure 1.8 Effect of using only QPSK modulation over a UWB channel**

### 1.4 Aim and Outline of the report

The aim of the project is to investigate the reason why UWB technology has failed to realise its potential and to find the technical solutions.

Following the introductory chapter, the rest of the report is organised as follows:

- Chapter 2: The literature review and background theory of the UWB communication systems are presented.

- Chapter 3: UWB performance is evaluated using a UWB evaluation kit (AT91AP9A-DK Development kit) and Q-waves wireless USB data kit (built on MB-OFDM UWB technology). The evaluation is carried out in different scenarios, in order to determine the general performance.
- Chapter 4: This chapter covers the UWB channel modelling, measurement procedures and the channels considered.
- Chapter 5: Time variance in UWB channel is studied and evaluated in this chapter, with the objective of determining an acceptable feedback rate for adaptive system. This includes :
    I. Evaluation of SISO and SIMO system to examine the performance with varying speed to determine the behaviour of the UWB device as it moves in the indoor environments.
    II. Evaluation of adaptive modulation in a channel experiencing shadowing due to the movement of people or objects to establish an acceptable speed of a UWB device with optimum performance within the indoor environment.
    III. Detail Study of the performance of using receive diversity on devices. This will aim at investigating the feasibility of incorporating receive diversity in small portable devices that have a potential market for the technology.
- Chapter 6: This chapter provides an overview of the spatial processing techniques that can be used in UWB communication systems to enhance the link reliability using receive diversity. Multi antenna systems will be used to extend and evaluate the performance of the receive diversity using the following techniques:

I. Antenna selection

II. Maximal Ratio Combining

Other techniques could be considered such as making the modulation adaptive in order to minimise the Bit Error Rate in the UWB system.

- Chapter 7: This chapter discusses the design and practical implementation of an UWB antenna selection circuit and test bed for MRC combining technique. Tests were carried out and the results were discussed. This is to evaluate and demonstrate the performance of using receive diversity over various antenna distance. This could establish the minimum distance between the antennas for optimal performance and show the possibility of achieving high data rate over three metres and beyond for multimedia within the indoor environment.
- Chapter 8: Conclusions are drawn and a road map for future work is provided.

### 1. 5 Novel work undertaken

The contributions to knowledge presented in this thesis are listed below in a chronological order:

1. Detailed evaluation and analysis of the MB OFDM communication system (looking at all the parameters)
2. Implementation of Adaptive bit loading on sub channels experiencing selective fading with a goal of improving the throughput of the UWB communication system.
3. Characterisation of UWB time varying channel to evaluate the rate at which the UWB channel changes with human movement in an indoor environment.
4. Implementing spatial processing techniques to improve performance and to achieve higher data rate. UWB channel modelling and system simulation for the SISO and SIMO schemes.
5. Circuit implementation of Antenna selection technique to evaluate the performance of the system. Implementation of Maximal ratio combining to evaluate the performance of the system.

### 1.6 List of publications

1. *Exploit Adaptive Modulation in UWB Power line Communication for Improved BER Performance*, Shuxian Chen**, Musa Magani**, Xiaodong Chen and Clive Parini. 15th IEEE International Symposium on power line communication, 2010, ISPLC 2010, Brazil

2. *Using Adaptive Bit Loading in MB-OFDM UWB System for Improved BER Performance*, **Musa Magani**, Lu Guo and Xiaodong Chen. ICUWB 2010, *2010* IEEE International Conference on Ultra-Wideband September 20-23, 2010 Nanjing, China

3. *Diversity Combining for Enhanced UWB System Performance*
**Musa Magani**, Lu Guo and Xiaodong Chen, 2011 Loughborough Antennas & Propagation Conference, 14th - 15th November (LAPC 2011) Loughborough, United Kingdom

4. *A Dual Band Planar Inverted F Antenna for Body-Centric Wireless Communications*
Mohammad M Khan, **Musa Magani,** Atiqur Rahman and Clive Parini . IET 3rd Annual Seminar on Passive RF and Microwave Components Savoy Place, London 26 March 2012

5. *Evaluation of MB OFDM UWB for High Data Rate Applications*

**Musa Magani,** Lu Guo, Yasir Alfadhl and Xiaodong Chen. Loughborough Antennas and Propagation Conference, LAPC 2012. 12-13 November 2012

6. A *Study of UWB Adaptive Bit Loading in Time Varying Channel*

**Musa Magani** , Lu Guo , Xiaodong Chen , Akram Alomainy

2013 International Workshop on Antenna Technology (iWAT) 4-6 March 2013 Karlsruhe Germany

**References**


1. Federal Communications Commission(FCC),"First Report and Order in The Matter of Re-vision of Part15of the Commission's Rules Regarding Ultra wideband Transmission Systems," ET-Docket98-153,FCC02-48,released April 2002.
2. Regulatory Comparison of Ultra-Wideband (UWB) Radio Systems between Japan and CEPT. MMAC Forum UWB Working Group, ARIB, Japan. MMAC-2008-0001. 2008
3. UWB (Ultra-Wideband) Radio Systems Ver. 1. 1, Assoc. of Radio Industries and Bus. Standard ARIB STD-T91, Japan. 2008
4. T. Kaiser and F. Zheng, Ultra Wideband Systems with MIMO. New York: Wiley,2010
5. Spectrum Allocations for Ultra Wide Band Communication Devices, Radio Spectrum Policy and Planning Group, Energy and Commun. Branch, Min of Econ Develop.Wellington, New Zealand. April 2008
6. O ppenmann, L. Stoica, A. Rabbachin, Z. Shekby, and J. Haapola, "UWB Wireless Sensor Networks: UWEN – a Practical Example," IEEE Communications Magazine, pp. S27-S32, 2004.
7. Wireless USB: The First High-speed Personal Wireless Interconnect, White paper, Intel Corporation, 2004
8. Werner Wiesbeck Introduction to Ultra Wideband Technology, Institut für Hochfrequenztechnik und Elektronik, Karsruhe institute of technology, April 2012
9. S. Ullah, M. Ali, A. Hussain, and K. S. Kwak, "Applications of UWB Technology," The 5th annual International New Exploratory Technologies Conference 2008 (NEXT 2008), pp. 225-232, Turku, August 2008.
10. What Is a Wireless Sensor Network?, White paper, National Instrument , May 2012
11. X. Huang, E. Dutkiewicz, R. Gandia, D. Lowe, "Ultra-Wideband Technology for Video Surveillance Sensor Networks," IEEE International Conference on Industrial Informatics, pp. 1012-1017, 2006.

12. J. Li, T. Talty, “Channel Characterization for Ultra-Wideband Intra-Vehicle Sensor Networks,” Military Communications conference (MILCOM), pp. 1-5,2006.
13. V. Mehta, M. EI Zarki, “An Ultra Wide Band (UWB) Based Sensor Network for Civil Infrastructure Health Monitoring,” 1st European Workshop on Wireless Sensor Networks (EWSN), Berlin, Germany, January 19-21, 2004.
14. S. Gezici, Z. Tian; G.B. Giannakis, H. Kobayashi, A.F. Molisch, H.V. Poor, Z. Sahinoglu, “Localization via ultra-wideband radios: a look at positioning aspects for future sensor networks,” IEEE Signal Processing Magazine, Vol. 22, pp. 70-84,2005.
15. L. Yuheng, L. Chao, Y. He, J. Wu, Z. Xiong, “A Perimeter Intrusion Detection System Using Dual-Mode Wireless Sensor Networks,” Second International Conference on Communications and Networking in China, pp. 861-865, 2007.
16. R.S. Thoma, O. Hirsch, J. Sachs, Zetik, R., “UWB Sensor Networks for Position Location and Imaging of Objects and Environments,” The Second European Conference on Antennas and Propagation (EuCAP), pp. 1-9, 2007.
17. F. Granelli, H. Zhang, X. Zhou, S. Maranò, “Research Advances in Cognitive Ultra Wide Band Radio and Their Application to Sensor Networks,” Mobile Networks and Applications, Vol. 11, pp. 487-499, 2006.

# CHAPTER 2

**LITERATURE REVIEW AND THEORY OF UWB**

## 2.1. Introduction

In this chapter, the early development about the UWB system is discussed. The discussion starts from its invention to the current state of art. Secondly, the theory behind the Impulse response (IR UWB) and the Orthogonal Frequency Division Multiplexing Ultra wideband (OFDM UWB) systems are discussed with more emphasis on the OFDM UWB system. Finally, the chapter concludes with the discussion of existing MB OFDM UWB communication products.

## 2.2. Critical review and early development

This section provides a critical review of the state of art of UWB technology. It is intended not to cite all the work performed in the area of UWB systems but to cite important accomplishment to the development of UWB technology. It is interesting that the earliest wireless communication systems are pulse based signals and had their origin in the spark gap transmission design by Heinrich Hertz and Marconi in the late 1890s [2]. These were later replaced by communication systems using carriers, since the pulsed based signal could not be effectively recovered at the receiver at that time. It was until early 1960s that the techniques of generating sub nanoseconds baseband pulses were developed which gave UWB a new engineering outlook that can be effectively used for several applications.

In 1960s, pioneering contribution to the development of UWB RF signals were done by Ross and Robinson at Sperry Rand Corp., Harmouth at Catholic University of America and Paul Van Effen at the US Air force (USAF) Rome development centre [3]. The first UWB patent awarded for UWB communication systems was to Dr. Gerald F. Ross on 17$^{th}$ April, 1973 [3]. This patent was a landmark in UWB communication and radar and it also includes coding schemes.

By 1975, the basic component of UWB systems could be constructed from Tektronic component either for communication or radar [2]. These components were pulse generator, pulse train modulators, switching pulse train generators, detection receiver and wideband antennas. By 1978, Ross and Bennett summarised the known pulse generation methods and since then, only innovative improvement in the UWB field were done on subsystem level and

not on the overall system concept itself. From 1977 to 1989, the USAF founded a UWB system development program headed by Col. J D Taylor and were able to organise a UWB workshop for US Department of Defence DDR & E in 1988 [3]. Over the next two decades UWB technology was extensively researched and developed for military radars and communications due to its immunity to multipath and low probability of intercepting.

In late 1990s, the communication industry moved to commercialised UWB communication system and devices. This led to the formation of two companies, namely; Time Domain and XtremeSpectrum later bought by Motorola [2] to build consumer UWB electronics. In 2002, interest in the UWB consumer electronics soared when the Federal Communication Commission (FCC) defined the emission mask and fractional bandwidth of UWB [4]. The FCC allocated a wideband of 7.5 GHz between 3.1 and 10.6 GHz for use within the Personal Area Network (PAN). This makes UWB suitable for high data rate applications within the PAN range under the current FCC regulation, or for low data rate applications over a longer distance. Some applications of UWB are home networking, wireless body area networks (WBAN) and accurate location based services.

Recently, a book titled UWB systems with MIMO [1] has been published by Wiley with Thomas Kaiser and Feng Zheng as its authors. They showed the progress in UWB MIMO research and the writers' focus in the book is on Impulse Response UWB (IR-UWB) systems and not MB-OFDM systems due to the following reason given by the authors. The authors believe IR-UWB based systems have already found their niche in indoor applications such as wireless indoor localisation. They investigated the benefits of combining UWB systems and MIMO technology in five promising and interesting fields, namely, channel Capacity, Channel Measurement, Space time Coding (STC), beamforming, UWB-MIMO relay and time reversal (TR) system.

They investigated the potential channel capacity that can be realised when both UWB and MIMO are combined together. This was shown in terms of its ergodic capacity, outage probability on a channel with channel state information (CSI) and unknown channel state information (CSI). In terms of STC, they presented a novel work in IR-UWB space time coding on MISO using STC scheme of 1S/2S (one information symbols and two transmit antennas) and 2S/2S (two information symbols and two transmit antennas). The performance was compared using antenna selection and equal gain combining and also presented a concept on STC with OFDM-UWB with MIMO. The large scale and small scale pathloss experienced by wideband systems with UWB system is discussed. Simulation results were presented on the performance Optimal Power Spectrum Allocation (OPSA) and Uniform Power Spectrum Allocation (UPSA) in UWB MIMO system. The results show that at low SNR, OPSA out performs the UPSA, while at higher SNR both scheme tend to have similar performance. It was demonstrated that the

efficiency of UPSA is lower than 0.61 when the SNR is low. With OPSA, the transmission rate can be increased roughly more 1.6 times [31]. A test bed for channel measurement is developed and demonstrated which consists of two arbitrary waveform generators (AWG) and one digital phosphor oscilloscope (DPA) that can provide four channels.

Not much research has been presented on MB-OFDM UWB with MIMO while a considerable number of research presentations have been done on IR-UWB system with MIMO. Some of the research work presented [6] did not put into consideration, the constraints in UWB technology such as power limit, which makes it difficult to implement. Also, some research only cover the channel capacity and channel modelling [7-14] with little work done on spatial multiplexing and diversity based on the MB OFDM UWB MIMO model.

In [15], MIMO UWB (pulse –based) in Nakagami fading has been investigated and in [16], the authors have investigated the benefit of using adaptive transmit and receive diversity under the constraint of power and overall bit rate. This shows that much research is needed to provide novel solutions and techniques to improve the performance of MIMO MB-OFDM UWB system while complying with the power regulation placed on UWB technology.

### 2.3. Multiple Input Multiple Output (MIMO)

The earliest development of MIMO could be traced back to 1984 where Jack Winter of Bell Laboratories published an article titled “Optimum combining in digital mobile radio with co-channel interference” [17]. Since then, many contributions have been made to the understanding and development of MIMO systems. In 1991, Emire Telatar wrote a paper “Capacity of multi-antenna Gaussian Channel” [18], in which he calculated the Shannon capacity of an isotropic fading MIMO channel. He stated that channel capacity increases proportionally with the number of transmit or receive antennas. This information drew a lot of interest in MIMO to exploit its potential benefit.

Both Greg Raleigh and Gerard J Foschini [19] in 1996 wrote a paper each, which redefined the approaches to MIMO technology. They considered configurations, where multiple antennas are co-located at one transmitter to improve the throughput effectively [20]. Bell Laboratories became the first in 1998 to perform a successful technology demonstration under laboratory conditions. A year later, Giga Bit Wireless Inc and Stanford University did a successful demonstration outdoor [21].

### 2.4. Overview of UWB

FCC provides the following definitions for UWB signalling:

• UWB bandwidth: This is the frequency band based on the complete transmission system which includes the antenna, bounded by the points that are 10dB below the highest permitted

radiated emission. The upper boundary of the frequency band is designated as $f_h$ and the lower boundary is $f_l$. The frequency at which the highest radiated emission occurs is $f_m$.

• Centre frequency ($f_c$): This is the average of upper Boundary ($f_h$) and lower boundary ($f_l$) expressed as

$$f_c = \frac{f_h + f_l}{2} \qquad 2.1$$

• Fractional bandwidth ($f_b$): FCC requires UWB to have a fractional bandwidth equal to or greater than 20% or an absolute bandwidth that is either equal to or greater than 500MHz.The fractional bandwidth is defined as

$$f_b = 2\frac{f_h - f_l}{f_h + f_l} \qquad 2.2$$

• Equivalent Isotropic Radiated Power (EIRP): This is apparent power transmitted towards the receiver, if it is assumed that the signal is radiated equally in all directions, such as a spherical wave emanating from a point source. EIRP could also be regarded as the arithmetic product of the power supplied to an antenna and its gain. The FCC power requirement is -41.3dBm/MHz which is equal to 74.13 nW/MHz.

UWB transmission has two signalling techniques developed by two different groups. Namely Carrier Free Ultra Wide Band which is also called Impulse Response Ultra Wide Band (IR- UWB) and Multiband Orthogonal Frequency Division Multiplexing Ultra wideband (MB OFDM UWB).

### 2.4.1 Impulse Response Ultra Wideband (IR –UWB)

IR- based UWB signalling technique is a carrier free system that sends train of short pulses without carriers at a very high speed as compared to narrow band carriers. The duration of the pulses are very short, measured in nanoseconds which results in a very wide band in the frequency domain. In IR-UWB system, the popular pulse waveforms are the first and second derivative of the Gaussian monopulse [22]. These are expressed as

I. First derivative

$$\omega_1 = \zeta_1 t\, exp\left[-2\pi\left(\frac{t}{\tau_p}\right)^2\right] \qquad 2.3$$

II. Second derivative

$$\omega_2 = \zeta_2\left[1 - 4\pi\left(\frac{t}{\tau_p}\right)^2\right] exp\left[-2\pi\left(\frac{t}{\tau_p}\right)^2\right] \qquad 2.4$$

Where $\zeta_1$ and $\zeta_2$ are constants to normalise the amplitude of $\omega_1$and $\omega_2$ respectively and $\tau_p$ adjusts the pulse width. The original Gaussian monopulse is not used because it contains a DC component in its power spectrum. Figures 2.1-2.2 shows the time domain representation of the first and second derivative of the Gaussian monopulse respectively.

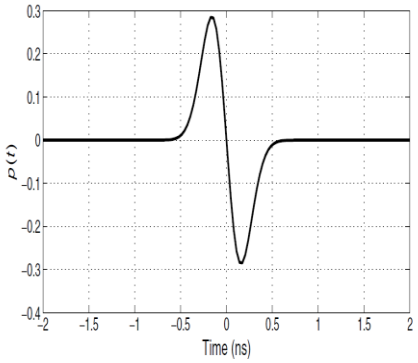


Figure 2.1 1st derivative of Gaussian pulse

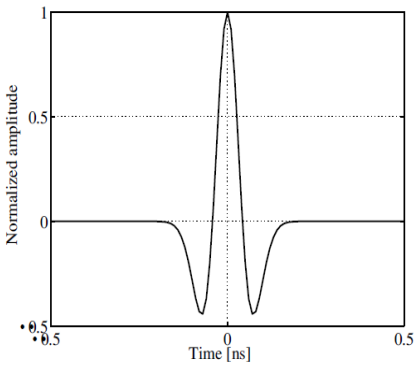


Figure 2.2 2nd derivative of Gaussian pulse

The signal data can be embedded either in the amplitude, position or both of the impulse train, there by resulting into Pulse Amplitude Modulation (PAM), Pulse Position Modulation (PPM), and Pulse Shift Keying (PSK). The generic transmit and receive IR-based UWB signal in a single user environment are written as

$$s_k(t) = \sum_{j=-\infty}^{\infty} \sqrt{\frac{E_s}{N_s}}\, \beta_j \alpha\, a_k\left(\lfloor j/N_f \rfloor\right)\, w\left(t - jT_f - c_k(j)T_c - \delta d_k\left(\lfloor j/N_f \rfloor\right)\right) \quad 2.5$$

$$r_k(t) = \sum_{j=-\infty}^{\infty} \sqrt{\frac{E_s}{N_s}}\, \beta_j\, a_k\left(\lfloor j/N_f \rfloor\right)\, w\left(t - jT_f - c_k(j)T_c - \delta d_k\left(\lfloor j/N_f \rfloor\right)\right) + n(t) \quad 2.6$$

where $s_k(t)$ and $r_k(t)$ are the transmitted and received signal for the $k^{th}$ user respectively. $w(t)$ is the monopulse of duration $T_w$,$T_f$ is the frame duration, $T_c$ is the chip duration, $N_f$ is the number of frames for one data symbol, $\delta$ is the modulation index, ($\lfloor x \rfloor$) is the integer floor of x, $E_s$ is the energy per symbol, $N_s$ is the number of pulses per symbol, the pulse amplitude is represented by $\frac{E_s}{N_s}$, $a_k$ and $d_k$ are the transmitted and received data symbols and $n(t)$ is the AWGN with double-sided spectrum [25] .

### 2.6 MB-OFDM UWB

In 2004, the WiMedia group proposed a UWB signalling using Multiband Orthogonal Frequency Division Multiplexing (MB-OFDM)[25]. The bandwidth is split into multiple sub bands to ensure that the total UWB spectrum is efficiently utilised. The advantages of this approach over IR-based approach are:

- having better co-existence with other current wireless technologies.
- it enables worldwide interoperability of UWB devices as different regions in the world have different spectrum allocation.
- having the ability to avoid strong narrowband interference where they exist. For example, the frequency band occupying 5.2GHz can be avoided when WiMax device are in operation.

### 2.4.2 Frequency band allocation

MB-OFDM divides the 7.5GHz available bandwidth for UWB communication into fourteen bands having 528MHz per band. The bandwidth is divided into five groups. The first four groups have three bands each while the fifth group contains only two bands. . Based on the FCC regulation, the minimum bandwidth should be less than 500MHz. This gives insight why a entire 7.5GHz bandwidth is divided into fourteen 528MHz bands. Table 2.1 summaries the frequency allocation of each of the group and their sub bands. The relationship between the band number and the center frequency is

$$\text{Band centre Frequency} = 2904 + 528 \times n \text{ (MHz)} \qquad 2.7$$

Where *n*= band number from 1 to 14

Table 2.1 MB OFDM UWB Frequency band allocation [25]

| Band Group | Band_ID | Lower Frequency | Centre Frequency | Upper Frequency |
|---|---|---|---|---|
| 1 | 1 | 3168MHz | 3432MHz | 3696MHz |
| | 2 | 3696MHz | 3960MHz | 4224MHz |
| | 3 | 4224MHz | 4488MHz | 4752MHz |
| 2 | 4 | 4752MHz | 5016MHz | 5280MHz |
| | 5 | 5280MHz | 5544MHz | 5808MHz |
| | 6 | 5808MHz | 6072MHz | 6336MHz |
| 3 | 7 | 6336MHz | 6600MHz | 6864MHz |
| | 8 | 6864MHz | 7128MHz | 7392MHz |
| | 9 | 7392MHz | 7656MHz | 7920MHz |
| 4 | 10 | 7920MHz | 8184MHz | 8448MHz |
| | 11 | 8448MHz | 8712MHz | 8976MHz |
| | 12 | 8976MHz | 9240MHz | 9504MHz |
| 5 | 13 | 9504MHz | 9768MHz | 10032MHz |
| | 14 | 10032MHz | 10296MHz | 10560MHz |

### 2.5.1 ORTHOGONAL FREQUENCY DIVISION MULTIPLEXING (OFDM)

A baseband UWB OFDM signal is expressed as

$$s_{rf}(t) = Re\left\{\sum_{n=0}^{N-1} s_n\left(t - nT_{sym}\right) \exp(j2\pi f_c(q(n))t)\right\} \qquad 2.8$$

where Re(.) represents the real part of the signal, $N$ is the number of symbols in the packet, $f_c$ is the centre frequency of the frequency band, $q(n)$ is a function that maps the $n^{th}$ symbols to the appropriate frequency band and $s_n$ is the complex based band signal for the $n^{th}$ symbol. The structure of $n^{th}$ symbol depends on its location within the packet as follows

$$s_n(t) = \begin{cases} s_{sync,n}(\mathrm{t}) & 0 \le \mathrm{n} \ge N_{sync} \\ s_{hdr,n-N_{sync}}(\mathrm{t}) & \mathrm{N_{sync}} \le \mathrm{n} < \mathrm{N_{sync}} + \mathrm{N_{hdr}} \\ s_{frame,n-N_{sync}-N_{hdr}}(\mathrm{t}) & \mathrm{N_{sync}} + \mathrm{N_{hdr}} \le \mathrm{n} < N \end{cases} \qquad 2.9$$

where $s_{sync,n}(\mathrm{t})$, $s_{hdr,n}(\mathrm{t})$ and $s_{frame,n}(\mathrm{t})$ describe the $n^{th}$ symbol of the preamble, header and Physical Sequence Data unit (PSDU) respectively. $N_{sync}$,$N_{hdr}$ and $N_{packet}$ are the number

of symbols in the preamble, header and packet respectively [23]. Table 2.2 shows the parameter values of the MB OFDM UWB as proposed by the WiMedia group.

Table 2.2 parameter values proposed by the WiMedia group [25]

| Parameter | Description | Value |
|---|---|---|
| fs | Sampling frequency | 528 MHz |
| $N_{FFT}$ | Total number of subcarriers (FFT size) | 128 |
| $N_D$ | Number of data subcarriers | 100 |
| $N_P$ | Number of pilot subcarriers | 12 |
| $N_G$ | Number of guard subcarriers | 10 |
| $N_T$ | Total number of subcarriers used | 122 (= $N_D$ + $N_P$ + $N_G$) |
| $\Delta f$ | Subcarrier frequency spacing | 4.125 MHz (= $f_s / N_{FFT}$) |
| $T_{FFT}$ | IFFT and FFT period | 242.42 ns ($\Delta f$ -1) |
| $N_{ZPS}$ | Number of samples in zero-padded suffix | 37 |
| $T_{ZPS}$ | Zero-padded suffix duration in time | 70.08 ns (= $N_{ZPS} / f_s$) |
| $T_{SYM}$ | Symbol interval | 312.5 ns (= $T_{FFT}$ + $T_{ZPS}$) |
| $F_{SYM}$ | Symbol rate | 3.2 MHz (= $T_{SYM}$ -1) |
| $N_{SYM}$ | Total number of samples per symbol | 165 (= $N_{FFT}$ + $N_{ZPS}$) |

In OFDM, Inverse Fast Fourier Transform (IFFT) is used to provide an effective means of summing the signals from sub carriers. IFFT produces orthogonal set of sinusoid in time domain. Due to the orthogonality between sub carries using OFDM, sub carrier can overlap without causing interference. This property makes OFDM a preferred choice over the traditional techniques because higher data rate can be achieved. Considering the following

$$r_{data,k}(t) = \sum_{n=0}^{N_{SD}} c_{n,k} \exp(j2\pi M(k)\Delta_F (t - T_{CP})) + p_k \sum_{n=-N_{ST}/2}^{N_{ST}/2} P_n \exp(j2\pi k\Delta_F (t - T_{CP})) \qquad 2.10$$

$r_{data,k}(t)$ =OFDM symbol, M (k) =Mapping from the indices 0 to 99, $N_{SD}$ = number of sub carriers, $N_{ST}$= total sub carriers, $c_{n,k}$ =Sub carrier n of OFDM symbol k , $\Delta_F$ = sampling period in the frequency domain. Applying IFFT to a sampled data that has been mapped into a complex based on the equation 2.10

$$\begin{aligned} ifft(X + jY) &= \sum_{k=0}^{N} (X + jY) \cdot e^{\frac{2\pi jnk}{N}} \\ &= \sum_{k=0}^{N} (X + jY) \cdot (\cos\phi + j\sin\phi) \\ &= \sum_{k=0}^{N} X \cdot \cos\phi + jX \cdot \sin\phi + jY \cdot \cos\phi - Y \cdot \sin\phi \\ &= \sum_{k=0}^{N} (X \cdot \cos\phi - Y \cdot \sin\phi) + j(X \cdot \sin\phi + Y \cdot \cos\phi) \end{aligned} \qquad 2.11$$

Where n = sub carrier, K=OFDM symbol, N=number of subcarriers

The proposed MB OFDM UWB standard utilises 128-point IFFT/FFT, to correspond to the available sub carriers in each band. Each band is divided into 128 sub carriers with 100 channels as data carriers, 10 channels as guard interval carriers, 12 channels as pilot carriers, 5 channels are unused and 1 channel is for zero DC as shown in Figure 2.3.

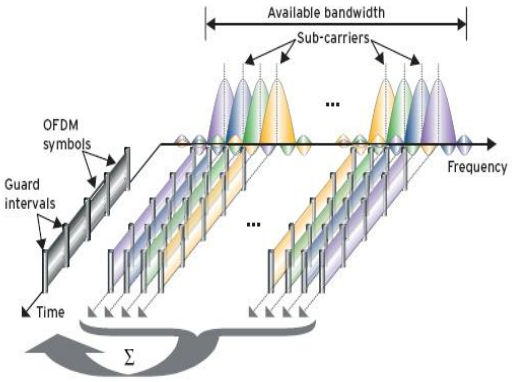


Figure 2.3 UWB OFDM structure showing the sub carriers and guard intervals [26]

A cyclic prefix of 60.6ns is used to be able to capture the multipath energy. Cyclic prefix refers to prefixing of a symbol with a repetition at the end. This allows the linear convolution of a selective multipath channel to be modelled as circular convolution, which in turn may be transformed to the frequency domain using discrete Fourier transform. This approach allows simple frequency domain processing such as channel estimation and equalisation [23].

The cyclic prefix length needs to be chosen to minimise the impact due to ISI and maximise the collection of multipath energy, while keeping the over head due to cyclic prefix low. However, instead of using cyclic prefix, the same robustness can be obtained by using zero padding (ZP). The only modification required is at the receiver. The receiver is to collect additional samples corresponding to the length of the prefix and to use an overlap-and-add method to obtain the circular convolution property. The advantage of using ZP prefix is that power back off at the transmitter can be avoided. The UWB emission are limited by the FCC, therefore power back off will be required if there are ripples in the PSD. When cyclic prefix is used, redundancy is introduced in to the transmitted signal and the correlation in the signal leads to ripples in the average PSD. When prefixing with zero padding, the ripples in the PSD can be reduced to zero with enough averaging [24]. Figure 2.4 shows the ripples experienced in PSD for OFDM UWB system that uses cyclic and zero padding prefix.

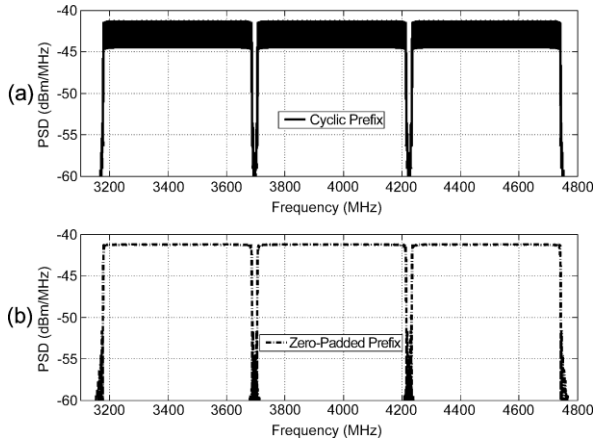


Figure 2.4 PSD Plots for an MD OFDM system using (a) Cyclic prefix and (b) Zero padding

### 2.5.2 Guard interval

The guard intervals are inserted to ensure that only a single RF transmitter and RF receiver chain are needed for all channel environments and all data rate, Also there is sufficient time for the transmitter and receiver to switch the carrier frequency to the next channel [23].

### 2.5.3 Pilots

The pilots are used to allow coherent detection and to provide robustness against frequency offset and phase noise. The pilot signals are placed in a logical frequency sub carrier -55,-45,-35,-25,-15,-5, 5, 15, 25, 35, 45, 55 [25]. Figure 2.4 depicts the position of the pilot carriers.

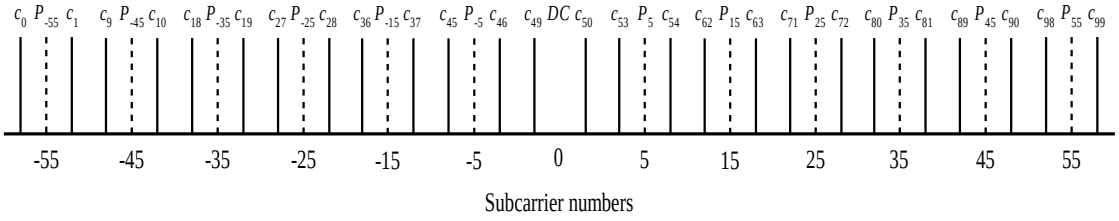


Figure 2.4 Showing positioning of subcarriers numbers[23]

The pilot carriers carry signal in order that the receiver can coherently detect the signal against frequency offset and phase noise. The pilot and guard intervals are inserted and the Inverse Fast Fourier Transform (IFFT) is employed to transform a frequency domain signal to a time domain signal. Appended with zero padding the time domain signal is passed through a band pass filter and transmitted with frequency hopping over the three sub bands. The receiver is similar to the transmitter but in the reverse direction, except it contains channel estimation and compensation. At the receiver, the reversed process is done with the Fast Fourier Transform (FFT) used to transform the time domain signal to frequency domain signal. The received data is demodulated, de-interleaved, decoded and forwarded to the MAC layer. The channel estimation and compensation helps form an estimation of the amplitude and phase shift caused by the vulnerability of the wireless channel to high noise and distortion. This estimation is done by the receiver analyzing the time domain component of received wave and separating the signal from the noise component based on the available pilot information. Figures 2.5 and 2.6 show the layout of the OFDM UWB transmitter and receiver respectively. The theory about the coding, interleaving and modulation used in MB OFDM UWB technology is described in the appendix A.

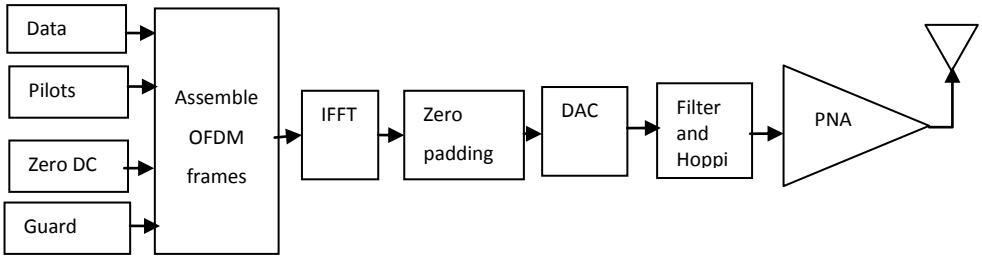


Figure 2.5 MB-ODFM UWB Transmitter

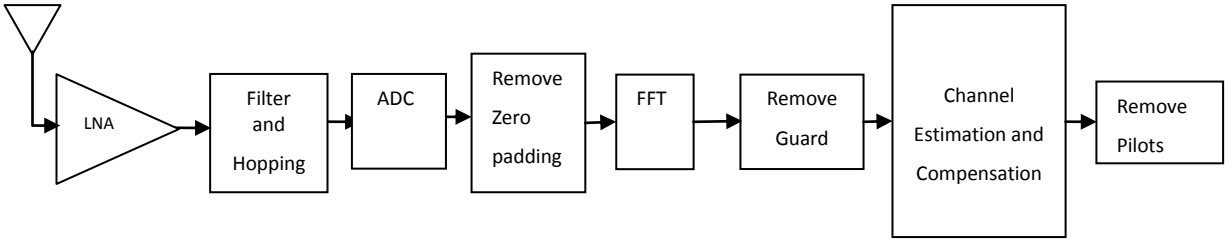


Figure 2.6 MB-ODFM UWB Receiver

The MB-OFDM system hops over specific pattern in each of the sub group (sub band). An example of OFDM symbols transmission in a MB-OFDM is shown in Figure 2.7. It shows one realisation of a time-frequency code where the first symbol is transmitted over channel 1, the second symbol is transmitted over channel 2, the third symbol is transmitted over channel 3 , the fourth symbol is transmitted over sub band 1 and so on. Here, a single realisation of the time- frequency code is illustrated but in practice there are different time–frequency codes. This approach provides frequency diversity and multiple accesses. Table 2.3 shows the hopping pattern.

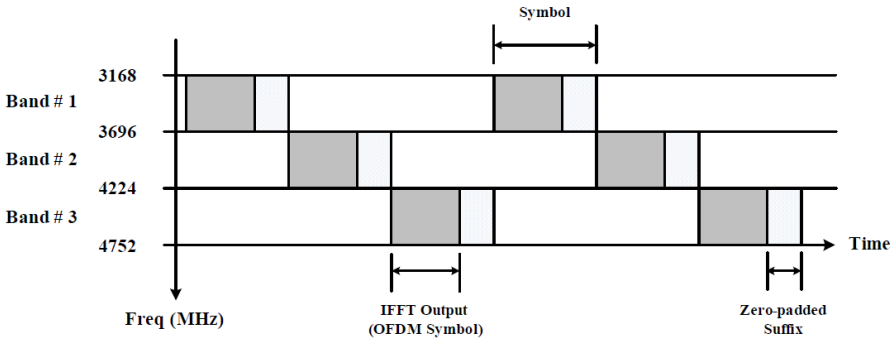


Figure 2.7 Example of time frequency coding for the multiband OFDM system [23]

Table 2.3 Time-Frequency Codes for Band Group 1[16]

| Channel Number | TFC Number | BAND_ID for Time-Frequency Codes for Band Group 1 | | | | | |
|---|---|---|---|---|---|---|---|
| 9 | 1 | 1 | 2 | 3 | 1 | 2 | 3 |
| 10 | 2 | 1 | 3 | 2 | 1 | 3 | 2 |
| 11 | 3 | 1 | 1 | 2 | 2 | 3 | 3 |
| 12 | 4 | 1 | 1 | 3 | 3 | 2 | 2 |
| 13 | 5 | 1 | 1 | 1 | 1 | 1 | 1 |
| 14 | 6 | 2 | 2 | 2 | 2 | 2 | 2 |
| 15 | 7 | 3 | 3 | 3 | 3 | 3 | 3 |

## 2.6 The State-of the Art of UWB Technology

Although UWB technology has been widely used in radar and information sensing over three decades, new interest was developed in using UWB technology for communication when the FCC defined a free spectrum to be used without license. Since the introduction of UWB for communication in 2002, not many products are available in the market. Some of the available UWB products are listed below.

### 2.6.1 Q WAVES

Q-waves is one of the companies providing wireless USB products based on the UWB technology. It currently has three products which are wireless AV kit, wireless USB data kit shown in Figure 2.8 and wireless audio kit. The products are designed in compliance to the WiMedia group standard and specification for the physical and MAC layer. The wireless USB operates within the frequency band of 3.1 GHz and 4.8GHz using the MB OFDM technology, within a of 10metres. A more detailed analysis of this product will be given in chapter 3.

Figure 2.8 Q-waves wireless USB data kit [27]

The UWB chipset used in this product is developed by Wisair. Wisair is a semiconductor company providing MB OFDM Ultra Wideband (UWB) and Wireless USB solutions based on its CMOS single chip. The latest chipset from the Wisair Company is WSR601, designed to be suitable for a wide range of applications such as notebooks, PC peripherals, consumer electronics, and portable devices. Figure 2.9 shows the block diagram of the WSR601 chipset.

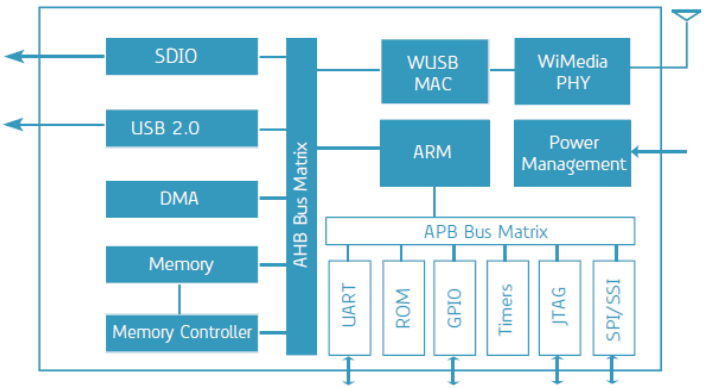


Figure 2.9 WSR601 UWB Chipset [28]

### 2.6.2 ALEREON INC

Alereon Inc. is a semiconductor company that develops wireless USB and WiMedia Ultra wideband (UWB) chipsets that are incorporated into devices. Some of its products are wireless USB adapter, wireless USB VGA adapter and wireless USB half mini card. The products are designed to work in band group 1, 3 and 6 and to support the entire data rate from 53.3Mbps to 480Mbps. This gives user's access to more than 10 channels which can be used in region without any hard ware modification. The band group number needs to be changed based on the region regulation. Alereon Inc. wireless USB adapter is shown in Figure 2.10.


Figure 2.10 Alereon wireless USB adapter [29]

### 2.6.3 GEFEN INC

Gefen Inc is specialised in audio and video connectivity with a wide selection of signal switches, extenders, scalers, splitters and home theatre accessories. Its objective is to enable audio, video and computer systems to be easily integrated and extended to maximise performance. Recently they foray into wireless video extension and have developed a product based on the Wimedia MB OFDM UWB technology to extend HDMI video.

The Gefen EXT-WHDMI wireless HDMI and component extender, shown in Figure 2.11, is used to send video with resolution of up to 1080p/30 (1080 line of vertical resolution and 30 progressive frames per second). It operates in the 3.1-4.8G Hz frequency range which is the band group one and offers a data rate of 65Mbps. The Gefen wireless HDMI extender has 2 video input which comprises of 2 HDMI and 1 component input on its transmitter. The transmitter box can be used to simultaneously send 2 videos/ TV channels to the receiver box. This enables users to switch and watch up to two videos.

Figure 2.11 Gefen EXT-WHDMI wireless HDMI and component extender [30]

**2.7 Summary**

In this chapter, the discussion covers the invention and the early development about the UWB system to the current state of art. It provides a critical review of the UWB technology, starting with the history of UWB systems, when it was invented in 1890s and continuing with major developments over t

3he years. The theory behind the Impulse response (IR UWB) and the Orthogonal Frequency Division Multiplexing Ultra wideband (OFDM UWB) systems are discussed with more emphasis on the OFDM UWB system. Finally, the chapter highlights a few existing MB OFDM UWB communication products. The evaluation of one typical product will be given in the next chapter.

**References**


1. T. Kaiser and F. Zheng, *Ultra Wideband Systems with MIMO*. New York: Wiley,2010
2. R. J. Fontana," *A brief History of UWB* 2", Multispectral Solution Inc Germantown, MD 1999
3. T. W. Barrett , "History of Ultra Wideband (UWB) Radar and Communications" , Pioneers and Innovators Progress In Electromagnetics Symposium 2000 (PIERS2000), Cambridge, MA, July, 2000
4. Federal Communications Commission(FCC),"First Report and Order in The Matter of Re-vision of Part15of the Commission's Rules Regarding Ultra wideband Transmission Systems," ET-Docket98-153,FCC02-48,released April 2002.
5. MIMO. High Capacity Digital Communication Laboratory. University of Alberta
6. K. Ampoma et al, "*Capacity & Performance Issues in a MIMO Based MB-OFDM Ultrawide Band Communication System*", 2nd Int. Conference on Adaptive Sci. & Tech (ICAST), Accra. Ghana 2009
7. J. Keignart, "*UWB SIMO channel measurement and simulation*". IEEE Trans. Microwave Theory Technique 2006

8. W. Q Malik, “Spatial *correlation in ultra wideband channels”*. IEEE trans wireless communication, 2008 pp 604 - 610
9. W. Q Malik and D J Edwards. *“UWB impulse radio with triple polarisation SIMO*”. IEEE Global Telecommunications Conference, (GLOBECOM '07). Washington, D**C** 2007 p**p** 4124 – 4128
10. T. Kaiser and M. El-Hadidy, “*A signal processing frame work for MIMO UWB channel with real antennas in real environments*”, IEEE Int. Conf on Ultra wideband Singapore 2007 pp. 111 – 116
11. M. El-Hadidy and T Kaiser, “*An Ultra channel Model considering angular impulse and polarization”.* In Proc. 2nd European conf on antennas and propagation 2007
12. A Martini, M Franceschetti and A. Massa, “*Capacity of wideband MIMO channels via space time diversity of scatter fields*”. Proc IEEE Asilomar Conf. Signals, systems and computers. Pacific Grove, CA, 2007 pp 138 - 142
13. F. Zheng and T Kaiser, “*On the evaluation of channel capacity of multi-antenna UWB indoor wireless systems”*. In proc IEEE Int. symp. Spread spectrum techniques and Application 2004 ,pp 6106 - 6113
14. F. Zheng and T Kaiser,” *On the evaluation of channel capacity of UWB indoor wireless systems*”. IEEE Int. Trans Signals Process. 2008 pp. 6106 - 6113
15. H. Liu R. C Qiu, Z. Tian,”*Error performance of pulse –based ultra wideband MIMO systems over indoor wireless channel”*. IEEE Transactions on wireless communication, 2005 pp 2939 - 2944
16. Z. Coa and J. W. Mwangoka,” *Adaptive modulated MIMO-OFDM for ultra wide band channel*”, IEEE international Symposium Microwave , antenna , propagation and EMC technologies for wireless communication , 2005,pp 1037 - 1040 Vol. 2
17. J. Winter,” *Optimum combing in digital mobile radio with Co-channel interference*” selected Areas comm. Special Issue on Mobile Radio Comm. IEEE journal. IEEE Trans on Vehicular Technology 1984, 528 – 539 Vol. 2 Issue 4
18. E. Telatar, “*Capacity of Multi antenna Gaussian Channels*”, *European Trans Telecommu,* Vol. 10, No. 6, Nov/Dec 1999,pp. 585-595
19. G. J. Foschini *"Layered space-time architecture for wireless communications in a fading environment when using multi-element antennas*". Bell Labs Technical Journal vol. 1 , Issue 2, 1996 pp 41–59
20. G. J. Foschini et al "*On limits of wireless communications in a fading environment when using multiple antennas*". Wireless Personal Communications vol. 6 Issue 3,Jan 1998, pp 311–335.

21. MIMO. High Capacity Digital Communication Laboratory. University of Alberta
22. M. Clark et al, "*Fixed-Point Modelling in an Ultra Wideband (UWB) Wireless Communication System*". MATLAB digest, May 2004
23. A Batra , "*Design of a Multiband OFDM System for realistic UWB Channel Environments*" , IEEE Transaction on Microwave Theory and Techniques Vol 52, No 9 September 2004
24. B Muquet et al "*Cyclic prefix or Zero padding for wireless multicarrier transmission?",* IEEE Trans. Commun. Vol 50, pp 2136-2148 Dec 2002
25. Phy Specification: Final Deliverable 1.5 Multiband OFDM Physical Layer Specification , WiMedia Alliance, Inc ,2009
26. X. Chen, *Improved BER Performance on MB-OFDM UWB System Using Adaptive Bit Loading-presentation Slides*. ICWB2010 Conference, Nanjing, China, 2010
27. Q waves and Xel solutions, Q waves wireless USB data kit user guide. [online] Available: http:q-waves .com
28. Wasir Inc, WSR601-Wireless USB Single Chip, 2010 [online] Available: ww.wisair.com
29. *Alereon*, Inc. *Worldwide Ultra Wideband (UWB) Radio Card Adapter (AL5616)*, 2010 [online] www.alereon.com
30. Gefen LLC , Wireless for HDMI UWB ext-WHDMI User Manual, 2010 [online] www.gefen.com
31. F. Zheng and T. Kaiser, On the evaluation of channel capacity of UWB indoor wireless Systems, [IEEE Trans. Signal Process. vol. 56, pp. 6106–6113, 2008.

# CHAPTER 3

## EVALUATION AND ANALYSIS OF UWB SYSTEMS

### 3.1 Introduction

In this chapter the UWB communication system is evaluated to determine the current performance of the system and seek ways of improving it. UWB technology has the potential of replacing other wireless technologies within the Personal Area Networks but more research and development are needed to be done. Testing the UWB system performance in terms of its packet error rate and other parameters has been conducted with a UWB evaluation kit to provide an in-depth evaluation and analysis of MB-OFDM UWB system. The Evaluation kit is configured and controlled through the NIOS EDS Command shell console and it is interfaced through USB blaster cables.

### 3.2 Hardware Description

The Atmel AT91CAP9 UWB – EK (Evaluation Kit) is used in order to generate the Multiband OFDM signal and evaluate its performance. The kit is compatible with the IEEE 802.15.3a standard as described in the specifications. The AT91CAP9 Ultra Wideband Evaluation Kit[1] comprises of

- Two AT91CAP9A-DKs, composed of three associated boards (Motherboard, Mezzanine and 3.3V Memory Extension) to be jointly used in order to develop AT91CAP9 applications.
- A CAP9 UWB PHY Transmitter Board.
- A CAP9 UWB PHY Receiver Board.

Figure 3.1 shows the AT91CAP9A Development Kit. After setting up the AT91CAP9 UWB Evaluation Kit, it can be used to transmit and receive WiMedia Multiband OFDM signals, using wireless transmission links. Both the transmitter and receiver boards are connected to the extension slot beside the memory extension slot on their respective AT91CAP9A board.

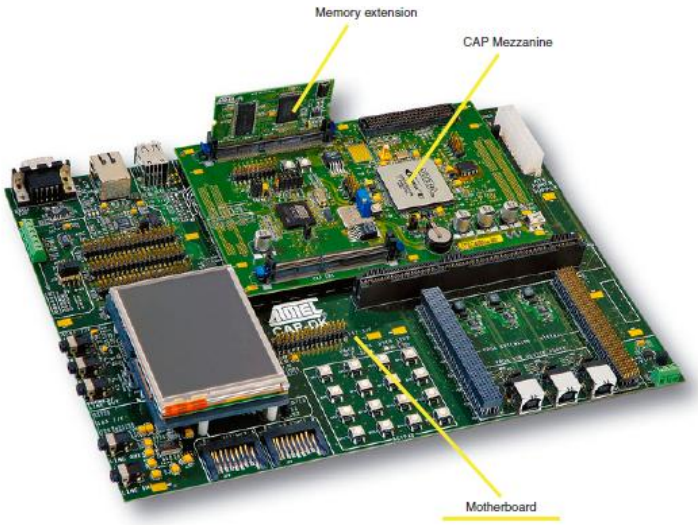


Figure 3.1 Overview of AT91CAP9A-DK Development Kit [1]

### 3.3 MB OFDM UWB Evaluation Setup

The AT91CAP9 UWB boards for both the transmitter and receiver were connected to the computer via USB blaster cables. This allows the evaluation kit to be configured with the desired parameters. For accurate measurement, similar parameters must be used for both the UWB transmitter and receiver boards. The UWB antenna used in this evaluation is a self-quasi-complementary antenna, designed and fabricated in QMUL (Queen Mary University of London) Antenna Laboratory [6]. Finally, a computer is used to monitor the data transmission quality of the system through the USB Blaster cable connected to the receiver board. Figure 3.2 gives the overview of the system setup and Figure 3.3-3.4 show the evaluation kit while measurement is taken. More information in how to operate the Kit is in the Appendix C.

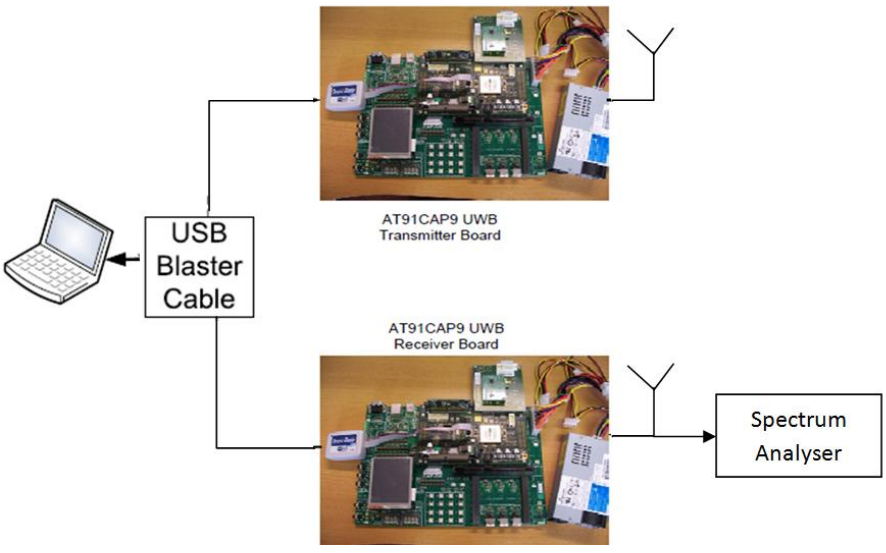


Figure 3.2 Measurement System setup diagram.

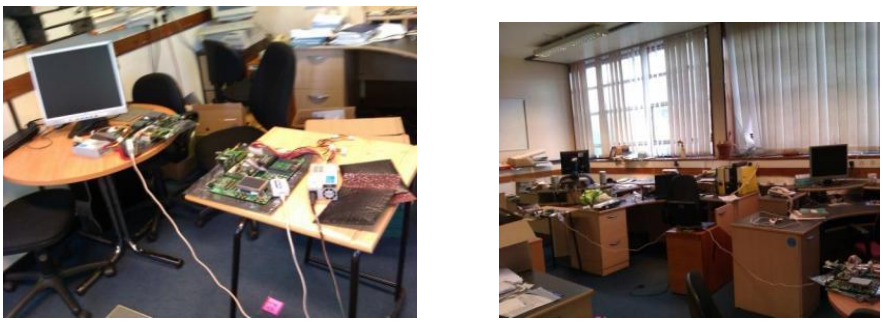

(a) (b)

Figure 3.3 Office environment used for UWB evaluation at 0.5 m and 3.0 m

Figure 3.4 Office environment used for UWB evaluation at 0.5 m and 3.0 m

The distance between the transmitter and the receiver is varied from 0.5 to 4.5m and the spectrum is measured using a spectrum analyser. Figure 3.5 shows the OFDM signal generated and transmitted from the UWB transmitter for hopping and non hopping scenario. It shows that the UWB Evaluation Kit (transmitter) complies with the regulation of the transmitted power for UWB transmission.

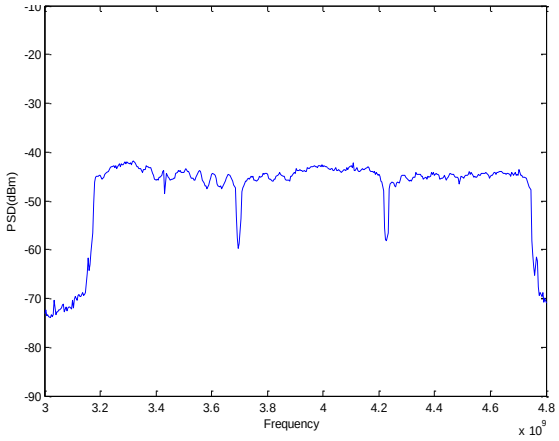


Figure 3.5 Transmit signal for band one from 3.168-4.752GHz

### 3.3.1 Packet Error Rate and distance

The packet error rate is calculated by sending 22,729 packets from the UWB transmitter to the UWB receiver. The number of packets received by the UWB receiver is subtracted from the total number of packets sent to get the number of packets that are lost. From the number of lost packets the packet error rate is calculated. Figures 3.6 - 3.8 show the variation of the packet error rate with increase in distance across channel 9 to 15 for different data rates with

a payload of 2048 bytes. The results illustrate that packets received in error increases with increase in the separating distance between the transmitter and receiver. The acceptable range for PER in UWB system is 8 %, this is define by the WideMedia MB OFDM UWB Specification. The variation in PER performances in the figure is to the different band hopping which depends on the logical channels. Logical channel 9 hops and logical channel 12 between the three bands; 3.168GHz to 3.696GHz, 3.696GHz to 4.224GHz, 4.224GHz to 4.752GHz in a sequential order. Logical channel 15 doesn't hop but remain on one band between 4.224GHz to 4.752GHz.

From Figure 3.6, it is evident that only the data rates of 53.3Mbps and 80Mbps have acceptable performance within a distance of 3m between the transmitter and receiver on channel 15. A data rate of 160 Mbps can be delivered over a distance of 2m with an acceptable packet error rate. It is therefore deduced that for a payload of 2048 with a throughput of 11.4Mbps, the UWB transmitter and receiver can support a maximum distance of 2 metres and the data rate of 160Mbps. A similar trend is observed for channels 12 and 9 (Figures 3.7-3.8.) A data rate of 53.5MBps can be used effectively over a distance of 4m with very low packet error rate on channel 9.

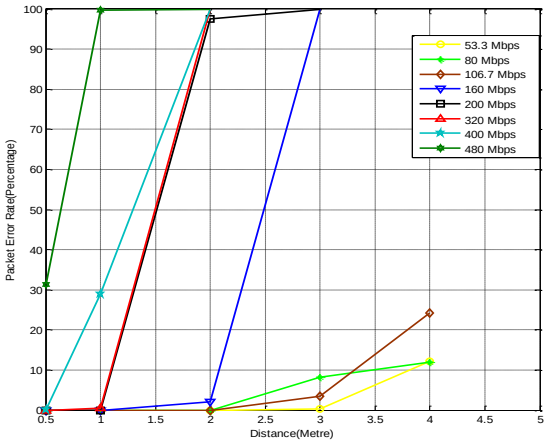


Figure 3.6 Channel 15

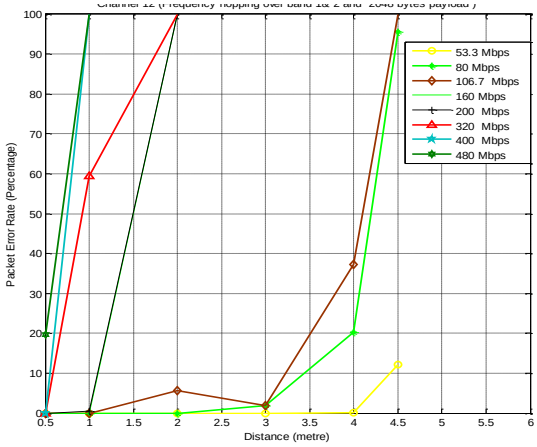


Figure 3.7 Channel 12

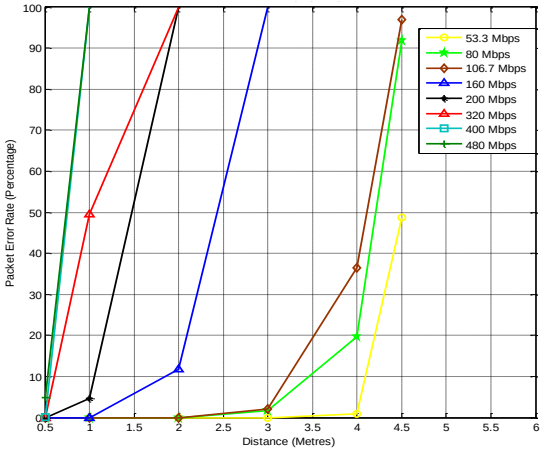


Figure 3.8 channel 9

### 3.3.2 Use of maximum allowable payload

Figures 3.9-3.11 depicts the UWB system performance using the maximum allowable payload of 4095 bytes. A very high packet error rate is observed in four channels for high data rate. The lower data rate of 53.3Mbps and 80Mbps have an acceptable packet error rate (PER) within two metres of distance between the transmitter and receiver. This is attributed to the power constraint of UWB transmit antenna that limits the spectral mask to be -41.3dBm/MHz. This reduces the Signal to Noise Ratio (SNR), decreasing the amount of information that can be transmitted per payload.

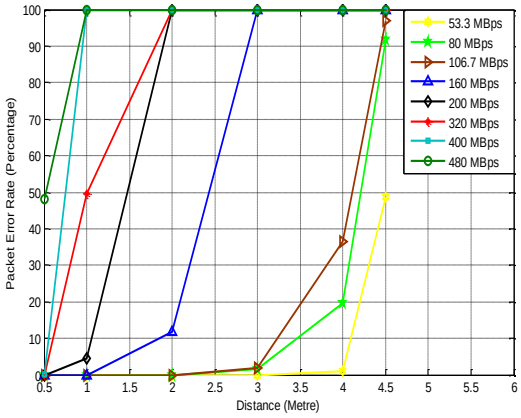


Figure 3.9 Channel 9 with 4095kb Payload

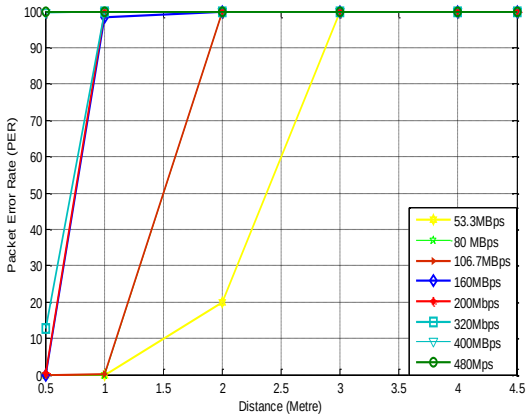


Figure 3.10 Channel 13 with 4095kb Payload

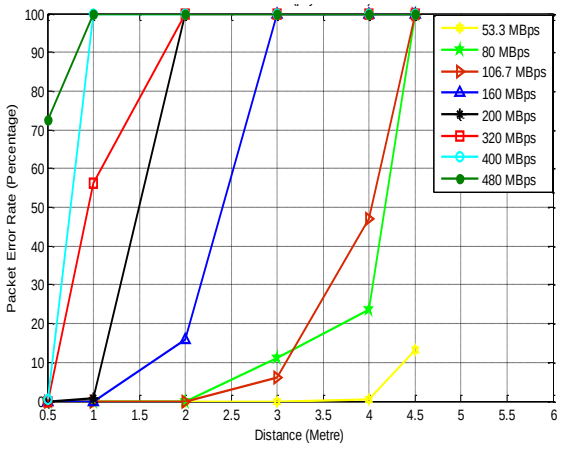


Figure 3.11 channel 15 with 4095 bytes Payload

### 3.3.3 Packet Error rate and payload

In this section, the UWB communication system performance is evaluated considering varying payload for different data rates and distances for each of the logical channels. The results shown in Figures 3.12-3.19 depicts that small payload have acceptable packet error rate. The acceptable range for PER in UWB system is 8 %. As the payload and/or distance increases, more packets are received in error which affects the throughput of the system. The logical channels cover different hopping sequence and frequency bandwidth. Detail of the hoping pattern and the frequency bandwidth is discussed in section C.2.2.

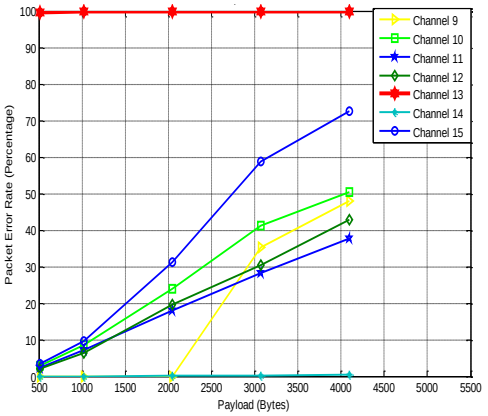


Figure 3.12 PER with 480Mbps at 0.5m

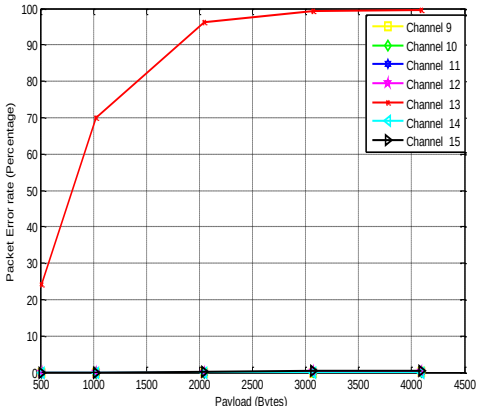


Figure 3.13 PER with 400Mbps at 0.5m

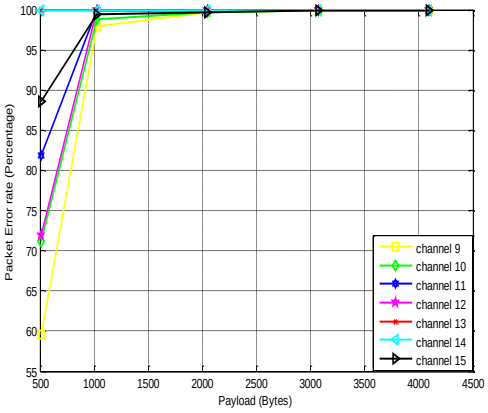


Figure 3.14 PER with 480Mbps at 1 m

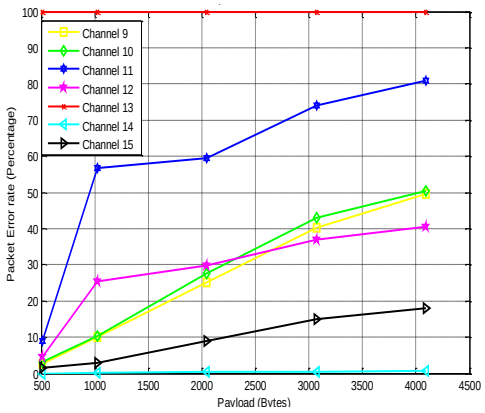


Figure 3.15 PER with 320Mbps at 1m

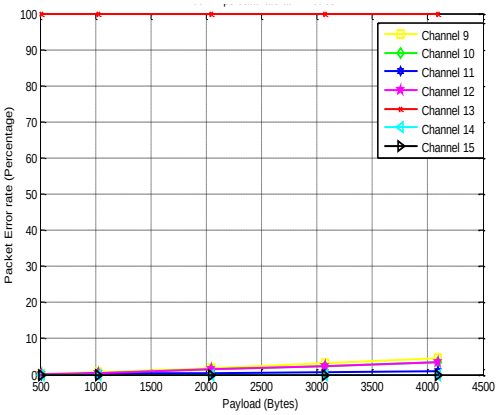


Figure 3.16 PER with 200Mbps at 1 m

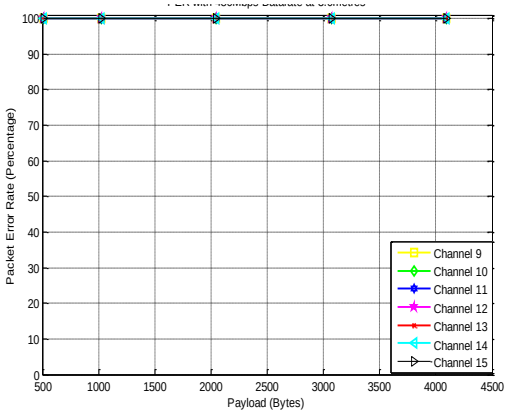


Figure 3.17 PER with 480Mbps at 3 m

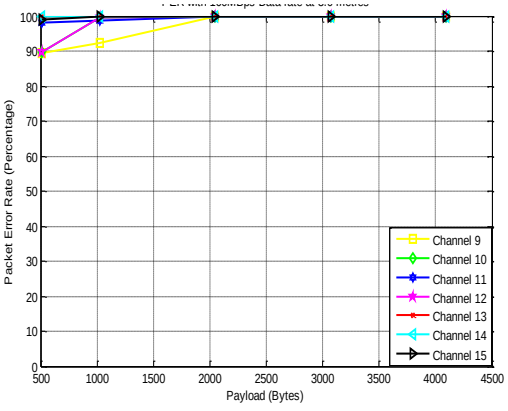


Figure 3.18 PER with 160Mbps at 3m

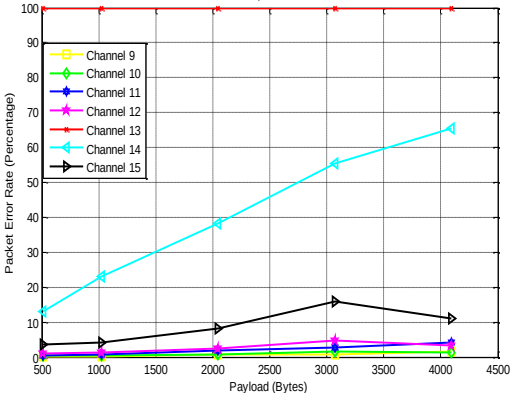


Figure 3.19 PER with 106.7 Mbps at 1m

From the figures above the PER increases as the Payload and this agrees with the theoretical behaviour as shown in Figure 3.20 in bits and Figure 3.21 in bytes. The PER can be calculated from the BER using the equation below

$$P_{PER} = 1 - (1 - P_{BER})^N \qquad 3.1$$

where $P_{PER}$ is the packet error rate, $P_{BER}$ is the bit error rate and N is the length of the payload. Increasing the payload increases in the total duration of the packet. In a time varying channel this will change the channel response when estimated using the training data.

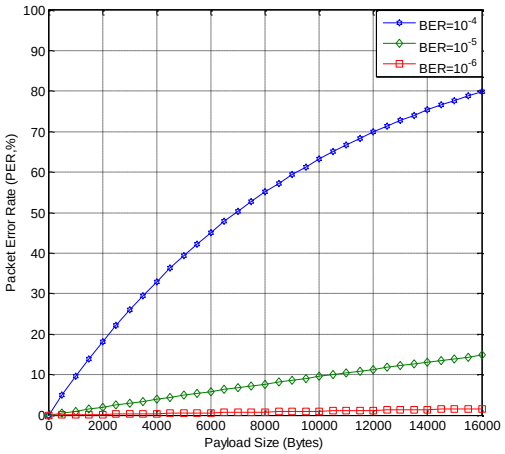


Figure 3.20 PER versus payload in bits

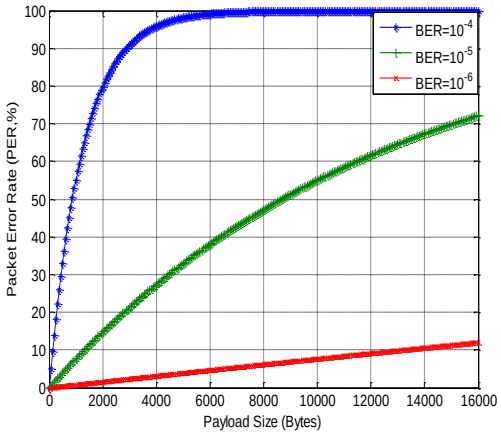


Figure 3.21 PER versus payload in bytes

In Figure 3.19 above, the advantages of frequency diversity can be seen. Channel 13, 14 and 15 have no frequency domain spreading, and occupy the frequency band between 3168MHz-3696MHz, 3696MHz-4224MHz and 4224MHz-4752MHz respectively. It can be noted that all the packets are received in error using channel 13. For channel 14, the error rate starts from 12% and increases with increasing payload. An acceptable PER performance is observed for channel 15 with different payloads. When the signal is spread by hoping over the 3 frequency bands occupied by channels 9 to 12, the packet error rate is dropped to 8% for the largest payload. Figure 3.24 shows the variation of SNR over distance with a range from 0.5 to 4.5m.

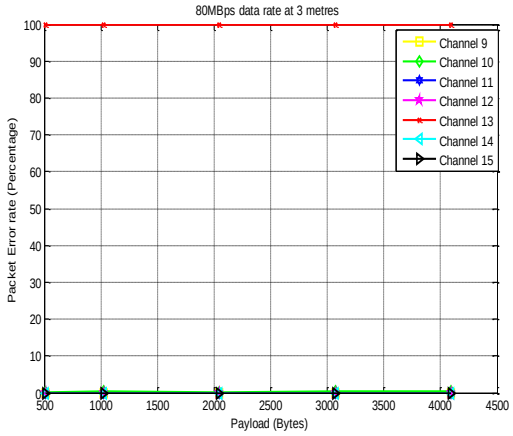


Figure 3.22 PER with 80Mbps at 3m

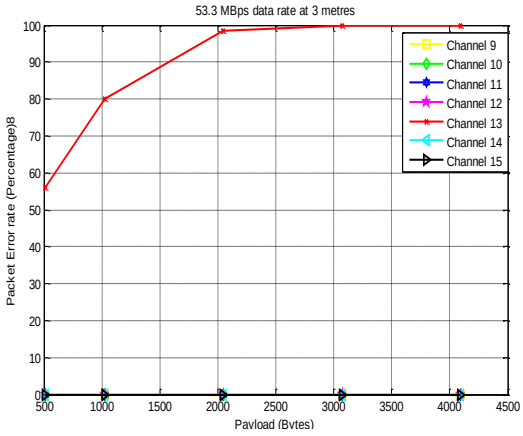


Figure 3.23 PER with 53.3Mbps at 3m

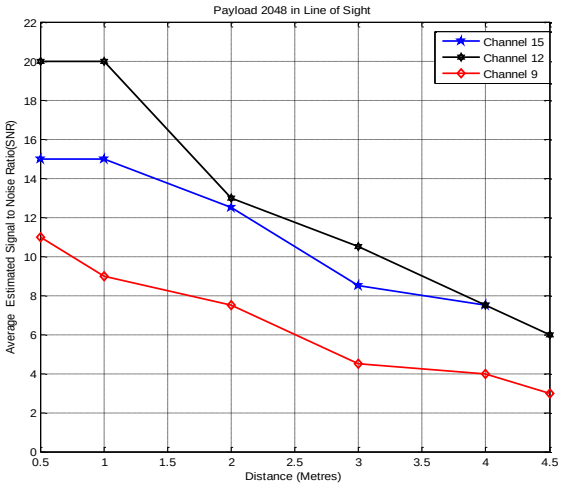


Figure 3.24 Estimated Signal to Noise ratio and distance

### 3.5 System Performance using a commercial MB-OFDM UWB product

A commercial UWB product, Q-waves Wireless USB Adapter, has been tested. The performance of the device under test (DUT) is determined by analysing its throughput over varied distance. The DUT is designed as a USB extender with the following specification

- WiMedia MB OFDM UWB certified PHY and MAC
- Operates within the WiMedia Band group 1 (3.168GHz to 4.752GHz)
- Supports the PHY channel 9 to 15
- Has an onboard Omni-directional Antenna
- Power consumption 1W @ 5VDC

The wireless adapter has a type-A male connector, providing an easy interface to any USB device. Since the device is a consumer product, flexibility of different parameters including data rate, SNR, coding etc are limited. Most of the parameters are either already fixed by the manufacturer or cannot be measured. The only available option, a throughput test, is used to evaluate the performance of the wireless USB. Figure 3.25 shows the throughput measurement and Figure 3.26a shows the throughput over a distance of 6 metres.

The throughput has been estimated by calculating the average transfer time of a large HD video signal sent over the wireless link. Based on the calculated throughput, the data rate used by the Q-waves' Wireless USB Adapter is determined by making comparison to the measured throughput over varying distances using the evaluation kit (Figure 3.26b). The calculated throughput of the Q-waves wireless USB agrees with the measured throughput when the data rate is 53Mbps with a payload of 4095bytes and when the data rate is 80Mbps with a payload of 512bytes.

While watching HD video clip over the wireless link, the video jitters every 5 seconds. This indicates that the current throughput is not sufficient for a HD video clip to be watched over

the wireless USB. It is shown that the required throughput for HD video clip to be watch effectively is 10Mbps which is higher than the throughput achieved by the Q-waves Wireless USB Adapter [3]. The measured throughput for 0.5m is 6.4Mbps, which is lower than the required throughput for a HD video to be played effectively.

Figure 3.25 Throughput measurement of Wireless USB(LOS and NLOS)

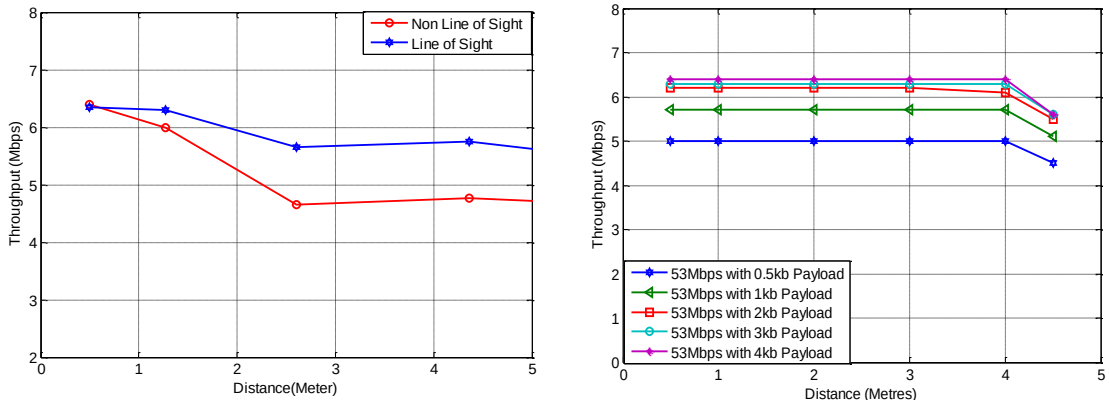


(a) (b)

Figure 3.26 (a) Throughput measurement of Q-waves wireless USB adapter. (b) Throughput measurement using the UWB Evaluation Kit (LOS)

### 3.6 Summary

This chapter provides evaluation and analysis of MB-OFDM UWB system. The performance is based on key parameters including payload, distance, SNR, data rate and throughput. A commercial available wireless USB adapter has been evaluated which shows that commercial UWB products still use low data rate for transmission. The results show that more research is needed to develop a system that can utilise the full potential of UWB technology.

**References**


1. AT91CAP9 UWB-EK Evaluation kit, User guide and technical documents 6457B–CAP–19-Jan-10
2. Embedded Design Handbook, Altera Co, San Jose, CA, 2001
3. PHY Specification: MB OFDM Physical Layer Specification, WiMedia Alliance, Inc, 2009
4. Key Performance Benefits of 802.11n, Cisco white paper, Cisco Systems, 2009 Inc.
5. A. Batra, "*Design of a Multiband OFDM System for realistic UWB Channel Environments*", IEEE Trans on Microwave Theory and Techniques Vol 52, No 9 Sept 2004
6. L. Guo et al, "*A Small Printed Quasi-Self-Complementary Antenna for Ultra wideband Systems* " IEEE Antennas and Wireless Propagation Letters, VOL. 8, 2009

# CHAPTER 4

## UWB CHANNEL MODELLING AND ADAPTIVE MODULATION

### 4.1 Introduction

Designing UWB communication system requires accurate knowledge and good understanding of UWB radio channel. This chapter will provide insight into the wave propagation mechanism in the UWB technology. This study will help to design a receiver with good performance.

### 4.2 UWB channel Model

Conventional Channel modelling for narrow band signals cannot be used for UWB due to its wideband nature. The narrow band channel modelling is based on the assumption that the signals undergo flat fading only. This reduces the complexity of the system. On the other hand, frequency selective fading is needed to be considered in case of UWB signals as the signal takes multiple paths to arrive at the receiver. In MB OFDM UWB, subchannels are considered to undergo flat fading.

Wireless signals interact with the physical environment in a complex manner. A transmitted signal can reach the receiver through a LOS path and several other paths, depending on the environment. The multiple paths occur due to three major propagation mechanisms, including reflection, scattering and diffraction. These phenomena causes the signal to undergo distortion and fading. The extent of the impact of these factors on the transmitted signal depends on the physical environment, as each environment has a unique channel impulse response. In a LOS environment, reflection tends to dominate over diffraction and scattering while in a NLOS environment, any of the phenomena can dominate depending on the nature of the environment and shadowing. Figure 4.1 shows a typical indoor scenario where the transmitted signal is reflected off objects in the room creating multiple copies of the signal at the receiver with different delays.

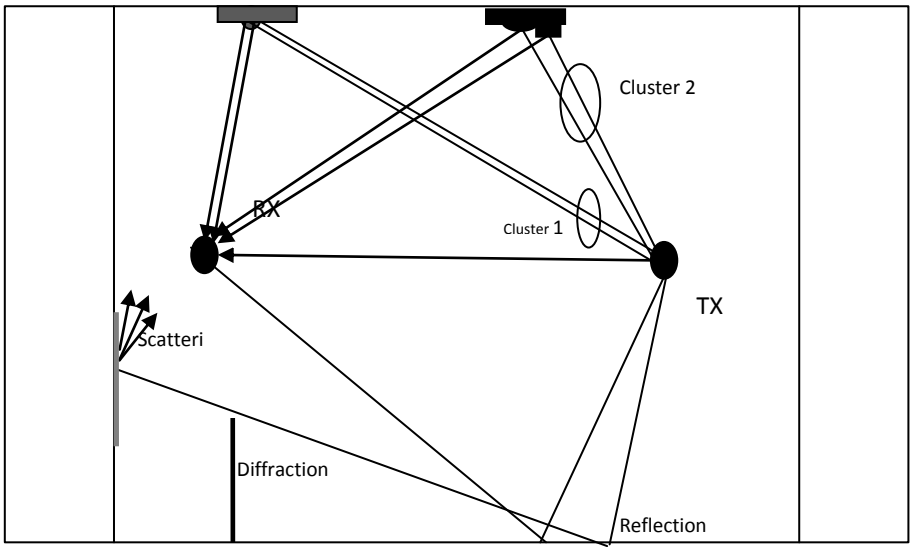


Figure 4.1 Signal propagation in an indoor scenario

Wireless propagation can be characterised according to the variability of the signal power level into either large scale channel characterisation or small scale channel characterisation.

### 4.3 Larger scale channel characterisation

#### 4.3.1 Path Loss

This is the ratio between the received power and the transmitted power. For a narrow band channel, the received power, $P_r$, can be modelled using Friis equation and it is expressed as

$$P_r = \frac{P_t G_t G_r \lambda^2}{(4\pi d)^2} \qquad 4.1$$

Where $P_t$ is the transmit signal power, $G_t$ and $G_r$ is the antenna gain for transmitter and receiver respectively, $d$ is the distance between the transmitter and receiver and $\lambda$ is the wavelength. The above equation shows that path loss depends both on a fixed frequency and the separation distance. In a narrow band, the dependency on frequency has a minimal effect and can be neglected but in UWB, it is significant due to the large bandwidth. Both the frequency and distance need to be accounted for while modelling path loss in a UWB channel. Hence, [1]

$$PL(f,d) = PL(f).PL(d) \qquad 4.2$$

where $PL(f)$ is frequency dependent path loss and $PL(d)$ is the distance dependent path loss.

#### 4.3.2 Distance dependent Path Loss

This is the attenuation of the median power as a function of distance and can be obtained from measured channel transfer function by frequency averaging over the measured bandwidth for each set of data at each received location. It is expressed in decibel as [4 ]

$$PL(d) = PL_0 + 10.n.log_{10}\left(\frac{d}{d_0}\right) + S\,; \quad d \geq d_0 \qquad 4.3$$

Where $PL(d)$ is the signal power received at a distance $d$, $PL_0$ is the free space path loss in the antenna far field at the reference $d_0$ and is computed based on the mid band frequency, S is the parameter for shadowing and n is the PL exponent. The path loss exponent is obtained by performing least square linear regression on the logarithmic scattered plot of the average received power versus the distance to equation above [1]

#### 4.3.3 Frequency dependent Path Loss

The Frequency dependent Path Loss can be modelled using two methods. In [2], it is modelled as

$$PL(f) \propto \exp(-\delta, f) \qquad 4.4$$

Where $\delta$ is the frequency decaying factor, with values between 1 and 1.4. The frequency decaying factor is determined as the average slope of the channel transfer function. Kunisch et al [3] have modelled the frequency dependent path loss as

$$PL(f) \propto f^{-\delta_2} \qquad 4.5$$

With the $\delta_2$ varying between 0.8 and 1.4.The IEEE 802.15.4a adopted equation 4.5 as the standard expression of modelling the frequency dependent path loss [4].

### 4.4 Shadowing

It is the slow variation of mean strength and is due to the movement of shadowing objects on the signal path. It varies randomly from one location to another and is modelled as a random Gaussian distribution with zero mean.

### 4.5 Small scale channel characterisation

#### 4.5.1 Clusters and Rays

Due to the wideband nature of UWB pulse, rays tend to arrive in clusters at the receiver. Clusters are defined as a group of rays with similar propagation characteristics and have similar interaction point in the line of propagation [19-20]. The number of these clusters can be modelled by a Poisson distribution. From [4], the average numbers of clusters are approximately between 3 -14 and 1-11 for LOS and NLOS scenarios, respectively. The clustering is a result of various structures located in the environment such as furniture, doors, windows, frames etc. When rays are reflected from an object, they tend to have slightly different arrival times. These multiple reflections may exist in the regions surrounding the receiver or the transmitter and are generally referred to as cluster. Figure 4.1 shows two

clusters with two rays each. The rays in each cluster have small inter arrival rate while the clusters have larger inter arrival rates as shown in Figure 4.2. For example, different parts of the same furniture piece can give rise to several rays which could be resolved by the receiver. The IEEE 802.153a standard body selected this model in order to reflect the unique characteristics of the channel [16].

The number of rays per cluster is modelled using PDF f(k) in [5] and k generally increase from LOS to NLOS scenarios. Some of the factors that affect the number of multipath are

a) Distance between the transmitter and receiver
b) The resolution of the parameter estimation technique
c) Location of the transmitter or receiver
d) Physical layout of the environment
e) The dynamic range of the measuring system

### 4.5.2 Arrival time of rays and cluster

The distribution of the arrival times of clusters and rays can be modelled by two Poisson distribution. The cluster inter- arrival times and the rays intra-arrival times are described by two independent exponential PDF as follows [4]

$$P(T_l|T_{l-1}) = \Lambda \exp[-\Lambda(T_l - T_{l-1})], \;\; l > 0 \qquad 4.6$$

$$P\left(\tau_{k,l}\middle|\tau_{k-1,l}\right) = \gamma \exp\left[-\gamma\left(\tau_{k,l} - \tau_{k-1,l}\right)\right], \;\; k > 0 \qquad 4.7$$

Where $\Lambda$ is the mean cluster arrival rate,$\gamma$ is the mean ray arrival rate and $\gamma \gg \Lambda$ i.e. each cluster has many rays.

### 4.5.3 Power decaying Phenomenon in Cluster and Rays

The average power of the rays per cluster is assumed to decay exponentially and is given by [4 ]

$$a^2{}_{k,l} = a^2{}_{0,0} e^{-T/\Gamma} e^{-\tau_{k,l}/\gamma} \qquad 4.8$$

Where $a^2{}_{0,0}$ is the expected power of the first arriving ray, $\Gamma$ is the decay exponent of the rays within a cluster. The expected power of the rays per cluster decays faster than the first ray of the next cluster. Figure 4.2 shows an illustration of the power decay phenomenon.

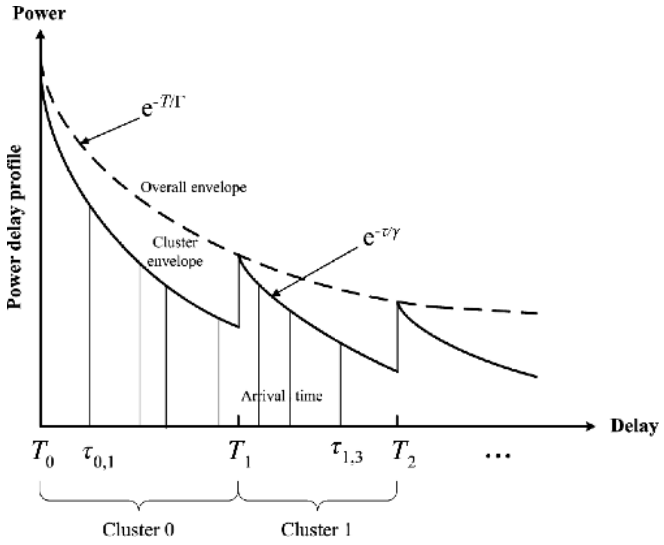


Figure 4.2 Figure showing pulses arriving in clusters [6]

### 4.6 Mean excess delay and RMS delay spread

RMS delay spread is one of the most important characteristics of fading because it determines the ISI between two signals sent in sequence. If the transmit rate is high and the signal spreads in a large area then subsequent signals will interfere and distort the previous signal. The RMS delay spread is the square root of the second central moment of power delay profile (PDP) and express as [7]

$$\tau_{rms} = \sqrt{\tau_m^2 - (\tau_m)^2} \qquad 4.9$$

And ${\tau_m}^2$is expressed as

$${\tau_m}^2 = \frac{\sum_k P(\tau_k)\tau^2{}_k}{\sum_k P(\tau_k)} \qquad 4.10$$

Where $\tau_m$ is the mean excess delay and is defined as the weight mean of the PDP or the first moment PDP expressed as

$$\tau_m = \frac{\sum_k P(\tau_k)\tau_k}{\sum_k P(\tau_k)} \qquad 4.11$$

### 4.7 SISO Channel

In a single input and single output channel, both the transmitter and receiver have one antenna each thereby having a single channel between the two antennas. Figure 4.3 illustrate the behaviour of the SISO channel

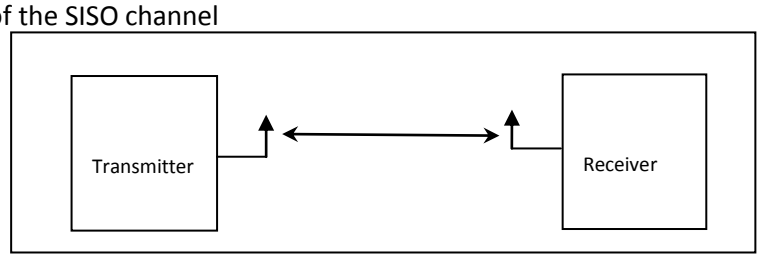


Figure 4.3 Single out single input channel

Single output single input channel model can be described as [1]

$$h(t) = \sum_{l=0}^{l-1} \sum_{k=0}^{k-1} \alpha_{k,l} \delta(t - T_1 - \tau_{k,l}) \qquad 4.12$$

Where $\alpha_{k,l}$ is the multipath gain coefficient, *k* and *l* refer to the cluster and rays within cluster, respectively. $\tau_{k,l}$ is the delay of the $k_{th}$ multipath component relative to $l_{th}$ cluster arrival time $T_1$, $T_1$ is the delay of the $l_{th}$ cluster. In a time invariant environment the relationship between the transmit and receive signal can be expressed as

$$y(t) = h(t)x(t) + \eta(t) \qquad 4.13$$

Where $x(t)$ is the transmit signal, $y(t)$ is the receive signal and $\eta(t)$ is the noise.

**4.8 SIMO Channel**

For a single input multiple output (SIMO), a single antenna is used for transmission while multiple receive antennas are used to receive the signal. The multiple received signals can then be combined using any combining technique. Figure 4.4 describes the behaviour of a SIMO channel.

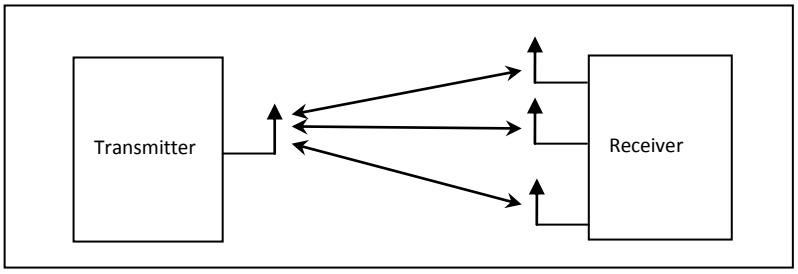


Figure 4.4 Single out Multiple input channel

A SIMO channel, can be decomposed into a number of SISO channels with each receive antenna forming a pair with the transmit antenna. This can be described by a 1x $n_r$ CIR matrix where $n_r$ is the number of the receive antennas. The channel modelling can be done based on the following consideration

1. When the receive antennas are closely packed, much less than the wavelength of the centre frequency, they will experience similar clustering. This can be expressed as [1]

$$H(t) = \sum_{l=0}^{l-1} \sum_{k=0}^{k-1} A_{k,l} \delta(t - T_k - \tau_{k,l}) \qquad 4.14$$

Where $H(t) = \begin{bmatrix} h_1(t) \\ \vdots \\ h_{n_n}(t) \end{bmatrix}$, $A_{k,l} = \begin{bmatrix} \alpha^1{}_{k,l} \\ \vdots \\ \alpha^{n_r}{}_{k,l} \end{bmatrix}$

2. If the receive antenna are sufficiently far, greater than the wavelength of the centre frequency, any two transmit-receive antenna pair will experience different clustering structure. Therefore the channel can be modelled as follows

$$H(t)=\begin{bmatrix} h_1(t) \\ \vdots \\ h_{n_n}(t) \end{bmatrix}$$

Where $h_1(t)$ is the CIR of channel from the transmit antenna to the 1st received antenna is expressed as

$$h_{i_1}(t)=\sum_{k=1}^{k}\sum_{l=1}^{L}\alpha_{k,l}^{i_1}\ \delta(t-T_k^{\ i_1}-\tau_{k,l}^{i_1}) \qquad 4.15$$

Where $\alpha_{k,l}^{i_1}$, $T_k^{\ i_1}$, $\tau_{k,l}^{i_1}$ have the same meaning as the SISO channel model but specifically to the channel from the transmit to the $i_{1th}$ receive antenna. In this scenario it assume that all the parameters ( $\alpha_{k,l}^{i_1}$, k=1....K, l=1....L, $i_1$=1..$N_r$,$i_2$=1...$N_t$ ) are independent of each other . The input –output relationship using a transfer function can be describe as

$$Y(t)=\begin{bmatrix} y_1(t) \\ \vdots \\ y_{n_n}(t) \end{bmatrix}=\begin{bmatrix} h_1(t) \\ \vdots \\ h_{n_n}(t) \end{bmatrix}x(t)+n\begin{bmatrix} n_1(t) \\ \vdots \\ n_{n_n}(t) \end{bmatrix} \qquad 4.16$$

Where $y_i(t)$, $\eta_i(t)$ and $h_i(t)$ is the receive signal, noise and channel fading respectively on the i[th] antenna.

**4.9 MIMO channel**

In multiple input and multiple output channel, multiple antennas are used at both the transmitting and receiving sides. Figure 4.5 describes the behaviour of a MIMO channel with each pair of transmit and receive antenna having different channel

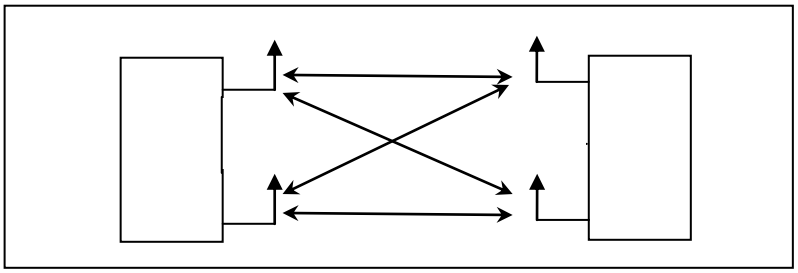

Figure 4.5 MIMO channel

In a MIMO channel, the system is described by a channel Impulse Response (CIR) matrix. The CIR matrix is an $N_r$ x $N_t$ matrix where $N_r$ represents the number of the receiving antennas and $N_t$ represents the number of the transmitting antennas. The MIMO channel can be modelled under three scenarios

1. If the transmit antennas and receive antennas are sufficiently close then it's assumed that the transmit–receive pairs will experience similar clustering structures and is modelled by [1]

$$H(t) = \sum_{l=0}^{l-1} \sum_{k=0}^{k-1} A_{k,l}\,\delta(t - T_k - \tau_{k,l}) \qquad 4.19$$

Where $H(t)$ is the system CIR matrix, $A_{k,l}$ is amplitude fading matrix, which describes the path fading in amplitude for $k_{th}$ cluster and $l_{th}$ ray. $\tau_{k,l}$ is delay of $l_{th}$ multipath component relative to $k_{th}$ cluster arrival time, $T_1$ is delay of the $k_{th}$ cluster. The entry of $A_{k,l}$ is denoted by $A^{k,l}_{i_1,i_2}$ and is the tap gain from the $i_{2th}$ transmitting antenna to the $i_{1th}$ receiving antenna for the $k_{th}$ cluster and $l_{th}$ ray.

2. If the transmit antennas and the receive antennas are sufficiently far, any two transmit-receive antenna pair will experience different clustering structure. Therefore the channel can be modelled as follows

$$H(t) = \begin{bmatrix} h_{11}(t) & h_{12}(t) & \dots & h_{1Nt}(t) \\ h_{21}(t) & \ddots & \ddots & \vdots \\ \vdots & \ddots & \ddots & \vdots \\ h_{Nr1}(t) & h_{Nr2}(t) & \dots & h_{Nr,Nt}(t) \end{bmatrix}$$

Where $h_{11}(t)$ is the CIR of channel from the 1st transmit antenna to the 1st receive antenna and is expressed as

$$h_{i_1,i_2}(t) = \sum_{k=1}^{k} \sum_{l=1}^{L} \alpha_{k,l}^{i_1,i_2}\ \delta(t - T_k^{\,i_1,i_2} - \tau_{k,l}^{i_1,i_2}) \qquad 4.20$$

Where $\alpha_{k,l}^{i_1,i_2}$, $T_k^{\,i_1,i_2}$, $\tau_{k,l}^{i_1,i_2}$ have the same meaning as the SISO channel model but specifically to channel from the $i_{2th}$ transmit to the $i_{1th}$ receive antenna. In this scenario it assume that all the parameters ( $\alpha_{k,l}^{i_1,i_2}$, k=1....K, l=1....L, $i_1$=1..Nr,$i_2$=1...$N_t$ ) are independent on each other .

3. If the scattering is rich with many objects that scatter the rays, the channel model can be described as

$$H(t) = \sum_{l=0}^{l-1} A_i\,\delta(t - (l-1)\Delta\tau) \qquad 4.21$$

Where $\Delta\tau$ is the sampling interval, $A_i$ =1.....L are the amplitude fading matrices. Considering a single user communication model and a point-to-point link where the transmitter has $N_t$ transmitting antennas and the receiver has Nr receiving antennas, the model is expressed as

$$y(n) = H(n)x(n) + \eta(x) \qquad 4.22$$

Where $x(n) = [x_1(n).....x_{Nt}(n)]$ is the received signal vector $N_t$ x 1, $y(n) = [y_1(n).....y_{Nr}(n)]$ is the received signal vector Nr x 1 and the channel transfer matrix with $N_r$ X $N_t$ is expresses as

$$H(n) = \begin{bmatrix} h_{1,1}(n), h_{1,2}(n),.....h_{1,N}(n) \\ h_{2,1}(n), h_{2,2}(n),.....h_{2,N}(n) \\ \vdots \\ h_{Nr,1}(n), h_{Nr,2}(n),.....h_{Nr,N}(n) \end{bmatrix}$$

**4.10 Channel Measurement**

The availability of a realistic and suitable channel model which reflects a typical multipath environment is an essential prerequisite for the assessment of UWB communication system. In an indoor scenario, wave propagation is complicated due to the effect of reflection, refraction and absorption. This could lead to severe fading due to the multipath. Different multipaths have different path lengths, which makes a single pulse radiated from the transmitter to be received as a train of pulses by the receiver.

Modelling a channel through measurement gives a realistic view of the channel in a particular environment. The channel characterisation is achieved by performing measurements either in the frequency domain or time domain. The time invariant radio channel measurement can be done using a Vector Network Analyser (VNA) to obtain the channel transfer function in the frequency domain. The received signal is modelled as follows

$$y(t) = x(t)h(t) + n(t) \qquad 4.23$$

Where *y* is received signal, h is channel estimate, n is additive white Gaussian noise with zero mean and *x* is transmitted signal. The characteristics of UWB channels can be measured in the time domain by measuring the impulse response h(t) or the frequency domain by measuring the transfer function H(f). In this study, the magnitude and phase of the $S_{21}$ is measured in the frequency domain between 3.0 to 11 GHz using VNA. The pre-processing techniques describe in [8]-[11] are employed in this work. The $S_{21}$ samples are directly proportional to the channel transfer function as shown in Equation 4.24**.**

$$S_{21}(f) \propto H(f) = \frac{Rx(f)}{Tx(f)} \qquad 4.24$$

Where *f* signifies the frequency domain, *Tx* is the transmitted signal and *Rx* is the received signal. For this study, only the required $S_{21}$ measurement for band group one, (3.168 to 4.752

GHz) are used for all the scenarios. Both the magnitude and the phase of the $S_{21}$ were taken and transformed to the complex domain by using the following equation

$$H(f) = |H(f)|e^{j\omega} \qquad 4.25$$

Where *f* signifies the frequency domain, $|H(f)|$ is the magnitude of the $S_{21}$ and $\omega$ is the phase. The complex transfer function is then mirrored to the negative frequencies by adding the conjugate reflection of the positive spectrum. This will lead to the complete desired real spectrum expressed as

$$H(f) = H_{VNA}(f) + H_{VNA}{}^{*}(-f) \qquad 4.26$$

Where $H_{VNA}{}^{*}(-f)$ is the complex conjugate of $H_{VNA}(f)$ . The transfer function is transformed to the time domain by employing the Inverse Fast Fourier Transform (IFFT) as shown in the following equation

$$h(t) = IFFT\ \ [H(f)] \qquad 4.27$$

The channel impulse response is interpolated to conform to the sampling time of the system model, which is 315.66ps and is then translated to baseband from pass band using the equation [9].

$$h_b[n] = h_p[n].e^{j*2\pi*f_c[n]T_s} \qquad 4.28$$

Where $h_p$ and $h_b$ are the channel impulse responses of the pass band and the baseband respectively, the centre frequency $f_c$ = 3960MHz for band group one and the sampling time of the system $T_s$ =315.66ps. The start of the process is truncated to remove any delay introduced in the pre-processes and the baseband impulse response is normalized before putting it into the system model. Due to the normalisation process, information regarding the antenna gain and antenna path loss is lost.

### 4.11 Adaptive Modulation

Wireless channel generally experiences fading, which affects the capacity and performance of the system. In narrowband systems, fading is generally assumed to be flat while in wideband system such as MB-OFDM UWB, the fading is selective across the entire band and each subchannel experiences different degree of flat fading.

In most wireless systems, an average SNR is estimated and used to determine the modulation scheme to be used. This approach doesn't always utilise the channel effectively as some subchannels will have higher SNR than others making it possible to send more information through such subchannel. In order to utilise the wireless channel effectively, an adaptive modulation technique is proposed to improve the BER performance in a frequency selective fading channel. The modulating bits are varied across the sub-channels depending on the

signal to noise ratio (SNR). Sub-channels experiencing severe fading employ lower or no bit-loading while sub-channels with little or no fading utilise higher bit-loading to maintain a constant system data rate. The data subcarrier can use any of the following modulation technique: BPSK, QPSK, 8PSK and 16 PSK. When considering the use of bit adaptive loading, each subcarrier can be differently loaded depending on the SNR of the carrier to exploit the channel more efficiently.

The Matlab template for MB-OFDM UWB system model proposed by Mark Clark et al [10] is modified to make the modulation adaptive instead of using only QPSK, while maintaining the data rate at 200Mbps. The MB OFDM UWB system hops between the three sub-bands in a special pattern as specified in [3]. In this model, the frequency hopping is reduced to only one sub-band to make the implementation of the adaptive modulation simple. The adaptive modulation is performed over the sub-band two, although any of the sub bands in the group one can be used since frequency hopping is not implemented. Sub band two lies between 3696MHz and 4224MHz with a centre frequency of 3960MHz. Figure 4.6 shows the block diagram of the adaptive UWB system used on this model. The UWB antenna used in this model is a small printed quasi-self-complementary antenna shown in Figure 4.8**.** This antenna has been which was designed and fabricated in Antenna Measurement Laboratory at Queen Mary University of London (QMUL). It offers an ultra wide impedance bandwidth with satisfactory radiation properties [11].

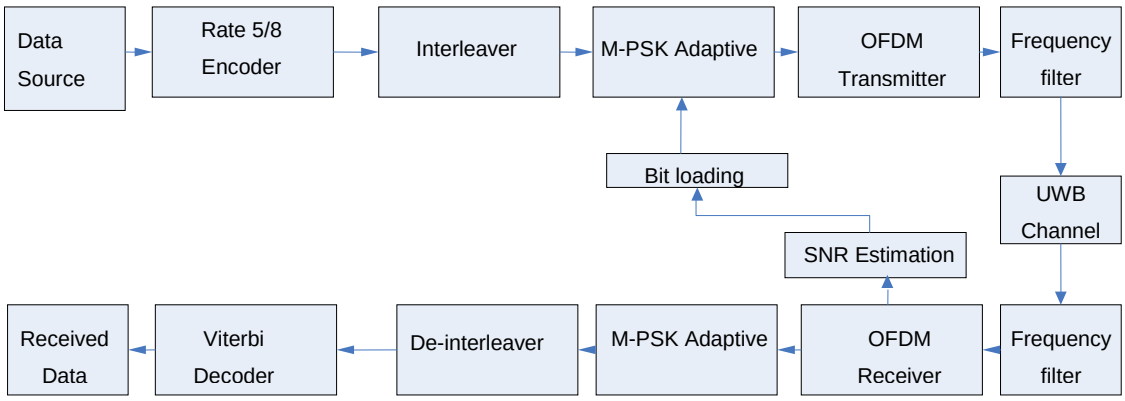


Figure 4.6 Block Diagram of Adaptive MB OFDM UWB System

The antenna dimensions include a length and width of the substrate of L=16mm and W=25mm, the height and width of the triangular notch is $L_2$ =4.8 and $W_s$=6mm, height and width of the microstrip line is $L_1$=8.9 and $W_f$=2.4mm and the thickness of the substrate is 1.6mm. The $S_{21}$ measurements are carried out using the VNA considering two antenna configurations namely, side-by-side and face-to-face orientation. For the side-by-side

orientation, the two antennas are placed in the Y-direction with the half-circular disc of each antenna pointing towards the other antenna. For the face-to-face orientation, the two antennas are placed with the half-circular disc facing each other in the X-direction. Figure 4.7 shows the two antenna orientation and the geometry of the quasi-self-complementary antenna used. Figure 4.9 shows the layout of the room where the measurements were carried out.

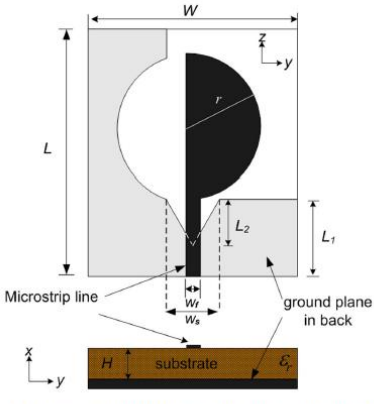


Figure 4.7 Antenna dimensions

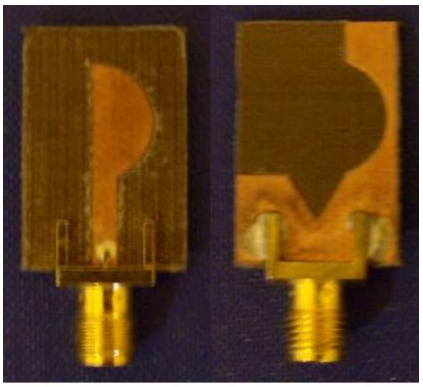


Figure 4.8 Prototype of the antenna

TABLE 4.1 Setup Measurement Parameters

| **Parameter** | **Value** |
|---|---|
| Frequency range | 3-11GHz |
| Number of Frequency points | 6000 |
| Tx Antenna height | 0.86m |
| Rx Antenna Height | 0.86m |
| Distance between antennas | 1 and 3 meters |

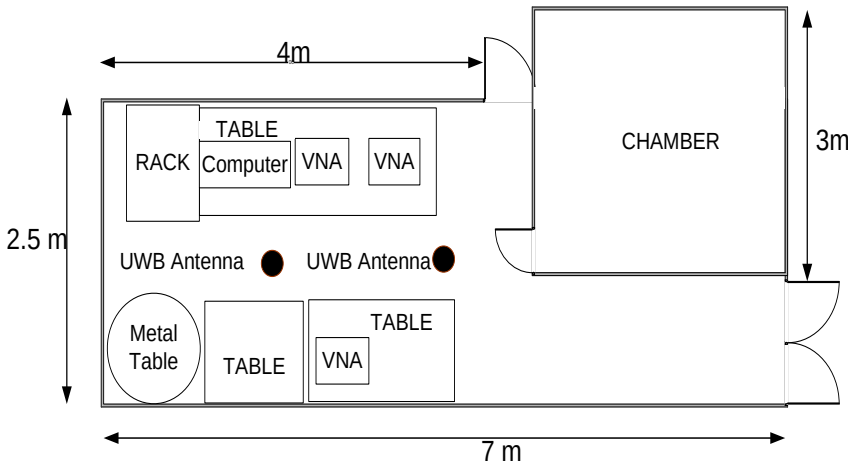


Figure 4.9 Room layout for the measurement

TABLE 4.2 Channel scenarios

| Orientation | Sight | Distance (m) |
|---|---|---|
| side by side | LOS | 1 and 3 |
| side by side | NLOS | 1 and 3 |
| face to face | LOS | 1 and 3 |
| face to face | NLOS | 1 and 3 |

This system uses BPSK, QPSK, 8PSK and 16PSK modulation schemes for the adaptive modulation. The choice of the modulation scheme used in each sub channel is based on the signal to noise ratio of each of the sub channel. Training data is used for channel estimation, which is known by both the transmitter and the receiver. QPSK modulation is used for training data. The SNR per sub carrier is expressed as [14]

$$SNR(i,\ j) = \frac{[H(i,\ j)]^2.[X(i,\ j)]^2}{\varepsilon(i,\ j)^2} \qquad 4.29$$

Where $SNR(i,\ j)$ is the signal to noise ratio of the $i_{th}$ sub channel in the $j_{th}$ OFDM symbol, $H(i,\ j)$ is the channel coefficient of the $i_{th}$ sub channel in the $j_{th}$ OFDM symbol, $\varepsilon(i,\ j)^2$ is the noise variance per subcarrier, $X(i,\ j)$ is the transmitted symbol of the $i_{th}$ sub channel in the $j_{th}$ OFDM symbol [15]. The absolute square of the transmitted symbol is one since QPSK modulation is used. Therefore, Equation 4.29 can be expressed as

$$SNR(i,\ j) = \frac{[H(i,\ j)]^2}{\varepsilon(i,\ j)^2} \qquad 4.30$$

Rearranging Equation 4.30 in decibels

$$SNR(i,\ j)(dB) = [H(i,\ j)]^2\,(dB) - \varepsilon(i,\ j)^2\,(dB) \qquad 4.31$$

In obtaining the channel coefficient, the least square channel estimator is used. This is expressed as [16]

$$H(i,\ j) = \frac{Y(i,\ j)}{X(i,\ j)} \qquad 4.33$$

Where $Y(i,\ j)$ is the received symbol of $i_{th}$ sub channel in the $j_{th}$ OFDM symbol without noise. The channel coefficient of each sub-channel is estimated in the channel with no white noise. The noise variance per sub carrier is estimated using the following equation [17]

$$\varepsilon^2 = \left|\hat{Y}(i,\ j) - X(i,\ j).H(i,\ j)\right|^2 \qquad 4.34$$

Where $\hat{Y}(i,\ j)$ is the received symbol with noise of the $i_{th}$ sub channel in the $j_{th}$ OFDM symbol. The SNR for each sub carrier is estimated and the most efficient subcarrier modulation that offers a BER performance of less than $10^{-4}$ is selected. The average power across all the sub carriers is assumed to be the same. The threshold used to determine the modulation rate is based on the theoretical BER performance of BPSK, QPSK, 8PSK and 16PSK modulation in white

noise. To ensure that the data rate remains constant, the summation of the data modulated across all the sub-channels must always be 200 bits. The channel is adjusted using a channel adjustment algorithm. The receiver receives the transmitted OFDM symbol, which includes the training data, and then calculates the channel coefficient of each sub channel from the training data. The signal to noise (SNR) is calculated from channel coefficient and the noise. Each sub channel's SNR is compared to the threshold value and the most suitable modulation index is selected for the sub channel. Table 4.3 shows the threshold range and the corresponding modulation index.

TABLE 4.3 Modulation Index Assignments

| **Threshold range (dB)** | **Modulation** | **Index** |
|---|---|---|
| $SNR_i \leq 5$ | Skip Channel | 0 |
| $5 \leq SNR_i \leq 8$ | BPSK | 1 |
| $8 \leq SNR_i \leq 12$ | QPSK | 2 |
| $12 \leq SNR_i \leq 17$ | 8PSK | 3 |
| $SNR_i \geq 17$ | 16PSK | 4 |

### 4.12 Simulink Modulation Block limitation

Unavailability of some required blocks such as adaptive modulation block in simulink, lead to a development of new blocks in simulink to implement the ideas of the adaptive system. This was made possible with a function called Matlab embedded function which is used in developing user defined block and to incorporate it into the simulink model. The created blocks are modulation block, demodulation block, SNR block, channel adjustment block, threshold and modulation index block.

#### 4.12.1 Modulation block

A modulation block is designed to modulate the incoming data either by using BPSK, QPSK, 8PSK or 16PSK on a particular sub carrier depending on the modulation index from the feedback channel. With a modulation index of zero, no data is modulated on the sub carrier which means the sub channel is skipped and this is due to severe fading on the sub channel. Figure 4.10 shows the structure of the modulation block. Sample and frame conversion blocks are used because the adaptive modulation is sample based while the interleaver and OFDM blocks are frame based. The modulation block has to be sample based because the data bits are modulated differently across the frame. Please refer to the Appendix B for the code of the block.

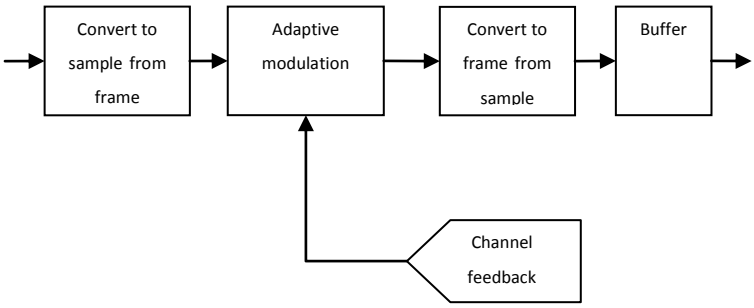


Figure 4.10 Adaptive modulation block

### 4.12.2 Demodulation Block

A demodulation block is designed to demodulate the signal in the same format that was used in modulating the data by the transmitter. The demodulation block receives the modulation index for each subcarrier and demodulates the signal base on the modulation index which could be BPSK, QPSK, 8PSK and 16PSK. However, when the demodulation block receives a modulation index of zero, no data is demodulated over the specified sub carrier which means the sub carrier is skipped. Figure 4.11 illustrate the structure of the demodulation block .

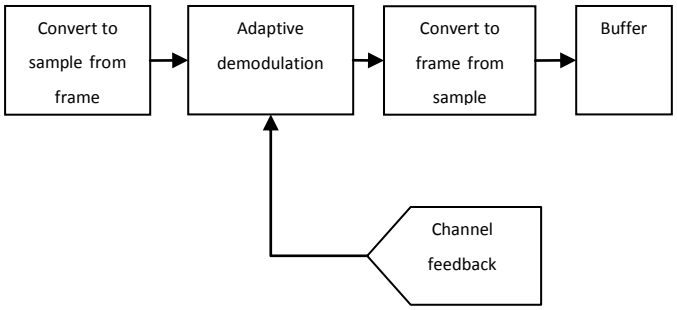


Figure 4.11 Adaptive demodulation block

### 4.12.3 Channel Adjustment Block

The channel adjustment block is designed to ensure that the total number of modulating bit is always 200. This is achieved by summing and readjusting the modulation index of the sub channels when the total is not equal to 200. When the total number of bits is more than 200 after assigning the modulation, the block reduces the highest modulation index. However, when the total number of bits is less than 200 after assigning the modulation index, the lowest modulation index is increased by one. Figure 4.12 describes the block diagram showing the channel estimation block, SNR calculation block, threshold and channel readjustment block. Please refer to the Appendix B for the code of the block

### 4.12.4 Threshold Block

The threshold block is designed to compare the signal to noise ratio of each of the sub channel and to assign a modulation index to the sub channel base on a set threshold. This will ensure that only the appropriate number of bits is modulated on a particular sub carrier.

### 4.12.5 SNR Block

This calculates the SNR of each of the data sub channel based on the fading and the AGWN (Addictive Gaussian White Noise). The block uses the channel estimate from the channel estimation block to compute the SNR.

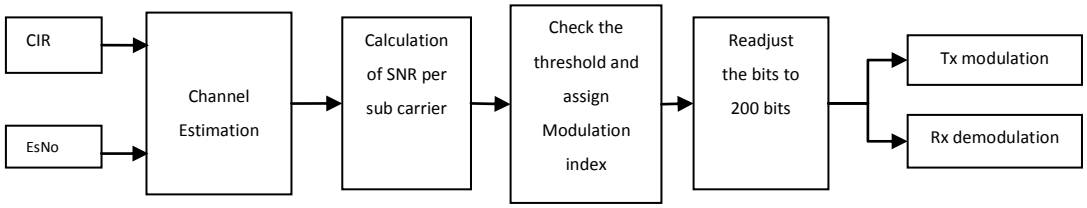


Figure 4.12 Channel estimation, SNR calculation block, threshold and channel readjustment

The system behaves as a non-adaptive system at lower SNR because 8PSK and 16PSK modulation will be only effective from 12dB Es/No and above. This makes the system to use only QPSK modulation on all the sub-channels at lower SNR. Figures 4.13 to 4.16 show how the modulation index is assigned to each of the sub-channel in the four considered cases. The four channel scenarios that are considered in this study including side-by-side antenna configuration placed 1m apart with LOS, side-by-side placed 3m apart with LOS, face-to-face having 1m separation with NLOS and face-to-face having 3m separation with NLOS. For brevity, only four samples are shown. The SNR of each channel is overlaid on the modulation indexes to give more clarity on how the channel fading affects the bit allocation of each sub channel. Due to the frequency selective fading, the total allocated bits are not always up to 200. The channel algorithm is used to adjust the total sum of the bits to 200 bits, ensuring that the data rate is the same.

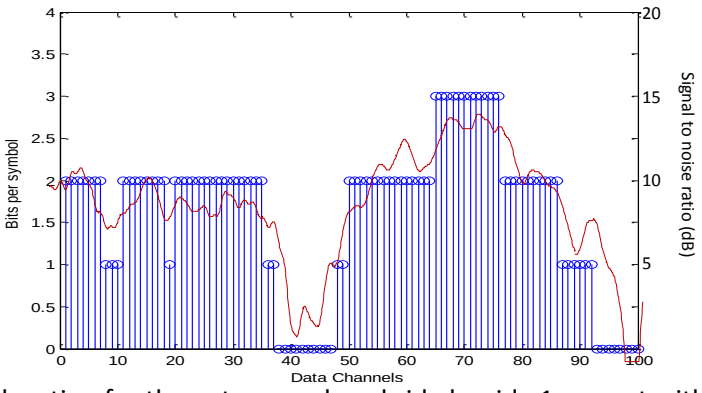


Figure 4.13 Bits allocation for the antennas placed side by side 1m apart with LOS at 10dB

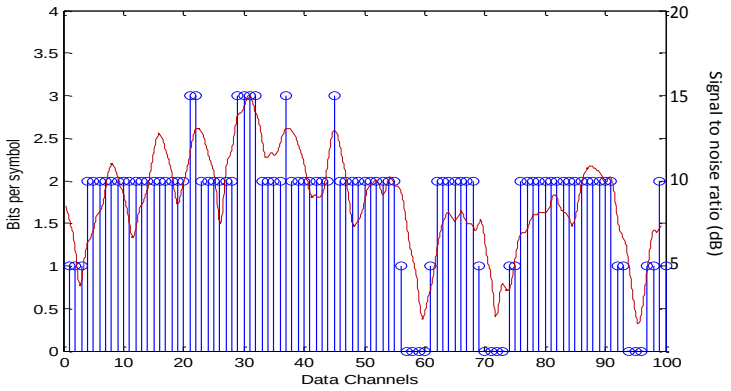


Figure 4.14 Bits allocation for the antennas placed side by side 3m apart with NLOS at 10dB

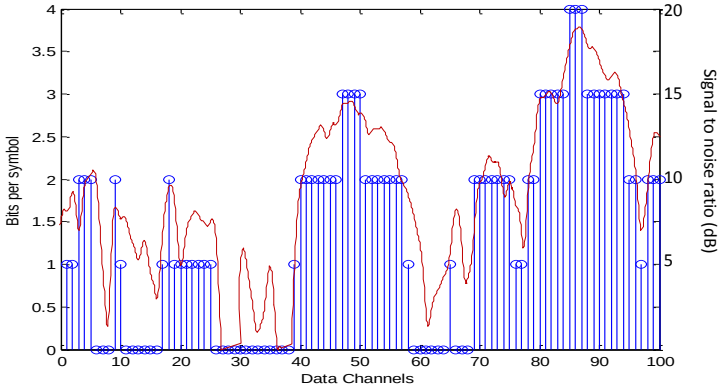


Figure 4.15 Bits allocation for the antennas placed face-to-face 1m apart with NLOS at 14dB

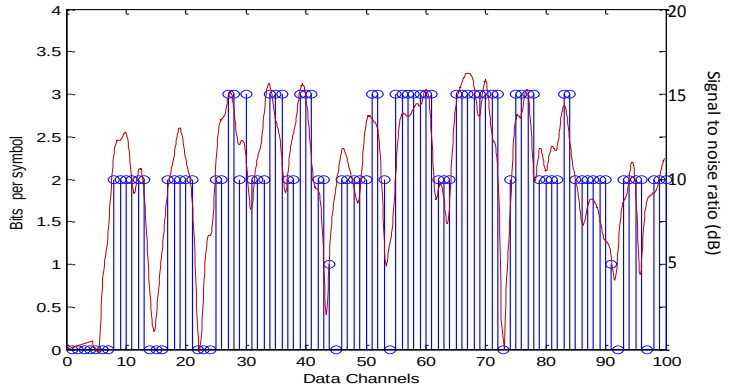


Figure 4.16 Bits allocation for antennas placed face to face 3m apart with NLOS at 14dB

Figures 4.17 to 4.20 show the magnitude responses of all the channel scenarios considered. The antennas placed face-to-face and side-by-side with a distance of 1 and 3 meters respectively, for both LOS and NLOS are studied. Since the channel has been normalised, the magnitude responses shown are not the actual measured $S_{21}$. The adaptive modulation uses the section of the spectrum with little or no fading to send more information at a BER of $10^{-4}$, which makes it possible to maintain real time communication in the channels experiencing severe selective fading.

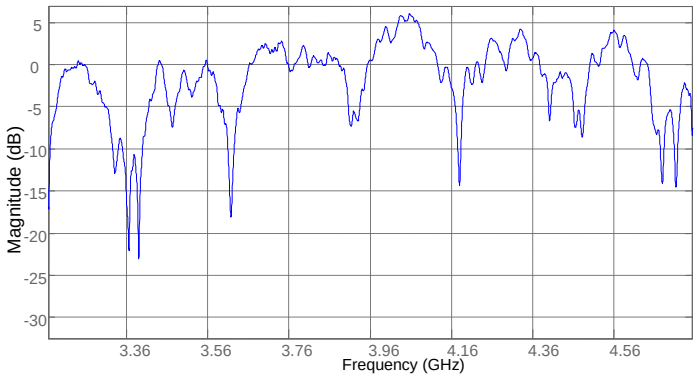


Figure 4.17 UWB Channel with the antennas placed side–by-side 1m apart with LOS

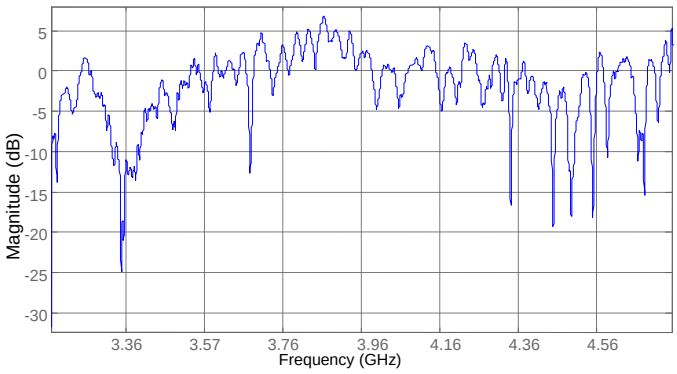


Figure 4.18 UWB channel with the antennas placed side –by-side 3m apart with NLOS

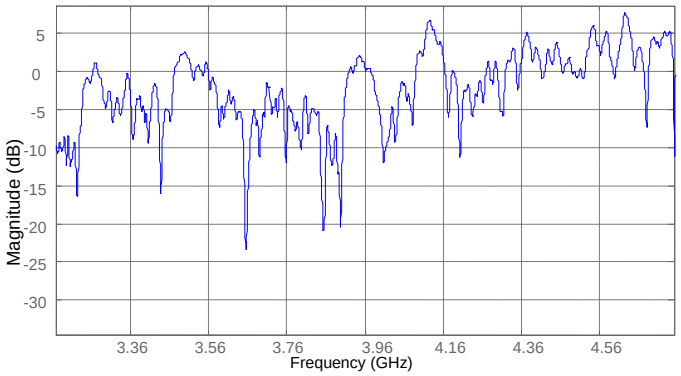


Figure 4.19 UWB channel with the antennas placed face-to-face 1m apart with LOS

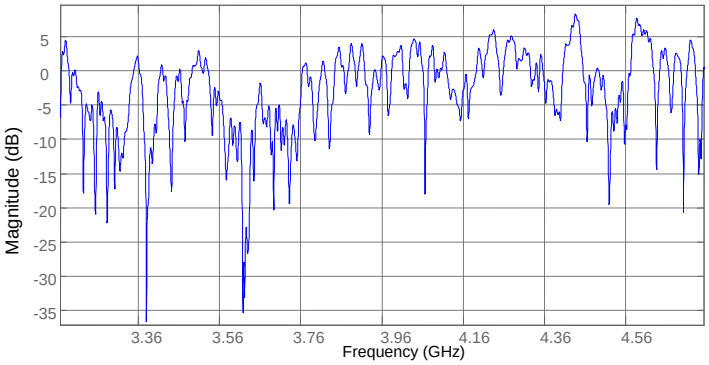


Figure 4.20 UWB channel with the antennas placed face-to-face 3m apart with NLOS

### 4.13 MB OFDM UWB system simulation

The system is simulated using the modified MB-OFDM UWB Matlab model, evaluating the BER variation with the Es/No for different indoor channels. The fading causes large variation in the channel frequency response over the bandwidth. However, with the application of OFDM and the adaptive modulation, the frequency selective fading can be mitigated. Figures 4.21 and 4.22 show the BER performance for the antennas placed 1-meter apart, side-by-side and face-to-face with LOS and NLOS respectively. Considering the channel of side-by-side with LOS, it is observed that the BER performances of the adaptive and non-adaptive modulation are the same until 10dB of Es/No. The relative magnitude response of the channel is shown in Figure 4.13. It describes that sub band 2 (3.696-4.224GHz) experiences little fading compared to sub band 1 (3.168–3.696GHz) and sub band 3 (4.224-4.752GHz). Therefore, the non-adaptive modulation scheme doesn't have more bit errors than the adaptive modulation scheme. For the case of side-by-side orientation with NLOS, a gain of 4dB is achieved by using the adaptive modulation (black curves).

For the cases of face-to-face antenna orientation with LOS and NLOS, gains of 4dB and 3dB have been achieved using the adaptive modulation. It shows that the adaptive modulation reduces the level of required power to less than half to give a BER performance of $10^{-4}$ compared to the non-adaptive system. Figure 4.23-4.24 show the BER performance for the antennas placed 3-meters apart, side-by-side and face-to-face with LOS and NLOS respectively. For the side-by-side setting, a gain of 4dB is achieved in both the LOS and NLOS scenarios. The performance of the LOS side-by-side setup is quite interesting as both the adaptive and non-adaptive modulations have the same performances up to 16dB of the Es/No. This indicates that the non-adaptive modulation scheme doesn't suffer more bit errors than the adaptive modulation scheme in a good LOS channel.

For the LOS and NLOS face-to-face setting, a gain of 8dB has been achieved by using the adaptive modulation at a BER of $10^{-4}$. This shows that the adaptive system will require only one sixth of the power used by the non-adaptive system to deliver the same BER performance. It is evident from these results that for a certain power level, much higher data rates can be delivered by using adaptive system as compared to a non-adaptive system. Therefore, adaptive modulation is an important tool that can be used to improve the system performance significantly.

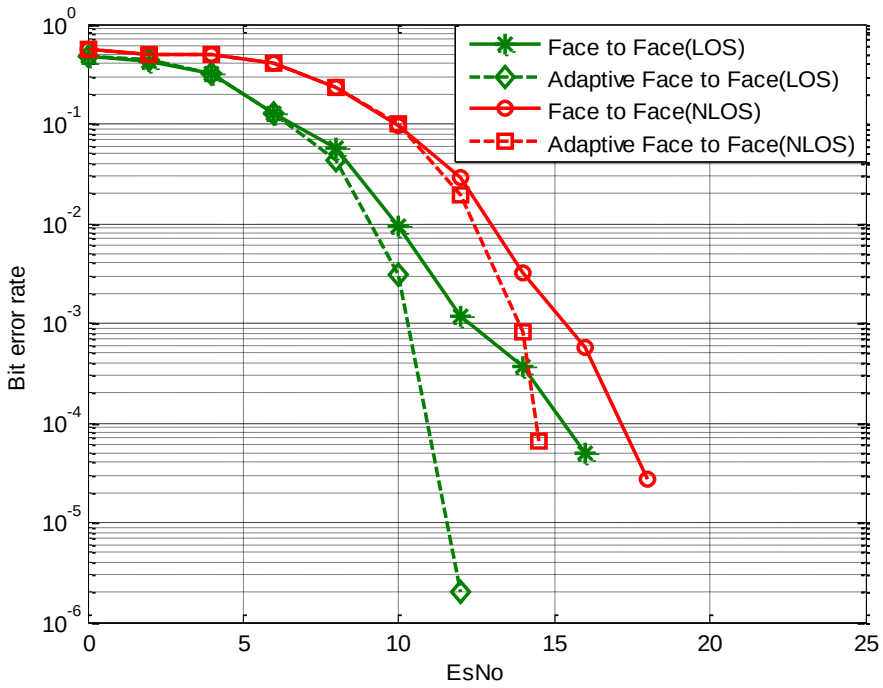


Figure 4.21 BER performance of a UWB channel with the antennas placed face-to-face 1 meter apart in dense multipath environment

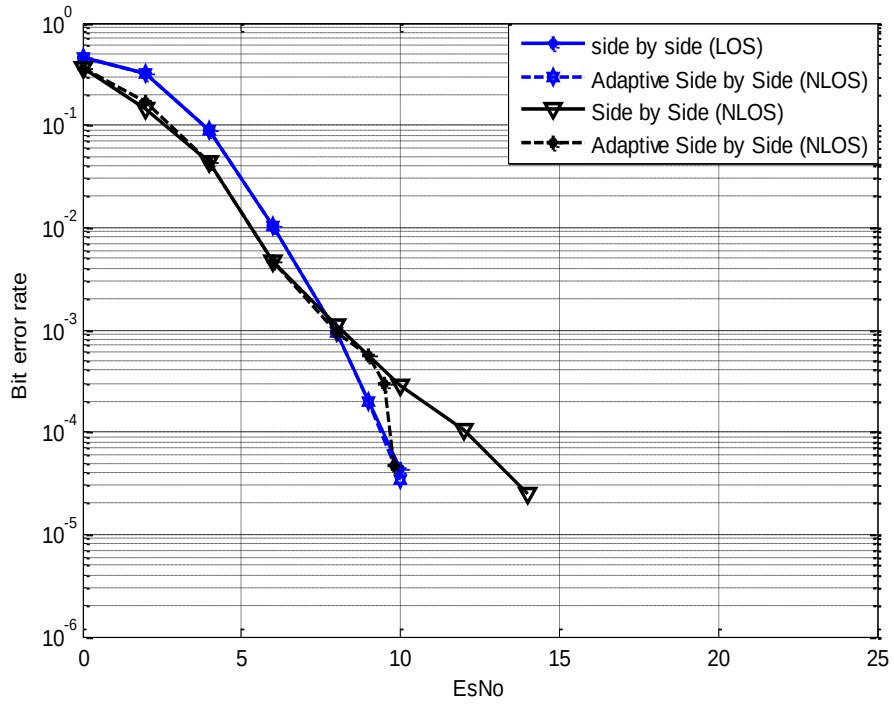


Figure 4.22 BER performance of a UWB channel with the antennas placed side-by-side 1 meter apart in dense multipath environment

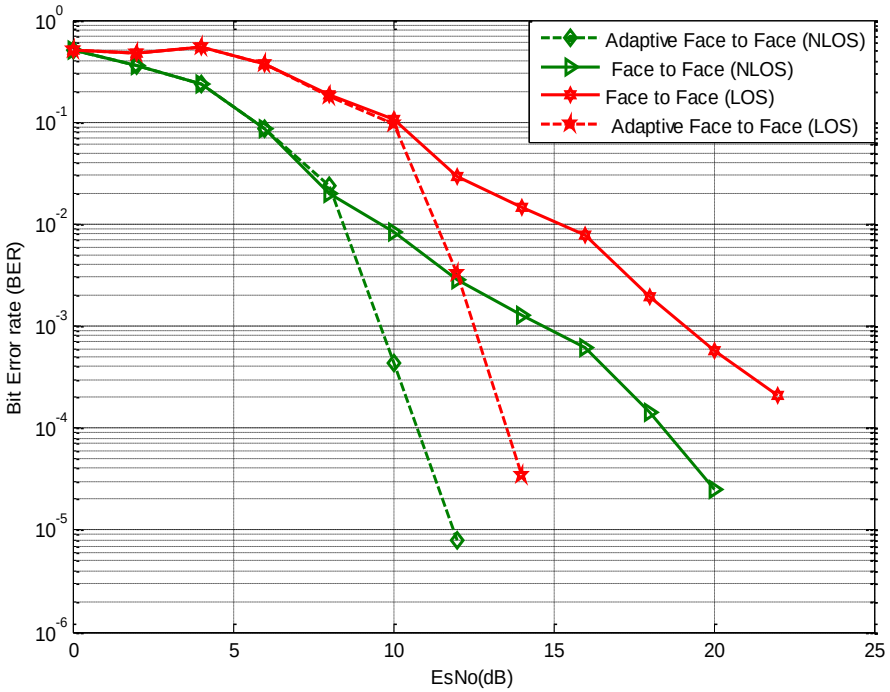


Figure 4.23 BER performance of a UWB channel with the antennas placed face-to-face 3 meter apart in dense multipath environment

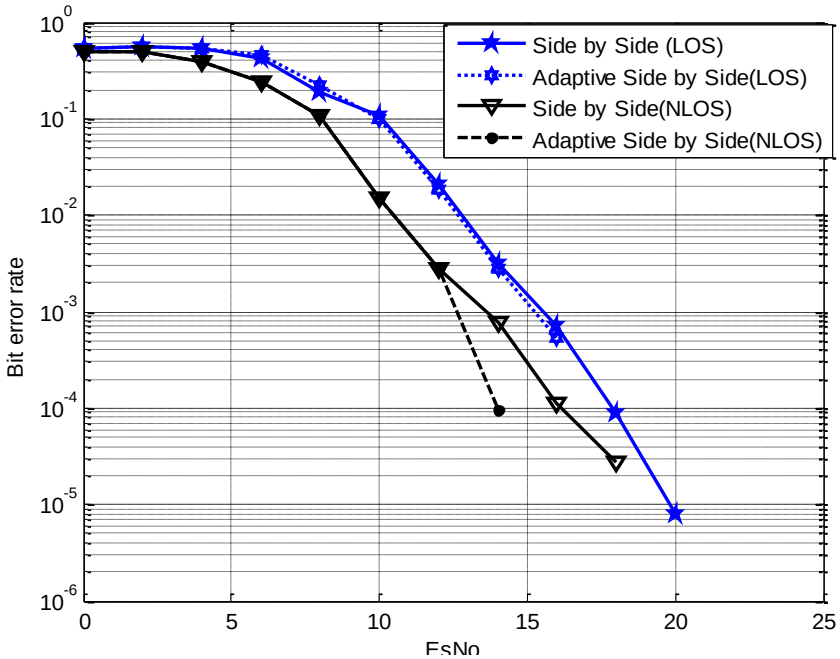


Figure 4.24 Figure 4.24 BER performance of a UWB channel with the antennas placed side-by-side 3 meter apart in dense multipath environment

### 4.14 Summary

In this chapter, the characteristic of the UWB channel was considered in SISO, SIMO and MIMO models. UWB channel modelling is different from the narrow band channel due to its frequency selective fading. The channel was characterised based on a large scale fading and a small scale fading due to the multiple clusters and rays arriving at different times at the receiver. The post processing technique of modelling a realistic channel was also discussed based on the measurements. A novel technique of using adaptive modulation was presented as a way of utilising the channel efficiently in a channel experiencing frequency selective fading. The results show that a better BER performance can be obtained using adaptive modulation while maintaining the data rate of the system.

### References


1. T. Kaiser and F. Zheng, *Ultra Wideband Systems with MIMO*. New York: Wiley,2010
2. H. Arslan et al (Ed), "*Ultra Wideband Wireless Communication"* New York: John Wiley & Sons, Inc, 2006
3. J. Kunisch and J. Pamp, "*Measurement results and modeling aspects for the UWB radio channel*" , Proc. IEEE Conf. UWB Systems and Technologies (UWBST02), Baltimore,MD, May 2002, pp. 19–23.
4. A. F. Molisch, et al "IEEE 802.15.4a channel model—final report," IEEE 802.15-04-0662-00-004a, November 2004.
5. A. Alvarez et al "*New channel impulse response model for UWB indoor system simulations*," Proc. IEEE Vehicular Technology Conf. (VTC 2003-Spring), Jeju, May 2003, pp. 1–5.
6. J. Keignart and B. DenisPost "*Processing Framework for Enhanced UWB Channel Modelling from Band-limited Measurements*" IEEE Conf. Ultra Wideband Systems and Technologies, 2003
7. D. Manteuffel et al "*Impact of Integration of Consumer Electronics on the Performance of MB-OFDM UWB*". Int. Conf. Electromagnetics Advanced Applicat. ICEAA 2007, Torino, 2007, pp 911-914
8. J. Kim et al," *Performance Analysis of Channel Estimationin OFDM Systems*". IEEE Signal Processing Letters, VOL. 12, NO. 1, January 2005
9. A. Molisch," *Ultra-Wide-Band Propagation Channels*". Proceedings of the IEEE, 2009 , vol 97,Issue 2 pp 305
10. M. Clark et al, " Fixed-Point Modeling in an Ultra Wideband (UWB) Wireless Communication System" MATLAB digest, May 2004

11. L. Guo et al, "*A Small Printed Quasi-Self-Complementary Antenna for Ultra wideband Systems* " IEEE Antennas and Wireless Propagation Letters, VOL. 8, 2009
12. K. Cao, "*A Bit Allocation Algorithm for MB-OFDM UWB with Spectral Mask Constraint*" 4th IEEE Int. Conf. Wireless Commun, Networking and Mobile Computing, (WICOM '08) Dalian 2008.
13. S. Coleri et al "*A Study of Channel Estimation in OFDM Systems*". IEEE 56th Proceedings Vehicular Technology Conference, VTC 2002-Fall. 2002,pp 894
14. D. M.S. Baek et al "Performance Evaluation of Adaptive UWB System with Multiple Antennas", Song Progress In Electromagnetics Research C, Vol. 5, 1–12, 2008
15. R. S Manzoor et al, "*DWPT Based FFT and ITS Application to SNR Estimation in OFDM Systems*" Signal Processing: An International Journal (SPIJ) Volume (3): Issue (2)
16. J. Foerster et al ,"*Channel Modelling Sub-committee Report Final",* IEEE P802.15 Working Group for Wireless Personal Area Networks (WPANs) IEEE P802.15- 02/490r1-SG3 ,February 2003
17. Phy Specification: Final Deliverable 1.5 Multiband OFDM Physical Layer Specification , WiMedia Alliance, Inc ,2009
18. S. V. Schell, "*Analysis of Time Variance of a UWB Propagation Channel* " IEEE P802.15 Working Group for Wireless Personal Area Networks (WPANs) IEEE P802.15-02/452r0-SG3a Alviso, CA 2002
19. O. Francis, Y. Quitin, C. Oestgesy, F. Horlin and P. De Doncker Clustered Channel Characterization for Indoor Polarized MIMO Systems Personal, IEEE 20th International Symposium on Indoor and Mobile Radio Communications, 2009 , Tokyo
20. *E. Haddad et al,* Optimization of 3D Ray Tracing for MIMO Indoor Channel ,General Assembly and Scientific Symposium, 2011 XXXth URSI , August 2011, Istanbul

# Chapter 5

**Time Varying UWB Channel Measurement and Adaptive Modulation**

## 5.1 Introduction

An evaluation of the UWB system in a time varying channel is necessary to analyse the performance of the system while implementing adaptive modulation. It gives insight on the parameters to be used when prototyping the system and also to estimate an acceptable feedback rate in a UWB time varying channel when implementing adaptive modulation.

## 5.2 Measurement setup

The measurements were carried out in two different places: Body-Centric Wireless Sensor Laboratory and open indoor space (Foyer) on the south side of the Body-Centric laboratory as shown in Figure 5.1. Human body movement are considered in measurements in Body-Centric Wireless Sensor Laboratory and in the Foyer space with people moving around. The transmitter and receiver were placed at different positions while measurements were taken. For the open indoor space, a gap of 5m is first considered between the transmit and the receive antenna and then subsequently the distance was reduced to 1m.

Measurements were taken over the fixed links as people move across the link, obstructing the LOS and other dominant paths of the signal. Measurements were also carried out with no human movement to determine the degree of variation. The number of persons moving during the measurements is varied from 1 to 3. Two types of human movement are studied; first people walked together on a straight line vertically across the link and secondly, the people walked randomly across the link. During the vertical movement, the spacing between two human subjects is about 1m. Each set of measurement consist of 2500 channel measurements over the measurement duration. The measurements were also carried out for varied antenna height. The human movement is at an average speed of 1m/s which generates an expected maximum Doppler shift of 13.2Hz at a centre frequency of 3.960GHz (band 1 centre frequency). Agilent PNA-X Vector Network Analyser was used for the measurements. The transmitting and receiving antennas are self quasi complementary UWB antennas designed and fabricated in the QMUL antenna laboratory [1].

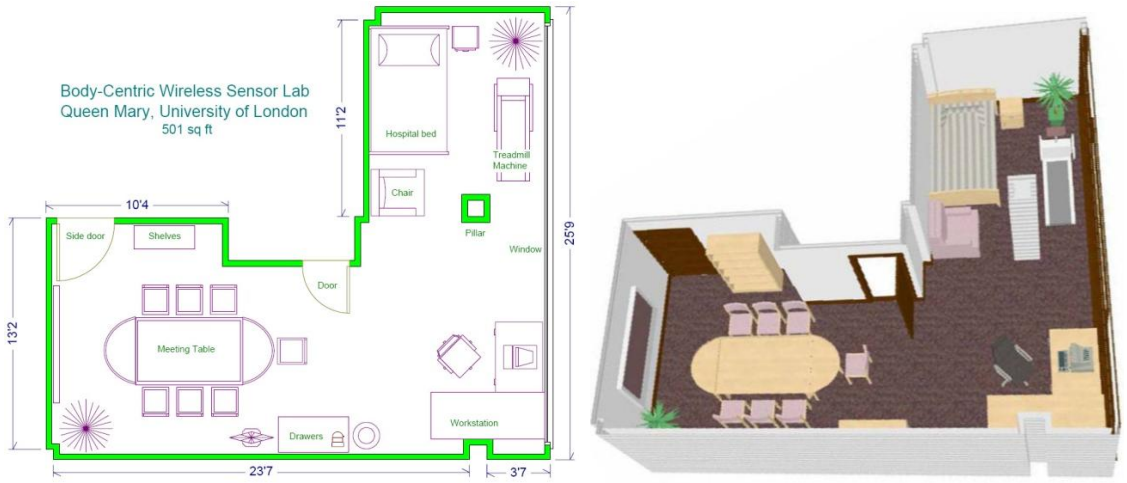


(a) Layout (b) 3D- Layout

Figure 5.1 The body-centric lab

## 5.3 Channel Measurement

### 5.3.1 Measurement Set-up

Measuring the channel response at small time interval while people are moving would help to understand the effect of time variance in a UWB channel. This will enable small changes in the channel response to be seen. A small cycle time is required to be able to capture such change. A cycle time comprises of the sweep time, retrace time and band crossing time. The total time to carry out the operation depends on multiple factors such as type of sweep, frequency range, IF bandwidth, number of points, types of correction being applied. Also for external triggering, the transport layer for LAN, USB, General Purpose Interface Bus (GPIB) could be used but the processing time could increase the total time needed to carry out a set of measurement.

Many techniques were experimented to determine which one is the suitable approach for the required measurement. An approach of triggering the Agilent PNA-X Vector Network Analyser for a complete sweep and then transfer the data is adopted eventually. The minimum measurement time per point is in order of 1/ (IF bandwidth). The smaller the IF bandwidth, the larger the sweeping time and vice versa. For an IF bandwidth of 600 kHz, the measurement time per port is 1.667µs and for 1 kHz it is 1ms. This time does not include the dwell time for each point. Sweep time is the time taken for the hardware to apply the stimulus and acquire data for sweep. This does not include the time PNA-X takes to process, calibrate, display results and save data. The sweep time can be computed using the following expression

$$S = N * P * \left(D + \frac{1}{B}\right) \qquad 5.1$$

where S is the sweep time, N is number of points, P is the number of measurement port, D is dwell time and B is IF bandwidth. Conventionally, 50µsec is used as the dwelling time, though the exact value can change depending on the frequency band [2]. Some frequency bands have faster dwelling time while some have slower dwelling time. For a 2-port measurement the sweep time will be 2 times than the displayed time of a PNA-X because it has to sweep in both forward and reverse mode. Figure 5.2 illustrates the PNA-X measurement process. It includes the time for the hardware data acquisition process to complete its cycle. Time taken for additional data processing, display and correction are not considered. There is also a time lag (T1) between the first trigger input and the start of data acquisition which varies depending on the model of the digital signal processing (DSP) board used in the PNA-X. This value could be in the range of microseconds (µs). For example, for 20GHz N5230A, the time is within a range of 650ns to 850ns. There is also a time difference (T2) between the last acquired point and the negative edge of the sweep end trigger. This difference (T2) is not defined by Agilent [3].


Figure 5.2 Timing diagram for a 3 point sweep[3]

### 5.3.2 Parameter Settings

The following parameters were used for the measurement settings

1. Frequency Span: Due to the desire to achieve a fast measuring cycle, one sub-band was measured at a time with a frequency bandwidth of 528 MHz
2. Number of Points: 128 points were selected to enable each sub channel have a channel response that can be used for simulation and further analysis. Using 128 points, the PNA-X generates an auto sweep time of 363µs. This is the quickest possible sweep time for current settings.
3. IF Bandwidth: An IF bandwidth of 600 KHz was used to reduce the cycle time. It can produce an acceptable trace. An average factor of 5 was used. The noise reduction

settings were changed to decrease the sweep time while achieving an acceptable measurement.

4. Display: According to PNA-X 5244 data sheet [4], turning the display off while taking measurement reduces the total measurement cycle by 21ms. Therefore, the display is turned off using an external PC.
5. Other programs: other programs like antivirus increases the overhead on the processors and that could increase the data processing time. Turning off these programmes during the measurement can be helpful. Doing the measurement via a remote connection results in an additional latency and overhead on the data transmission triggering time.

### 5.3.3 Measuring Channels

The data logger is used to save traces on the PNA-X first before transferring it to the external PC to reduce any overhead by the network. Using the Agilent connection expert software, commands are sent to the PNA-X to turn the display off to improve the measuring speed. Moreover, some functions including markers, smoothing, limit testing and math functions that are not required for the measurement are turned off in order to increase the sweep speed. When turned on, the analyser must update all information for active functions for every sweep. Table 5.1 Summarise different measurement scenarios. Figure 5.3-5.8 shows the set-up of different measurement scenarios done in the wireless sensor laboratory and in the open indoor space. The pictures show human movement while carrying out measurement.

Table 5.1 Scenarios and conditions used to take the measurements.

| **Distance (Metre)** | **Movement** | **Number of people** | **Antenna Height (metre)** |
|---|---|---|---|
| 5 | No Movement | 0 | 1 |
| | Straight movement and Random movement | 1 | 1 |
| | Straight movement and Random movement | 2 | 1 |
| | Straight movement and Random movement | 3 | 1 |
| | Straight movement and Random movement | 1 | 1.5 |
| | Straight movement and Random movement | 2 | 1.5 |
| | Straight movement and Random movement | 3 | 1.5 |
| | Straight movement and Random movement | 1 | 2 |
| | Straight movement and Random movement | 2 | 2 |
| | Straight movement and Random movement | 3 | 2 |
| 4 | No Movement | 0 | 1 |
| **Distance (Metre)** | **Movement** | **Number of people** | **Antenna Height (metre)** |
| | Straight movement and Random movement | 1 | 1 |

| | | | |
|---|---|---|---|
| | Straight movement and Random movement | 1 | 1.5 |
| | No Movement | 0 | 2 |
| | Straight movement and Random movement | 1 | 2 |
| 3 | No Movement | 0 | 1 |
| | Straight movement and Random movement | 1 | 1 |
| | No Movement | 0 | 1.5 |
| | Straight movement and Random movement | 1 | 1.5 |
| | No Movement | 0 | 2 |
| | Straight movement and Random movement | 1 | 2 |
| 2 | No Movement | 0 | 1 |
| | Straight movement and Random movement | 1 | 1 |
| | No Movement | 0 | 1.5 |
| | Straight movement and Random movement | 1 | 1.5 |
| | No Movement | 0 | 2 |
| | Straight movement and Random movement | 1 | 2 |
| 1 | No Movement | 0 | 1 |
| | Straight movement and Random movement | 1 | 1 |
| | No Movement | 0 | 1.5 |
| | Straight movement and Random movement | 1 | 1.5 |
| | No Movement | 0 | 2 |
| | Straight movement and Random movement | 1 | 2 |
| Centric Lab | The transmit antenna placed on a small table on a projector while the receive antenna is place on the TV. | 0 | Transmit:1<br>Receive:2 |
| | A person doing a Presentation with the transmit antenna placed on a projector while the receive antenna is on the wall mounted TV. | 1 | Transmit: 1<br>Receive: 2 |
| | A person sitting and moving (hands, Body and chair) on a table with transmit and receive antennas placed across the table. | 1 | Transmit :1<br>Receive:1 |
| | Three walking and sitting on the table in a random pattern. | 3 | Transmit: 2<br>Receive:2 |
| | Transmit antenna place 5 metres from the receive antenna with a height of 1.10m and the receive antenna is placed on a wall mounted TV. | 3 | Transmit: 1.1<br>Receive:2 |

Figure 5.3 Two people in a straight

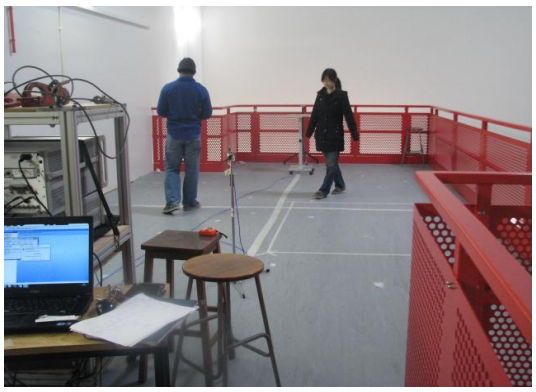

Figure 5.4 Two people in random

Figure 5.5 Three people in random

Figure 5.6 Three people in a straight

Figure 5.7 Walking and sitting on the table

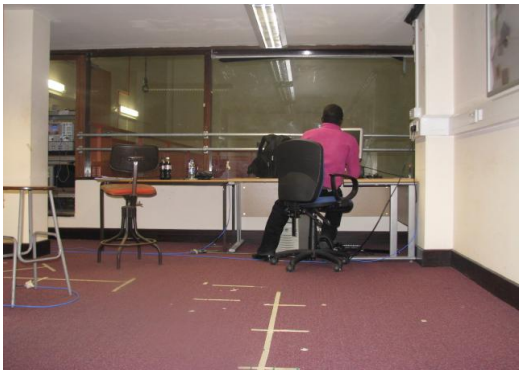

Figure 5.8 Sitting and moving hands and Body

In order to determine the best way to analyse the measurement, the correlation coefficient is calculated between successive channels varying time interval from 20ms to 140ms. Thirty four successive points are considered to give pictorial view of the variation of the channel over the points with 20ms time interval. It covers a duration of 680ms. The average height of people involved in the measurement is 163cm which is higher than some of the antenna positions. The antennas are placed at heights of 1m, 1.5m and 2m. Figures 5.9- 5.11 give an idea on the channel variation when thirty two successive points are captured and overlaid. The results

show large variation in some channel scenarios while small variation (or none in some cases) can be seen in other channel scenarios.

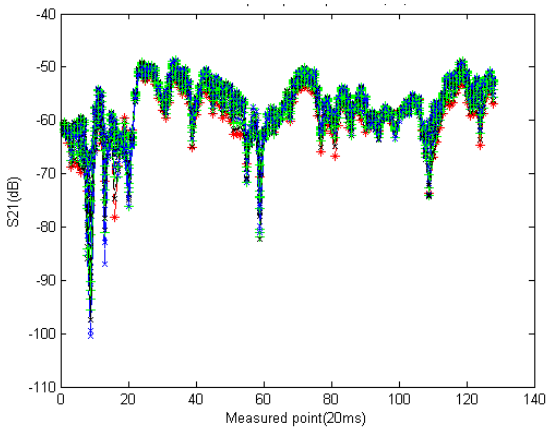


Figure 5.9 Thirty four points (680ms) while three people moved randomly across transmit and receive antennas with height of 1.5m and 5m apart

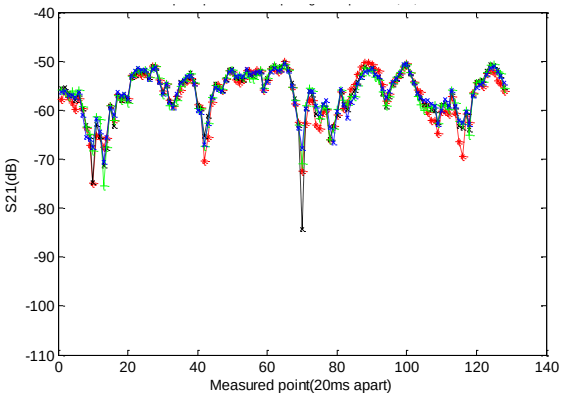


Figure 5.10 Thirty four points (680ms) while three people moved randomly across transmit and receive antennas with height of 2m and 5m apart

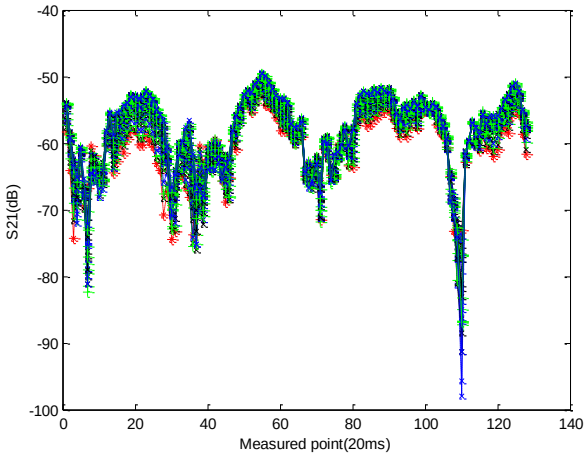


Figure 5.11 Thirty four points (680ms) while three people moved randomly across transmit and receive antennas with height of 1m and 5m apart

Channel responses over time are plotted in 3D to analyse the effect of humans blocking the LOS between the transmitter and receiver. These plots give a pictorial view on how movement in an environment can affect the channel response. For brevity, only a few scenarios are shown. Figure 5.12s show 3-D plot of a person moving in a random pattern with the antenna at 2m height. Little variation in the channel over the entire duration of the measurement is observed. Figure 5.13 shows 3-D plot of one person moving in a random pattern with the antenna placed at 1m height. The human height is higher than the antenna in this case. Therefore, the human movement intermittently blocks the LOS signal between transmit and receive antenna.

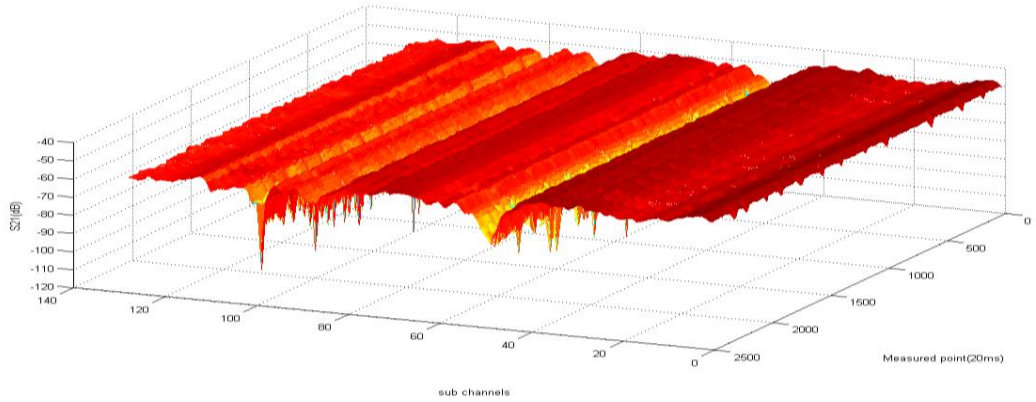


Figure 5.12 One man in a random movement with antenna height of 2m and 5m apart over 50s with 20ms interval

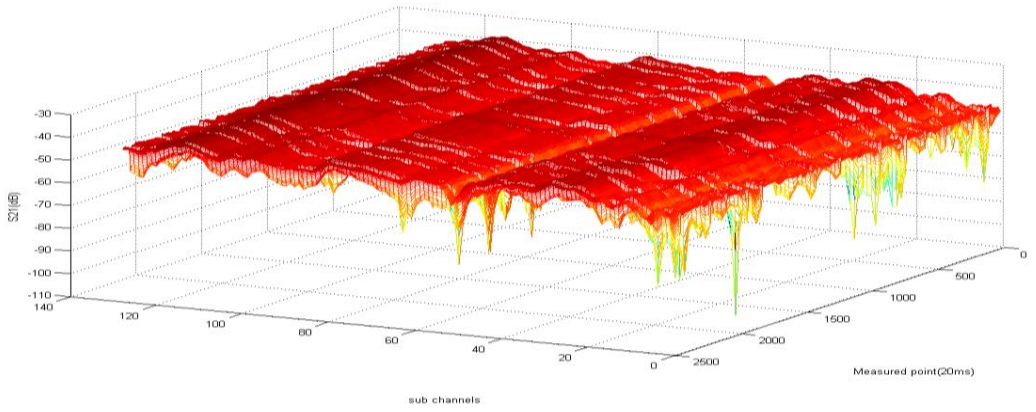


Figure 5.13 One man in a random movement with antenna height of 1m and 1m apart over 50s with 20ms interval

Figure 5.14 shows 3-D plot of one person moving in the wireless sensor laboratory. The transmit antenna is attached to a wall mounted display screen while the receive antenna is attached to a desktop PC 2m away from the transmitter. The plot shows visible lines indicating the effect of one person moving across of the channel. Figure 5.15 shows the 3-D plot of three people moving in between the transmitter and receiver placed 5m apart. The antenna heights are both 1m. The plot shows a higher degree of variation in the channel which is due to greater number of people walking across the channel, with average height greater than the height of

the antennas. The LOS is clearly blocked by this human movement as they are moving across the channel. Figure 5.16 shows the 3-D plot of three people moving between the transmitter and receiver. Lesser variation in the channel is noted as compared to Figure 5.15 where the antennas are lower than the average height of the people.

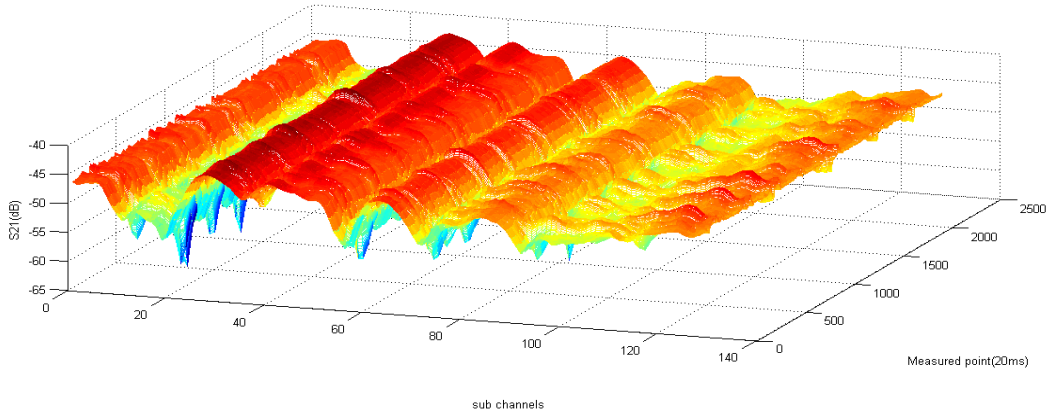


Figure 5.14 Receive antenna attached to the TV and the transmit antenna to flat desktop PC on a table with One man moving within the environment over 50s with 20ms interval

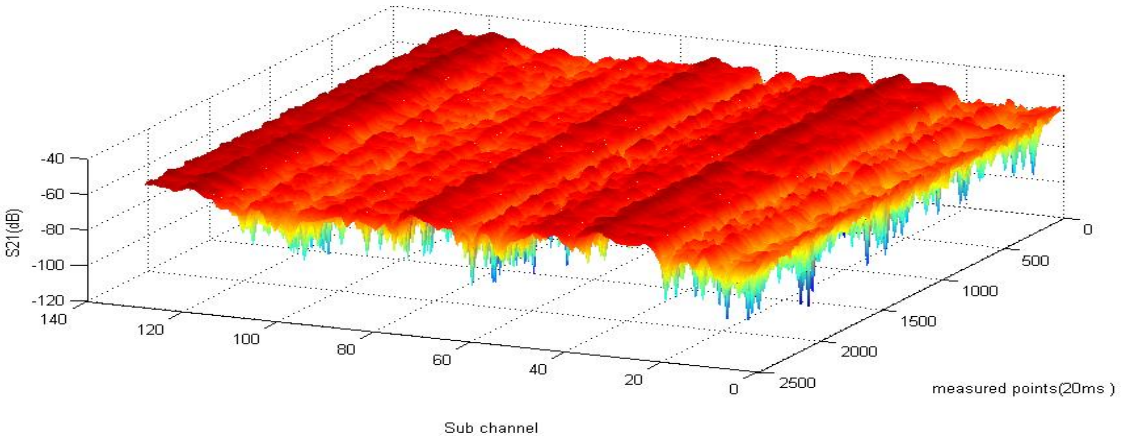


Figure 5.15 Three Men in a random movement with antenna height of 1m and 5m apart over 50 s with 20ms interval

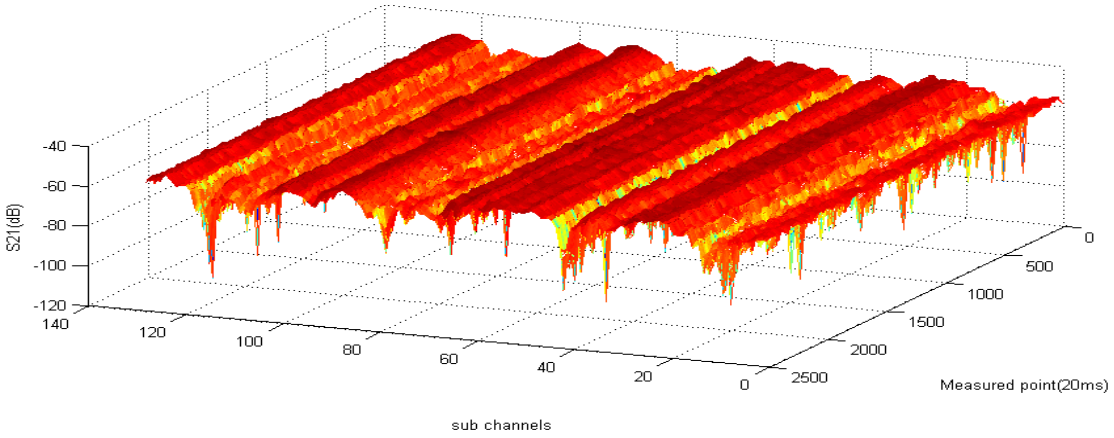


Figure 5.16 Three Man in a random movement with antenna height of 2m and 5m apart over 50s with 20ms interval

### 5.4 Correlation between channel measurements

The channel analysis is done using the correlation coefficient. This makes it easier to see how the responses of two successive channels vary in a time varying channel. Correlation coefficient is calculated from the channel responses using the following expression [9]:

$$\rho(H_1, H_2) = \frac{\varepsilon\{H_1 {H_2}^{\dagger}\} - \varepsilon\{H_1\}\varepsilon\{{H_2}^{\dagger}\}}{\sqrt{\left(\varepsilon\{{H_1}^2\} - |\varepsilon\{H_1\}|^2\right)}\sqrt{\left(\varepsilon\{{H_2}^2\} - |\varepsilon\{H_2\}|^2\right)}} \qquad 5.2$$

Where $\rho$ denote spatial correlation coefficient, $\varepsilon\{.\}$ is the expectation and $\{.\}^{\dagger}$ represents conjugate. For the UWB channel, $H_1$ and $H_2$ represent the channel transfer function for the two channels. Figures 5.17, 5.18 and 5.19 show the correlation of 3 people in a random movement between the transmitter and receiver with height of the antenna at 2, 1.5 and 1m, respectively. The correlation coefficients from Figure 5.17 are above 0.9, which could be considered quasi stationary. It describes the effect of antenna height on the channel response. Figure 5.18 shows there is much scattering in the environment due to higher number of people moving in the environment. It results in larger variation between the correlation coefficients, when the antennas are placed at a height of 1.5m. Lower time interval gives higher correlation as shown in Figure 5.18b. Figure 5.19 shows the largest channel variation as the antennas are 1m high, which was easily affected by shadowing as the human subject move around.

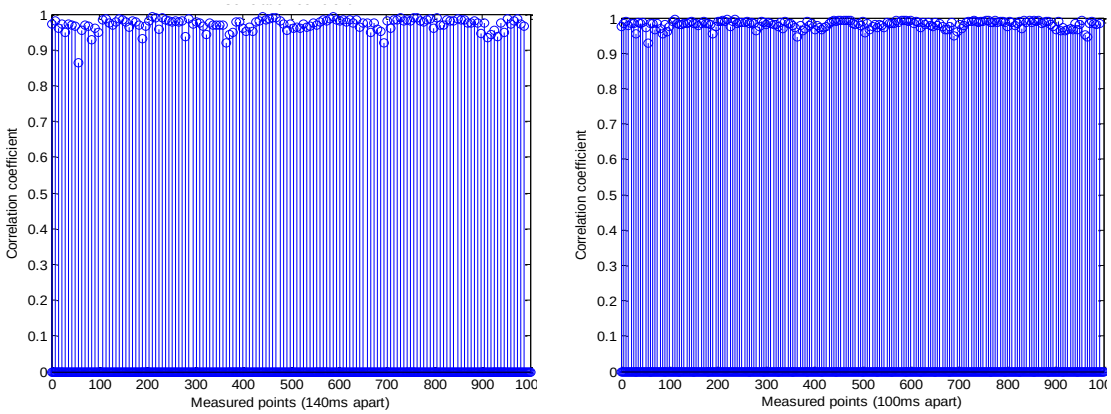


(a) (b)

Figure 5.17 Correlation coefficient for successive points with (a) 140ms and (b) 100ms time interval while three people move in a random movement with antennas place 2m high.

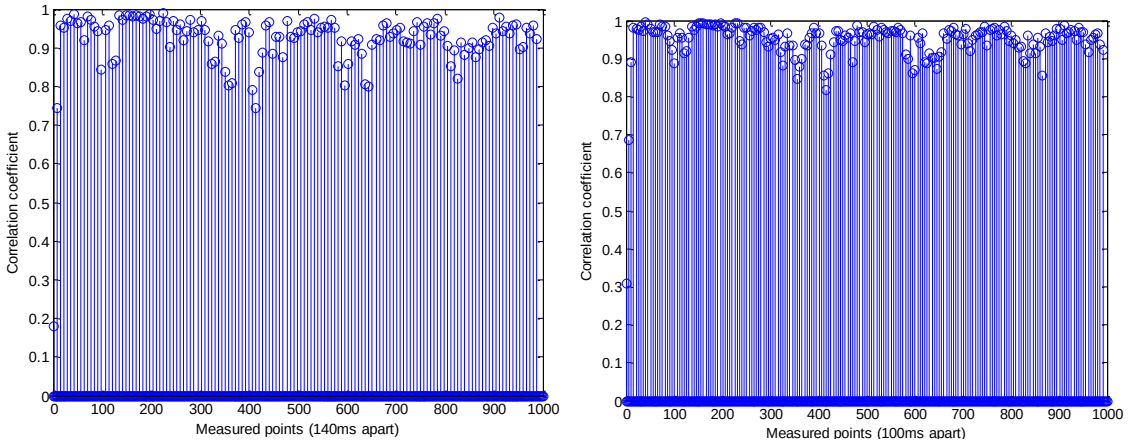


(a) (b)

Figure 5.18 Correlation coefficient for successive points with (a) 140ms and (b) 100ms time interval while three people move in a random movement with antennas place 1.5m high.

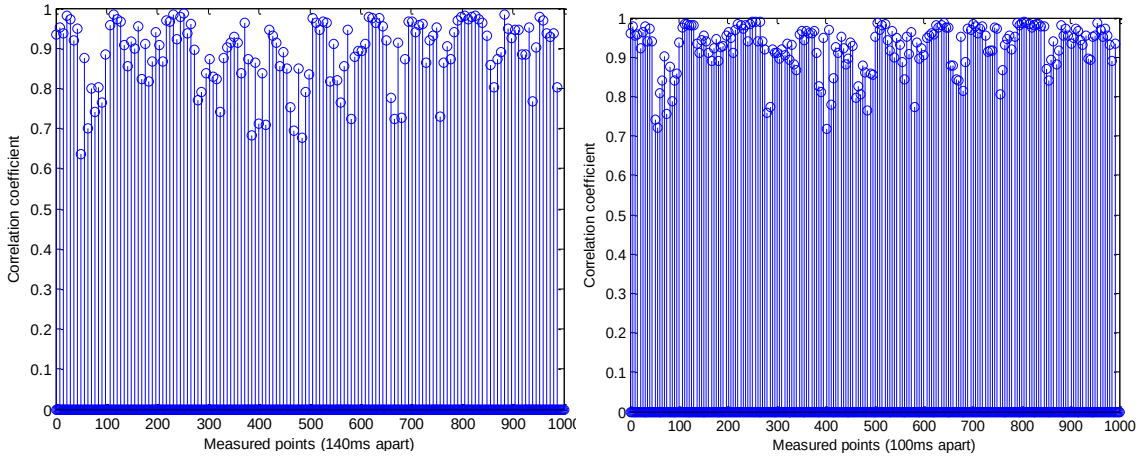


(a) (b)

Figure 5.19Correlation coefficient for successive points with (b) 140ms and (b) 100ms time interval while three people move in a random movement with antennas place 1m high.

Figure 5.20 shows the correlation coefficient for a TV to desktop scenario, where a receiving antenna is attached to the TV and the transmitting antenna is connected to a flat desktop PC. It represents a play back video device placed on a table with a person moving across the channel but not crossing the line of sight. The results show a very high correlation across all the measured points. The 3-D plot is shown in figure 5.14 where the effect of the movement is visible. In this scenario, larger time interval can be used and will still deliver optimum performance.

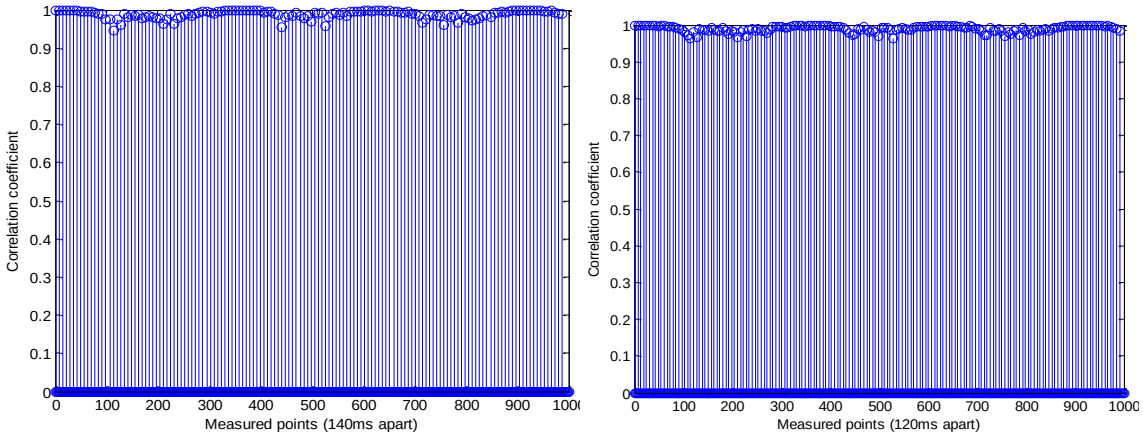


(a) (b)

Figure 5.20 Correlation coefficient for successive points with (a) 140ms and (a) 120ms time interval correlation coefficient for a TV to desktop scenario

Figure 5.21 shows the correlation coefficient of three men in a random movement while the receiving and transmitting antennas are placed in the body-centric laboratory. The antennas have a spacing of 5m with height of 2m and 1.1m, respectively. The results also show a significant amount of scattering in the environment. More results are shown and discussed in the Appendix D.

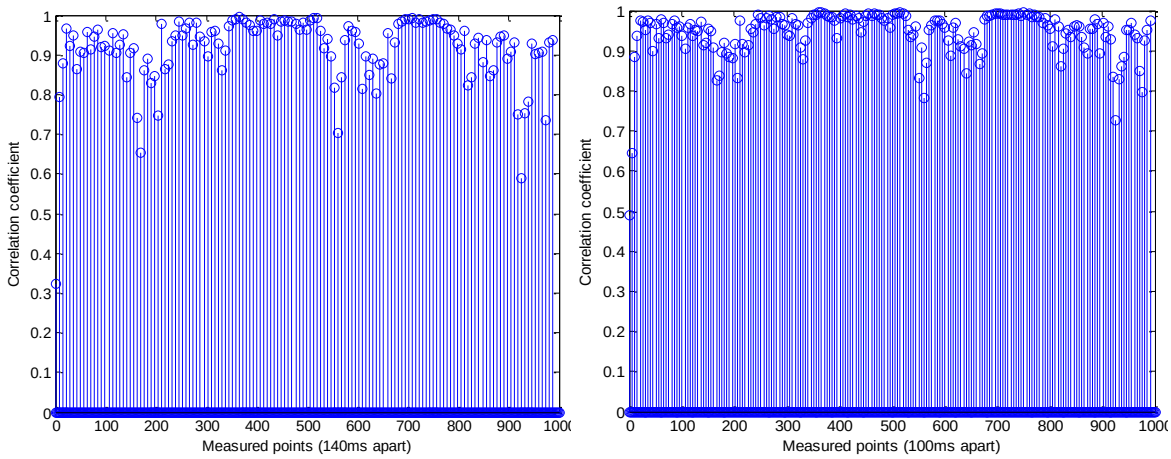


(a) (b)

Figure 5.21 Correlation coefficient for successive points with (a) 140ms and (a) 100ms time interval while three people move in a random movement and 5m apart in the centric lab.

### 5.5 Deviation between the Correlation coefficient

In this section, the maximum deviation between successive correlations is evaluated. Each measurement scenario has 2500 channel measurements which are 20ms apart. The correlation between two successive points is calculated over all the channel measurements. It could help to get the rate at which the channel can be fed back to the transmitting device without affecting the performance while implementing adaptive modulation. Table 6.2 shows

the rate at which channel information state is fed back to the transmitting device by other communication technologies.

Table 5.2 The rate at with the channel is feedback to the transmitting device[4-5]

| SYSTEM | Time interval | Modulation |
|---|---|---|
| WLAN (OFDM) | Included in packet | BPSK, QPSK,16QAM or 64QAM |
| HSDPA | 2ms | QPSK, 16QAM, 64QAM |
| WiMax | 10ms | BPSK, QPSK, 16QAM, 64QAM |

For MB-OFDM UWB technology, no study is available in open literature that could suggest an acceptable feedback rate for UWB adaptive systems. In most communication technologies, the bandwidth is considered as narrowband where one modulation index could be applied to all subchannels. For example, IEEE 802.11g uses only one index across all 64 channels. This modulation index could be binary phase-shift keying (BPSK), Quadrature phase-shift keying (QPSK), 16-Quadrature amplitude Modulation (16-QAM) or 64-Quadrature amplitude Modulation (64-QAM). These give different data rates depending on the selected modulation index. For narrow band systems, the channel state information can easily be included into the packet header as only few bits are needed due to single modulation index. For wideband systems that experiences frequency selective fading e.g. OFDM UWB, applying a single modulation index will not utilise the channel efficiently.

Therefore, it is necessary to study and suggest an acceptable channel quality feedback rate that a receiving UWB system can send channel state information to the transmit device while maintaining optimum performance. The maximum deviation is the maximum difference between two successive correlation coefficients

$$d = Max[\, abs(coef_i - coef_{i+1})] \qquad 5.3$$

Where d is the maximum deviation, $coef_i$ is the correlation coefficient between two successive channel measurements, $i$ is one of the 2500 measured points.

### 5.5.1 Open (Foyer) Indoor Space Measurements

Figure 5.22 shows the maximum correlation coefficient deviation over different antenna spacing of 4, 3, 2 and 1m. The antennas are 1m high, which is below the average height of the human subjects involved in the measurement. The average height of the three human subjects is 163cm. The result shows that at time intervals 20 and 40ms the maximum deviation for all the scenarios is less than 0.1. That could be acceptable when implementing an adaptive system. As the measurement time increases, the deviation has increased to 0.6 when the antennas were 3m apart. A larger variation is observed for time interval between 60ms and 140ms.

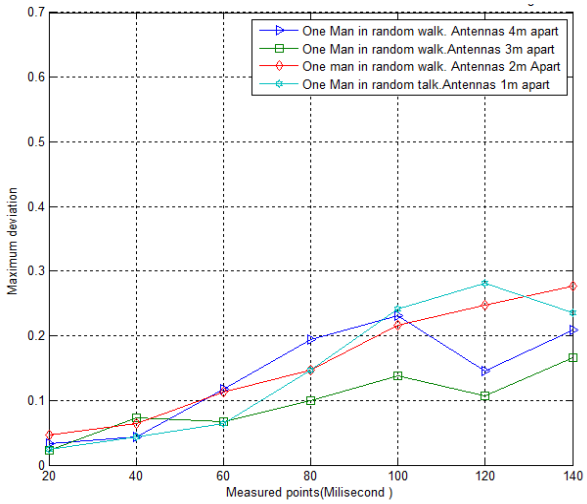


Figure 5.22 Maximum deviation of correlation coefficient between two measured points while the antennas are both 1m high

Figure 5.23 shows the maximum deviation between successive correlation coefficient while the antennas are 1.5m high. The deviation between correlation coefficients is on the x-axis while the measured points are on the Y-axis. Very low deviation over 20ms and 40ms interval is observed while very large variation over interval more than 60ms is noted. This clearly shows that implementing adaptive modulation for a system with larger feedback rate will compromise the system's performance. This is important when the height of the antenna is lower than the human height.

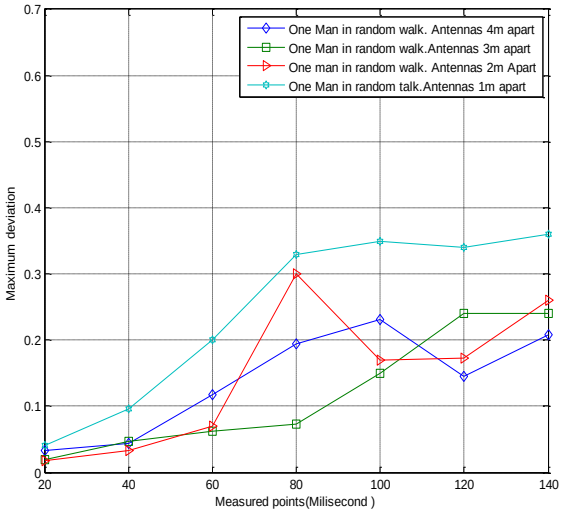


Figure 5.23 Maximum deviation of correlation coefficient between two measured points while the antennas are both 1m high

Figure 5.24 shows the maximum deviation between successive correlation coefficients when the antennas are 2m high. The results show that over the entire interval from 20ms to 140ms, the deviations between the correlation coefficient are quite low over the entire measurement duration. The antenna height could be a key playing factor here.

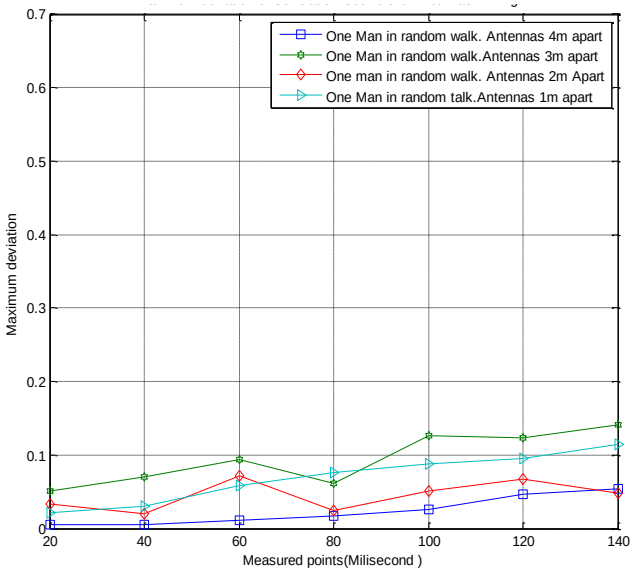


Figure 5.24 Maximum deviation of correlation coefficient between two measured points while the antennas are both 2m high

Figure 5.25 shows the maximum correlation coefficient deviation for different number of people walking across the channel when the transmitter and receiver were placed 1.5m high. The figure shows that using small time interval yields high correlation and better performance. From 40ms and below, the maximum deviation between the correlation coefficient is less than 0.1.

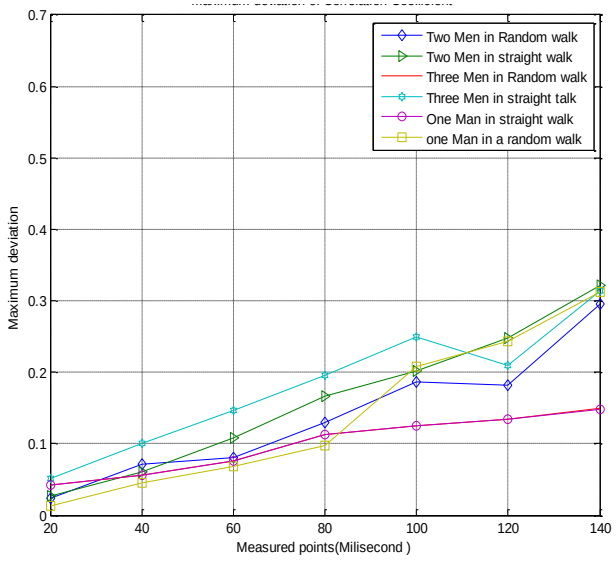


Figure 5.25 Maximum deviation of correlation coefficient between two measured points while the antennas are 1.5m high and 5 m apart.

### 5.5.3 Open Indoor Space Measurements over distance of 5m

Figure 5.26 shows the maximum correlation coefficient deviation for different number of people walking across the channel when the transmitter and receiver are placed 2m high. The results show that over the entire measurement from 20ms to 140ms time interval, the

deviations between the correlation coefficients are very low. The maximum deviation is about 0.12 and this is due to the longer height of the antenna of 2m. Figure 5.27 shows the maximum correlation coefficient deviation for different number of people walking across the channel when the transmitter and receiver are placed 1m high. As the measurement time increases, the deviation also increases. For all the time intervals lower than 40ms, the deviations are less than 0.1, while for time intervals between 60ms and 140ms, larger variation can be seen.

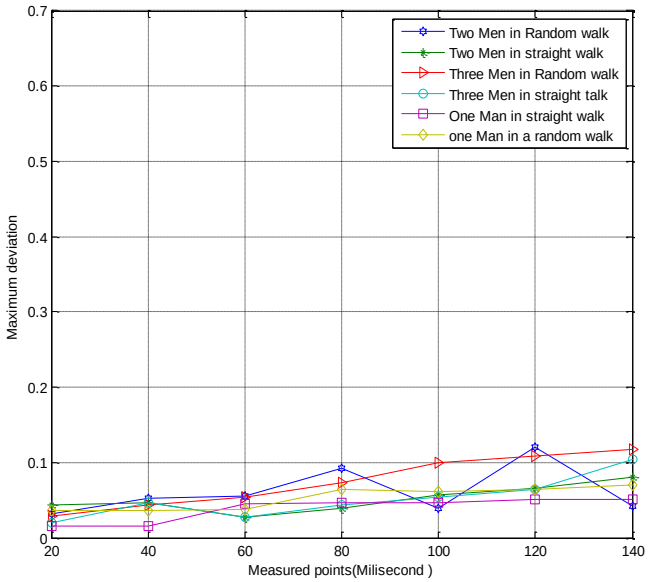


Figure 5.26 Maximum deviation of correlation coefficient between two measured points while the antennas are 2m high and 5 m apart.

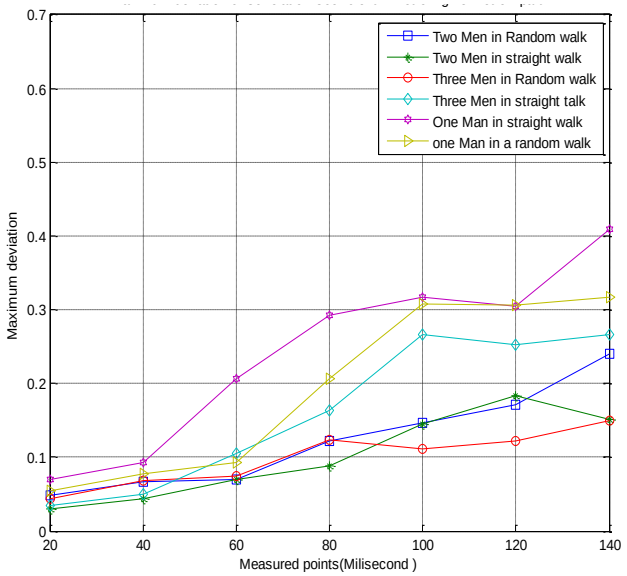


Figure 5.27 Maximum deviation of correlation coefficient between two measured points while the antennas are 1m high and 5 m apart.

Considering average human indoor speed and the rate at which the channel measurements were taken, at 20ms only 2cm distance is covered and at 40ms only 4cm distance is covered. This little change seems to introduce small variation in the channel. Increase in the time of measurement increases the effect of people moving. Figures 5.22-5.27 show a common

characteristic irrespective of the number of people that the maximum deviation of the correlation coefficients is about 0.1 for 40ms interval. It is independent of the separating distance between the antennas.

### 5.5.4 Body-Centric Laboratory Measurements

Figure 5.28 shows the maximum deviation between successive correlation coefficient. The measurements are carried out in the Body-Centric laboratory where furniture and equipments are present. The measurements are done using different set-ups with human activity that represents realistic scenarios

1. The transmit antenna is placed on a small table on a projector while the receive antenna is placed on the TV.
2. A person doing a Presentation with the transmit antenna placed on a projector while the receive antenna is on the wall mounted TV.
3. A person sitting and moving (hands, body and chair) on a table with transmit and receive antennas placed across the table.
4. Three people sitting on a meeting table and the antennas are placed across the table.
5. Three people walking and sitting on the table in a random pattern.
6. Transmit antenna is placed 5 m from the receive antenna. The transmit antenna serves as a mobile station with a height of 1.1m and the receive antenna is placed on a wall mount TV display.

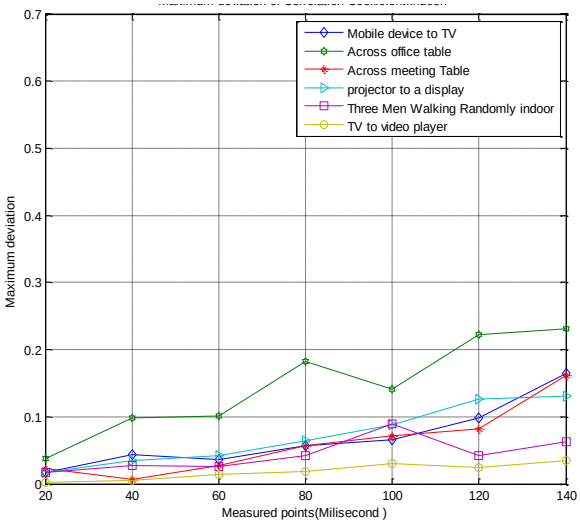


Figure 5.28 Maximum deviation of correlation coefficient between two measured points in the wireless sensor laboratory

### 5.6 Effective Data rate with Feedback Channel

The effective data rate while implementing adaptive modulation is expressed as

$$eD = \frac{D*T_i}{T_i+F_r} \qquad 5.4$$

Where $eD$ is the effective data rate per seconds due to the feedback channel, D is the normal data rate, $T_i$ is the time interval and $F_r$ is the duration used to feedback the channel. The communication is Time division duplex (TDD). Due to the time required to feedback the channel state information to the transmit device, the effective data rate will be lower than the normal expected data rate. The receive device just need to send one packet that contains the CSI with the modulation index. The duration of a packet used in this study with a payload 2990bytes is 40µs. The time used in calculating the effective data rate is 240µs which is 6 times the packet duration. This includes other factors such as time taken to compute the modulation index etc.

Figure 5.29 shows the effective data rate for all time intervals from 20ms to 140ms used in Equation 5.3. An effective data rate of 395.2Mbps is noted for 20ms time interval which is 4.8Mbps less than the normal expected data rate of 400Mbps. Considering that adaptive modulation improves the BER, having a data rate reduced by 4.8Mbps can be negligible. It will be better to use the 395.2Mbps data rate with a higher BER performance and throughput.

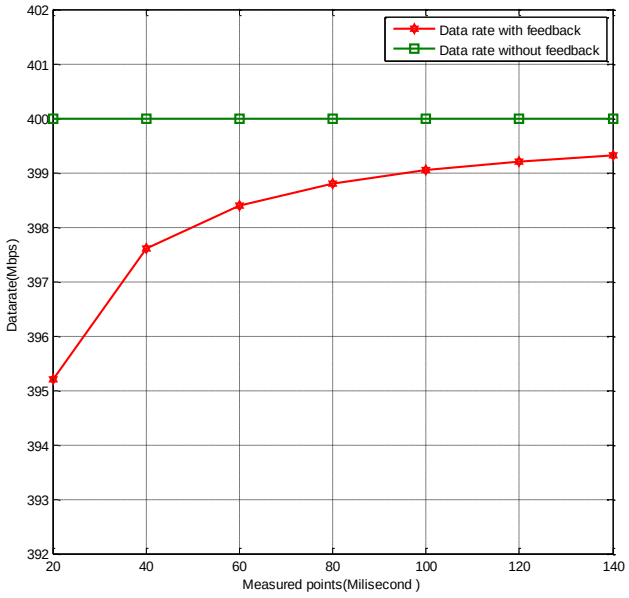


Figure 5.29 Effective data rate at different feedback time interval

### 5.7 UWB Packet Size

A UWB packet contain a header, preamble and payload which is expressed as [8]

$$N_{Packet} = N_{Preamble} + N_{Header} + N_{Payload} \qquad 5.5$$

Every OFDM packet contains a preamble, header and payload. The preamble contains the packet/frame synchronisation and channel estimation sequence. MB-OFDM packets have 2 modes

1. Standard mode: It has 30 symbols in its preamble and is used in all packets for low data rate. In high data rate (from 320 and above) only the first packet is a standard packet while the remaining are burst packets.
2. Burst mode: This mode has 18 symbols in its preamble and is used mainly in the high data rate mode.

The design and simulation of UWB system is done in burst mode to exploit high data rate in the system. The simulation considers the performance of an adaptive modulation in a time varying channel. It provides an overview of UWB communication system performance when the adaptive modulation is implemented. Also for ease of implementation, packet duration of 40µs is selected that is equivalent to 128 symbols per packet in burst mode. The duration of a symbol is 3.125e-07. The breakdown of the packet is given in Table 5.3.

Table 5.3 UWB packet

| | | | |
|---|---|---|---|
| Preamble | 18 symbols | 5.625us | Packet , Frame and Channel Estimation sequence |
| Header | 12 symbols | 3.75us | Header details |
| Payload | 98 symbols | 30.625 | Contains data and FCS |
| | 128 | 40us | |

The following equation is used to determine the length of payload to use with a data rate of 400Mbps [8]

$$6\left(\frac{8\times length+32+N_{tail}}{N_{ibp6s}}\right) \qquad 5.6$$

where, Length = Payload in bytes, 32= size of the FCS

$N_{ibp6s}$ = Information per 6 OFDM symbols

This gives a payload of 2996 bytes and shows that a payload of 98symbols can be used to deliver slight more than half of the maximum allowable payload. System is simulated considering in realistic scenarios where the channels change due to the movement of human subject and the effect of other objects in the vicinity. The UWB channel model is updated every 20ms.

The channel pre-processing stages done on the measured channel before inputting to Simulink were discussed in Chapter 4. Each measurement scenario contains 2500 channel measurements captured at 20ms interval. The test set-ups represent different realistic situations. 2500 CIR are loaded to the workspace in Matlab where Simulink retrieves the required channel at the required time. The entire 2500 CIRs can't be loaded as the file size is very big which could easily generate errors. From the equation

$$Y = H * X + N \qquad 5.7$$

where *Y* is received signal, *X* is transmitted signal, *H* is channel response and *N* is noise. *H* changes every 20ms and the system is designed to update its channel information state every 20ms. After every 20ms, the receiver computes the SNR for each channel from the channel state information and determines the modulation index of each channel. It then sends it to the transmit system where the transmit system update its modulation index and changes the modulation on each of the sub channel based on the feedback. This operation continues throughout the system simulation.

### 5.8 Implementation of Adaptive Modulation

Implementing the proposed adaptive modulation technique requires a feedback channel to inform the transmitter of the state of the channel. This approach is found in many wireless and wired adaptive systems. The uniqueness of this adaptive modulation scheme is the fact that the adaptive modulation will be done based on the fading of each sub carrier. It is different from the existing adaptive system where same modulation index is applied across the entire OFDM sub carriers, such as in IEEE802.11g/n [7, 8]. Training signals can be used by both the transmitter and the receiver for channel sounding.

A time variance channel study with a human movement of 3km/hr concludes that when a person moves from one position to another, the body movement can be sampled at 61ms (milliseconds) [9]. Hence, within the duration of 61ms, the human can be considered as stationary and not affecting the state of the channel. The WiMedia physical layer specifications states that a 1024 octet data packet for a data rate of 480Mbps will have time duration of 88.75µs [8]. Therefore, over 500 packets could be transmitted while considering the channel to be time invariant. Sending one packet after every 500 to update that channel state information will only increase the overhead by $^{1}/_{500}\%$. This shows that the UWB channel behaves differently from mobile networks channel where devices are expected to move at speeds of up to 200Km/hr or more. Implementing the proposed adaptive modulation technique will improve UWB system in the indoor environment. However, further investigation will be carried out to address the issues of adaptive modulation implementation in a MB-OFDM.

Below are the steps that need to be considered in implementing the CSI (Channel State Information) update process

1. Transreceiver 1 sends the first packet which contains the packet synchronization (PS), frame synchronization (FS) and channel estimation (CE) sequence to the transreceiver 2.
2. Transreceiver 2 receives the packets and estimates the channel using the channel estimate sequence. It then calculates the SNR and assign modulation index to the data sub channels.
3. Transreceiver 2 sends the modulation index of each sub channel to transreceiver 1. Transreceiver 2 will send this information in its packet which also contains the PS, FS and CE sequence to transreceiver 1.
4. Transreceiver 1 receives the packet and estimates the channel using the channel estimate sequence. It will then calculate the SNR and assign modulation index to the data sub channels.
5. Transreceiver 1 sends the modulation index of each sub channel to transreceiver 2. Transreceiver will send this information in its packet which also contains the PS, FS and CE sequence to transreceiver 2.
6. Both transmitter 1 and 2 are updated with channel state. The channel sounding will be repeated periodically or after every 500 packets in order to update the channel state information on both transmitters.

A flow chart for the implementation of the adaptive modulation system is given in Figure 5.30. The PS, FS and CE sequence are the packet synchronisation, frame synchronisation and channel estimation sequence respectively that are already included in the specification of MB-OFDM UWB packets by the WiMedia group [8]. These are contained in the PLCP (Physical Layer Convergence Protocol) preamble. The PLCP preamble is appended to standard data unit before the header and the payload.

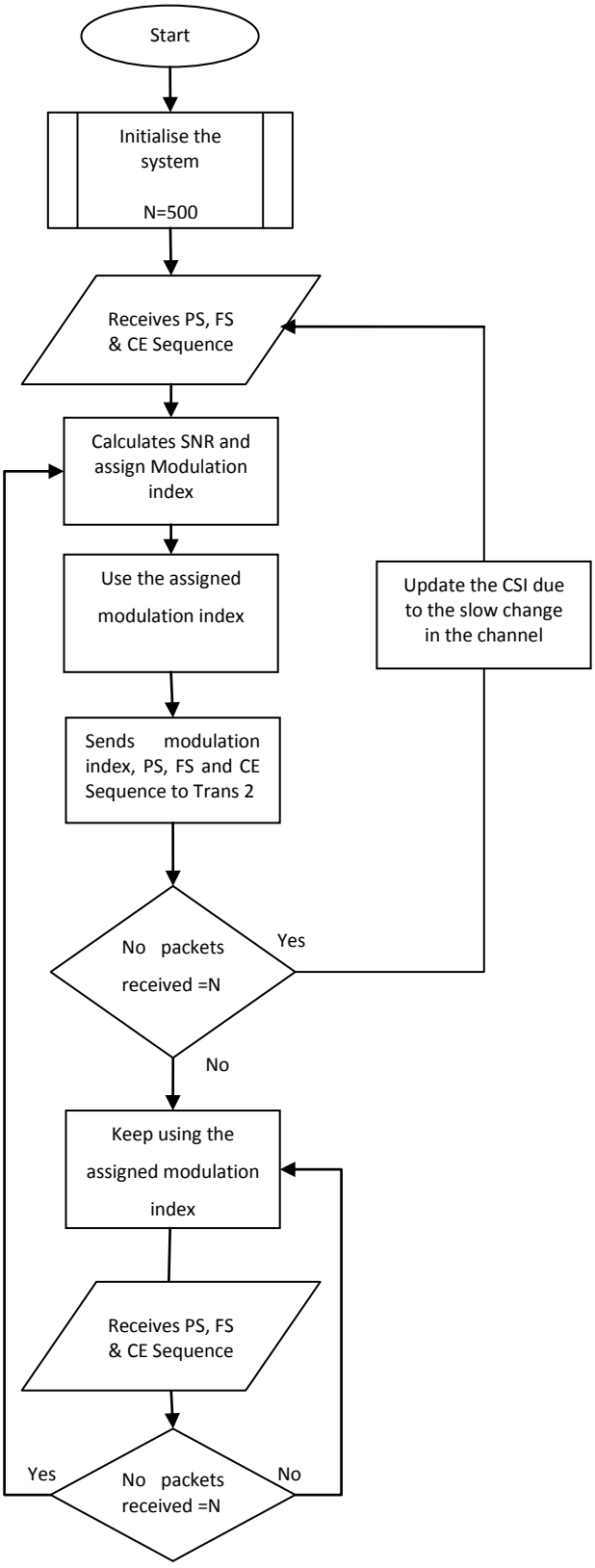


Figure 5.30 Flow chart for CSI (Channel State Information) update

### 5.9 Time varying channel and system simulation

The entire system is simulated using a data rate of 400Mbps. A packet contains 128 OFDM symbols per packet (98 symbols for data). Figure 5.31 shows the Time varying channel block diagram. Since the channel changes every 20ms, the equivalent number of OFDM symbols transmitted with the time frame is 64000. This gives 500 packets when using 128 OFDM symbols per packet at every 20ms. The time varying channel counts the number of symbols and changes the channel impulse response every 500 packets. A counter is used to keep track of the symbol rate which is 3.125e-07s to determine the changes in CIR response 20ms. The model loads a new CIR into the system and then forwards it to the filter block to be combined with the transmitting signal after every 20ms. An embedded Matlab function is used to programme the time varying channel to ensure it synchronises with the system symbol rate.

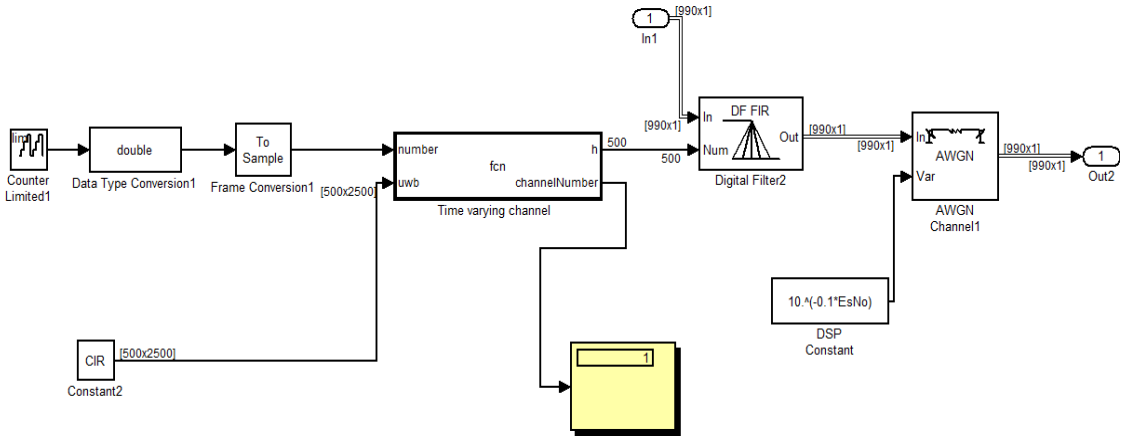


Figure 5.31 Time varying UWB channel

The simulation results for the BER performance of both the adaptive and non adaptive performance of the system are shown in Figures 5.32 -5.33. Figure 5.32 (non-adaptive) shows that for better performance, higher SNR is needed depending on the degree of selective fading in the channel. The more number of people in the vicinity of the device, the greater is the degradation of the channel due to their movement. On the other hand, Figure 5.33 shows the BER performance of the system while using adaptive modulation in time varying channel. An improvement of more than 4dB compared to the non adaptive system is observed. At 14dB, all the channel scenarios give similar performance. This could be due to the feedback rate used, which is 20ms for all the channels. Though the adaptive system has not achieved the full data rate of 400Mbps, it can deliver a closer data rate with a better bit error rate. A large feedback rate may not give the same performance due to various degree of change in the channel in various channels. For an average indoor walking speed at 20ms, a user movement changes by 2cm only while for 140ms the movement changes by 14cm. The adaptive modulation scheme is designed with a BER threshold of a $10^{-4}$. Overall, the results show that very good system

performance can be achieved by implementing 20ms feedback channel rate in the UWB MB-OFDM adaptive system.

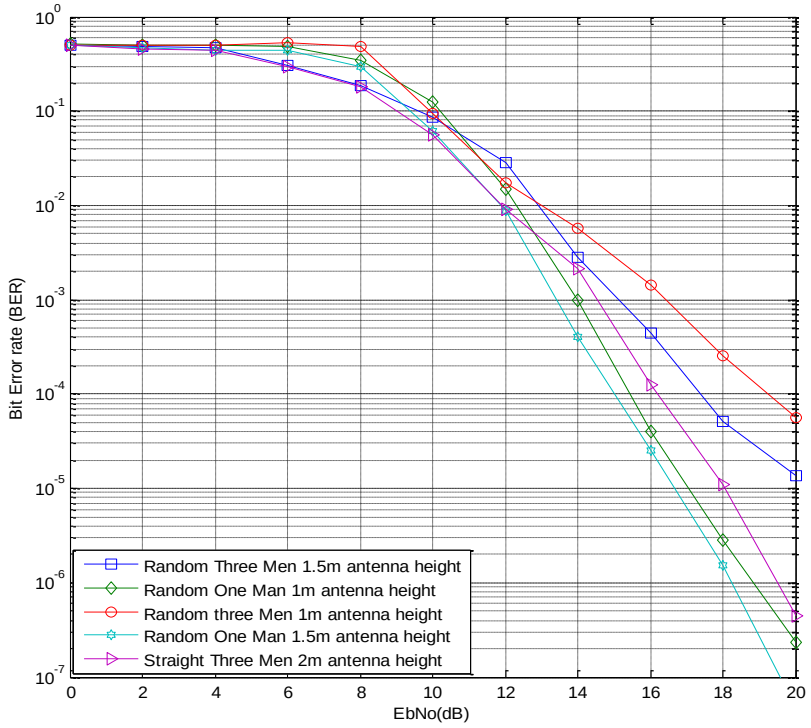


Figure 5.32 BER performances for non Adaptive Modulation with a data rate 400Mbps

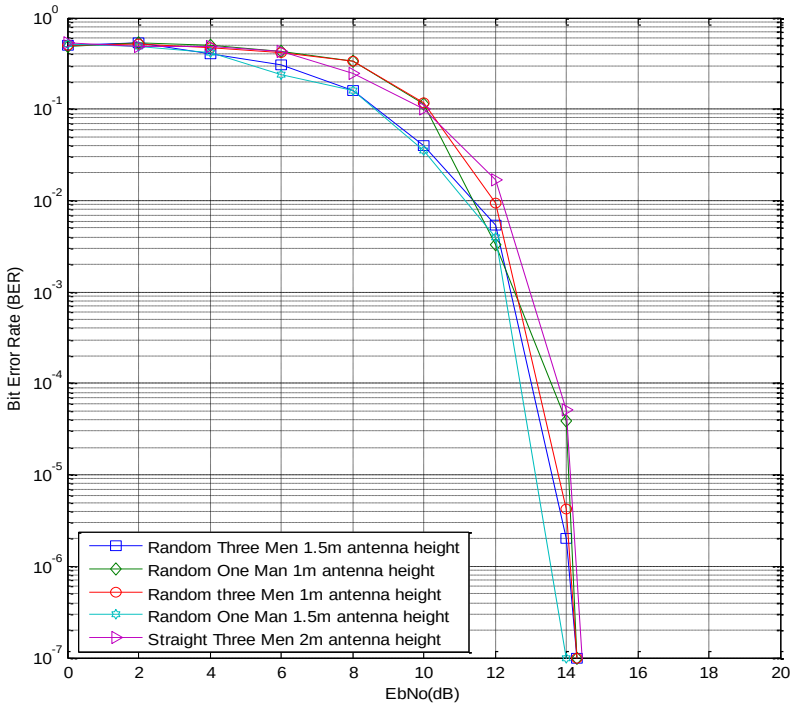


Figure 5.33 BER performances for Adaptive Modulation with a data rate 400Mbps

### 5.10 Summary

In this chapter the channel measurement of different scenarios has been carried out. The scenarios are realistic environments where UWB devices are operating. Effects of different number of human subjects in various movement patterns were studied.

Channel correlation was investigated to monitor the changes in the channel as people move across it. The results show that the number of people moving across the channel and the height of the antenna affect the correlation between the successive channels. Also, maximum deviation in the channel correlation was computed for each scenario.

Channel responses were inputted into the UWB system model to evaluate the system performance while using non-adaptive modulation and adaptive modulation with a feedback rate of 20ms. The results exhibit that implementing adaptive modulation in UWB system enhances the performance of the system. Currently, UWB devices operate below the expected performance which is largely due to its EIRP limit and frequency selective fading. This bottle neck can be eased by implementing the proposed adaptive modulation in the system.

**References**


1. L . Guo, S. Wang, X. Chen and C. Parini, "A Small Printed Quasi-Self-Complementary Antenna for Ultra wideband Systems" *IEEE Antennas and Wireless Propagation Lett*, VOL. 8, 2009
2. PNA Help /RevA.07.50.38, Agilent Technologies, Inc. Accessed 12-08-2011 http://na.tm.agilent.com/pna/help/WebHelp7_5/S0_Start/Using_Help.htm
3. *Service Guide*, Agilent N5224A and N5225A 2-Port and 4-Port PNA Microwave Network Analyzers. Agilent Technologies, Inc .Service Guide N5225-90001, 2011
4. M. Tran, A. Nix, A. Doufexi, "*Mobile WiMax: Impact of Mobility on the Performance of Limited Feedback Linear Precoding* ", 71st IEEE Vehicular Technology Conference (VTC 2010-Spring), 2010 , Taipei pp 1 – 5 , 2010
5. Bell Mobility, "HSDPA and 1xEV-DV Harmonization Opportunities", 2001 3GPP/3GPP2 Joint Meeting on Harmonization of High Speed Data Services. Nov 2001
6. J.E Cabral Jr and Y. Kim," *Multimedia systems for telemedicine and their communication requirement"*, IEEE Commun. Mag., 34:20-27 1996
7. J. Foerster et al ,"*Channel Modelling Sub-committee Report Final",* IEEE P802.15 Working Group for Wireless Personal Area Networks (WPANs) IEEE P802.15- 02/490r1-SG3 ,February 2003
8. Phy Specification: Final Deliverable 1.5 Multiband OFDM Physical Layer Specification , WiMedia Alliance, Inc, 2009

9. S. V. Schell, ”*Analysis of Time Variance of a UWB Propagation Channel* “ IEEE P802.15 Working Group for Wireless Personal Area Networks (WPANs) IEEE P802.15-02/452r0-SG3a Alviso, CA 2002

# CHAPTER 6

**UWB SPATIAL PROCESSING TECHNIQUES**

## 6.1 Introduction

When it comes to developing and enhancing wireless technologies, spatial processing techniques are truly the final frontier that can provide the expected demand. Like other areas, wireless communication also has certain theoretical boundaries which cannot be crossed. The amount of data that can be passed through a channel with noise governed by Shannon's law (Eq (1.1)) which defines the maximum rate at which error free transmission can take place with a given bandwidth. Shannon's law shows that other processing techniques are needed in order to achieve high data rate or provide better link reliability within the constraint of bandwidth. Multipath phenomenon occurs when signals are transmitted to receiver due to reflection, diffraction and scattering caused by various objects such as walls, windows, furniture etc. The multipath can be considered as interference but can also be used to increase the channel capacity and link reliability.

Although modulation plays a part in this, higher modulation scheme can be used to increase the data rate. However, it requires higher or better signal to noise ratio (SNR), which can be a bottle neck for the UWB system due to its regulation. There is a need for a trade off between the modulation scheme, the available SNR and power. Spatial techniques introduce spatial domains to the existing time and frequency dimension thereby increasing the degree of freedom and can be primarily classified into

1. Spatial Multiplexing
2. Spatial Diversity

## 6.2 Spatial Multiplexing

This type of multiplexing transmits different data through different independent spatial communication channels using multiple transmit antennas. These signals are received using multiple antennas at the receiver. This approach increases the data rate with increase in the number of transmit and receive antennas.

In the light of Edholm's law of bandwidth, combining multiple antennas and UWB system yields enormous data capacity in the order of several gigabits. It has been shown that the MIMO UWB Ergodic channel capacity increases approximately linearly with the minimum number of antennas under UWB Nakagami fading channel [1]. Its advantages include increase of data rate without need of additional power or bandwidth. However, combination of MIMO with MB-OFDM UWB needs a trade off between the coverage distance and number of antennas used. Due to the power limitation, the coverage distance is reduced when spatial multiplexing is applied to MB-OFDM UWB.

The feasibility of practical implementation of UWB and MIMO combination is quantitatively characterised by extending the WiMedia specification on link budget to a 2X2 MIMO and 4X4 MIMO scenarios. Figure 6.1 shows a simple link analysis for UWB performance for SISO, 2X2MIMO and 4X4 MIMO configurations using data rates of 110Mbps, 200Mbps and 480Mbps. The line of sight (LOS) case with a packet error rate of 8% is considered. The factors of mutual coupling channel cross correlation and antenna gain are not taken into account. It is observed that for a 4X4 MIMO at 480Mbps (per antenna), the distance between the transmitter and the receiver must be less than 1 metre. This limitation reduces the number of usable high data rate (> 1.5Gbps). The MB-OFDM UWB link budget is calculated as follows:

$$P_R = P_T + G_T + G_R - L_1 - L_2 \text{ (dB)} \qquad 6.1$$

Where $P_R$ is the received power, $P_T$ the transmitted power, $G_T$ is the transmit antenna gain, $G_R$ is the receive antenna gain, $L_1$ is the path loss at 1metre and $L_2$ is the path loss at distance d. $L_1$ is expressed as

$$L_1 = 20\log_{10}(4\pi f_c^{'} / c)) \qquad 6.2$$

With $c = 3\times10^8$ m/s and $f_c^{'}$ is the geometric centre frequency of waveform expressed as

$$f_c^{'} = \sqrt{f_{\min} f_{\max}} \qquad 6.3$$

Where $f_{\min}$ and $f_{\max}$ are the -10 dB edges of the waveform spectrum. The path loss at d called $L_2$ is expressed as

$$L_2 = 20\log_{10}(d) \qquad 6.4$$

The receiver sensitivity comprises of the minimum detectable threshold i.e. required Eb/No from the acceptable error level and is expressed as

$$N = -174 + 10*\log_{10}(R_b) + N_F + EbNo(dB) \qquad 6.5$$

Where $R_b$ is the data rate, $EbNo$ is the required signal to noise ratio able to decode the signal, $N_F$ is the receiver noise figure and -174dBm is the thermal noise per hertz. The

primary sources for the noise figure are the mixer and low noise amplifier (LNA). The implementation loss based on the WiMedia specification is set to be in the range of 2.5 to 3dB depending on the data rate. Table 6.1 summaries the WiMedia link budget specification for MB-OFDM UWB system.

Table 6.1 Wimedia MB-OFDM Link budget Specification [2]

| **Parameter: Mode 1 DEV (3-band)** | **Value** | **Value** | **Value** |
|---|---|---|---|
| Information data rate ($R_b$) | 110 Mb/s | 200 Mb/s | 480 Mb/s |
| Average Tx power ($P_T$) | -10.3 dBm | -10.3 dBm | -10.3dBm |
| Tx antenna gain ($G_T$) | 0 dBi | 0 dBi | 0 dBi |
| Geometric centre frequency of waveform | 3882 MHz | 3882 MHz | 3882 MHz |
| Path loss at 1 m $L_1$ | 44.2 dB | 44.2 dB | 44.2 dB |
| Path loss at $d$ m $L_2$ | 20 dB ($d$ = 10 m) | 12 dB ($d$ = 4 m) | 6 dB ($d$ = 2 m) |
| Rx antenna gain ( $G_R$ ) | 0 dBi | 0 dBi | 0 dBi |
| Rx power ( $P_R$ ) | -74.5 dBm | -66.5 dBm | -60.5 dBm |
| Average noise power per bit | -93.6 dBm | -91.0 dBm | -87.2 dBm |
| Rx NF Referred to Antenna Terminal ( $N_F$ ) | 6.6 dB | 6.6 dB | 6.6 dB |
| Average noise power per bit $P_N$ | -87.0 dBm | -84.4 dBm | -80.6 dBm |
| Required $E_b/N_0$ ($S$) | 4.0 dB | 4.7 dB | 4.9 dB |
| Implementation Loss(I) | 2.5 dB | 2.5 dB | 3.0 dB |
| **Link Margin** | 6.0 dB | 10.7 dB | 12.2 dB |
| **Proposed Min. Rx Sensitivity Level** | -80.5 dBm | -77.2 dBm | -72.7 dBm |

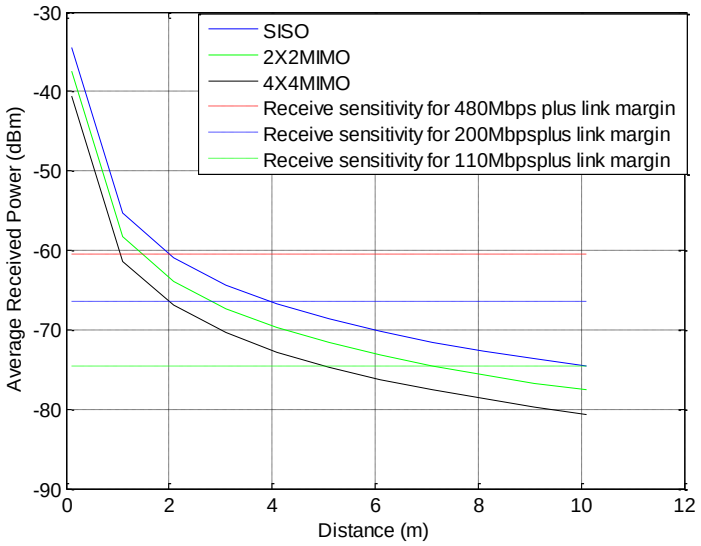


Figure 6.1 Link analysis based on Wimedia Link budget Specification for data rate of 110Mbps, 200Mbps and 480Mbps

The figure shows the trade off between the data rate and the distance where the performance will be acceptable. The higher the choice of data rate and antenna branches the small the distance. For high data rate, MIMO –OFDM UWB could only be used in applications where the separating distances is around 1m.

### 6.3 Spatial Diversity

A channel with deep fades can result in complete loss of signal. Spatial diversity is a technique used to reduce the effect of fading in the channel and improves the performance of the communication system. Signals are transmitted through one or multiple transmitter and are passed through independent channels making them to experience different and independent fading. These signal are then received through a number of receive antennas. When multiple copies of the same signal passes through different channels with independent fading, there is a high probability not all will experience deep fading. These different received signals can be compared or combined using different methods to increase the power and to enable better interpretation of the received signals. Spatial diversity can either be implemented on the transmitting side called transmit diversity or on the receiving side called receive diversity. For this study, antenna selection and Maximal Ratio Combining are used to implement spatial diversity in the UWB system.

#### 6.3.1 Antenna Selection (AS)

This method simply compares the SNR of different antennas and selects the one with the strongest SNR. Each element compared is considered to have an independent fading process. It can be expressed as

$$w_i = \begin{cases} 1, & y_i = \max(y) \\ 0, & otherwise \end{cases} \qquad 6.6$$

where $w_i$ is the weight factor and $y_i$ is the signal with the highest average SNR. In MB-OFDM UWB, each sub-channel is considered to have undergone flat fading. Hence, the SNR of one sub-channel differs from the other. In this case, the average SNR is used in the selection process and is expressed as

$$Avr.SNR = \frac{\sum_{i=1}^{N} \frac{[H_i]^2.[X_i]^2}{\varepsilon^2}}{N} \qquad 6.7$$

where Avr.SNR is the average signal to noise ratio of the OFDM symbol, H is the channel coefficient of the $i_{th}$ sub channel in the OFDM symbol, X is the transmitted symbol of the $i_{th}$ sub channel in the OFDM symbol and $\mathcal{E}$ is the noise variance in the OFDM symbol. This method is not the most efficient since some sub-carriers with little or no fading will be discarded when the average SNR is not the best among the three antennas. Figure 6.2 illustrates the simulation process of the antenna selection technique in simulink.

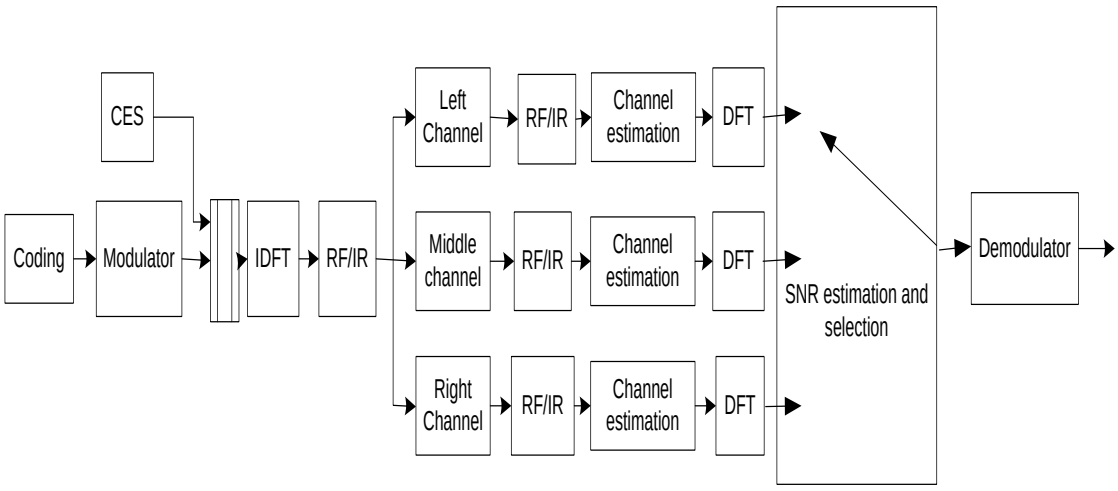


Figure 6.2 Antenna Selection technique

### 6.3.2 Maximal Ratio Combining (MRC)

In this method each of the received signals is weighted with a factor that is proportional to the signal amplitude. The branches with stronger signals are further amplified while the ones with weak signals are attenuated. This can be expressed as [8]

$$y_i = \sum_{j=1}^{J} r_{j,i}\, w_{j,i} = \sum_{j=1}^{J} (h_{j,i}\, x_i + n_{j,i})\, w_{j,i} \qquad 6.8$$

$$= \left( \sum_{j=1}^{J} h_{j,i}\, w_{j,i} \right) x_i + \sum_{j=1}^{J} n_{j,i}\, w_{j,i} \qquad 6.9$$

where $y_i$ is the received signal from all the antenna elements, $r_{j,i}$ is the signal received from antenna j, $w_{j,i}$ is the weight factor for the receive signal $r_{j,i}$ and for i sub channel, h is the CIR for sub channel i and signal j. x is the transmitted signal. The instantaneous SNR can be expressed as

$$\gamma = \frac{\left| \sum_{j=1}^{J} h_{j,i}\, w_{j,i} \right|^2}{\frac{1}{2} E\left[ \left| \sum_{j=1}^{J} h_{j,i}\, w_{j,i} \right|^2 \right]} \qquad 6.10$$

Where $\gamma$ is the instantaneous SNR. To get the maximum weight, the conjugate of the Channel Impulse Response (CIR) is used which can be express as

$$w_{j,i} = h_{j,i}^{*} \qquad 6.11$$

where $h_{j,i}^{*}$ is the conjugate of $h_{j,i}$. Since each sub-channel experiences different fading in OFDM UWB, the weight of each sub-channel is determined individually. Based on the WiMedia specification each packet has a Channel Estimation Sequence (CES) which can be used at the beginning to estimate the channel [2]**.** From the channel estimation sequence, the channel response can be determined. Figure 6.3 shows the implementation of the maximal ratio combining (MRC) technique in simulink. Each channel response from the SIMO channel

measurement is inputted into the model for simulation. Each channel is estimated using CES and the conjugate is taken. This amplifies stronger signals over the weaker signals. The signals from all the three antennas are then summed up and forwarded for demodulation.

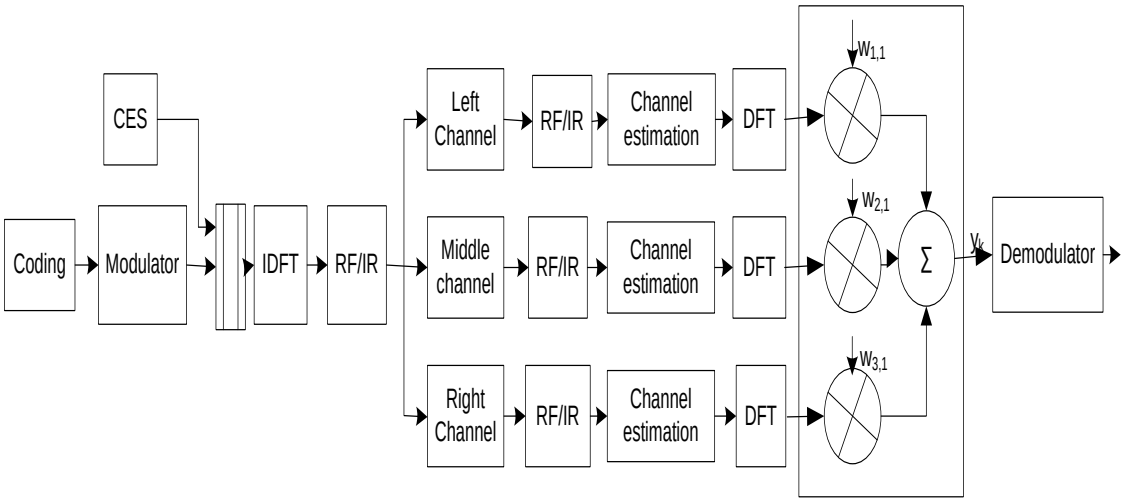


Figure 6.3 Maximal Ratio combining technique

### 6.4 SIMO Channel Measurement

SIMO channel measurements for a typical indoor environment are carried out in order to evaluate the impact of using the spatial diversity in the MB-OFDM UWB system. Figure 6.4 shows the LOS and NLOS environment while taking the measurement. The indoor environment used in the measurements is the Wireless Sensor Laboratory at Queen Mary, University of London. Layout of the laboratory is shown in Figure 5.1.

Figure 6.4 Pictures showing the LOS and NLOS measurements taking place

The channel model given in [6] can be used to express this scenarios as the receive antennas experience similar clustering when closely packed. This is expressed in Equation 4.14. An Agilent PNA N5230A Network Analyser is used to measure the channel in the UWB band 1 frequency range of 3.168GHz to 4.752GHz. The distance and height of transmit and receive antennas are 3m and 1.2m respectively. Table 6.2 gives the parameters used in the measurement setup. The measured channel transfer function is transformed to the time

domain. The Channel Impulse Response for each transmit-receiver pair is pre-processed using the technique described in [7], which is then used in the simulink model of the MB-OFDM UWB to evaluate the system performance.

TABLE 6.2 Parameters used for measurements

| **Parameter** | **Value** |
|---|---|
| Frequency range (GHz) | 3.162-4.572 |
| Number of Frequency points | 384 |
| Tx Antenna height (m) | 1.2 |
| Rx Antenna Height (m) | 1.2 |
| Distance between Tx and Rx antennas(m) | 3 |

Two types of UWB antennas were used for the SIMO measurements; they are patch antennas and monopole antennas. The patch antennas are quasi self complementary antennas which are designed and same as describe in chapter 4. The antennas offer UWB impedance bandwidth with satisfactory properties [5].Figure 6.5 shows the pictures of the antennas and Table 6.3 shows the ratio of the varied distances used to the wavelength of the centre frequency.

TABLE 6.3 Varying distances used for the channel measurements

| **Antenna Spacing (cm)** | **Band 1 ($f_c$=3.432GHz, $\lambda_1$=8.7)** | **Band 2 ($f_c$=3.96GHz, $\lambda_2$=7.6)** | **Band 3 ($f_{c=}$ 4.488GHz, $\lambda_3$=6.68)** |
|---|---|---|---|
| 2.5 | $0.27\lambda_1$ | $0.33\lambda_2$ | $0.37\lambda_3$ |
| 5 | $0.57\ \lambda_1$ | $0.66\ \lambda_2$ | $0.75\ \lambda_3$ |
| 7.5 | $0.86\ \lambda_1$ | $0.99\ \lambda_2$ | $1.12\ \lambda_3$ |
| 10 | $1.14\ \lambda_1$ | $1.32\ \lambda_2$ | $1.50_3$ |

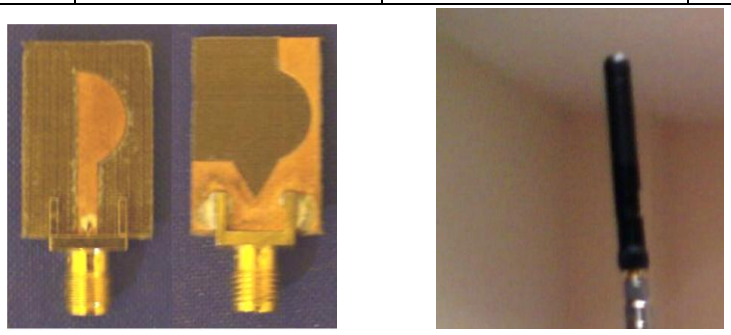

(a) (b)

Figure 6.5 (a) quasi-self-complementary antenna, front and back side. (b) Monopole antenna

### 6.5 Spatial Correlation

Spatial correlation can be interpreted as a correlation between a signal's spatial direction and the average received signal gain. In spatial diversity, the degree of correlation between the channels affect the performance of the diversity because the lesser the correlation the better the performance of the system. Spatial correlation coefficient is calculated from the set of channel responses in the frequency domain using the following expression [9]:

$$\rho(H_1, H_2) = \frac{\varepsilon\{H_1 {H_2}^{\dagger}\} - \varepsilon\{H_1\}\varepsilon\{{H_2}^{\dagger}\}}{\sqrt{\left(\varepsilon\{{H_1}^2\} - |\varepsilon\{H_1\}|^2\right)}\sqrt{\left(\varepsilon\{{H_2}^2\} - |\varepsilon\{H_2\}|^2\right)}} \qquad 6.12$$

Where $\rho$ denote spatial correlation coefficient, $\varepsilon\{.\}$ is the expectation and $\{.\}^{\dagger}$ represents conjugate. For the UWB channel, $H_1$ and $H_2$ represent the channel transfer function for the two channels. The spatial correlation coefficient signifies the correlation between the received signals at the different locations from the same transmitter. The value of correlation coefficient varies from 0 to 1. Most of the calculated spatial correlations of the measured signal fall below 0.6, which could be acceptable and can bring remarkable diversity base on the study carried out in [10].

In a narrow band system, an increase in the antenna spacing leads to a decrease in the correlation while a decrease in the spacing increases the correlation. This is different from the simulation results, which show close performance over different antenna spacing from 2.5 cm to 10cm. This is due to the wideband nature of the signal and the frequency selective fading the channel experiences as compared to the narrowband systems that only experiences flat fading.

Different antenna orientations were considered when taking measurement to study the performance of UWB systems. The orientations used are

1. Vertical orientation

   The antennas were place in a vertical position when taking measurement.

2. Horizontal Orientation

   For the horizontal orientation, the antennas were placed 90 degree from the vertical antenna.

Due to space and size limitations of consumer electronics, combining different antenna orientations could be the most desirable approach while implementing antenna diversity. Devices such as external drives, displays etc might require different antenna orientations to implement the diversity.

### 6.6 System Simulation and Discussion

The MB-OFDM UWB system is simulated using a data rate of 400Mbps. The data rate of 400Mbps is achieved with code rate of 5/8 without using frequency and time domain spreading. This model is a modified version of the one described in [11] to implement the MRC and antenna selection technique using 2 and 3 antennas. For Simulation results and discussion while using two antenna branches, please see appendix E. In Simulink, determining the delay between the transmitting data and the receiving data can be tedious but the best approach is

to trace the data block to block and estimate the delay introduced by each block. Estimating the delay accurately will synchronise the transmitted data with the received data for the error block to compute the BER. Different antenna orientations are considered in modelling and simulating the system in order to determine the performance of spatial diversity.

### 6.6.1 Three Patch Antennas in Vertical Orientation

First, three antennas in vertical orientation are investigated as shown in Figure 6.6. Figures 6.7 and 6.8 show the bit error rate (BER) performance for both the MRC and antenna selection technique with the antennas placed at different distances in a LOS and a NLOS environment. The antennas are placed vertically and are all patch antennas. The left and right antennas spaced from 2.5cm to 10cm away from the middle antenna. It is observed that the MRC technique generates similar performances for different antenna spacing.

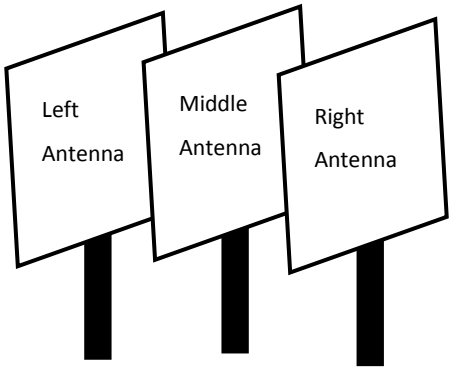


Figure 6.6 Simulation of three patch antennas placed in vertical orientation

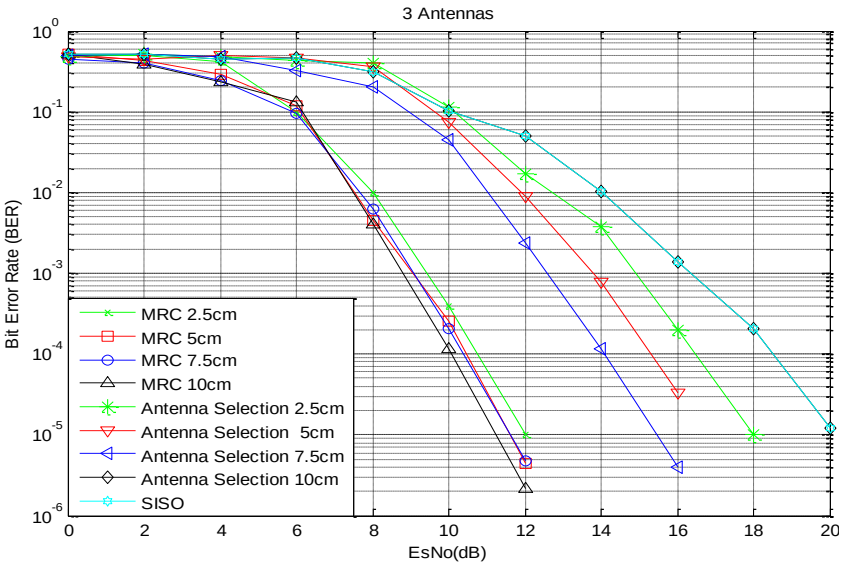


Figure 6.7 BER performance of the SIMO UWB system in a LOS environment

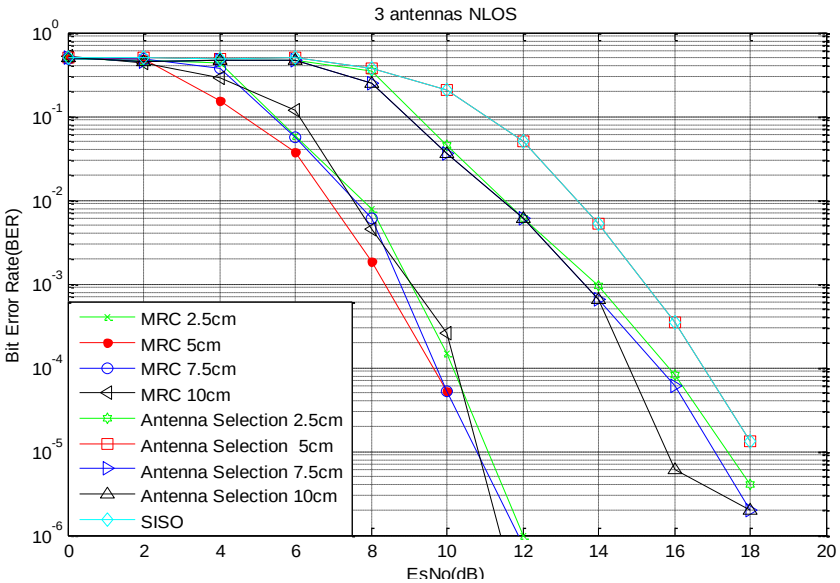


Figure 6.8 BER performance of the SIMO UWB system in a NLOS environment

The BER values at 12dB show that a good performance is achieved in both the NLOS and LOS environment. It should be noted that normalised values of CIR are used in the model. For the MRC, at an average EsNo of 12 dB, the BER performance lies between 9e-6 and 2.19e-6 for the antenna spacing of 2.5cm and 10cm respectively. This results in a PER of 2% for 2.5cm spacing while 0.5% for 10cm spacing using the following equation [12]

$$P_{PER} = 1 - (1 - P_{BER})^N \qquad 6.13$$

where $P_{PER}$ is the packet error rate, $P_{BER}$ is the bit error rate and N is the length of the payload. Table 6.4 summarises PER, LOS and NLOS scenarios while table 6.5 shows the spatial correlation between the channels. The results show that at 2.5cm antenna spacing, the correlation is 0.6 for the LOS measurement. It decreases when the antenna spacing increases. For the NLOS scenarios, the correlation is lower than 0.5 which gives good diversity gain. It could be seen that these values are well below the acceptable packet error rate (PER) threshold of 8% [3].

Table 6.4 PER of simulated result at an EsNo 12dB with a payload of 1kb with MRC

| **Antenna spacing (cm)** | **BER with 3 antennas (LOS)** | **Packet Error Rate (%)(LOS)** | **BER with 3 antennas (NLOS)** | **Packet Error Rate (%)(NLOS)** |
|---|---|---|---|---|
| 2.5cm | 9.99E-06 | 1.02 | 1E-06 | 0.1 |
| 5cm | 4.40E-06 | 0.45 | 1e-7 | 0.01 |
| 7.5cm | 4.80E-06 | 0.49 | 8E-07 | 0.08 |
| 10cm | 2.19E-06 | 0.23 | 1E-07 | 0.01 |

Table 6.5 Spatial correlation coefficient of the patch antennas

| Antenna Spacing | 2.5cm | 5cm | 7.5cm | 10cm |
|---|---|---|---|---|
| Middle and Left Ant with LOS | 0.6137 | 0.2916 | 0.4063 | 0.3617 |
| Middle and Right Ant with LOS | 0.6271 | 0.2619 | 0.3465 | 0.2489 |
| Middle and Left Ant with NLOS | 0.3707 | 0.0548 | 0.2790 | 0.2857 |
| Middle and Right Ant with NLOS | 0.2548 | 0.2058 | 0.2392 | 0.4727 |

### 6.6.2 Three Patch Antennas, One in Vertical Orientation and Two in Horizontal Orientation

Now, three antennas in different orientation are investigated. The orientation of the side antennas are varied 90 degree with respect to the middle antenna vertically positioned. Hence, the left and right antennas are horizontally oriented as shown in Figure 6.9.

Figure 6.10 and 6.11 shows the BER performances while using 3 antennas for both LOS and NLOS condition. The results show an average gain of 4dB for both the NLOS and LOS environment. This is 2dB less than the BER performance achieved with three antennas in vertical orientation (Figure 6.7 and Figure 6.8). The horizontal receive antennas are normalised to the magnitude of the vertical antenna to maintain the power difference between the antennas. It can be expressed as

$$E = \frac{h_x}{|h_m|} \qquad 6.14$$

Where $h_x$ is the CIR of either the left ($h_l$), middle ($h_m$), or right antenna ($h_r$), and $h_m$ is the CIR of the middle antenna (in vertical position). The antennas are linearly polarised and the transmit antenna is in a vertical position which will make the horizontally placed antennas at the receiver to receive lower power. In the NLOS environment, 4dB gain is achieved using the MRC technique for varied antenna spacing except for the 2.5cm spacing which achieved only a 2.5dB gain. In general, these results show that spatial diversity can be implemented in UWB devices where space is limited to improve the performance of the system such as small portable consumer electronics. Tables 6.6 and 6.7 summarised the PER and spatial correlation between the channels respectively. The correlation coefficients between the channels are low. The results show that for varying the antenna spacing, the correlation is 0.36 for LOS, while it is 0.42 for NLOS. This gives remarkably diversity gain. Also, the PER results show that error rates are below the acceptable value except for the 5cm NLOS spacing which has an error rate of 11%. It is evident from these results that the performance of the UWB system could be enhanced greatly using spatial diversity.

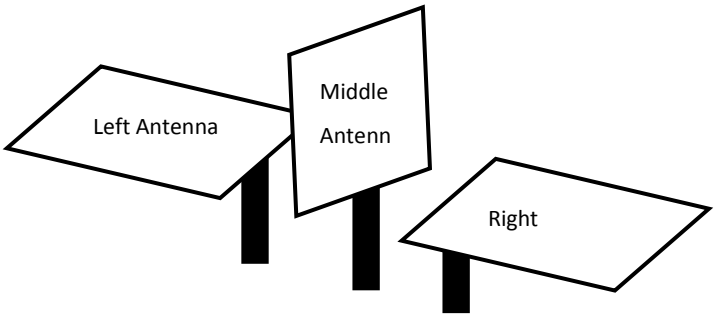


Figure 6.9 Simulation of three patch antennas, one placed in vertical orientation and two in horizontal orientation

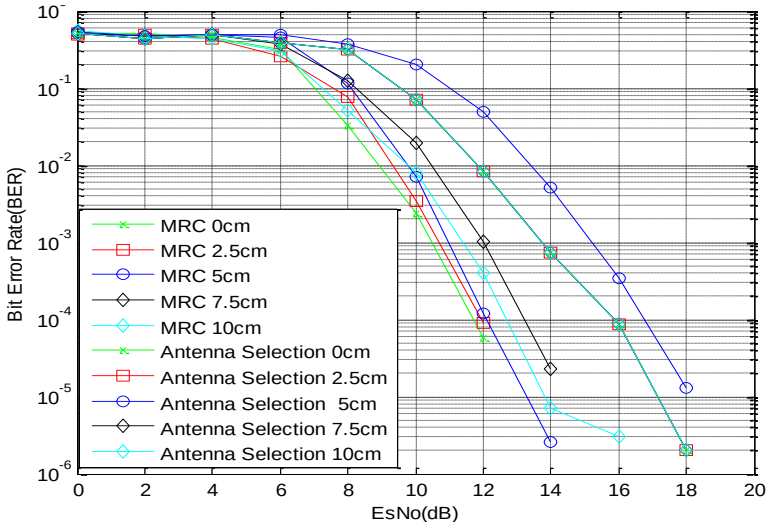


Figure 6.10 BER performance of the SIMO UWB system in a LOS environment

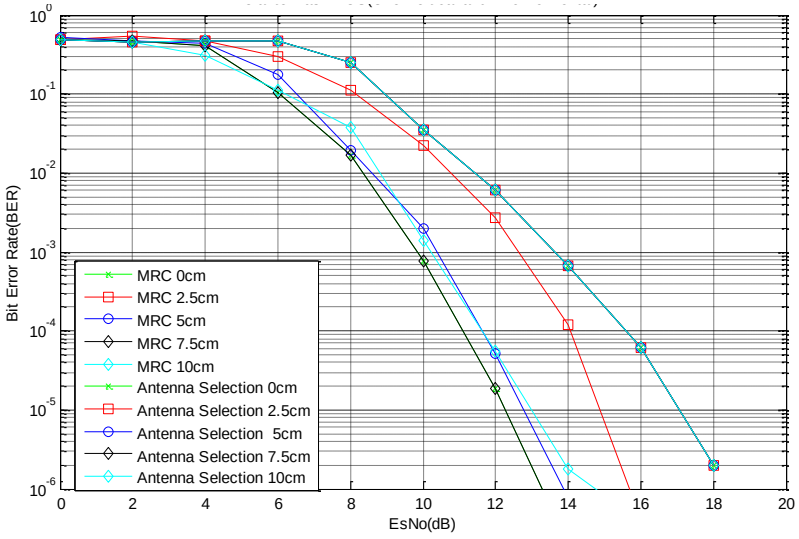


Figure 6.11 BER performance of the SIMO UWB system in a LOS environment

TABLE 6.6 PER of the simulated result using a payload size of 1kb at 14dB with MRC

| Antenna spacing (cm) | BER with 3 antennas (LOS) | Packet Error Rate (%)(LOS) | BER with 3 antennas (NLOS) | Packet Error Rate (%)(NLOS) |
|---|---|---|---|---|
| 0cm | 7e-6 | 0.7 | 1.8e-6 | 0.18 |
| 2.5cm | 1e-7 | 0.01 | 2e-7 | 0.02 |
| 5cm | 1e-7 | 0.01 | 0.00012 | 11.56 |
| 7.5cm | 2.6e-6 | 0.26 | 8E-07 | 0.082 |
| 10cm | 2.3 e-05 | 0.44 | 2E-07 | 0.02 |

Table 6.7 Spatial correlation coefficient of three patch antennas, one placed in vertical orientation and two in horizontal orientation antennas

| Antenna Spacing | 2.5cm | 5cm | 7.5cm | 10cm |
|---|---|---|---|---|
| Middle and Left Ant with LOS | 0.2259 | 0.1489 | 0.1009 | 0.3495 |
| Middle and Right Ant with LOS | 0.2923 | 0.0187 | 0.2365 | 0.3617 |
| Middle and Left Ant with NLOS | 0.1983 | 0.0064 | 0.1977 | 0.1790 |
| Middle and Right Ant with NLOS | 0.2457 | 0.2729 | 0.1472 | 0.2447 |

### 6.6.3 Three Monopole Antennas in Vertical Orientation

Three monopole antennas placed vertically are considered here as shown in Figure 6.12. Figure 6.13 and 6.14 shows the BER performance using three antennas for LOS and NLOS. An average gain of 6dB for both the LOS and NLOS environments can be observed. It shows a very interesting improvement, with the LOS case achieving a good performance at 6dB. Table 6.8 gives the PER while Table 6.9 summarises the spatial correlation between the channels. The table shows that at 10cm antenna spacing for the LOS measurement, the correlation is seen to be about 0.35, while it decreases for the other antenna spacing. For the NLOS scenarios, all the correlations are lower than 0.3. The results show a system performance with good diversity gain.

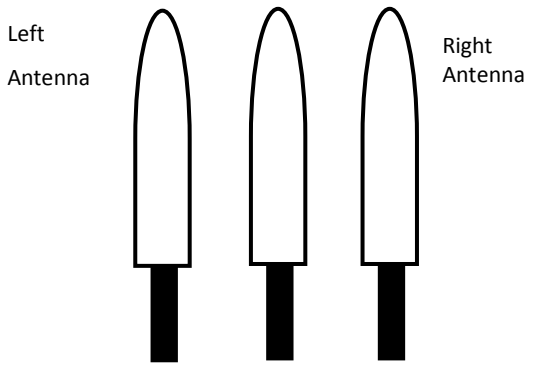


Figure 6.12 Simulation of three monopole antennas in vertical position

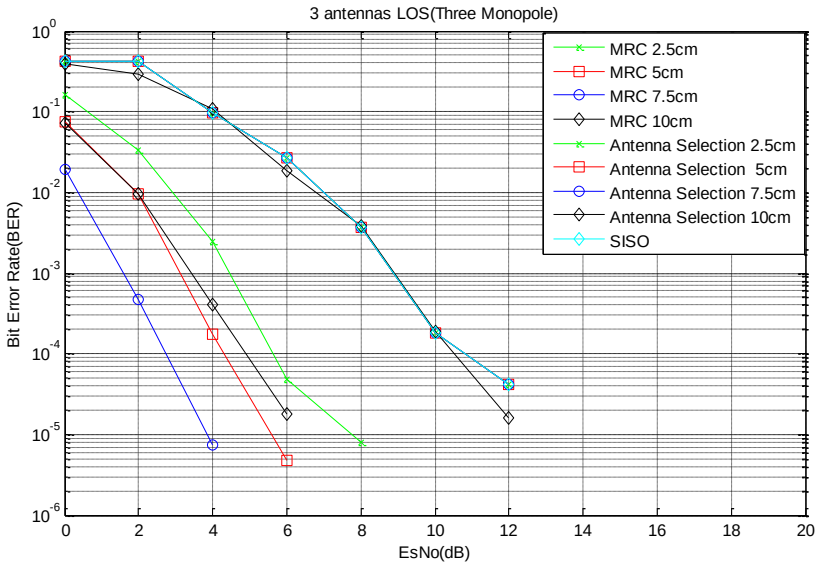


Figure 6.13 BER performance of the SIMO UWB system in a LOS environment

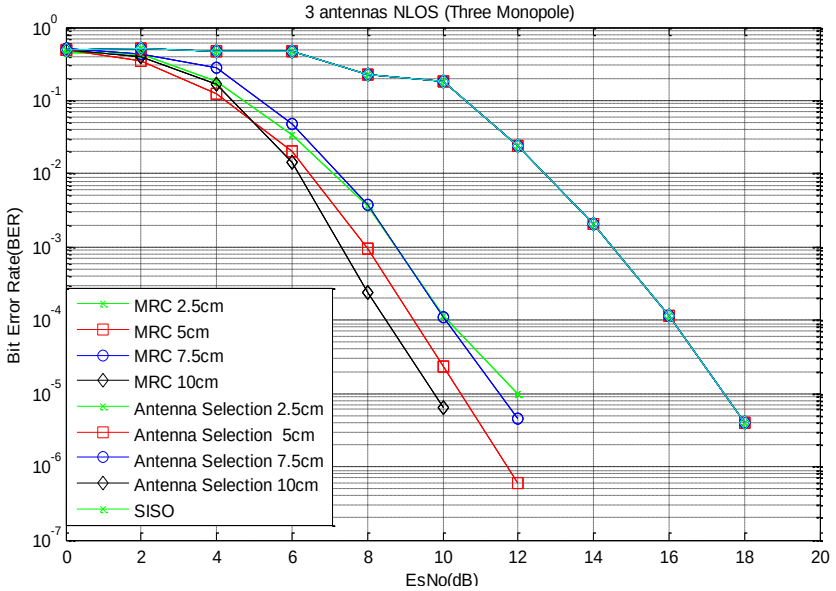


Figure 6.14 BER performance of the SIMO UWB system in a NLOS environment

TABLE 6.8 PER of the simulated result using a payload size of 1kb with MRC

| **Antenna spacing (cm)** | **BER with 3 antennas (LOS)- 6dB** | **Packet Error Rate (%)(LOS)** | **BER with 3 antennas (NLOS)- 12dB** | **Packet Error Rate (%)(NLOS)** |
|---|---|---|---|---|
| 2.5cm | 4.9e-5 | 0.1 | 1e-05 | 0.1 |
| 5cm | 4.8e-6 | 0.06 | 6.0e-07 | 0.06 |
| 7.5cm | 1-e07 | 0.01 | 4.6e-06 | 0.47 |
| 10cm | 1.76e-5 | 0.23 | 1e-07 | 0.01 |

TABLE 6.9 Spatial correlation coefficient three monopole

| Antenna Spacing | 2.5cm | 5cm | 7.5cm | 10cm |
|---|---|---|---|---|
| Middle and Left Ant with LOS | 0.2923 | 0.1075 | 0.2365 | 0.3495 |
| Middle and Right Ant with LOS | 0.2259 | 0.1489 | 0.1806 | 0.3617 |
| Middle and Left Ant with NLOS | 0.1983 | 0.0064 | 0.1472 | 0.1790 |
| Middle and Right Ant with NLOS | 0.2457 | 0.2729 | 0.1977 | 0.2447 |

### 6.6.4 Three Antennas, One monopole and two patch antennas

Two patch antennas in horizontal orientation and a monopole antenna in vertical orientation were used for this set-up as shown in Figure 6.15. Figure 6.16 and 6.17 shows the BER performance for the LOS and NLOS. An average gain of 4dB is realised by the MRC technique. Table 6.10 shows the PER results while Table 6.11 gives the spatial correlation between the channels. For the NLOS an average gain of 6dB is achieved. For the LOS environment, an average gain of 2dB is observed. From Table 6.7, the spatial correlations for the LOS is lower than 0.5. That should have improved the performance of the spatial diversity but only 2db gain is obtained. More results are shown and discussed in the Appendix E.

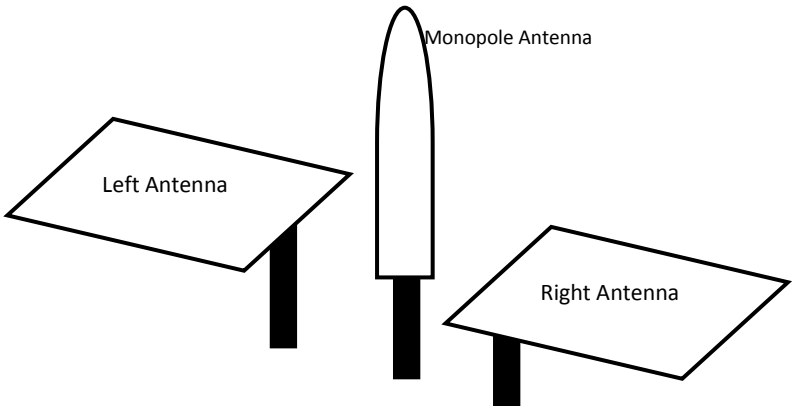


Figure 6.15 Simulation of three antennas, one monopole antenna placed in vertical orientation and two patch antennas in horizontal orientation

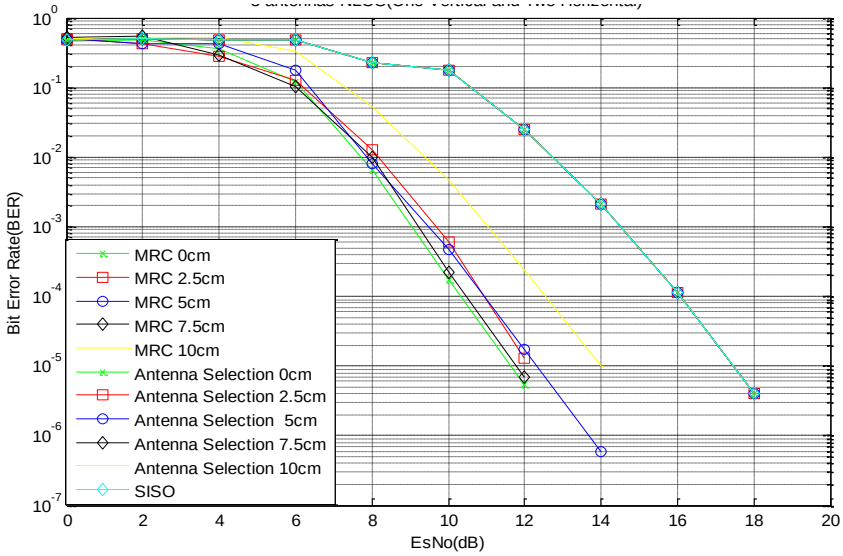


Figure 6.16 BER performance of the SIMO UWB system in a LOS environment

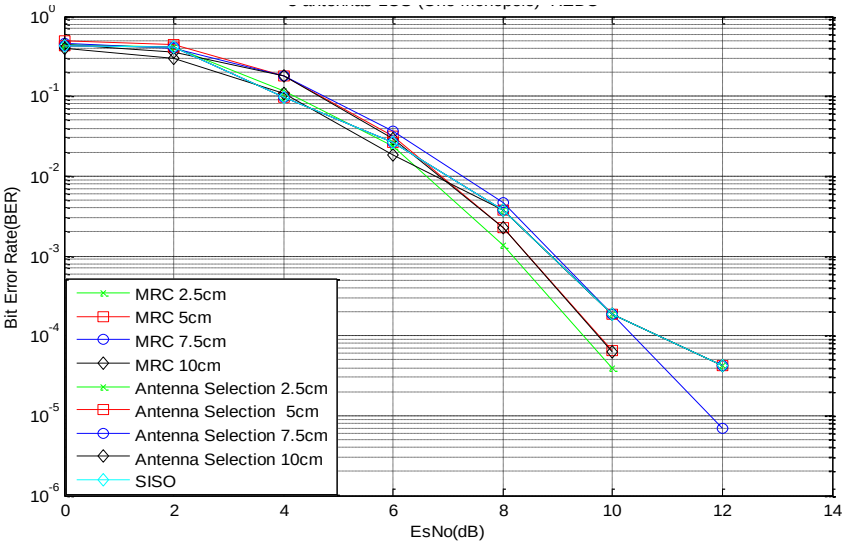


Figure 6.17 BER performance of the SIMO UWB system in a LOS environment

TABLE 6.10 PER of the simulated result using a payload size of 1kb at 12dB with MRC

| **Antenna spacing (cm)** | **BER with 3 antennas NLOS** | **Packet Error Rate (%)(LOS)** | **BER with 2 antennas LOS** | **Packet Error Rate (%)(NLOS)** |
|---|---|---|---|---|
| 0 | 3.6e-6 | 0.4 | 0.000237 | 21 |
| 2.5cm | 1e-7 | 0.01 | 5.5E-06 | 0.57 |
| 5cm | 1e-7 | 0.01 | 1.30E-05 | 1.4 |
| 7.5cm | 7e-6 | 0.71 | 1.74E-05 | 1.7 |
| 10cm | 1e-7 | 0.01 | 7E-6 | 0.71 |

TABLE 6.11 Spatial correlation coefficient of three antennas (one monopole and two patch)

| Antenna Spacing | 2.5cm | 5cm | 7.5cm | 10cm |
|---|---|---|---|---|
| Middle and Left Ant with LOS | 0.2659 | 0.0832 | 0.2293 | 0.1826 |
| Middle and Right Ant with LOS | 0.0025 | 0.1724 | 0.1670 | 0.3539 |
| Middle and Left Ant with NLOS | 0.1010 | 0.1418 | 0.1843 | 0.1952 |
| Middle and Right Ant with NLOS | 0.1213 | 0.0198 | 0.1069 | 0.0181 |

## 6.7 Comparison of spatial diversity techniques

MRC and AS techniques are compared in view of their SNR improvement and complexity. In terms of complexity, AS technique is the simplest and easiest to implement as it only requires the SNR of each antenna to be computed. After SNR computation, the antenna with the maximum SNR is selected. Information regarding the phase is not required and the combiner doesn't need to be coherent as the signals are only selected and not combined. On the other hand, MRC requires phase information and accurate gain measurement. For an OFDM system the technique requires the number of Discrete Fourier transform (DFT) processor to be the same as the number of the antennas. Hence, the computational complexity will increase as the number of antennas increases.

From the simulation results in Figures 6.7-6.17, the best SNR improvement is achieved using the MRC technique. The AS technique gave less improvement compared to the MRC technique. The antenna configuration that gives the best performance depends on the applications, whether the transmit and receive antennas are fixed or mobile. When the transmit and receive antennas are fixed, then placing the antennas in the same orientation gives the best performance. Considering when one or both antennas are mobile then placing at antenna in both vertical and horizontal orientation will give the best orientation.

## 6.8 Pre and post combining diversity scheme

In an OFDM system, the signals are first transformed using DFT processors and the OFDM signal divided into sub channels before combining the signals on sub channel by sub channel basis. The bandwidths of the sub channels are narrower than the coherent bandwidth of multipath fading channel.

Although the Post Combining Diversity scheme is optimum in terms of its BER performance, it increases the computational complexity, since it requires the same numbers of DFT processors as the number of antennas. This is not a major problem for stationary WPAN devices like DVD, TV, monitors as these have no space limitation. On the other hand, implementing Post DFT could be difficult in space-limited hand-held devices. In order to reduce the complexity of implementing diversity in OFDM, pre-DFT is preferred though pre-DFT introduced network overhead due to the feed back channel. A trade off between the feedback rate and the network overhead is required for optimum performance.

## 6.9 Summary

This chapter provides an overview of spatial processing techniques using multiple antennas. Multi antenna methods can be employed to exploit different properties of the radio channel to improve performance. Viability of a diversity system was demonstrated in measurements and the channels are combined using maximal ratio combining and antenna selection techniques.

Spatial diversity was employed to improve the system performance by achieving high data rates. The SIMO channel measurements were carried out for a typical indoor environment to replicate realistic channel scenario in the system simulation.

The limitation of MIMO-UWB when using spatial multiplexing was considered in terms of its expected coverage distance. The WiMedia link budget specifications for SISO are extended to the MIMO scenarios. The results show that the coverage distance reduces when implementing MIMO spatial multiplexing on MB OFDM UWB.

Different antenna orientations were used to model scenarios with space constraints. The results showed that good diversity gain could be achieved using different orientations. Also, different UWB antennas were used to study the performance of diversity in UWB system. The results showed that the performance can be improved using diversity. A minimum diversity gain of 4dB is achieved using three antenna configurations while a minimum gain of 2.5dB is achieved with two antennas. The performance could be improved further if circular polarised UWB antennas are used. The results of the simulink simulations show that both the LOS and the NLOS channel performance can be improved with spatial diversity.

**References**


1. H. Arslan et al (Ed) "*Ultra Wideband Wireless Communication* ".EURASIP Book Series on Signal Processing and Communications, Volume 5. New York, John Wiley & Sons, Inc. Publication 2006
2. A. Batra, "Multiband OFDM Physical Layer Proposal for IEEE 802.15 Task Group 3a" MBOA-SIG (Multiband OFDM Alliance) ,2004
3. PHY Specification: Final Deliverable 1.5 Multiband OFDM Physical Layer Specification , WiMedia Alliance, Inc ,2009
4. AT91CAP9 UWB-EK Evaluation kit, User guide and technical documents (6457A–CAP–11-Jun-09). Atmel,2009

5. L. Guo, S. Wang, X. Chen and C. Parini, “A Small Printed Quasi-Self-Complementary Antenna for Ultra wideband Systems” IEEE Antennas and Wireless Propagation Lett, VOL. 8, 2009
6. T. Kaiser and F. Zheng, Ultra Wideband Systems with MIMO. Wiley,2010
7. M. Magani, L. Guo and X. Chen, “Improved BER Performance on MB-OFDM UWB System Using Adaptive Bit Loading”, IEEE Int. Conf. on Ultra-Wideband (ICUWB2010), Nanjing, China, September 20-23, 2010
8. P. Ho, Diversity Techniques, ser. Lecture notes in Mobile and Personal Communications, Burnaby, BC, Canada.2006
9. W. Q. Malik et al**,** “Spatial and polarisation correlation characteristics for UWB impulse radio,” in Proc. IEEE Int. Conf. Ultra-wideband (ICU). Zurich, Switzerland, Sep. 2005
10. J. Liu, B. Allen, W. Q. Malik, and D. J. Edwards, BA measurement based spatial correlation analysis for MBOFDM ultra wideband transmissions, in Proc. Loughborough Ant. Propagat. Conf., 2005.
11. M. Clark, M. Mulligan, D. Jackson, and D. Linebarger, “ Fixed-Point Modeling in an Ultra Wideband (UWB) Wireless Communication System” MATLAB digest, May 2004
12. K. Dogan, G. Gurel, A. K. Kamci and I. Korpeoglu, “A Performance Analysis of Bluetooth Broadcasting Scheme,” *Springer Berlin /Heidelberg*, Vol. 3992/2006, pp. 996-999, May 2006.

# CHAPTER 7

**IMPLEMENTATION OF UWB SPATIAL DIVERSITY TECHNIQUES**

## 7.1 Introduction

In this chapter, the design of a UWB antenna selection circuit and MRC is discussed. Spatial diversity is a technique used to reduce the effect of fading in the channel and improves the performance of the communication system. Viability of a diversity system is demonstrated with improved system performance

## 7.2 UWB Antenna selection Circuit

The circuit is designed to work with the existing UWB kit, thereby improving the performance of the system. The circuit layout is categorised into three section namely, RF (Radio Frequency), ADC (Analogue Digital conversion) and Digital section. Figure 7.1 shows the overview of the Antenna Selection Circuit.

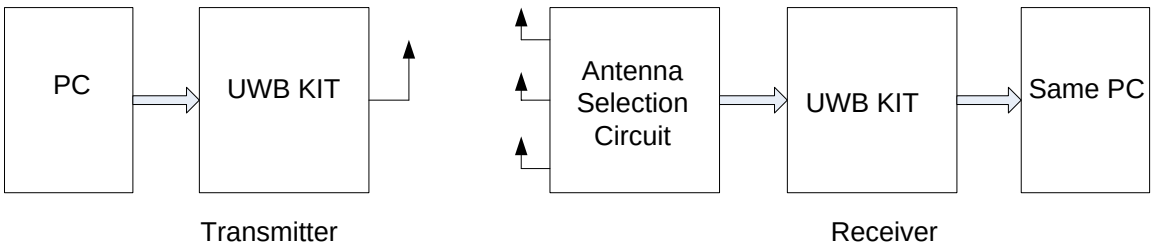


Figure 7.1 An Overview of the Antenna Selection Circuit

The antenna selection circuit is connected to an existing UWB receiver to improve the received signal by selecting the antenna with the best RSSI. Figure 7.2 shows the block diagram of the antenna selection circuit. The received signals are amplified and filtered before feeding to a 10dB coupler. The coupled signal from the coupler is fed to the Received signal strength indicator (RSSI) to give a voltage output proportional to the received signal. The voltage is fed to the digital circuit via a comparator which acts as a one bit analogue to digital converter (ADC). This approach is done for all the receive antennas. The output from the comparator is

digital, which compares the three signals to determine the one with the highest RSSI. The antenna with the highest RSSI is then connected to the UWB evaluation kit via the switch.

Due to the low power of the UWB signal, amplification of the received signal is necessary for the signal to be within the acceptable range of the RSSI indicator. The RSSI indicator used has a detecting range from -2 to -60dBm [1]. The RSSI indicator used has the lowest signal input level in the market and its bandwidth ranges from 1 to 8GHz. This makes it the most suitable to be used with the UWB signal but it is still higher than the range most UWB devices will receive signal. Considering the free space path loss equation expressed as

$$L = 20\ log\ \frac{4\pi d}{\lambda} \qquad 7.1$$

Where L is the path loss, d is the distance between the transmitter and the receiver and $\lambda$ is the wavelength. At 3GHz, a loss of 41.9dB will be experienced between a transmitter and a receiver 1m apart. With an EIRP of -41.3dB/MHz, it will be difficult for the RSSI indicator to operate. The need for amplification is necessary to cover such challenge.

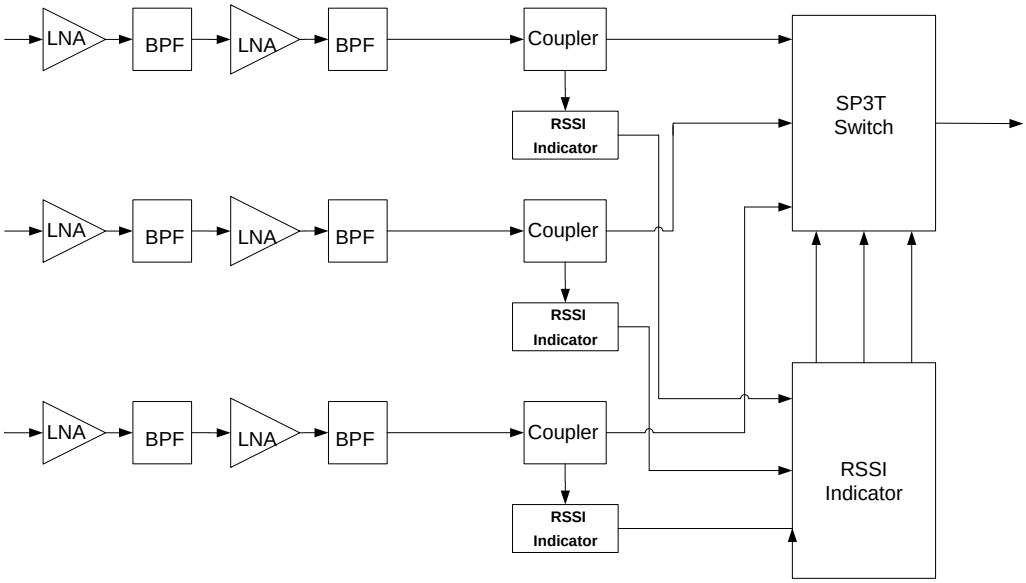


Figure 7.2 Antenna Selection block Diagram

### 7.3 Radio Frequency (RF) Design

The radio frequency (RF) section of the circuitry is simulated in ADS (Advance Design System). The main components used in the RF design are Band Pass Filter (BPF), Low noise Amplifier (LNA), High directivity coupler and SP3T switch which will be discussed below.

#### a) LNA (Low noise amplifier)

The LNA used is a surface mount device (SMD) manufactured by Avago technologies with a gain and noise figure of 17.5dB and 1.6dB at 4GHz respectively. It has an operating frequency range of 0.8-6GHz. This covers the required frequency range of 3.168-4.752GHz. For the required frequency range, no additional matching is required. The input and the output are

matched to 50 Ohm. Figure 7.3 shows the ADS circuit block diagram and Figure 7.4 shows the simulated gain and reflection coefficient of the LNA. [2]

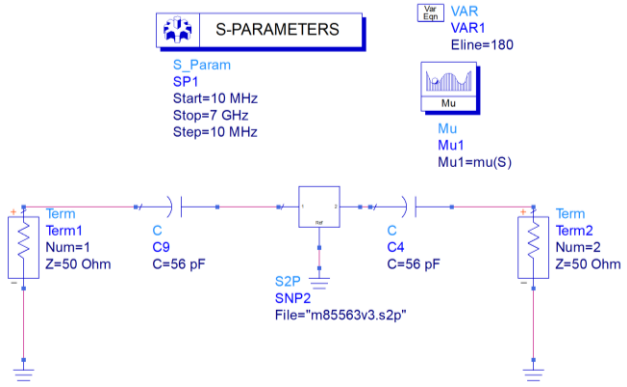


Figure 7.3 ADS simulation of the Low Noise Amplifiers

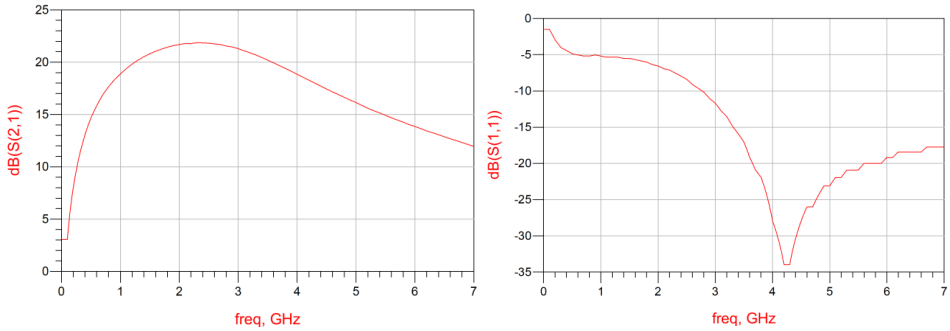


a. Gain of the LNA b. Reflection coefficient

Figure 7.4 Simulation parameters of the of the LNA

**b) Directional Coupler**

Directional couplers are four –ports circuits where one port is isolated from the input port. It is used to take a portion of the received signal after amplification for RSSI measurement. This enables the RSSI indicator to determine the strength of the signal. A directivity coupler is used to provide a -10dB coupled signal for the RSSI measurement. Figure 7.5 shows the ADS simulation circuit and Figure 7.6 and 7.7 show the S parameters of the 10dB coupler. [3]

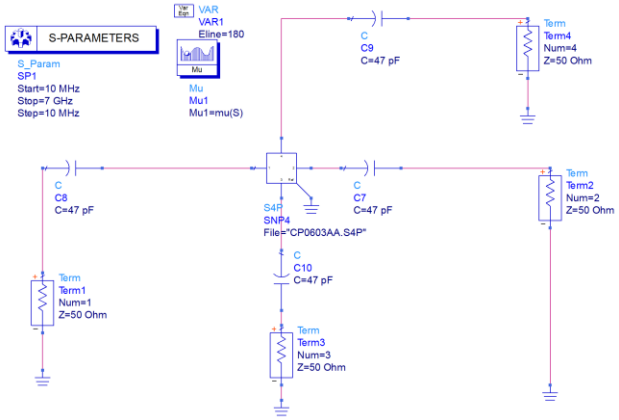


Figure 7.5 Directional Coupler the S21 is the forward port while the S41 is the coupled port.

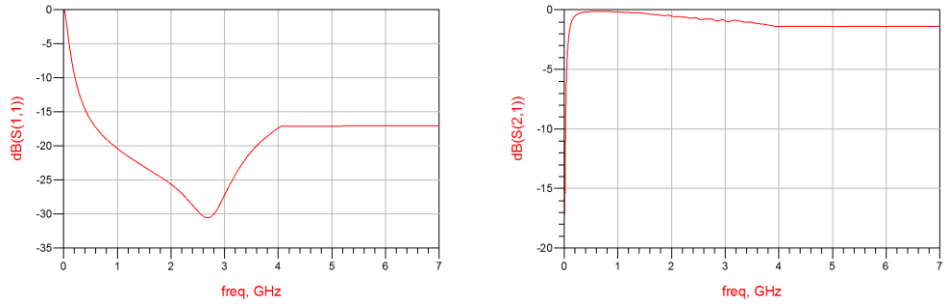


Figure 7.6 S11 and S21 parameters of the Directional coupler

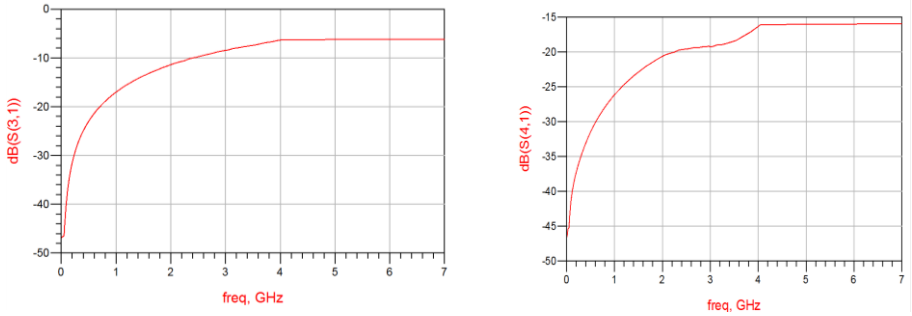


Figure 7.7 S31 and S41 parameters of the Directional coupler

**c) Band Pass Filter (BPF)**

The BPF used in the circuit is a TDK UWB filter that covers only UWB band 1 (3.168-4.752GHz). Figure 7.8 shows the ADS circuit and Figure 7.9 shows the simulation result. The BPF has good performance over the required frequency range. The result shows very good pass-band insertion loss across the desired frequency range, 3168 – 4752MHz. [4]

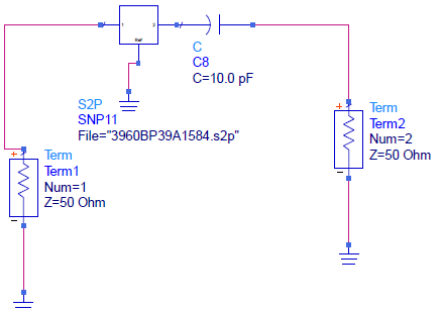


Figure 7.8 Band Pass filter (BPF)

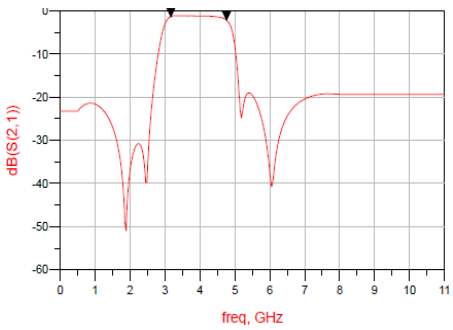


Figure 7.9 Band Pass filter (BPF)

**d) RF Switch**

An SP3T single-pole triple-throw antenna switch is used, which operates in the frequency range of 0.02-6GHz. The switch has 3 voltage inputs. Figure 7.10 and Figure 7.11-7.12 show ADS circuit and the performance of the RF switch. The Switch has an insertion loss of 0.7dB. Table 7.1 shows the truth table for the switch operation. Any state other than described in the table places the switch into an undefined state. [5]

Table 7.1 Sky13317-373LF Truth Table [5]

| Low insertion Loss path | V1(Pin 3) | V2 (Pin 6) | V3 (Pin 7) |
|---|---|---|---|
| RFC to RF 1 | High | Low | Low |
| RFC to RF2 | Low | High | Low |
| RFC to RF3 | Low | Low | High |

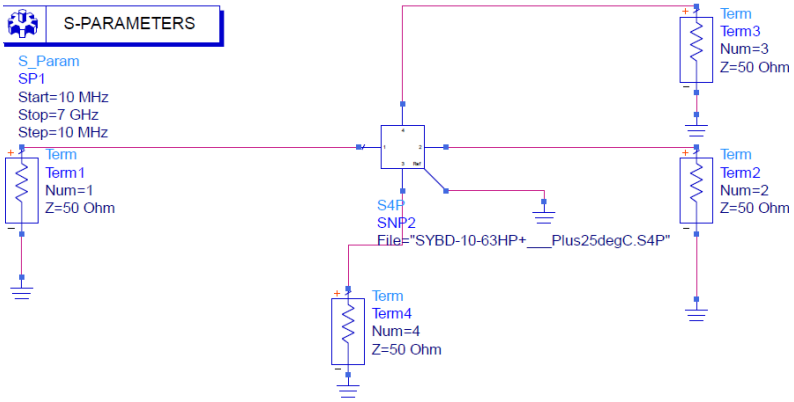


Figure 7.10 RF SP3T SKY Switch

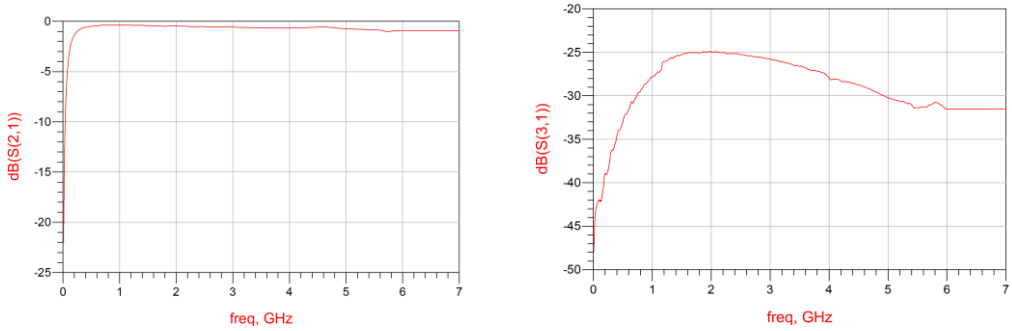


Figure 7.11 S31 and S41 Simulation results of the RF SKY Switch

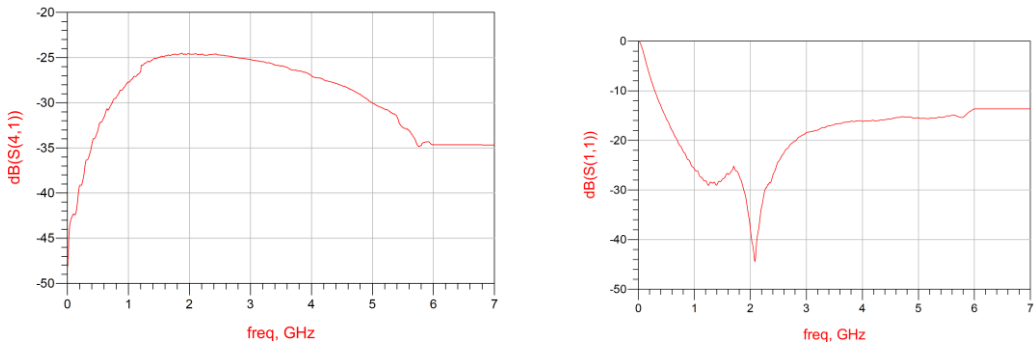


Figure 7.12 S11 and S21 Simulation results of the RF SKY Switch

### 7.4 RF Circuit

First, the circuit was simulated using the S parameters of the components without considering the transmission line. Figure 7.13 shows the circuit layout in ADS. This is to ensure the components give acceptable performance over the required frequency band. The components are double pair of LNA and BPF and a coupler. The simulation results show acceptable performance in Figures 7.14 and 7.15. The S21, S31 and S41 are the performances over the coupled signal, forward signal and the termination port respectively. The circuit has a signal gain of 37dB on the forward signal and 27dB on the coupled signal. This gain on the couple port will enable the signal to be within the RSSI measuring range of the circuit, to give an equivalent DC voltage for comparison. The S11, S22, S33 and S44 are well below the -13 dB. This is good for the system.

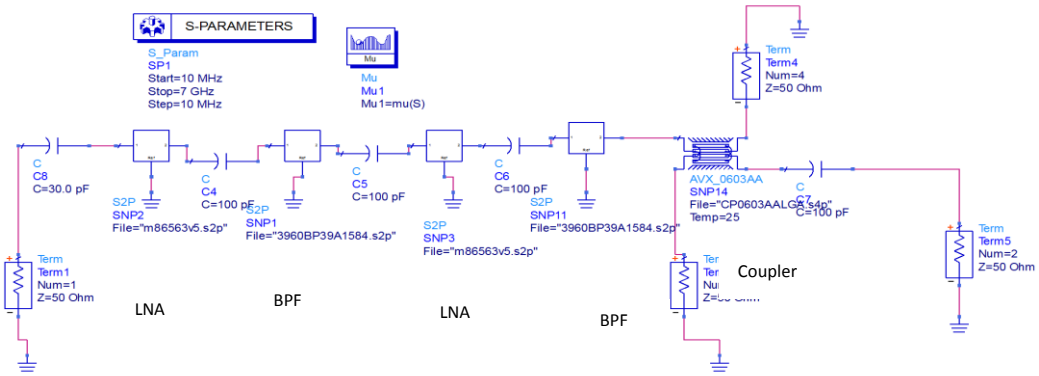


Figure 7.13 Circuit layout in ADS without transmission lines

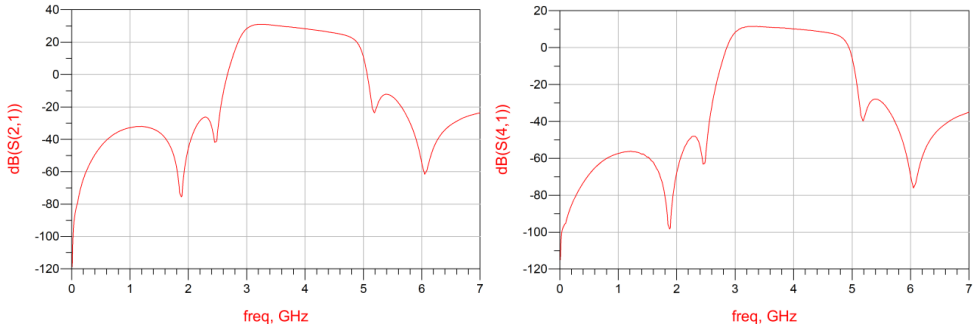


Figure 7.14 S21 and S41 Parameters of the circuit

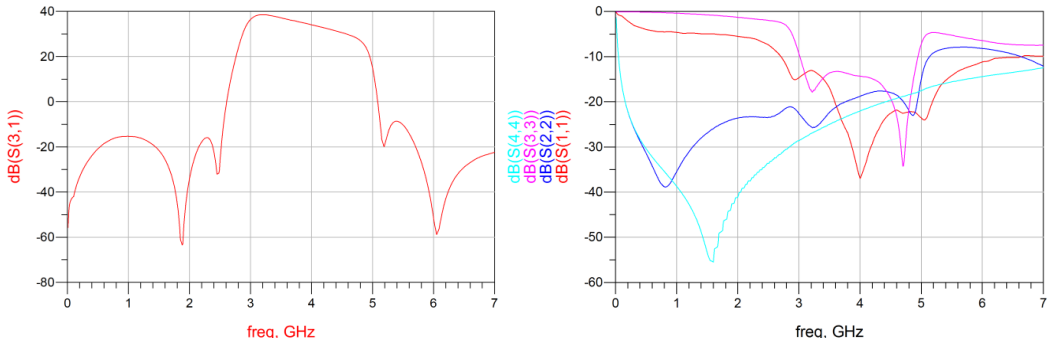


Figure 7.15 Figure 7.14 S11, S22, S33, S44 and S31 of the circuit

In this design, coplanar waveguide (CPW) is used for the transmission line so that the bottom layer is used for only dc lines routing. CPW is formed when a conductor is separated by a pair of ground planes, all on the same plane on the top of a dielectric medium. Table 7.2 shows the comparison of various transmission lines types. CPW is chosen because it is easier to design on a 2 layer PCB. The top layer is used for the CPW design, while the bottom is used for routing non transmission line. Table 7.3 shows the value of the parameters used for the design. Figure 7.16 shows the coplanar waveguide cross section with "a" as the width of the transmission and "b" as the distance between the two grounds labelled b. Figure 7.17 shows the ADS schematic diagram of the RF section with the transmission lines including tapering.

Table 7.2 Comparison of various transmission-line types [6]

| Transmission line | Chip mounting |
|---|---|
| Microstrip(dielectric) (GaAs, Si) | Difficult for shunt, easy for series |
| Stripline | Poor |
| Suspended stripline | Fair |
| Slotline | Easy for shunt, difficult for series |
| Coplanar waveguide | Easy for series and shunt |
| Finline | Fair |

Table 7.3 shows the value of the parameters used for the design

| Dielectric Constant (Er) | 4.6 |
|---|---|
| Height,(H) | 1.58mm |
| Thickness, (T ) | 70um |
| Width, (W) | 3mm |
| Space, (S) | 0.4mm |
| Impendence (Zo) | 51.7Ohm |

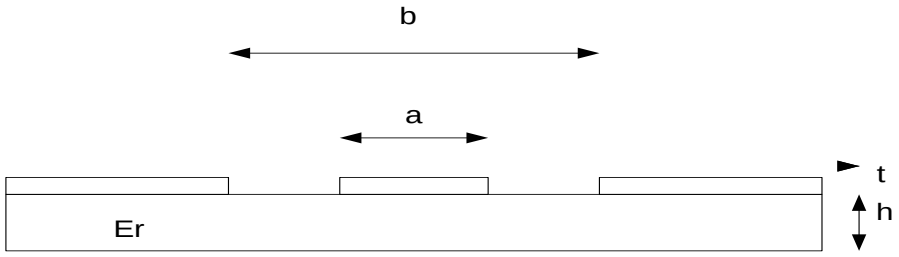


Figure 7.16 showing the coplanar waveguide cross section

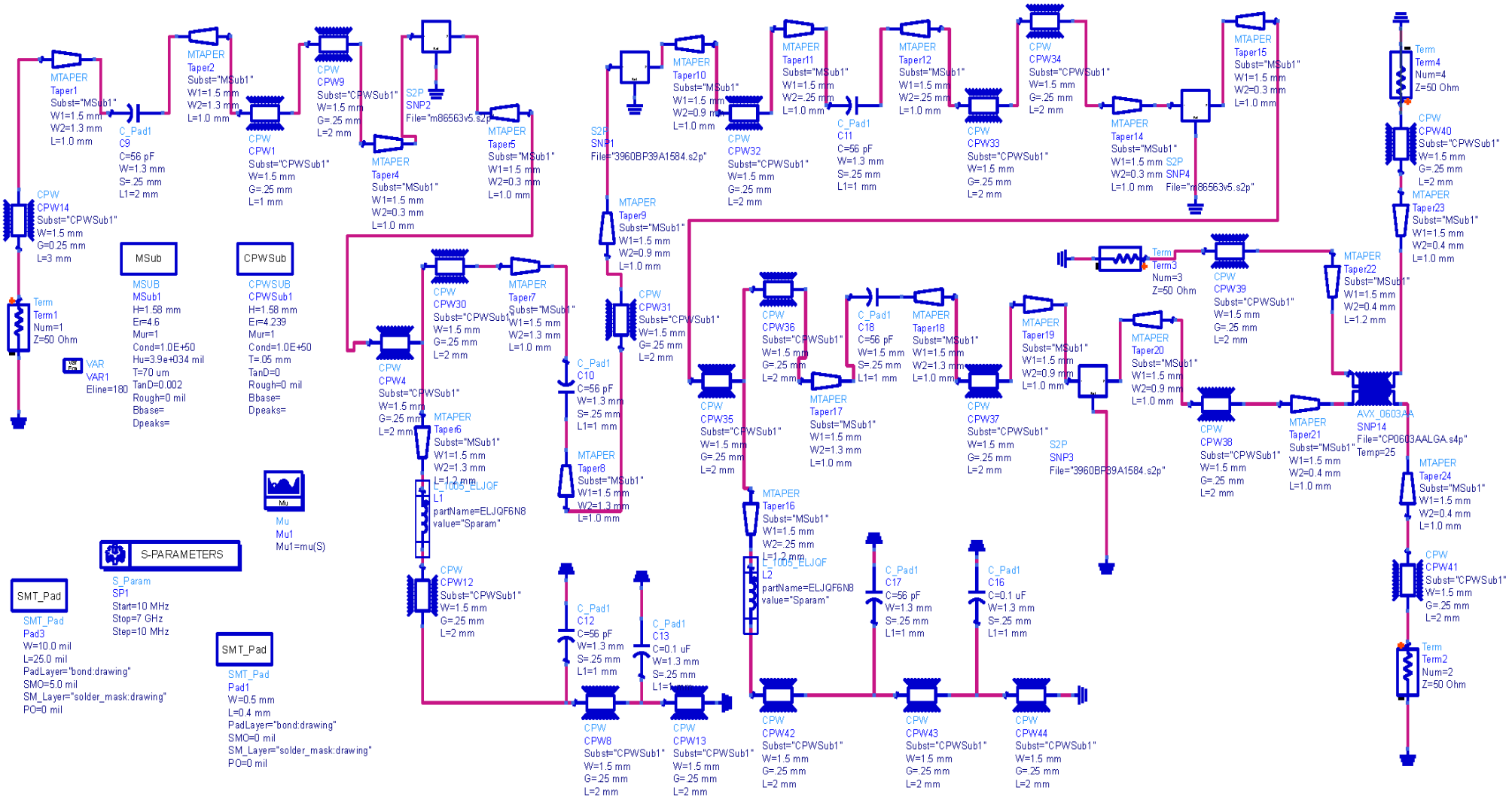


Figure 7.17 Schematic of the of the circuit diagram

Figure 7.18 and 7.19 show the S parameters for the whole RF circuit with the CPW transmission line. Port 3 is the forward port while port 4 is the coupled port. Port 2 is terminated with 50ohm impendence. The coupler used is a -10dB directional coupler as it can be seen from the performance in the Figure 7.19a, the signal via the transmitted port is 10 dB higher than the signal via the coupled port. The RF circuit is transferred from ADS to Ultiboard software to combine both digital, analogue and RF circuits.

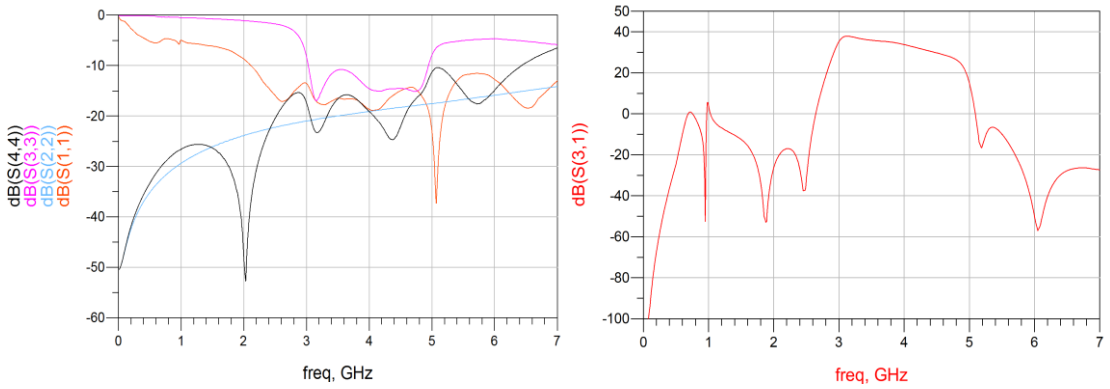


a. Insertion loss on the four ports b. Forward port

Figure 7.18 S parameters of RF design section

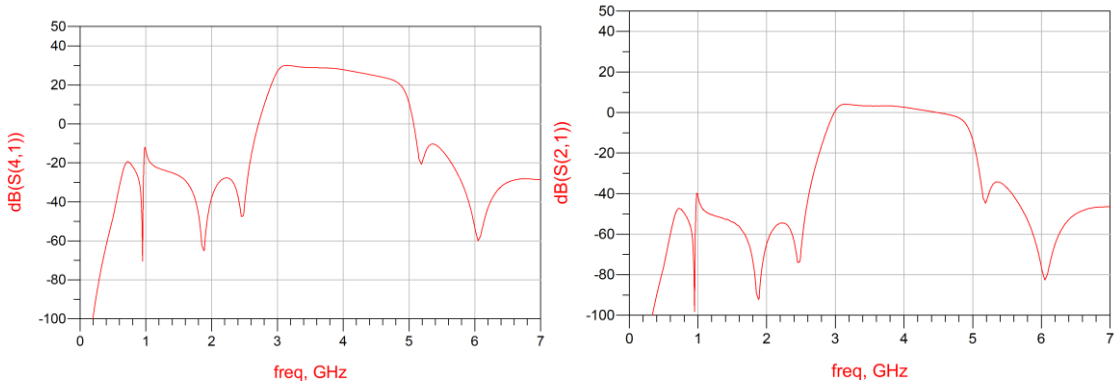


a. Coupled port b. Terminated port

Figure 7.19 S parameters of RF design Section

### 7.5 Analogue to Digital Converter (ADC) and Digital section

Voltage comparators are used to compare two voltages and to indicate which input voltage is larger. The voltages from the RF power indicator are connected in pairs to comparators to determine the larger one. The positive input ($V_1$) serves as the reference voltage while the negative input ($V_2$) serve as the input voltage. Figure 7.20 shows the diagram of the comparator.

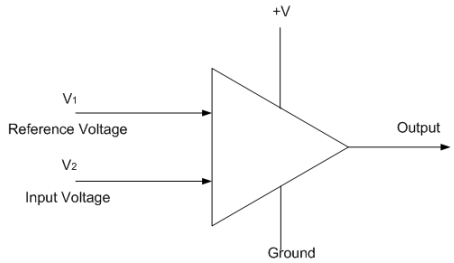


Figure 7.20 Diagram of the Comparator

One of the advantages of using comparators is that they can serve as one bit ADC (Analogue to Digital converter). Voltage comparators are used interfacing directly to digital circuit. The output of the comparators are in binary state as they either output $+V_{cc}$ when the $V_2 > V_1$ or 0V when $V_2 < V_1$. Figure 7.21 shows the states of the comparator.[7]

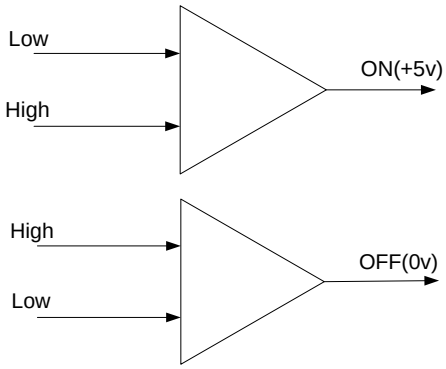


Figure 7.21 States of the comparator

Comparators are used to compare the RSSI at each antenna. Since the RF power detector IC output a voltage linearly proportional to the RSSI, the output voltage is connected to comparators. Fortunately, comparators can also act as one bit ADC (Analogue to Digital Converter) which means digital components can be used to achieve the desired response for the circuit to drive the switch. After comparison, a logic circuit is used to ensure that only one antenna is selected at a time. Three AND gates and two Inverter were used to determine that only the antenna with the highest RSSI has a high output while others are low. This is due to the possibility of having more than one comparator with a high output, which could cause undesirable system behaviour as the switch only works with one input high per time. Figure 7.22 shows the sub circuit that selects the antenna with the best RSSI and the logic circuit used to mitigate any undesirable behaviour in the circuit. Table 7.4 shows the truth table of the logic circuit which allows only one antenna to be selected from the three comparators while rejecting any other combination. The circuit will compare the Signal strength of each antenna and compare the one with the highest signal strentgh then switches to the antenna untill another antenna has a stronger signal.

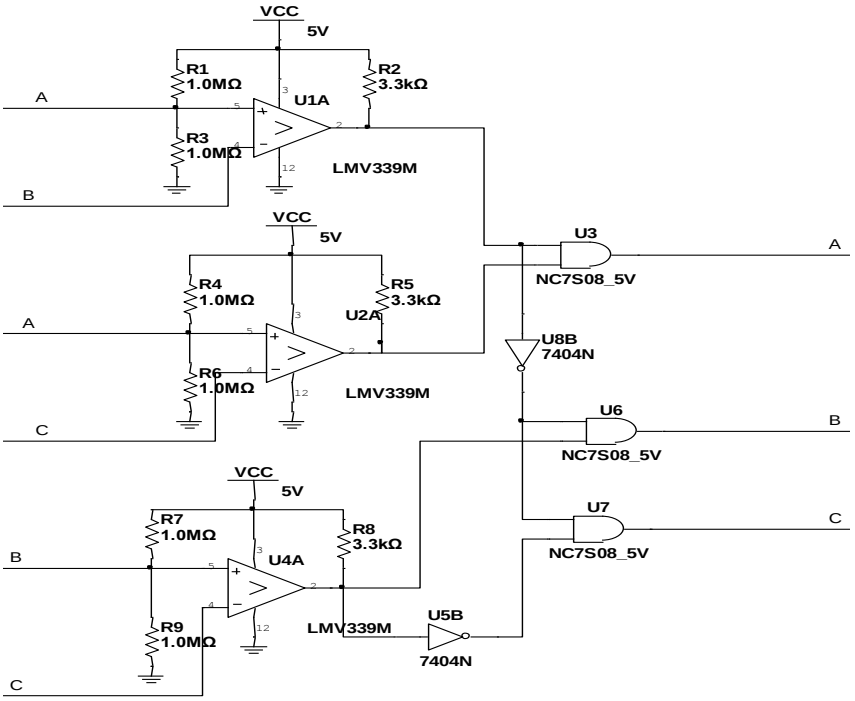


Figure 7.22 Comparators and selection Sub Circuit

Table 7.4. Truth table for activating the swtich

| **A** | **B** | **C** | **E** |
|---|---|---|---|
| 0 | 0 | 0 | 0 |
| 0 | 0 | 1 | 1 |
| 0 | 1 | 0 | 1 |
| 0 | 1 | 1 | 0 |
| 1 | 0 | 0 | 1 |
| 1 | 0 | 1 | 0 |
| 1 | 1 | 0 | 0 |
| 1 | 1 | 1 | 0 |

The following requirement must be met before an antenna is selected

1. To select antenna one the following expression must result to a high output

$$E = A\bar{B}\bar{C} \quad 7.2$$

2. To select antenna two the following expression must result to a high output

$$E = \bar{A}B\bar{C} \quad 7.3$$

3. To select antenna three the following expression must result to a high output

$$E = \bar{A}\bar{B}C \quad 7.4$$

Therefore only this combinations are required to select one of the antennas

$$E = A\bar{B}\bar{C} + \bar{A}B\bar{C} + \bar{A}\bar{B}C \quad 7.5$$

The IC used for detecting the signals strength, AD8318, is an IC from Analog Devices. The AD8318 provides a log-linear relationship between an RF/IF input voltage and its output.. Figure 7.23 shows the recommended power circuit diagram for measuring the RSSI using the AD8318. The AD8318 power detector measures the RSSI and outputs a voltage that is based on a linear relationship as shown in Figure 7.24.

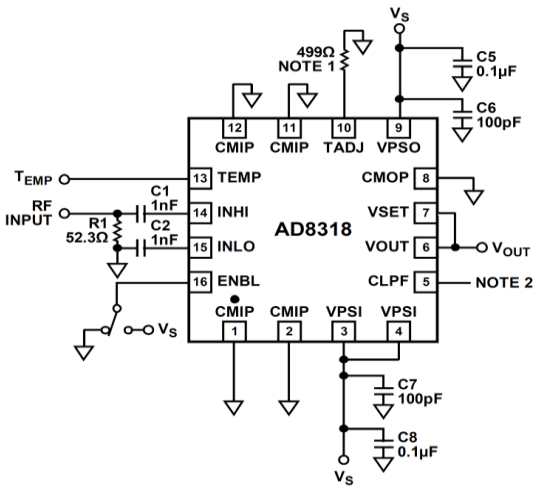


Figure 7.23 RF Power Detector Circuitry[1]

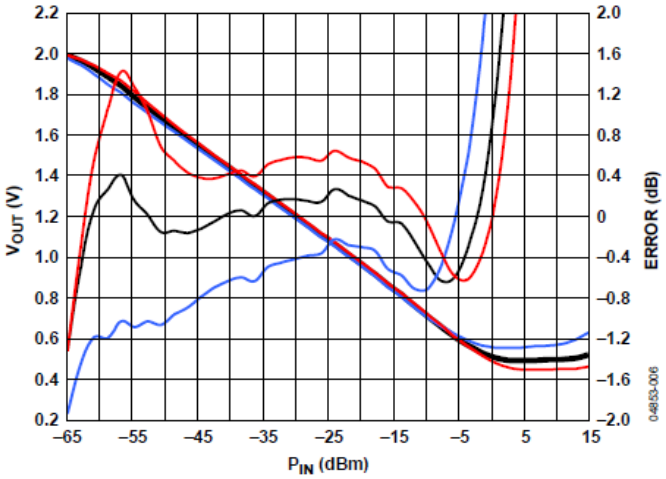


Figure 7.24 $V_{out}$,Log conformance Vs. Input Amplitude at 3.6GHz[1]

The outputs are passed to the shift registers where they are converted from serial input to 2 bit parallel output. Shift registers can serve as serial to parallel converter or parallel to serial converter. This is done by checking each antenna's performance over a period of 5 seconds. The shift register is a cascade of Flip-Flop. The flip-flop is connected to the next flip-flop on the chain. Figure 7.25 shows a four bit serial to parallel shift register.

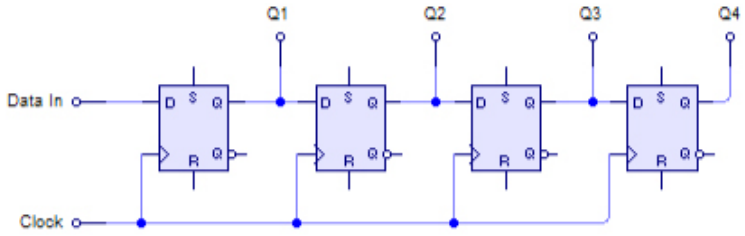


Figure 7.25 Shift Register [8]

The sub circuit showed in Figure 7.26 checks the performance of subsequent signals from the same antennas after five seconds. If a selected antenna has the highest RSSI over 5 seconds, the serial–in to parallel-out shift register will output two digital ones. When passed through the AND gate will output a digital one which will in turn select the antenna. When the selected antenna fails to maintain the highest RSSI, the antenna will not be selected. The selection process will be repeated until the selected antenna meets the requirement. A shift register is used to enable the circuit to capture subsequent states of the signals that are 5 seconds apart for comparison. The shift register used in this circuit is used as a serial to a parallel converter. The first input signal is stored in the first flip-flop until the next pulse from the 555 timer, and the signal is moved to the next flip-flop in the shift register and then replaced by the new signal. The two subsequent signals are compared if they are the same by "ANDing" them. A high output means that the selected antenna has the best RSSI over the 5 seconds interval.

The outputs from all the 3 shift registers are passed to a D-latch. This is to keep the selected antenna active until another antenna is selected and has satisfied the required condition of having the highest RSSI over 5 seconds. A 3 input OR-gate is used to enable the D-latch to switch to another antenna when it has the highest RSSI.

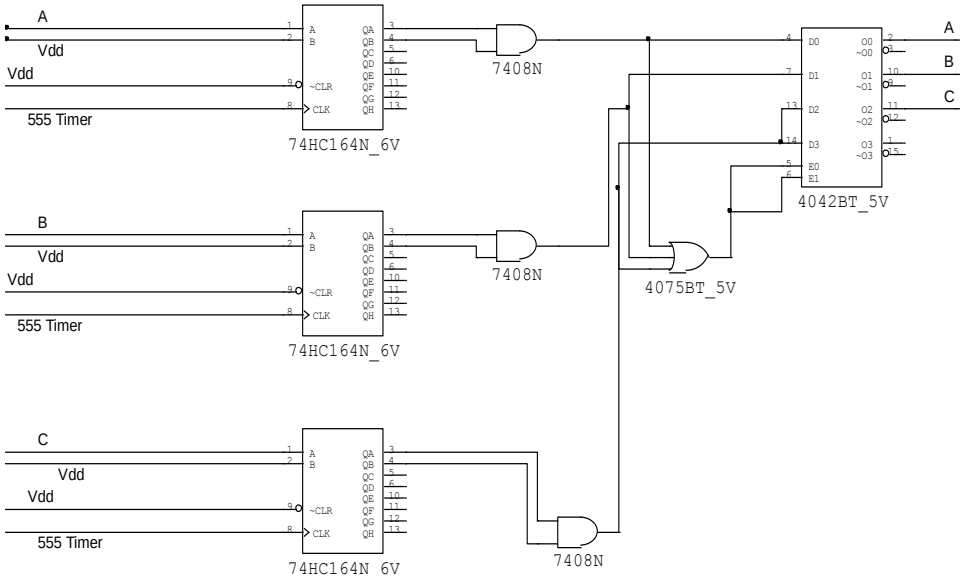


Figure 7.26 RSSI Comparison after 5s Sub Circuit

Figure 7.27 shows a sub circuit that uses a 3 input NAND-gate and an OR-gate after the quadruple D-Latch to ensure the 3rd antenna is selected at the beginning of reception before

the selection takes place. This is to prevent a case where no antenna RSSI is stable over first 5 seconds. To prevent the switch from not working for the first 5 seconds, a 3 input NAND-gate and a 2 input OR-gate were used to ensure that the third antenna is selected by default. The third antenna will be selected at the beginning for the first 5 seconds or when there are intermittent changes in the RSSI of the three antennas. The circuit will select the third antenna until there is stability in the RSSI. An SP3T sky switch is used to switch between the three antennas based on the one with the highest RSSI.

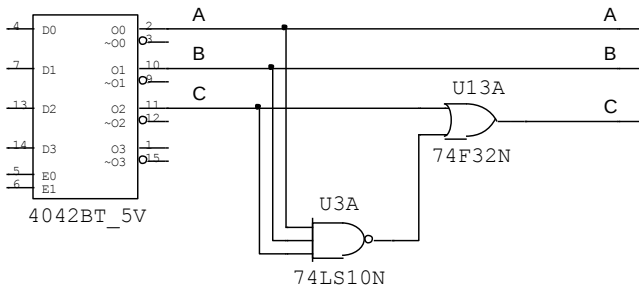


Figure 7.27 Circuit to ensure antenna three is selected

555 timers are used to provide pulse every 5 seconds to clock the sift register. 555 timers can be used to output a continuous stream of rectangular pulses having a specified frequency. It is used to generate rectangular pulses with 5 seconds interval. The pulses have high interval duration of 250ms to enable all the comparisons and selections to be made. Figure 7.28 shows the square pulses generated by the 555 timer in an astable state.

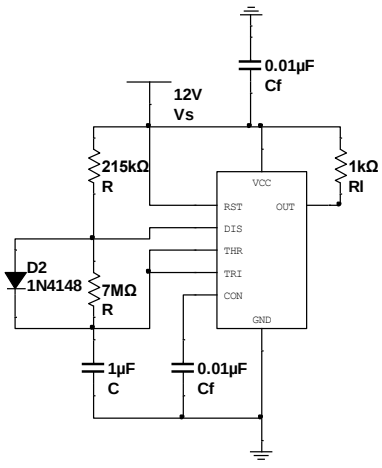


Figure 7.28 555 Timer Circuit with a diode in parallel to the 7Mohm resistor

In an astable mode, the frequency of the rectangular pulse depends on R1, R2 and C. It is expressed as [9]

$$f = \frac{1}{In(2) * C * (R_1 + R_2)} \qquad 7.6$$

$$f = \frac{1}{T} \quad 7.7$$

Where f is the operating frequency, c is the capacitance of the capacitor, R1 and R2 are resistors and T is the period of the pulse. The interval of the pulse are describe with the following equation

$$H = In(2) * C * (R_1 + R_2) \quad 7.8$$

$$L = In(2) * C * (R_2) \quad 7.9$$

Where H is the high interval and L is the low interval. The 555 timer outputs the pulse with a duty circle of 50% which does not give the 5s time interval clock the shift register. The duty cycle is the ratio of duration of the high time to the total period and is expressed as

$$D = \frac{\tau}{T} \quad 7.10$$

Where D is the duty cycle, $\tau$ is the duration of the high output and T is the total period of the pulse. When R1< R2, the duty cycle is less than 50%. A diode is placed in parallel with R2 towards the capacitor to bypass the R2 during the high part of the cycle. This makes the high interval to depend only on R1 and C.

$$H = In(2) * C * (R_1) \quad 7.11$$

Figure 7.29 is the captured timed measurement of the 555 timer circuit. The figure shows that the high output has about 250ms duration. The complete schematic, PCB design layout and bill of materials are shown in the Appendix F.

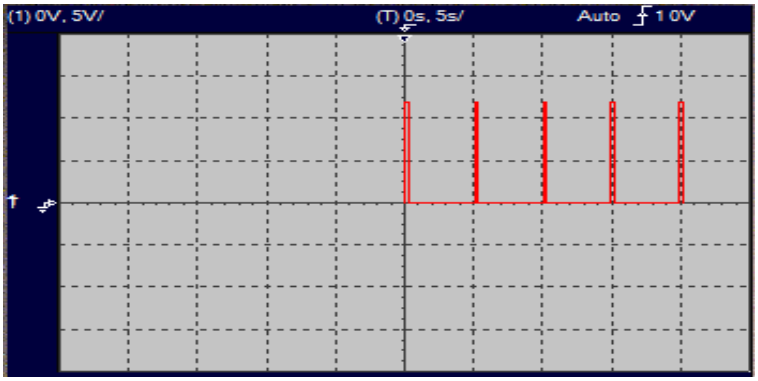


Figure 7.29 Using an Oscilloscope to capture the generated pulse. Pulse duration is 250ms while the interval is 5s

7.6 Demonstration setup and testing

The antenna selection circuit is connected to the UWB evaluation kit for testing in the body centric laboratory at QMUL. The setup procedure of the UWB evaluation kit was discussed in chapter 3. In the demonstration we considered the following parameters

1. Data rate: Varying data rate of 53.3, 80, 106.7 and 200MBps, were used for testing the performance of the circuit.

2. Payload: A payload of 1024bytes was used for data rates.
3. Distance: The antenna selection was placed 1m from the transmitting UWB evaluation kit.
4. Channel: Logical channel 15 is used for the testing .The channel occupies the band between 4224MHz and 4752MHz with a centre frequency at 4488MHz.

Figure 7.30 and Figure 7.31 show the picture of the body centric laboratory where testing was done and the positioning of the antennas respectively. The Figure shows two antennas in horizontal orientation and the third in a vertical orientation. The laboratory is a model of a realistic indoor environment with office furniture. Figure 7.31 shows the antenna selection circuit LEDs for the three antennas switching while taking measurement.

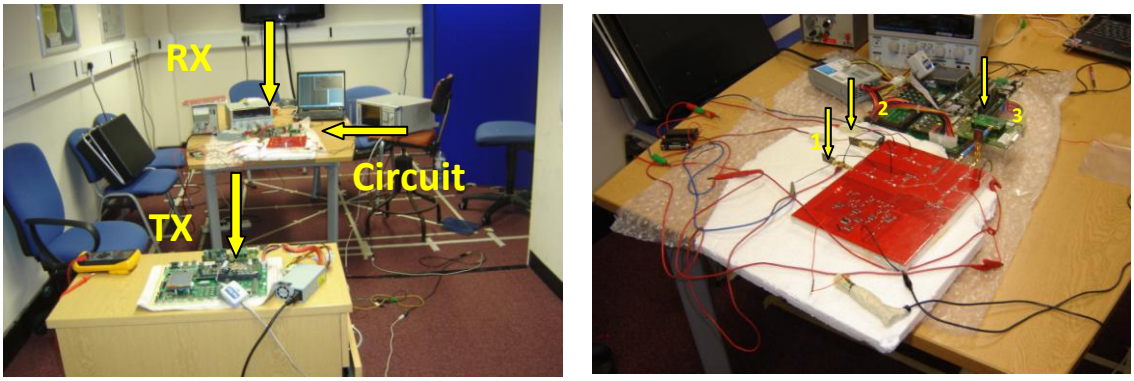


Figure 7.30 Picture showing Setup Demonstration and Testing of the antenna circuit

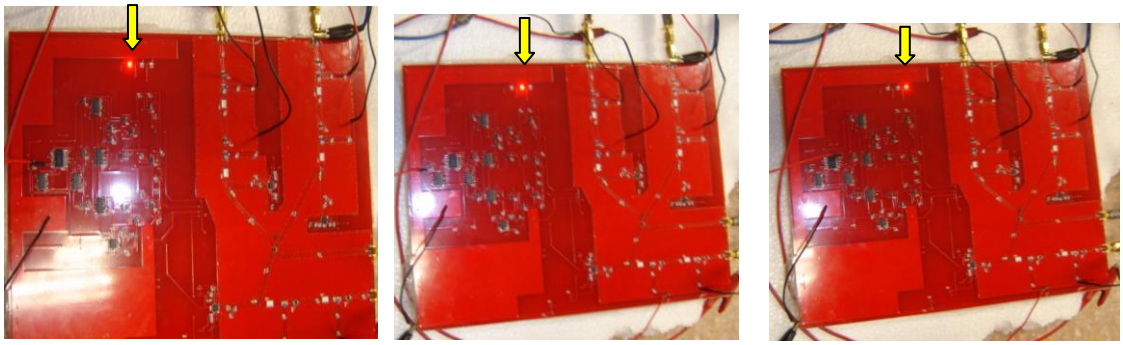

a. Antenna 1 selected b. Antenna 2 selected c. Antenna 3 selected

Figure 7.31 Antenna selection circuit LEDs

Figures 7.32 and 7.33 show the results of the packet error rate (PER) and throughput of the UWB evaluation kit connected to the antenna selection circuit respectively. Figure 7.32 shows antenna three has the lowest PER of the three antennas. Only the data rates for 53.3, 80 and 106MBps are shown as the higher data rate from 200MBps all gave a PER of 100%. Figure 7.33 shows the throughput of the UWB evaluation while connected to the antenna selection circuit. It also shows that antenna two has the worst throughput while antenna three has the best throughput over the three data rates.

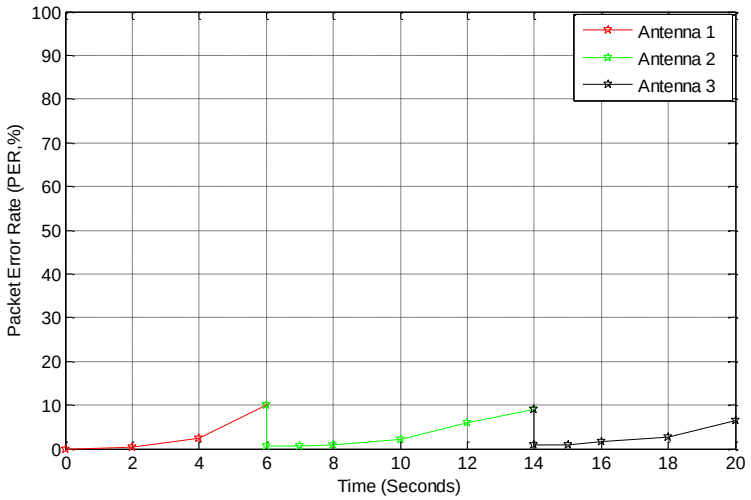


Figure 7.32 PER of the UWB Evaluation Kit with the antenna selection circuit.

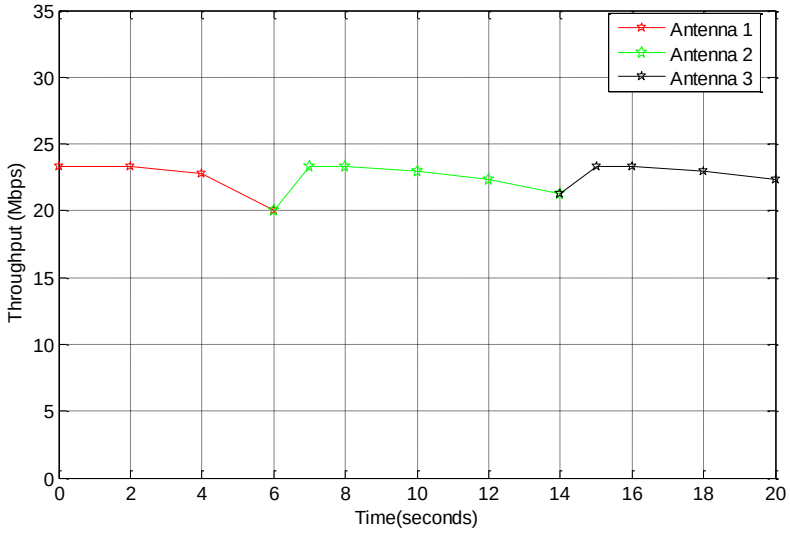


Figure 7.33 Throughput of the UWB Evaluation Kit with the antenna selection circuit at a data rate of 400Mbps at 1m apart.

### 7.9 Maximum Combining Ratio (MRC)

The design of the maximum ratio combining (MRC) MB OFDM UWB test bed is discussed in this section. Test bed gives a fundamental insight into the practical aspect of a developed approach and provides an important tool to verify the results of a model based design [1]. Acquiring system simulators for this specific purpose is beyond the cost and scope of this program. In order to simplify access of the real channel, a UWB evaluation kit is used to generate the OFDM packets and a Lecroy serial data analyzer is used to capture both the received and transmitted data which is then processed offline in Matlab. High data rate systems are targeted for high resolution media streaming applications over short distances. The MB OFDM UWB is proposed to deliver 480Mpbs over 3metre to enable streaming of high

resolution content within the Personal Wireless Area Network (WPAN). The MRC diversity technique is used to improve the performance of the MB OFDM UWB to enable it deliver the proposed 480 data rate over 3m. QPSK is used for data rate 55.3Mbps, 80MPbs, 106Mpbs, 160 Mbps and 200Mbos. For data rates 320Mbps, 400Mbps and 480Mpbs Dual Carrier Modulation (DCM) is used which is based on the 16-QAM Modulation technique. The SNR typically required for reliable detection in 16 QAM is usually higher than 16dB.

The tests were conducted in a typical office setting environment with desk, tables, computers, cupboard and different scattering objects. For the purpose of the measurement, four antennas were used with one as the transmit antenna and the three as the receive antennas. The antennas are place 80 cm above the floor and the separating distance between the transmit and receive antennas was varied from 0.5m to 3m. The receive antennas were aligned linearly with an inter-antenna separation distance of 10cm. This corresponds to the largest wavelength for the UWB signal under the FCC regulation.

A monopole UWB antenna is used as the transmit antenna which has an omnidirectional radiation. The receive UWB antennas used in this model are small printed quasi-self-complementary antenna shown in Figure 5.5.

The main components for the testbed are UWB Evaluation kit, Lecroy SDA 11000 serial Data Analyser and a PC with Matlab. The UWB evaluation kit is describe in Chapter 2 and it is used to generate the MB OFDM UWB signals. The signals are passed through a splitter and fed to both the transmit antenna and the Lecroy Serial Data Analyser simultaneously. This enable capturing of both the transmit and receive signal at the same time instant to be able to synchronize offline processing of the signal for MRC combining and BER evaluation. This is necessary as user defined OFDM UWB signal cannot be generated from the UWB kit. It only allows data rates, payload and logical channels to be changed. The Evaluation kit is design to work between 3.1GHz to 4.8GHz and this limits the test to only the first band group. The kit is used to specify the data rate, payload and the channel before sending the signal to the transmit antenna and to the Lecroy SDA as a reference signal.

The Lecroy SDA 11000 is a 40.0 GSa/Sec, 11.0 GHz Serial Data Analyser. It provides either four channels with up to 20GS/sec sampling rate and a frequency span of 6GHz or two channels with up to 40GS/sec sampling rate and a bandwidth of 11GHz. Therefore, with the four channels it is possible to do a setup for up to three receive antennas for MRC combining technique. The frequency band of interest is band 1 which is between 3.162 GHz to 4.752GHz and this bandwidth lies within the acceptable bandwidth for the Lecroy SDA. The Lecroy can capture and store UWB waveforms from the Evaluation kit without the need of an up/down conversion circuits and expensive UWB RF front ends. Each of the four channels has a

dedicated ADC (Analog to Digital Converter) and the voltage on each is sampled and measured at the same time instant. This allows for a very reliable measurement between the channels [16]. The Lecroy SDA has QPHY-UWB option software which enables the Digital Oscilloscope to perform WiMedia UWB PHY transmitter compliance measurement. The software performs in accordance to the Multiband OFDM (Orthogonal Frequency Division Modulation) Physical Layer Specification, version 1.0 [17]. This is used in estimating the channel and equalising the channel. Figure 7.34 shows the sketch of the testbed set up and Figure 7.35 shows the pictorial view of the measurement. Several alternatives of implementing the testbed were considered but the above is the preferred option due to the relative easiness in implementing, compared to other methods.

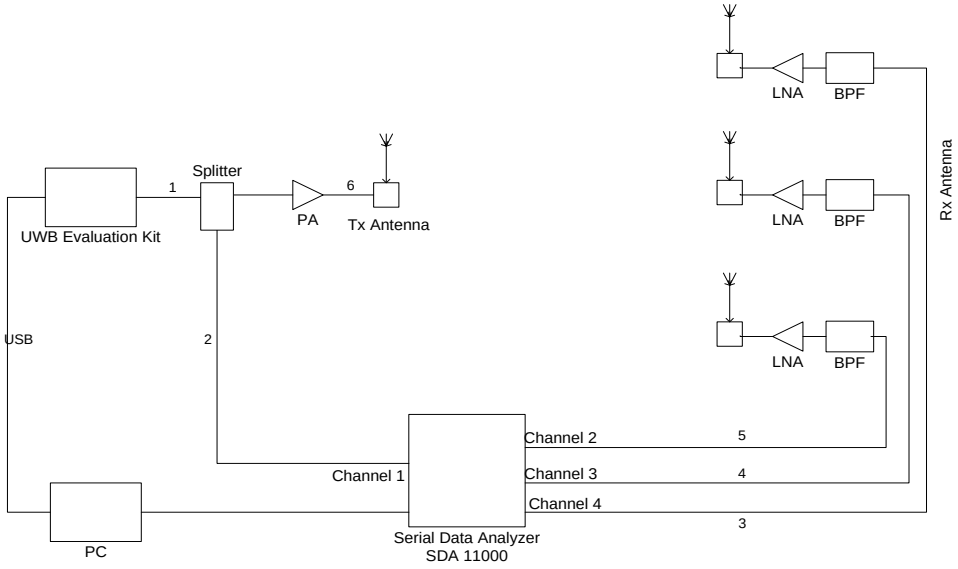


Figure 7.34 Measurement Testbed setup for the MB OFDM UWB System

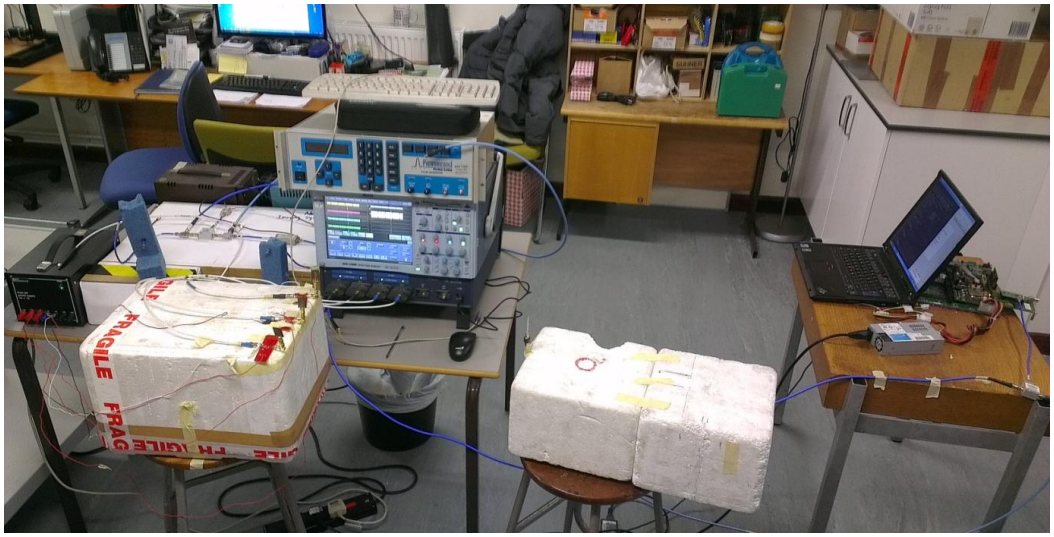

Figure 7.35 Pictorial view of the Measurement Testbed setup for the MB OFDM UWB System

On the receiver side, three UWB antennas are connected to the Lecroy SDA through a +15dB low noise amplifier for reliable signal acquisition. The three receive antennas uses channel 2-4, while channel one is connected directly to the UWB evaluation kit via the splitter and it is s also used to trigger the Lecroy SDA. A power amplifier is used to compensate the losses as a result of the cabling and components used. Table 7.5 shows the losses within the measurement setup.

Table 7.5 The losses within the measurement setup

| | | Material | Length | Loss dB ( 3-4GHz) |
|---|---|---|---|---|
| 1 | 141-15Sm | SMA Cable | 0.5 | 2.5 |
| 2 | ALCC-005 | SMA Cable | 1.5 | 2.5 |
| 3 | ALCC-0010 | SMA Cable | 0.7 | 2 |
| 4 | ALCC-0031 | SMA Cable | 1 | 2 |
| 5 | ALCC-0032 | SMA Cable | 1 | 2 |
| 6 | ALCC-001 | SMA Cable | 3 | 4 |
| 7 | 6882-812 | Amplifier | | 20(gain) |
| 8 | ZFSC-2-10G+ | Splitter | | 3 |

For the measurement, a payload of 1024 bytes size is used. The packets are transmitted and acquired and stored in the Lecroy. This is transferred to computer for further offline processing. Figure 7.36 shows the power spectrum of a received MB OFDM UWB Signal during the transmission. The figures show the effect of frequency selective fading on the signal. Figure 7.37 shows the received signal acquired directly from the UWB evaluation kit via the splitter and via the receive antenna at a distance of 0.5m. Figure 7.38 shows the hopping sequence of the UWB signal while transmitting on logical channel 9. Each logical channel defines a hopping pattern for the UWB signal as shown in table 2.2. The WiMedia group defined the sequence of hopping to enable multiuser channel access.

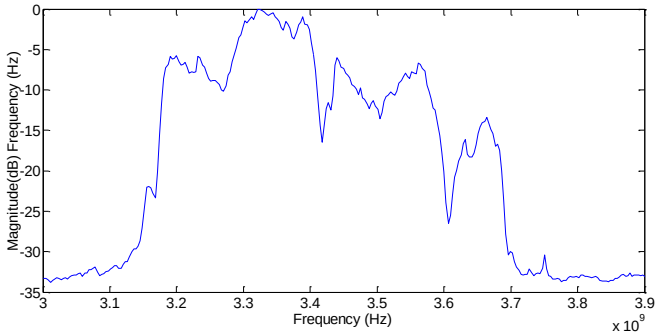


Figure 7.36 Received signal spectrum

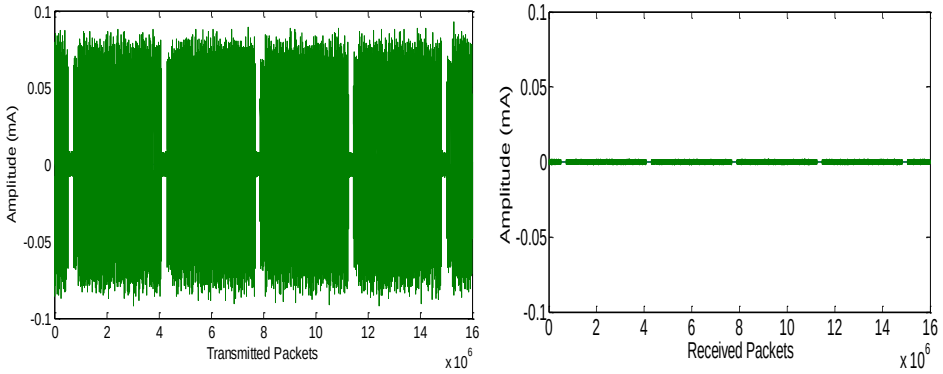


Figure 7.37 Transmitted and received signal with a separating distance of 0.5m

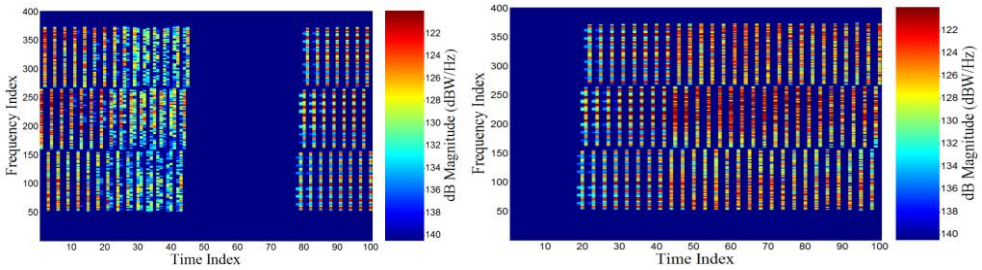


Figure 7.38 Frequency hopping of a single measurement.

The MB OFDM UWB has a known preamble added prior to the PLCP header to aid the receiver in timing synchronization; carrier offset recovery and channel estimation. The PLCP preamble consists of two portions: a time–domain portion (packet /frame synchronization sequence) and the frequency domain portion (channel estimation sequence). For symbol timing, cross correlation is performed between the received signal and a known reference signal. Equation 7.12 shows how to calculate the correlation

$$\hat{t}_s = \arg \max_n \left| \sum_{k=0}^{L-1} r_{n+k} t_k^* \right|^2 \qquad 7.12$$

Where $r_n$ is the received signal, $t_k^*$ is the conjugate of a known reference signal. MB OFDM UWB has two types of preambles namely; burst and standard mode. The value of n that corresponds to maximum absolute value of the cross correlation is the symbols timing estimate. The burst mode has 12 symbols while the standard mode has 24 symbols. Figure 7.39 shows the OFDM UWB Packet and Figure 7.40 shows the output of the cross correlator

that uses the first OFDM symbol in the preamble as the reference signal. The signal clearly shows the start of packets for all the four incoming packets. In the figure below the high peak at n=486, 1050, 1614 and 2178 clearly shows the correct symbol timing and the start of a packet which is the preamble.

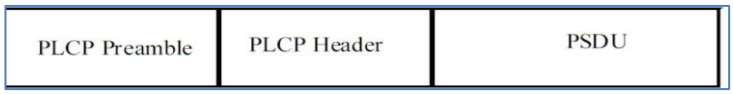


Figure 7.39 Figure 7.47 OFDM UWB Packet

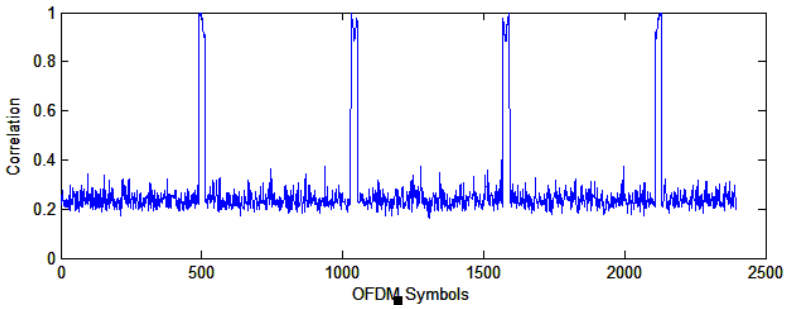


Figure 7.40 Response of the symbol timing cross correlator of one of the acquired data

In the PLCP preamble, after the packet/frame synchronization sequence is the channel estimation sequence. The channel estimation can be used to estimate the frequency response. Channel estimation in MB OFDM UWB systems is data aided. Training data is used for channel estimation, which is known by both the transmitter and the receiver. QPSK modulation is used for training data. In obtaining the channel coefficient, the least square channel estimator is used. This is expressed as

$$H(i,J) = \frac{Y(i,j)}{X(i,j)} \qquad 7.13$$

Where $Y(i,j)$ is the received symbol of $i_{th}$ sub channel in the $j_{th}$ OFDM symbol. The channel coefficient of each sub-channel is estimated in the channel with no white noise. The specified value of the training data can be obtained from reference [16].

Error vector magnitude (EVM) is the measure of error between the measured symbols and expected symbols. The error vector magnitude of the signal can be express as [17]

$$RMS_{error} = \frac{1}{N_f}\sum_{n=1+N_{Sync}+N_{Hdr}}^{N_{packet}} \left[\frac{\sum_{k=1}^{N_D}|R_{D,n}[k]+C_{D,n}[k]|^2+\sum_{k=1}^{N_P}|R_{P,n}[k]+C_{P,n}[k]|^2}{(N_D+N_P+N_{TN,n})N_{frame}P_o}\right] \qquad 7.14$$

where $N_f$ is the number of packets under test, $N_{packet}$ is the number of symbols in the packet, $N_{sync}$ is the number of symbols in the PLCP preamble, $N_{hdr}$ is the number of symbols in the PLCP header, $N_{frame} = N_{packet} - N_{sync} - N_{hdr}$ $r$ is the number of symbols in the PSDU, $ND$ is the number of data subcarriers, $N_P$ is the number of pilot subcarriers, $P_0$ is the average power over all

payload symbols of the data and pilot constellations is re-computed for each packet, $C_{D,n[k]}$ and $C_{P,n[k]}$ are the transmitted $k^{th}$ data subcarrier and $k^{th}$ pilot subcarrier for the $n$th OFDM symbol, respectively, and $R_{D,n[k]}$ and $R_{P,n[k]}$ are the observed $k^{th}$ data subcarrier and $k^{th}$ pilot subcarrier for the $n$th OFDM symbol, respectively. The values for $N_D$, $N_P$, $N_{sync}$, $N_{hdr}$, $N_{frame}$, and $N_{packet}$ are defined in Table 7.6. The RMS error shall be computed over the payload portion of the packet only. $N_{TN,n}$ is the number of data or pilot tones nulled in symbol $n$. If a data tone $k$ is nulled (i.e., the corresponding tone nulling element is set to zero according to a valid tone nulling mask) in symbol n then $R_{D,n[k]}$ and $C_{D,n[k]}$ are replaced with zero. If pilot tone $k$ is nulled in symbol $n$ then $R_{P,n[k]}$ and $C_{P,n[k]}$ are replaced with zero.

Table 7.6 parameter values proposed by the WiMedia group [17]

| Parameter | Description | Value |
|---|---|---|
| $N_D$ | Number of data subcarriers | 100 |
| $N_P$ | Number of pilot subcarriers | 12 |
| $N_G$ | Number of guard subcarriers | 10 |
| $N_T$ | Total number of subcarriers used | 122 (= $N_D + N_P + N_G$) |
| $N_{sync}$ | Number of symbols in the PLCP Preamble | Standard: 30,Burst: 18 |
| $N_{hdr}$, | Number of symbols in the PLCP Header | 12 |
| $N_{frame}$, | Number of symbols in the PSDU | $N_{packet} –(N_{sync} + N_{hdr})$ |
| $N_{packet}$ | Total number of symbols in the packet | $N_{sync} + N_{hdr} + N_{frame}$ |

Two modulating technique are used in the MB OFDM UWB technology namely; Quadrature Phase Shift Keying (QPSK) and Dual Carrier Modulation (DCM) technique. QPSK is used for data rate 55.3Mbps, 80MPbs, 106Mpbs, 160 Mbps and 200Mbos. For data rates 320Mbps, 400Mbps and 480Mpbs Dual Carrier Modulation (DCM) is used. Figure 7.41a and 7.41b show the constellation diagram of OFDM UWB transmitted data with data rate 200Mbps and 480Mbps respectively. The splitter is used at the transmitter to split the transmitted signal such that half of the transmitted signal is connected to the Lecroy SDA (Channel 1) to serve as the reference signal for the receive signals on channel 2 , channel 3 and channel 4. The second half of the transmitted signal is connected to the transmit antenna for transmission. Figure 7.42a and 7.42b show the constellation diagram of two receive antennas connected to the channel 3 and channel 4 on the Lecroy SDA. The receive antennas are 1.5 m apart from the transmit antenna with the data rate of 200Mbps and uses QPSK modulation. Figure 7.42a show larger degree of phase noise in the constellation. Figure 7.43a and Figure 7.43b show the constellation diagram of two of the receive antenna while receive data 480Mpbs. The transmit and receive antennas are 1.5 mm apart. The receive antenna are connected channel 3 and channel 4. Phase error seen could be due to the frequency offset and phase shift at the receive antennas.

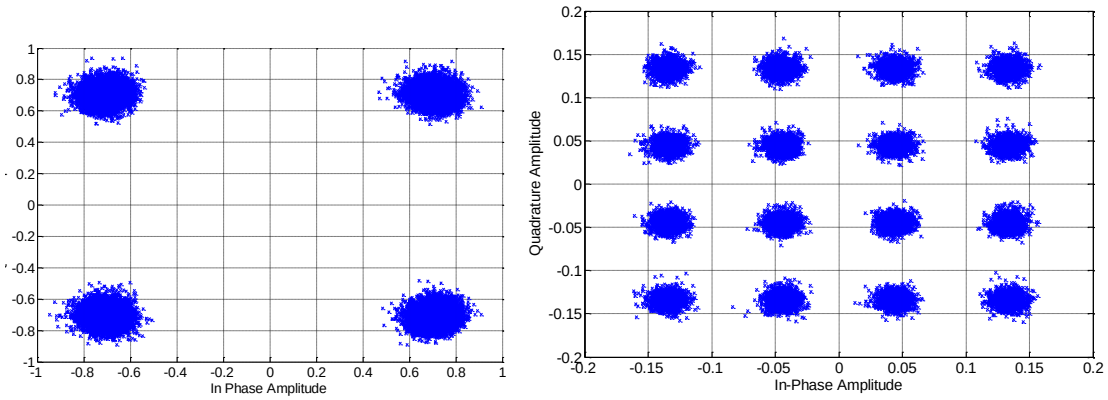


(a) 200Mpbs using QPSK (b) 480Mbps using DCM

Figure 7.41 Constellation diagram from the transmitter via the splitter (200Mpbs and 480Mpbs)

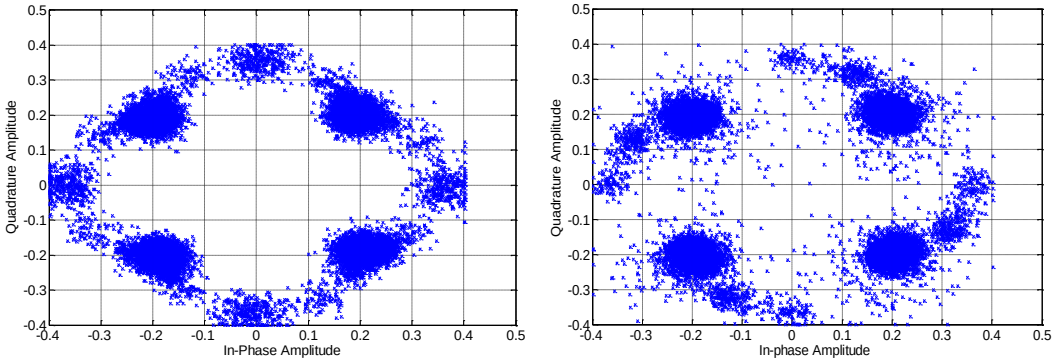


(a) 200Mpbsusing QPSK (b) 200Mpbs using QPSK

Figure 7.42 Constellation diagram 3 m from the transmitter (200Mbps)

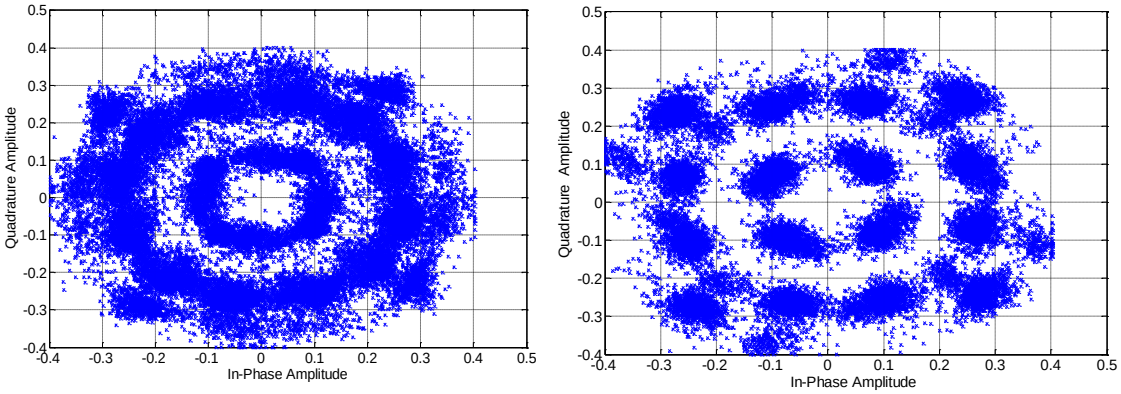


(a) 480Mbps using DCM (b) 480Mbps using DCM

Figure 7.43 Constellation diagram 1.5 m from the transmitter (480Mpbs)

In MRC, each of the received signals is weighted with a factor that is proportional to the signal amplitude. The branches with stronger signals are further amplified while the ones with weak signals are attenuated. The instantaneous SNR can be expressed as

$$\gamma = \frac{\left|\sum_{j=1}^{J} h_{j,i}\, w_{j,i}\right|^2}{\frac{1}{2}E\left[\left|\sum_{j=1}^{J} h_{j,i}\, w_{j,i}\right|^2\right]} \qquad 7.15$$

Where $\gamma$ is the instantaneous SNR. To get the maximum weight, the conjugate of the Channel Impulse Response (CIR) is used which can be express as

$$w_{j,i} = h_{j,i}^{*} \qquad 7.16$$

Where $h_{j,i}^{*}$ is the conjugate of $h_{j,i}$. Since each sub-channel experiences different fading in OFDM UWB, the weight of each sub-channel is determined individually. Based on the WiMedia specification each packet has a Channel Estimation Sequence (CES) which can be used at the beginning to estimate the channel [2]**.** From the channel estimation sequence, the channel response can be determined. Figure 7.44 shows the implementation of the maximal ratio combining (MRC) technique. The signals from all the three antennas are then summed up and forwarded for demodulation. The model is used in conjunction with the test bed to test the system performance. After combining the signal, the symbols are then demodulated either using QPSK or DCM modulation technique depending on the data rate. The data bits are de-interleaved and viterbi decoder is used to decode the coded bits by inserting the punctured bit and decoding it according to the code rate as specified in the WiMedia Specification 1.0 [17].

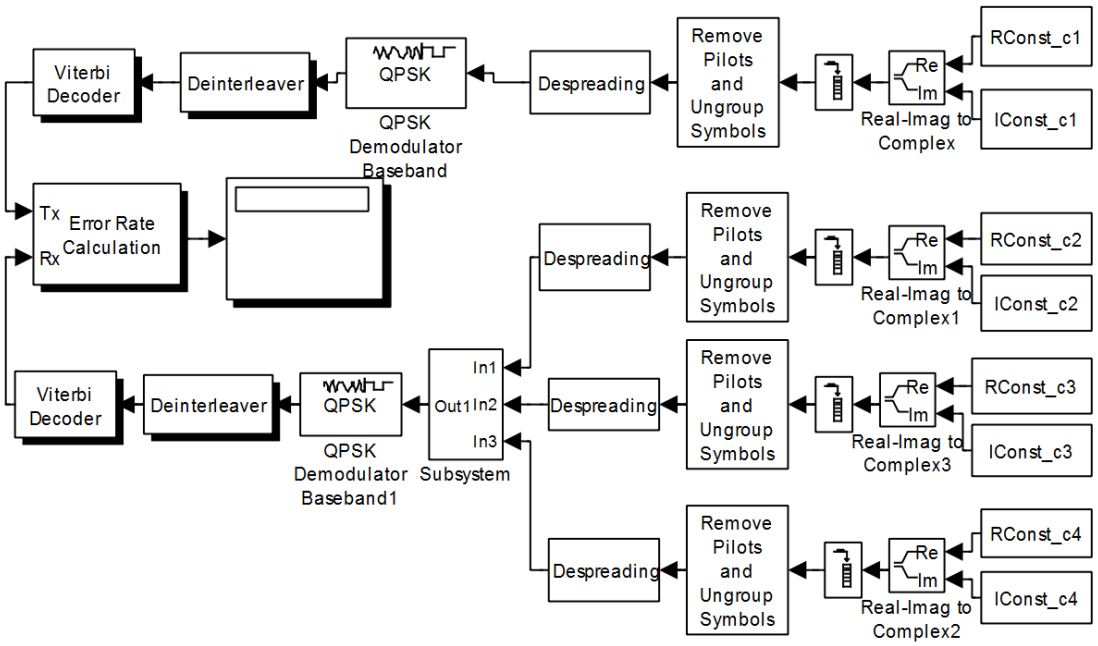


Figure 7.44 Combining the signal using MRC and calculating the BER rate.

The results provide insight into the practical implementation of spatial processing technique using multiple antennas. Table 7.7 shows the BER performance for OFDM UWM with MRC Technique in comparison with Antenna Selection Technique. The results show that over 3m 200Mpbs could be successfully achieved using MRC while transmitting a data rate of 480Mpbs is achieved over 1.5 m. The antenna selection technique could be used for transmitting data rate of 200Mbps over 2m but has a PER of 100% when the distance is more than 2m.

Table 7.7 BER performance for OFDM UWM with MRC Technique in comparison with Antenna Selection Technique

| Data Rate (Mbps) | Distance | MRC (PER) % | Antenna Selection (PER) % |
|---|---|---|---|
| 480 | 0.5 | 0 | 10 |
| 480 | 1 | 2.11 | 50 |
| 480 | 1.5 | 10 | 100 |
| 480 | 2 | 50 | 100 |
| 480 | 2.5 | 100 | 100 |
| 480 | 3 | 100 | 100 |
| 200 | 0.5 | 0 | 0 |
| 200 | 1 | 0 | 2.5 |
| 200 | 1.5 | 0 | 20 |
| 200 | 2 | 0 | 60.8 |
| 200 | 2.5 | 5 | 100 |
| 200 | 3 | 20 | 100 |

**7.10 Summary**

In this chapter, the design of an antenna selection circuit was presented. The objective of the circuit is to improve the performance of the UWB system in an indoor environment. The circuit was designed to work with AT90CAP9 UWB Evaluation kit. The circuit has three antennas connected to it and switches to the antenna with the highest RSSI. The circuit was designed using ADS for the RF part and Multisim for the digital and analogue section. The simulated result show acceptable parameters. The circuit was tested in the body centric laboratory. The results show that the antenna selection can be used to improve the performance of the UWB system.

Maximal Ratio combining technique was implemented using a test bed with post processing. The test bed mainly comprises of a Lecroy SDA used for capturing and sampling the data over its four channels and a UWB evaluation kit to generate MB OFDM UWB signals. Using diversity system techniques could aid the UWB technology of achieving its proposed target. The results show that MRC technique could be used to improve the performance of the system, delivering a higher data rate in streaming multimedia applications. The Performance of the MRC is better than the performance of the Antenna selection technique but will increase the complexity of the system.

**References**


[1] Analog Devices, Inc “1 MHz to 8 GHz, 70 dB Logarithmic Detector/Controller” AD8318 data sheet April 2007. D04853-0-4/07(B)

[2] Avago Technologies, “0.5 – 6 GHz Low Noise GaAs MMIC Amplifier” MGA-86563 Data Sheet. AV02-2514EN October 27, 2010

[3] AVX Corporation, “Thin-Film Directional Couplers CP0603 High Directivity LGA Termination“

[4] TDK Corporation, “Band Pass Filter for UWB” , DEA453960BT-3002B1 datasheet, August 2006 Ver.9

[5] Skyworks Solutions, Inc “SKY13317-373LF: 20 MHz-6.0 GHz pHEMT GaAs SP3T Switch” DATA SHEET 200914H January 11, 2011

[6] L.G. Maloratsky, "Reviewing the Basics of Microstrip Lines," Microwaves & RF, March 2000, pp. 79-88.

[7] Operational Amplifiers / Comparators Application note. Op-Amp/ Comparator Tutorial ROHM semi conductor, November 2011. Rev B

[8] *Shift Registers tutorial. accessed from : https://maxwell.ict.griffith.edu.au/yg/teaching/.../dns_module3_p3.pdf*

[9] 555 and 556 Timer Circuits John Hewes 2011, The Electronics Club, Accessed from: http://www.kpsec.freeuk.com/555timer.htm

[10] D. L. Jones, “PCB design Tutorial”, Rev A- 29th June 2004

[11] S. Mercer, Minimizing RF PCB electromagnetic emissions, RF Design Magazine January 1999

[12] J. Warner “Signal Loss: A Big Picture Approach to RF/MW PCB Design” Accessed from: http://mwexpert.typepad.com/rfmw_pcb_design/2011/10/signal-loss-a-big-picture-approach-to-rfmw-pcb-design.html

[13] R. Hartley, “Base Materials for High Speed, High Frequency PC Boards”. March 2002, Published in PCB & A

[14] L. Guo, S. Wang, X. Chen and C. Parini, “A Small Printed Quasi-Self-Complementary Antenna for Ultra wideband Systems” IEEE Antennas and Wireless Propagation Lett, VOL. 8, 2009

[15] Lecroy Serial Data Analyzer , Operator’s Manual , Lecroy Corporation Chestnut Ridge, Ny 10977–6499 November 2006

[16] PHY Specification: Final Deliverable 1.5 Multiband OFDM Physical Layer Specification , WiMedia Alliance, Inc ,2009

# CHAPTER 8

**CONCLUSION AND FUTURE WORK**

## 8.1 Summary

The need for high data rate wireless systems within the PAN cannot be over-emphasized. This is due to the increase in demand for multimedia communication. Though UWB technology has the potential of meeting the current demand, it still faces some challenges. These challenges are power limit, different regulations in different regions and frequency selective fading. A critical review on the development of UWB is carried out.

It is evident from the review that substantial research has been done on the IR–UWB with MIMO while little has been done on MB-OFDM UWB with MIMO.

Detailed evaluation and analysis of the current UWB systems was carried out using an evaluation kit. The evaluation was done over varied distances, payloads, logical channels, signal-to-noise ratio and data rates. The analysis showed that only lower data rates can be used effectively for commutation within an acceptable PER of 8%. To verify this, a UWB commercial product was purchased and the throughput was evaluated over varied distances. The result agrees with the throughput of the lowest data rate while using the evaluation kit. The throughput obtained in the commercial UWB product shows only 53.3Mbps instead of the expected data rate of 480Mbps. Also a MIMO link analysis was done to determine the coverage distance when both MIMO and UWB are combined based on the WiMedia link budget specification. The analysis shows that the coverage distance when MIMO and UWB are combined will be very short due to the power constrain on the UWB technology.

The channel model for both large and small scale loss for the case of an SISO, SIMO and MIMO are then considered. Large scale loss is as a result of the exponential loss of signals over a distance while the small scale losses are due to the arrival of signals in clusters and rays. The procedures for post processing channel measurement via VNA were discussed. The aim of the post processing is to prepare the measured channel for evaluation in modelling software such as simulink. Due to the problem of frequency selective fading in UWB channel, an adaptive modulation was proposed to improve the BER performance by varying the modulating bit

across the sub channels depending on the degree of fading. The simulation results show that using adaptive modulation to maintain a constant data rate features a better performance than using only QPSK modulation in a frequency selective fading channel.

Furthermore, maximal ratio combining and antenna selection were incorporated to the MB OFDM UWB system. Two different types of antenna were used (monopole and patch) and were placed at different orientation. The performance of the UWB system with the diversity technique shows remarkable gain of up to 8dB over short distances. The results show that diversity can be used to improve the performance of the system. The antennas are linearly polarised and when placed at an orientation perpendicular to each other, the gain is only up to 3dB.

Due to the frequency selective fading in the UWB channel using non-adaptive modulation will not efficiently utilise the channel. To understand the variation in the channel due to human movement, a measurement campaigned was carried out and the channel is analysed. Different measurement scenarios were considered with different number of people. The measurements were carried out in the body centric laboratory. These measurements show that adaptive modulation could be used in a UWB channel to improve the bit error rate performance without introducing much over head. An antenna selection circuit is design, fabricated and assembled. The circuit is design to be used with the AT90CAP UWB evaluation kit. The Circuit has three antennas and it checks their RSSI to select the antenna with the best RSSI.

Maximal Ratio combining technique is implemented using a test bed. The test bed mainly comprises of a Lecroy SDA used and for capturing and sampling the data over its four channels and a UWB evaluation kit to generate MB OFDM UWB signals. Using diversity system techniques could aid the UWB technology of achieving its proposed target. The results show that MRC technique could be used to improve the performance of the system and to enable delver higher data rate capable of streaming multimedia applications.

## 8.2 Key Contributions

The contributions in this thesis are detailed as follows

### 8.2.1 Detailed evaluation and analysis of the MB OFDM communication system.

- A MB-OFDM UWB evaluation Kit used was for carryout detail evaluation considering key parameters such as payload, distance, SNR, data rate and throughput. The evaluation results showed only lower data rates of 55.3Mbps, 80Mbps and 106.7Mbps have acceptable performances.
- A commercial available wireless USB adapter was evaluated which shows commercial UWB

products use low data rate for transmission. This means MB OFDM UWB product are yet to offer the proposed 480Mpbs over 3metres.

### 8.2.2 UWB channel modelling Implementation of Adaptive bit loading

- UWB channel modelling was demonstrated using channel measurements .The channel was characterised based on large scale fading due to the path loss and small scale fading due to the multiple clusters and rays arriving at different times at the receiver. The post processing technique of modelling a realistic channel and using it in simulink was also demonstrated based on the measurements.
- A novel technique of using adaptive modulation was presented as a way of utilising the channel efficiently in a channel experiencing frequency selective fading. The results show that a better BER performance can be obtained using adaptive modulation while maintaining the data rate of the system.

### 8.2.3 Time varying UWB channel measurement with adaptive modulation.

- Time varying UWB Channel modelling was demonstrated to capture shadowing in the channel. A 20ms time interval between successive channels was achieved in channel measurement while human subjects where moving.

- Effects of different number of human subjects in various movement patterns and in different scenarios are studied. The scenarios were realistic environment where UWB devices are operating. Channel correlation is used investigated and monitor the changes in the channels as people moved across it. The results showed that the number of people moving across the channel and the height of the antenna affect the correlation between the successive channels. Also, maximum deviation in the channel correlation is computed for each scenario.

- Channel responses were inputted into the UWB system model to evaluate the system performance while using non-adaptive modulation and adaptive modulation with a feedback rate of 20ms. Result exhibit that implementing adaptive modulation in UWB system enhances the performance of the system.

### 8.2.4 Implementing spatial diversity techniques to improve the performance.

- Multi antenna methods were employed to exploit different properties of the radio channel to improve performance. Viability of a diversity system was demonstrated in measurements in

and the channels were combined using maximal ratio combining and antenna selection techniques. Spatial diversity was employed to improve the system performance by achieving high data rates. The SIMO channel measurements were carried out for a typical indoor environment to replicate realistic channel scenario in the system simulation.

- Different antenna orientations were used to model scenarios with space constraints. The results have showed that good diversity gain could be achieved using different orientations. Also different UWB antennas were used in study the performance of diversity in UWB system. A minimum diversity gain of 4dB is achieved using three antenna configurations while a minimum gain of 2.5dB is achieved with two antennas. The results of the simulink simulations show that both the LOS and the NLOS channel performance can be improved with spatial diversity.

### 8.2.5 Implementation of Antenna selection circuit and testbed for MRC technique

- Implementation of the antenna selection circuit is demonstrated. The objective of the circuit is to improve the performance of the UWB system in an indoor environment. The circuit is designed to work with AT90CAP9 UWB Evaluation kit. The circuit is designed using ADS for the RF part and Multisim for the digital and analogue section. The simulated result show acceptable parameters. The results show that the antenna selection can be used to improve the performance of the UWB system.

- Maximal Ratio combining technique is implemented using a test bed. The test bed is built consisting Lecroy SDA, UWB evaluation kit, PC and built RF end. Using diversity system techniques could aid the UWB technology of achieving its proposed target. The results show that MRC technique could be used to improve the performance of the system and to enable delver higher data rate capable of streaming multimedia applications

## 8.3 Future work

Further research will be carried out to seek novel solution that will improve the performance of UWB systems. Therefore the following will considered as future work of the research project

- Carrying out further detailed UWB channel analysis in realistic environment to able to identify and tackle relevant challenges while implementing the novel solution. This should establish the minimum distance between the antennas for optimal performance and show the possibility of achieving high data rate over three metres and beyond for multimedia

within the indoor environment.

- Testing and Extensive study will be carried out to determine the system performance under different channel conditions
- Develop technique on combining adaptive modulation and receive diversity to improve the BER performance of the system and to increase the coverage distance. This will provide a novel approach in enhancing the capacity and performance in a diversity scenario.
- Extend the diversity to include MIMO using both space time diversity and spatial multiplexing. This will be done in consideration of the maximum distance to achieve optimum performance as discussed in chapter three. This study include
    a. Developing technique for channel estimation for MIMO MB-OFDM UWB
    b. Improve the channel spectral efficiency for capacity gain over short distances. This includes developing a MIMO MB-OFDM model to establish the data rate supportable by the system under the current regulation and power constrain.
    c. Validation and testing of the results and any optimization needed
- Study on using Field-Programmable Gate Array (FPGA) in designing and developing Communication systems
- Development of algorithms and architecture to satisfy the requirement for Multiuser and low cost. This could include modification of algorithm where the performance of existing algorithm or technique does not meet the expected requirement.
- Development of an experimental improved UWB communication system prototype using Field-Programmable Gate Array **(**FPGA) for further testing and experimental evaluation.

# APPENDIX A

**CODING, INTERLEAVING AND MODULATION**

**A.1 Coding and interleaving**

The convolution encoder used in the MB-OFDM UWB physical model uses a code rate of 1/3 with the generator polynomials, $g_o = 133_8, g_1 = 165_8, g_2 = 171_8$. Different code rates are obtained by puncturing. Puncturing is the procedure used to remove some encoded bits thus reducing the number of bits that will be sent. The receiver inserts a dummy zero metric into the decoder to replace the omitted bits at the receiver [1]. Figure A.1 shows the convolution encoder structure while Figure A.1 illustrates the puncturing procedure. The generator polynomials in octal numeral system are expressed as $g_0$, $g_1$, $g_2$

$$g_0 = 133_8, g_1 = 165_8, g_2 = 171_8$$

While in binary system is

$$g_0 = 1011011_2, g_1 = 1110101_2, g_2 = 1111001_2$$

These are expressed in polynomials as follows

$$g_0 = x^6 + x^4 + x^3 + x + 1 \qquad 2.8$$

$$g_1 = x^6 + x^5 + x^4 + x^2 + 1 \qquad 2.9$$

$$g_2 = x^6 + x^5 + x^4 + x^3 + 1 \qquad 2.10$$

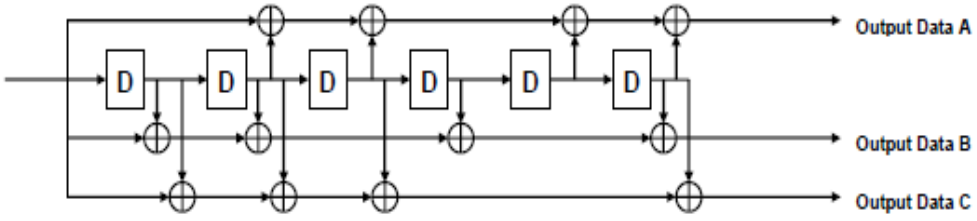


Figure A.1 Convolution encoder [2]

Puncturing is a technique used to make an n/m rate code from basic code rates such as $\frac{1}{2}$ and $\frac{1}{3}$ codes. It is done by deleting some of the bits in the encoder output. The bits are deleted according to the puncturing matrix, which in this case for a $\frac{5}{8}$ code is

$$\begin{bmatrix} 1 & 0 & 1 & 0 & 1 \\ 1 & 0 & 1 & 0 & 1 \\ 0 & 1 & 0 & 1 & 0 \end{bmatrix}$$

The puncture vector is a binary vector with 1 indicating that the bit in the corresponding position is sent to the output vector while 0 indicates that the bit in the corresponding position is discarded. At the receiver, dummy bits are inserted back in the matrix where the bit is zero before forwarding the frame to the decoder.

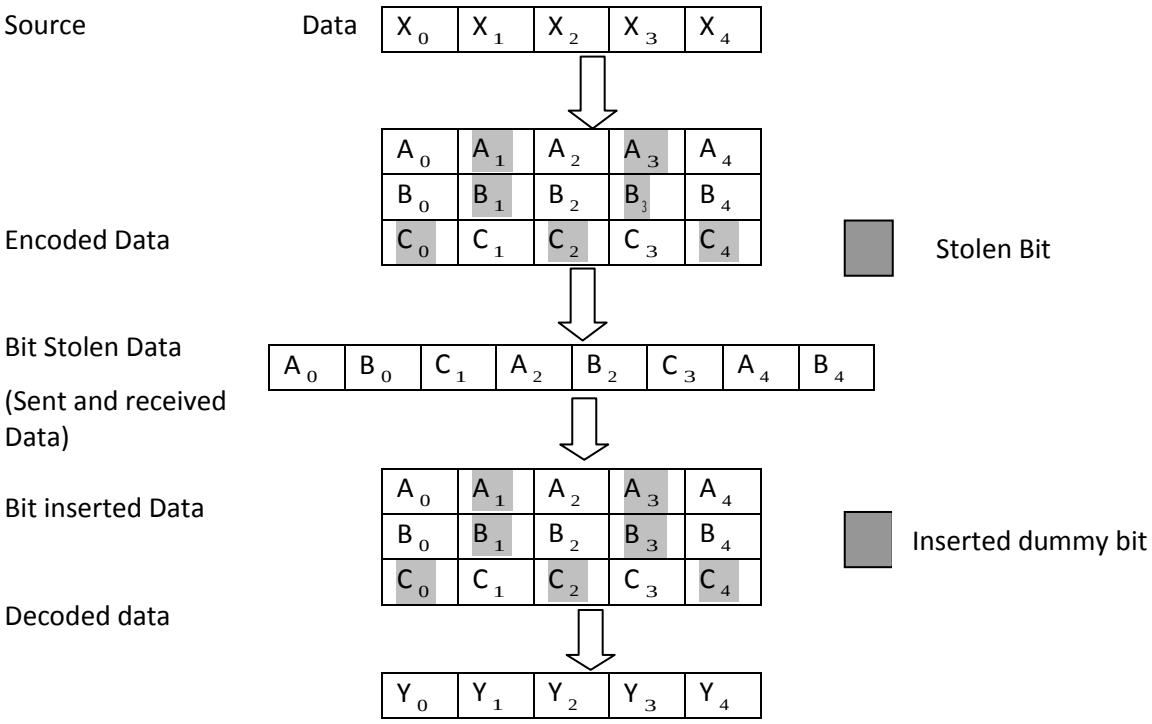


Figure A.2 Example showing the procedure used in puncturing [2]

After coding the information, the data are then interleaved. Bit interleaving is done to provide robustness against burst errors. The data bits are rearranged in order to reduce burst errors. This is carried out in two stages

1. Interleaving across the OFDM frames
2. Interleaving within the OFDM frames

**A.2 Modulation**

Phase shift keying (PSK) is a widely used scheme in data transmission and it is well suited for synchronous communication. For a given energy information per bit, PSK gives lower bit error rate in a communication system with unrestricted bandwidth. The modulation scheme used in the MB OFDM UWB model is Quadrature Phase shift keying (QPSK**).** Figure A.3 BPSK and QPSK constellation bit encoding. The following equation describes the Q-PSK modulation scheme

$$m_i(t) = \begin{cases} \sqrt{\frac{2E}{T}} \cos\left[ 2\pi f_c t + (2i-1)\frac{\pi}{4} \right] & ,0 \le t \le T \\ 0 \end{cases} \qquad 2.11$$

Where i = 1, 2, 3 and 4, E= transmitted signal energy, T=Symbol duration and $f_c$ = frequency

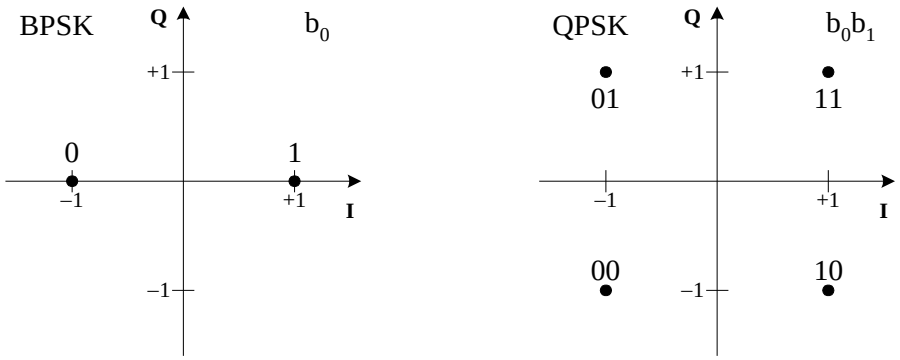


Figure A.3 BPSK and QPSK constellation bit encoding

Gray coded constellation is used in mapping the data base on the require modulation scheme. Gray coding is a technique often used in multilevel modulation scheme to minimise the bit error rate by ordering the symbols so that the binary representation of adjacent symbols differs only one bit.

# APPENDIX B

**MATLAB EMBEDDED CODES**

### B.1 Modulation

```
function y = fcn(u,channelInfo)
% This block supports an embeddable subset of the MATLAB language.
%
w=0;
x=0;
count=0;
yIn=complex(0);

y = complex(zeros(100,1));

for x=1:100
 % if channelInfo(x)==0 % To Avoid Algebraic Loop Making sure that when there No feed use the default
   if channelInfo(x)==4
      w=count+1;
      n=u(w)*2^3+u(w+1)*2^2+u(w+2)*2^1+u(w+3)*2^0;
     yIn =pskmod(n,16,0,'gray');
     y(x)=yIn;
     count=count+4;
   end

   if channelInfo(x)==3
      w=count+1;
      n=u(w)*2^2+u(w+1)*2^1+u(w+2)*2^0;
     yIn = pskmod(n,8,0,'gray');
     y(x)=yIn;
     count=count+3;
   end

   if channelInfo(x)==2
     w=count+1;
     n=u(w)*2^1+u(w+1)*2^0;
     yIn = pskmod(n,4,0,'gray');
     y(x)=yIn;
      count=count+2;
   end

  if channelInfo(x)==1
      w=count+1;
     n=u(w)*2^0;
     yIn = pskmod(n,2,0,'gray');
     y(x)=yIn;
```

```
  count=count+1;
   end

   if channelInfo(x)==0
      y(x)=0;
   end
 end
```

**B.2 Demodulation**

```
   function y = fcn(u,channelInfo)
% This block supports an embeddable subset of the MATLAB language.
%
    y =zeros(200,1);
   %yInt=0;
   w=0; % Counting the bits in order to demodulate correctly

   for x=1:100
     % if channelInfo(x)==0 % To Avoid Algebraic Loop Making sure that when there No feed
use the default

      if channelInfo(x)==4

         yIn=pskdemod(u(x),16,0,'gray'); % demodulating using 16 Psk
         yStr=num2str(yIn);
         yInt=str2num(yStr);
         w=w+4;

         for t=0:3 % Covert decimal to Binary and arrange the bits in order
            r=mod(yInt,2);
            y(w)=r;
            a=yInt/2;
            e=fix(a);
            yInt=e;
            w=w-1;
         end
         w=w+4;
      end


      if channelInfo(x)==3

          yIn=pskdemod(u(x),8,0,'gray'); % demodulating using 8Psk
         yStr=num2str(yIn);
         yInt=str2num(yStr);
         w=w+3;

         for t=0:2 % Covert decimal to Binary and arrange the bits in order
            r=mod(yInt,2);
            y(w)=r;
            a=yInt/2;
            e=fix(a);
```

```
        yInt=e;
        w=w-1;
      end
      w=w+3;
    end


    if channelInfo(x)==2

      yIn=pskdemod(u(x),4,0,'gray');  % demodulating using QPsk
      yStr=num2str(yIn);
      yInt=str2num(yStr);
      w=w+2;
      for t=0:1  % Covert decimal to Binary and arrange the bits in order
        r=mod(yInt,2);
        y(w)=r;
        a=yInt/2;
        e=fix(a);
        yInt=e;
        w=w-1;
      end
      w=w+2;
    end

     if channelInfo(x)==1
      yIn=pskdemod(u(x),2,0,'gray');  % demodulating using BPsk
      yStr=num2str(yIn);
      yInt=str2num(yStr);
      w=w+1;
      y(w)=yInt; % sine the ouput are already in Binary NO need for conversion

          end

    if channelInfo(x)==0  % Skip demodulating
    end

  end
```

**B.3 Channel Adjustment**

```
% This block supports an embeddable subset of the MATLAB language.
%% to readjust the channel bit to be 200 from any number
function newChannelBits  = fcn (channelBits)

[bits,noOfCHWith4bits,noOfCHWith1bits]= getBits(channelBits);
count=1;
bits;

while bits~=200
 if  bits> 200
  if channelBits(count)==4 % checking to reduce modulation rate if the bits are more than 200
    channelBits(count)=channelBits(count)-1;
     else if channelBits(count)==3 && noOfCHWith4bits==0
     % checking to reduce modulation rate and making sure that all 4 bit are reduce first
```

```
      channelBits(count)=channelBits(count)-1;
          end
   end
   else if bits <200
    if channelBits(count)==1 % checking to increase modulation rate if the bits are less than
200
      channelBits(count)=channelBits(count)+1;
   % checking to increase modulation rate and making sure that all 1 bit are increase first
 else if channelBits(count)==0 && noOfCHWith1bits==0
     channelBits(count)= channelBits(count)+1;
    end
    end
     end
 end

 count =count+1;
 if count ==101
    count=1;
 end
 [bits,noOfCHWith4bits,noOfCHWith1bits]= getBits(channelBits);
end
 newChannelBits =channelBits;

 % function to calculate the sum of bits an their individual  bit numbers
 function [sum,noOfCHWith4bits,noOfCHWith1bits]  =  getBits(channelBits);
sum=0;
noOfCHWith4bits=0;
noOfCHWith1bits=0;
for i=1:100
   sum=sum+channelBits(i);
   if channelBits(i)==4
      noOfCHWith4bits=noOfCHWith4bits+1; % get current number of channels with four bits
   end
    if channelBits(i)==1
      noOfCHWith1bits=noOfCHWith1bits+1; % get current number of channels with 1 bit
    end
end
```

**B.4 Matching the SNR to a modulation index**

```
function y = fcn(u)
% This block supports an embeddable subset of the MATLAB language.
%

y=zeros(100,1);
for i=1:100
   %  for 16Psk
 if u(i)<=150 && u(i)>=17
      y(i,1)=4;

    % for 8 Psk
   else if u(i)<=17 && u(i)>=12

      y(i,1)=3;
```

```
      % for 4 psk
      else if u(i)<=12 && u(i)>=7
      y(i,1)=2;

      % for bpsk
         else if u(i)<=8 && u(i)>=5
        y(i,1)=1;
           else if u(i)<=5 %:Test: Trying to avoid zero to get the system working
           y(i,1)=0;
           end
         end
      end
  end
  end
end
%%y=zeros(100,1)+2;%
```

**B.5 Calculating the SNR of data sub carrier**

```
function y = fcn(CM,EsNo)
% This block supports an embeddable subset of the MATLAB language.

y=zeros(100,1);
HCM=complex(ones(122,1));

 %EsNo=12;
N=10^(-0.1*EsNo); % noise variance
SNR1=zeros(100,1);
SNRdB=zeros(100,1);
pilot=7;
channel=1;
for i=6:117 % Data channels start from channel number 6 and end on channel number 118
  %  if i==63

   % else
      if i==pilot
         pilot=pilot+10; % to remove the Pilot channels , leaving only the Data Channels
         if i ==57
          pilot=pilot-1; % since the DC is removed subsequent pilots will in the last digit of 6s and
NOT 7s
         end
      else
         SNR1(channel)=(abs(HCM4(i))^2)/N; % calculate the Signal to noise ratio
                channel=channel+1;
      end
end
 y=SNR1;
```

# APPENDIX C

**UWB EVALUATION KIT SOFTWARE SETUP**

## C.1 Software Setup

The Evaluation kit is configured and controlled using the NIOS Embedded Design Suite (EDS) Command shell console and it is interfaced through USB blaster cables. Figure A.1 shows the NIOS II EDS Command Shell interface to set the system parameters. The connection between the USB blaster cables and the computer is checked using "Jtagconfig" command**.** The JTAG command, as defined by the IEEE sts.-1149.1 standard, is an integrated method for testing interconnection on printed circuit boards (PCBs) implemented on the IC level [3].

The USB Blaster cable of the CAP9 UWB transmitter and receiver board when connected flashes (blue light) in sequence. The sequence of the flash corresponds to the cable connection to the computer. The first flash indicates the cable number is 0 and the second flash indicates the cable is number 1. If the transmitter board is connected to USB Blaster cable 0, the following command is used in the command shell to access the transmitter menu:

**Nios2-terminal - -cable = "USB-Blaster [USB-0]"**

The user interface shown in Figure C.1 appears displaying a menu which can be used to configure the system. The following parameters of channel, payload, rate, power level and transmission can be used to configure the system. By pressing "T" on the command prompt, transmission is activated and the LED-DS3 on the transmitter board will begin to flash, indicating the board is transmitting.

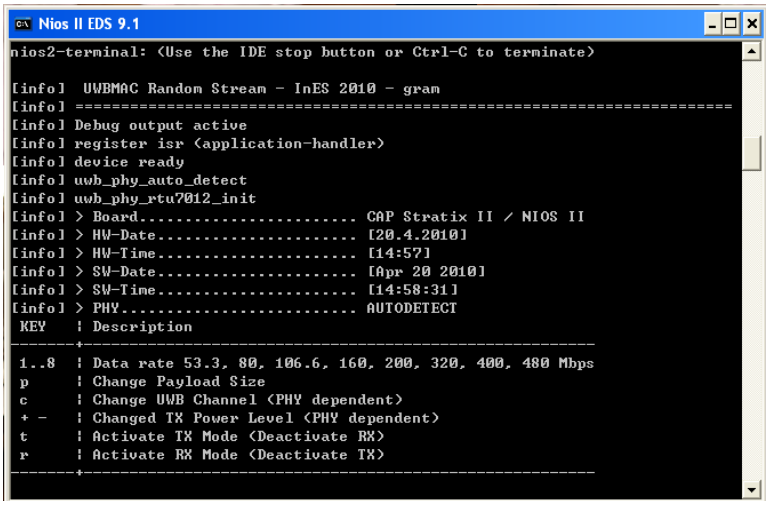


Figure C.1 Interface for setting the Transmitter/Receiver parameters.

For the receiver, another NIOS II command shell needs to be opened to display the receiver information by following the same procedure as for the transmitter. After logging to the NIOS EDS console, the following command line used:

**Nios2-terminal - -cable = "USB-Blaster [USB-1]"**

When the USB cable 1 is connected to the receiver board, another interface same as Figure 3.4 will appear. Reception of data is activated by Pressing "R". The LED-DS4 on the receiver board will begins to flash, indicating the board is receiving the data. Note that the settings for the transmitter and receiver boards must be the same for data to be received. Table C.1 shows the list of keys used in configuring the transmission and reception of data. Transmission and reception must be deactivated and then reactivated for any change to be effective.

Table C.1 Keys to configure the data transmission and reception of the development board.

| Key | Description |
|---|---|
| '1'….'8' | Data rate 53.3Mbps….480Mbps |
| 'p' | Change payload Size for (TX) |
| 'c' | Change UWB Channel (For TX and RX) |
| '-'/'+' | Change TX Power level (For TX) |
| 't' | Activate TX |
| 'r' | Activate RX |
| 's' | Show settings (during RX and TX) |
| 'o' | Deactivate RX/TX (during RX and TX). Use this to change a setting and then reactivate RX/TX |

## C.2 Test Parameters

UWB Evaluation kit is used to test MB-OFDM UWB system based on the following parameters

### C.2.1 Data rates

The transmission data rates proposed by the WiMedia group for the MB-OFDM model are 55, 80, 110, 160,200,320,400,480,640,800, 960 and 1024Mbps but the AT91CAP9A Development kit only supports 53.3, 80,106.6,160,200,320,400 and 480Mbps. Table C.2 summaries the MB-OFDM data rates with their dependent parameters. [4]

Table C.2 MB-OFDM UWB Data Rate-Dependent Parameters

| Rate (Mb/s) | Modulation | Coding Rate (*R*) | Freq domain Spreading(FDS ) | Time domain Spreading (TDS) |
|---|---|---|---|---|
| 53.3 | QPSK | 1/3 | YES | YES |
| 80 | QPSK | 1/2 | YES | YES |
| 106.7 | QPSK | 1/3 | NO | YES |
| 160 | QPSK | 1/2 | NO | YES |
| 200 | QPSK | 5/8 | NO | YES |
| 320 | DCM | 1/2 | NO | NO |

| | | | | |
|---|---|---|---|---|
| 400 | DCM | 5/8 | NO | NO |
| 480 | DCM | 3/4 | NO | NO |
| 640 | MDCM | 1/2 | NO | NO |
| 800 | MDCM | 5/8 | NO | NO |
| 960 | MDCM | 3/4 | NO | NO |
| 1024 | MDCM | 4/5 | NO | NO |

### C.2.2 Logical channels

Logical channels which are defined by the WiMedia group are characterised by different time-frequency codes and are used to improve the performance. Table C.3 shows time-frequency codes for band group 1 and Figure C.3 illustrate the frequency band and allocations. For example, if channel number 9 is selected, the system will use the time frequency code number 1. This will make the system to transmit the first signal in band 1, second signal in band 2, third signal in band 3, fourth signal in band 1, fifth signal in band 2 and so on. This pattern is repeated for all the signals with the transmitter. For channel 13, 14, and 15, the code indicates that all signals will be sent only through band 1, 2 and 3 respectively. This shows that when either channel 13, 14 or 15 is selected, frequency hopping is not in use.

Table C.3 Time-Frequency Codes for Band Group 1[2]

| Channel Number | TFC Number | BAND_ID for Time-Frequency Codes for Band Group 1 | | | | | |
|---|---|---|---|---|---|---|---|
| 9 | 1 | 1 | 2 | 3 | 1 | 2 | 3 |
| 10 | 2 | 1 | 3 | 2 | 1 | 3 | 2 |
| 11 | 3 | 1 | 1 | 2 | 2 | 3 | 3 |
| 12 | 4 | 1 | 1 | 3 | 3 | 2 | 2 |
| 13 | 5 | 1 | 1 | 1 | 1 | 1 | 1 |
| 14 | 6 | 2 | 2 | 2 | 2 | 2 | 2 |
| 15 | 7 | 3 | 3 | 3 | 3 | 3 | 3 |

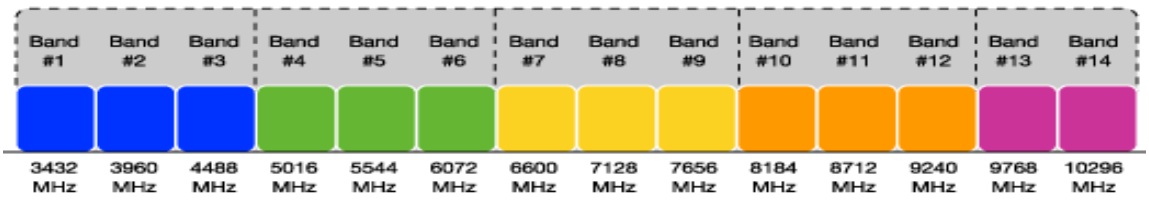


Figure C.3 Multiband OFDM Frequency bands [5]

### C.2.3 Transmit power control

Eight Transmit power level, numbered 0 to 7 (as shown in the table C.4) provides support for power control by attenuating the transmit power in a step of 2dB down the level. It enables the

minimisation of the transmit power spectral density when coexisting with other wireless technologies while providing reliable link. The power control is for three transmit modes namely time-frequency Interleaving over band 1 (TFI1), time-frequency Interleaving over band 2 (TFI2) and Fixed- Frequency Interleaving.

TABLE C.4 Transmit power levels [2]

| LEVEL | TX Power Attenuation for TFI Modes | TX Power Attenuation for TFI2 Modes | TX Power Attenuation for FFI Modes |
|---|---|---|---|
| 0 | 0 dB | 0 dB | 0 dB |
| 1 | 2 dB | 2 dB | 2 dB |
| 2 | 4 dB | 4 dB | 4 dB |
| 3 | 6 dB | 6 dB | 6 dB |
| 4 | 8 dB | 8 dB | 8 dB |
| 5 | 10 dB | 10 dB | RESERVED |
| 6 | 12 dB | RESERVED | RESERVED |
| 7 | RESERVED | RESERVED | RESERVED |

### C.2.4 Payload

The UWB evaluation kit supports different payload sizes ranging from 0 to 4095bytes. For analysis of the system performance, the payload sizes of, which are 512, 1024, 2048, 3071 and 4095 bytes are considered. Figure C.4 depicts a screen shot of the NIOS command shell of the receiver, giving information about the performance of the system. The fields are interpreted as follows:

- RSSI: Received Signal Strength.
- LQE: Link Quality Estimation (estimated SNR).
- Rate: Physical Layer Data Rate.
- Size: Payload Size.
- Rcvd: Packages Per Second Successfully Received.
- PER: Packer Error Rate.
- Date rate: Data Throughput Rate.

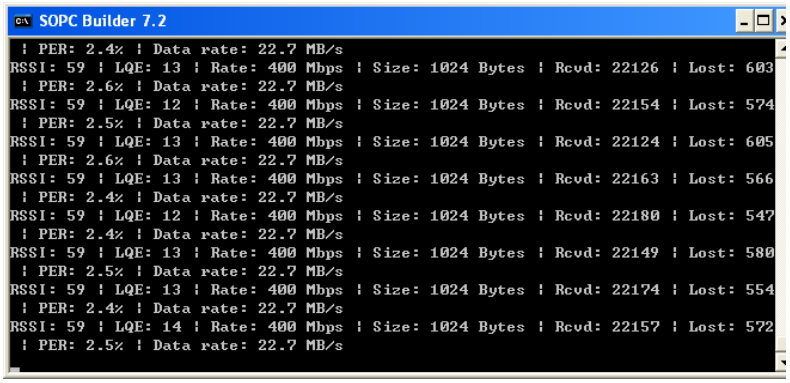


Figure C.4 screen shot of NIOS command shell of the receiver

# APPENDIX D

**RESULTS FOR UWB TIME VARYING CHANNEL**

**D.1 Acquiring data**

Two methods were considered for triggering in order to determine the better method to use.

1. Labview: The first method used was with Labview. The time taken to complete a measurement cycle plus saving the data is noted to be about 1s which is not suitable for the intended measurement. This could be due to the network overhead and number of cycles it takes to store one measurement.
2. Data logger: This program triggers each sweep as fast as possible and the trigger is then kept in a hold mode to enable it read and transfer the entire data taken before the next sweep. The application allows user to automatically store trace data over long periods of time. Although this utility is not primarily designed for fast speed applications, using the above stated settings results in a better performance compared to the Labview.

Taking measurements while keeping the Agilent PNA-X Vector Network Analyser in a continuous triggering mode is not the best approach to use in capturing data. This is because the PNA stores data in its buffer sequentially during a sweep. In this mode when an external program sends a command to transfer data, it's not possible to determine whether the data is a new data, old data or mixture of both. This has no effect on a time invariant measurement but a time varying channel measurement is very sensitive to this effect.

**D.2 Other measurement Results**

Figure D.1and Figure D.2 show the correlation coefficient of two men in a random movement with antenna height of 1m and the distance between the antennas is 5m. The results show that the correlation reduces with the reduction in the measured time between two successive points. With the measured points at 60ms as shown in Figure D.2, all correlation coefficients are above 0.9, which makes it quasi-stationary. For 140ms, substantial variation between the subsequent measurements could be seen. For longer time interval, large variation in the correlation is observed. This observation is however not a suitable feedback rate for the

adaptive system. Hence, lower time interval is required to achieve a higher correlation that could be acceptable for the adaptive modulation.

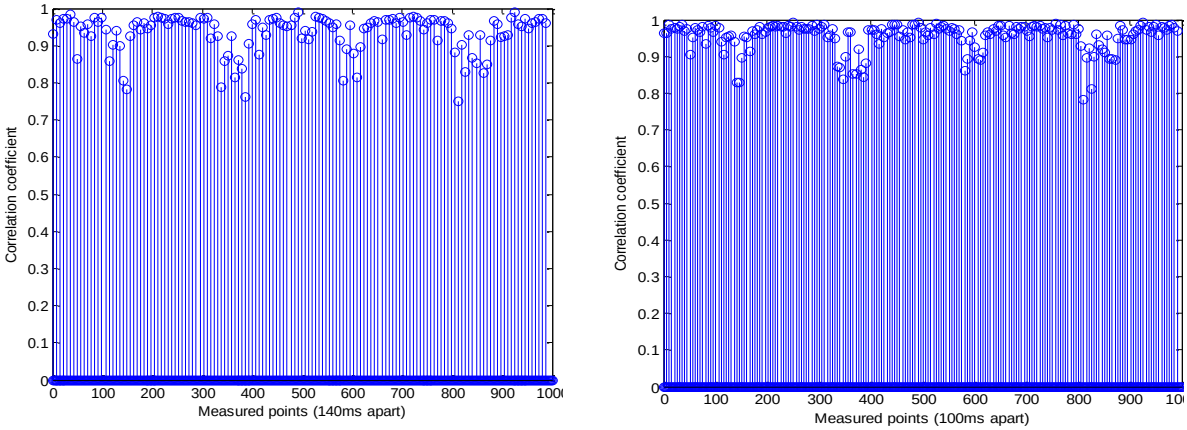


(a) (b)

Figure D.1 Correlation coefficient for successive points with 140ms and 100ms time interval while two people move in a random movement with antennas place 1m high.

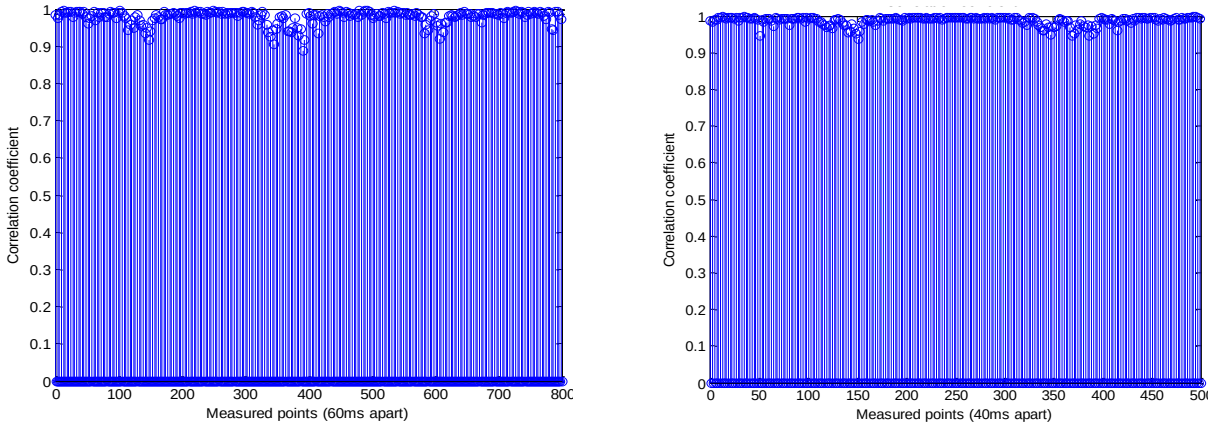


(a) (b)

Figure D.2 Correlation coefficient for successive points with 140ms and 100ms time interval while two people move in a random movement with antennas place 1m high.

Figure D.3 presents the correlation coefficients of two men in a random movement with antenna height of 2m and spacing of 5m. The results show that at 140ms, almost all the correlation coefficients are above 0.9 which can be considered quasi-stationary. The transmitter and receiver are placed 2m high which is above the average height of human subjects. Therefore, when implementing adaptive modulation on devices that are placed at a height higher than the average human, larger time interval can be used to feedback the channel state information. Figure D.4 shows the correlation coefficient of two men in a random movement with antenna height of 1.5m and gap of 5m. The results show that considering 140ms time interval, the correlation coefficients were 0.7. At lower time interval the correlation coefficients are above 0.9.

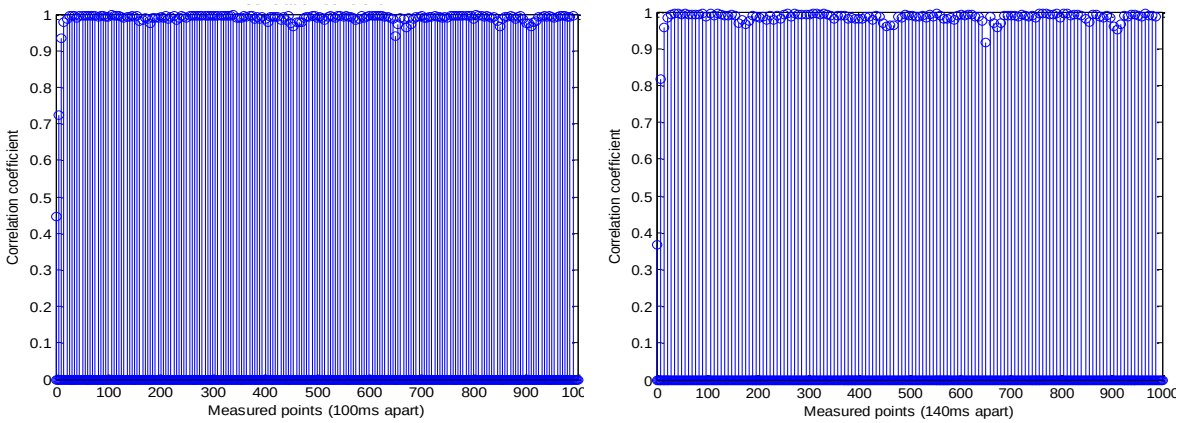


(a) (b)

Figure D.3 correlation coefficient for successive points with 140ms and 100ms time interval while two people move in a random movement with antennas place 2m high.

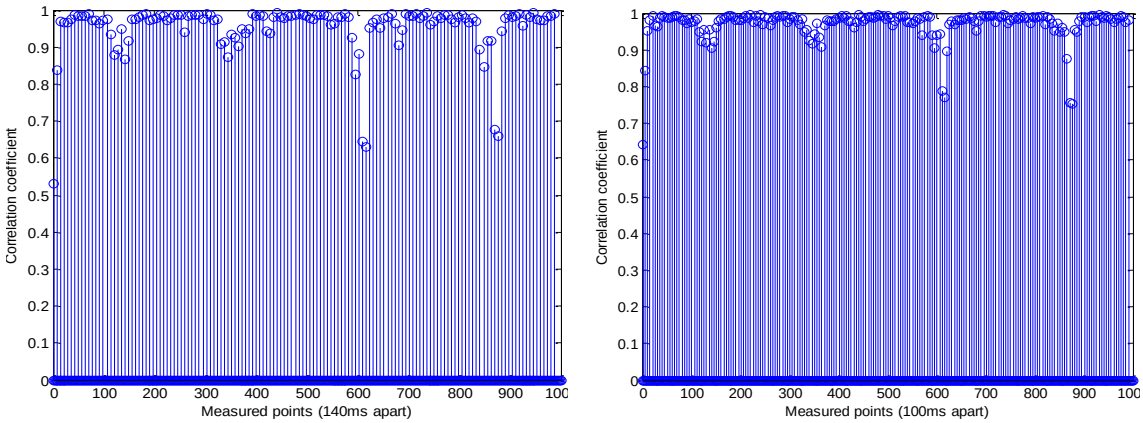


(a) (b)

Figure D.4 Correlation coefficient for successive points with 140ms and 100ms time interval while two people move in a random movement with antennas place 1.5m high.

The correlation coefficient of one man in a random movement with antenna height of 1m placed at a distance of 2m is shown in Figure D.5. The results also show that there is much variation in the environment when the person crosses the line of sight link. Figure D.6 shows the correlation coefficient of one man in a straight movement with antenna height of 1.5m and separation of 2m.

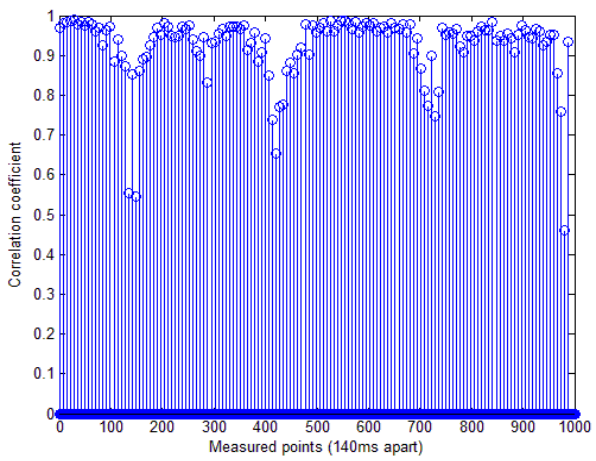


(a)

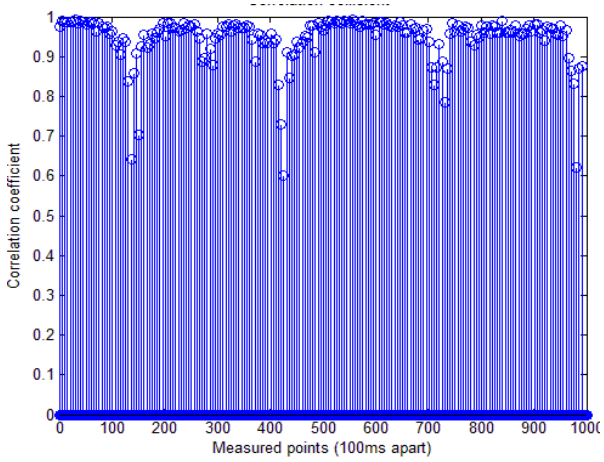


(b)

Figure D.5 Correlation coefficient for successive points with 140ms and 100ms time interval while one person moves in a random movement with antennas 1m high

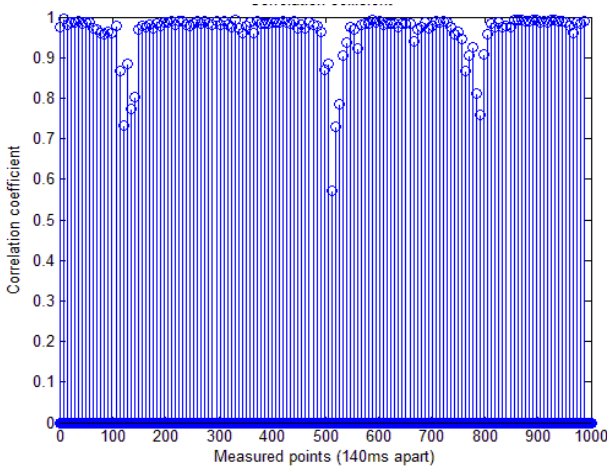


(a)

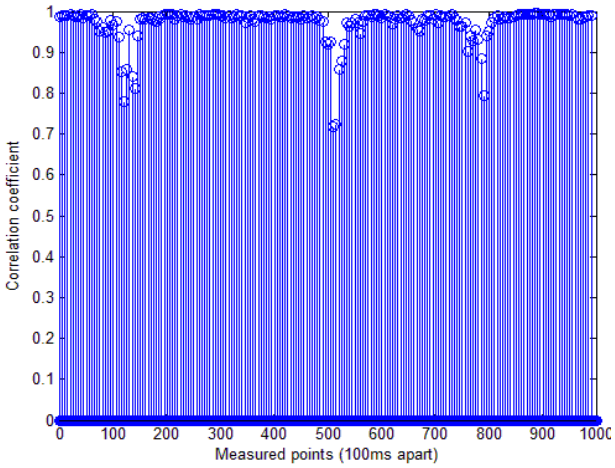


(b)

FigureD.6 Correlation coefficient for successive points with 140ms and 100ms time interval while one person moves in a random movement with antennas 1.5m high

Figure D.7 illustrate the correlation coefficients of one man in a straight movement with antenna height of 2m and spacing of 5m. It is observed that the scattering effect due to one man is negligible when the antenna is higher than the moving object in the environment. The results also show that at 140ms, all the correlation coefficients are above 0.9 which can be considered quasi stationary. As compared to Figures D.5and D.6, it shows that the antenna height greatly affects the degree of scattering in the environment.

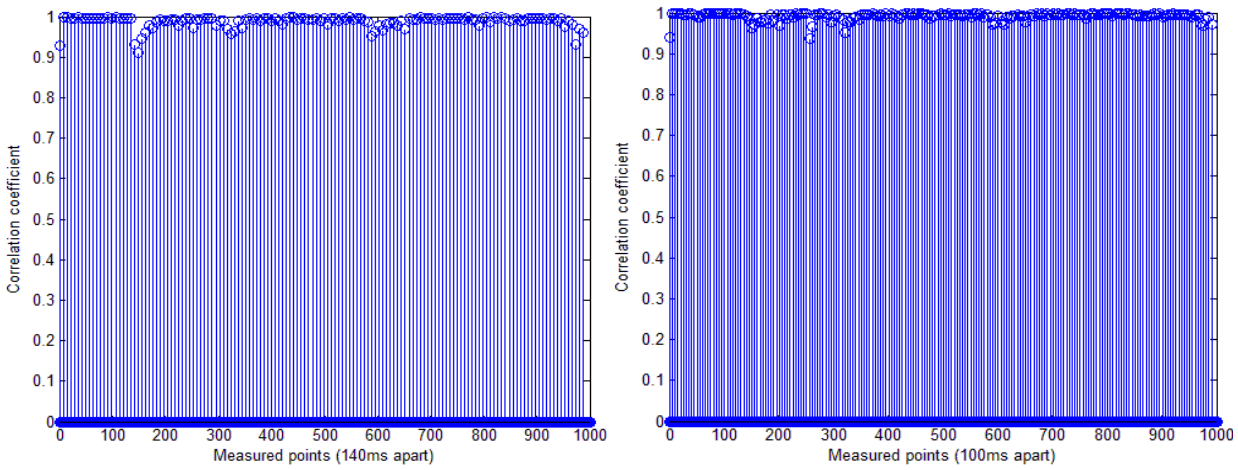


(a) (b)

Figure D.7 Correlation coefficient for successive points with 140ms and 100ms time interval while one person move in a random movement with antennas place 2m high .

# APPENDIX E

**RESULTS FOR ANTENNA DIVERSITY FOR TWO ANTENNAS**

**E.1 Two Patch Antennas in Vertical Orientation**

The next simulation is done using two antennas with vertical orientation as shown in Figure E.1. Performance is evaluated considering different spacing between the two antennas. Figures E.2 and E.3 illustrate the BER performance of both the MRC and antenna selection technique for both LOS and NLOS case. The performances for the NLOS are similar to the LOS when using the MRC combining technique. The results indicate that the MRC combining technique can be used to improve the gain up to 6dB with an antenna spacing less than one third of the wavelength. This clearly shows that implementing the spatial diversity in the UWB system enhances the system performance, thereby making high data rate achievable.

The MRC technique using 2 antennas generated close performance with the one observed using 3 antennas but with a difference of up to 2dB. Therefore, a 2 receive antenna solution can be used in hand—held devices with limited space. This could be implemented in hand held devices that don't have space. Tables E.1 and E.2 give the PER results and spatial correlation between the channels respectively.

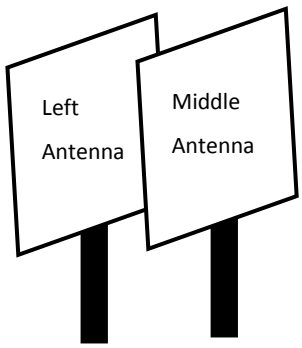


Figure E.1 Simulation of two patch antennas placed in vertical orientation

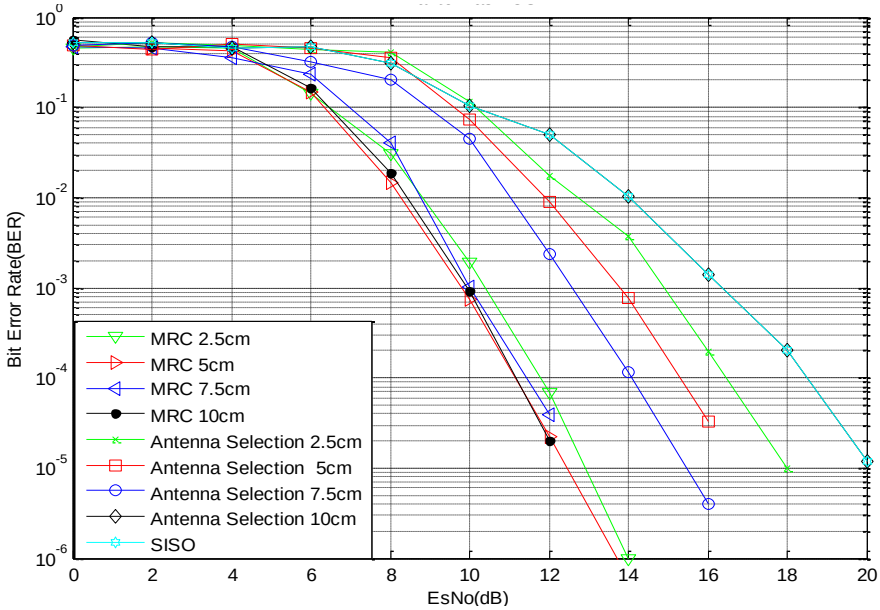


Figure E.2 BER performance of the SIMO UWB system in a LOS environment

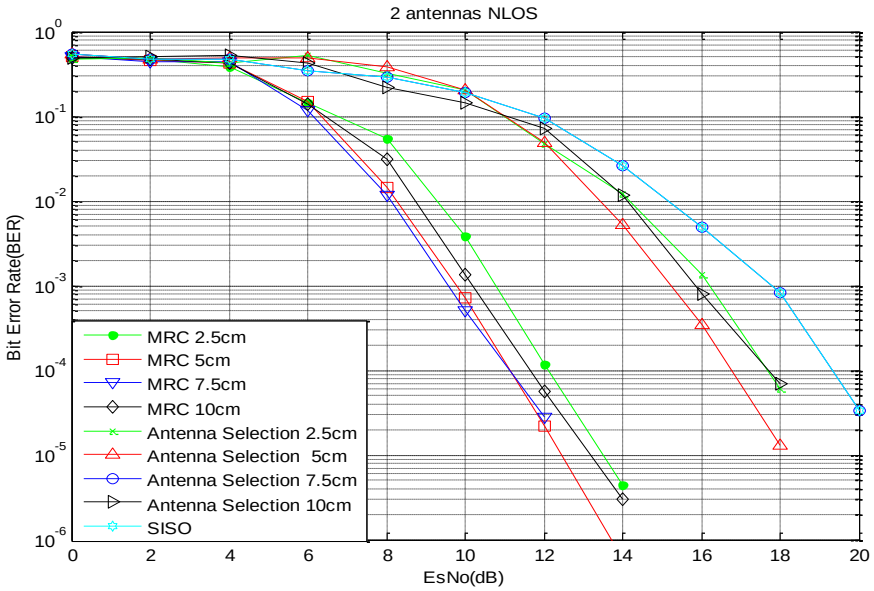


Figure E.3 BER performance of the SIMO UWB system in a NLOS environment

TABLE E.1 PER of the simulated result using a payload size of 1kb at 12dB with MRC

| **Antenna spacing (cm)** | **BER with 2 antennas (LOS)** | **Packet Error Rate (%) ( LOS)** | **BER with 2 antennas (NLOS)** | **Packet Error Rate (%)(NLOS)** |
|---|---|---|---|---|
| 2.5 | 6.96E-05 | 6.7 | 1.19E-04 | 11.5 |
| 5 | 2.20E-05 | 2.2 | 2.2E-05 | 2.2 |
| 7.5 | 3.84E-05 | 3.8 | 2.76E-05 | 2.8 |
| 10 | 1.97E-05 | 2 | 5.7E-05 | 5.67 |

Table E.2 Spatial correlation coefficient of the two patch antennas

| **Antenna Spacing** | **2.5cm** | **5cm** | **7.5cm** | **10cm** |
|---|---|---|---|---|
| Middle and Left Antenna with LOS | 0.6137 | 0.2916 | 0.4063 | 0.3617 |
| Middle and Left Antenna with NLOS | 0.3707 | 0.0548 | 0.2790 | 0.2857 |

### E.2 Two Patch Antennas, One in Vertical and One in Horizontal Orientation

Here, two patch antennas in different orientation are studied. Figure E.4 shows the orientation for two antennas, one in vertical position and the other in horizontal position. The BER results for LOS and NLOS environments are shown in Figures E.5 and E.6. For the LOS, a 4dB gain is achieved for different antenna spacing, while for NLOS environment, some spacing achieved a gain of 4dB and others 2dB. The results are similar to the one shown in Figure E.1 which could be due to low received power by the horizontal antenna. Tables E.3 and E.4 show the PER at 14dB with a payload of 1kb and spatial correlation respectively. This PER for MRC at 0cm and 2.5cm are quite high having 30% and 18% respectively, but is still an improvement compared to the performance observed using the antenna selection technique in the same scenario. It should be noted that simulating at higher SNR will further reduce the PER but the focus here is to study the performance over low SNR.

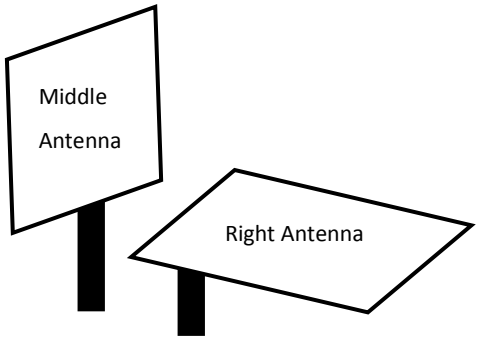


Figure E.4 Simulation of two patch antennas, one placed in vertical orientation and one in horizontal orientation

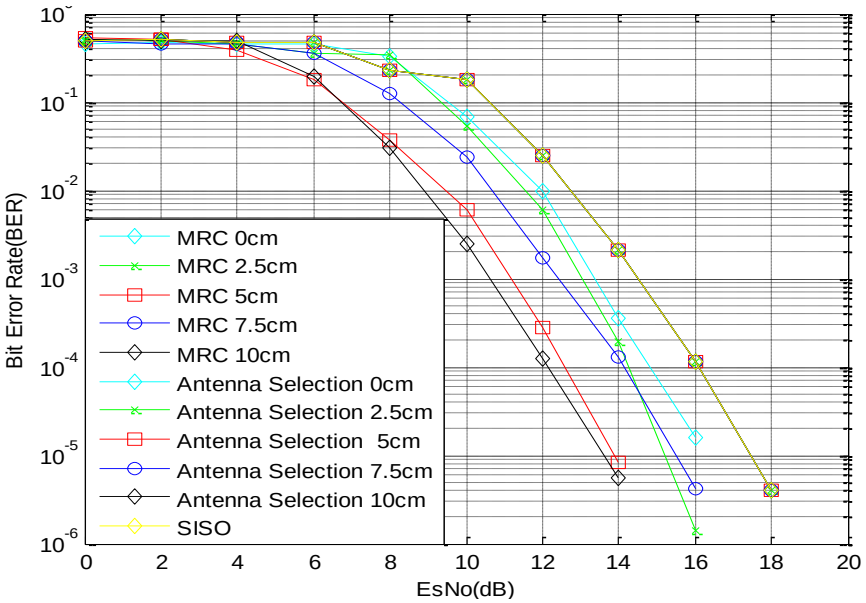


Figure E.5 BER performance of the SIMO UWB system in a LOS environment

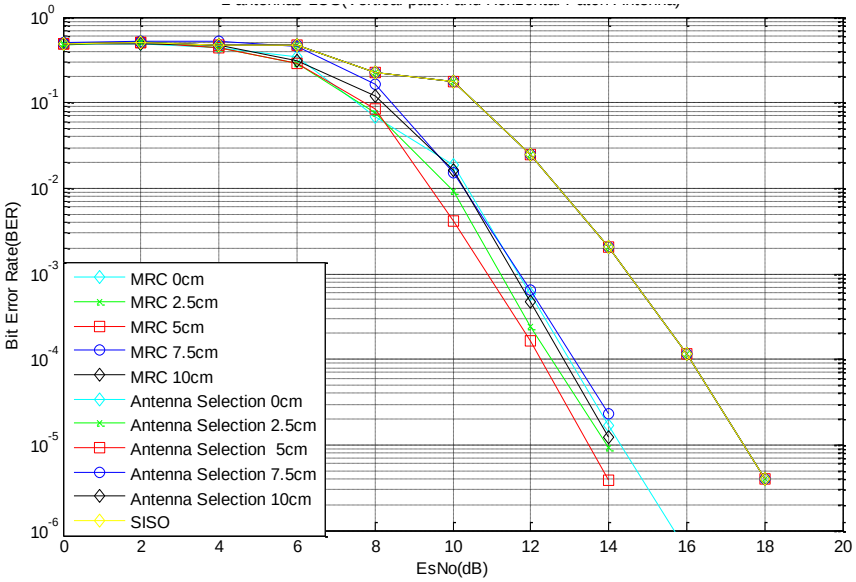


Figure E.6 BER performance of the SIMO UWB system in a NLOS environment

TABLE E.3 PER of the simulated result using a payload size of 1kb at 14dB with MRC

| Antenna spacing (cm) | BER with 2 antennas (LOS) | Packet Error Rate (%)(LOS) | BER with 2 antennas (NLOS) | Packet Error Rate (%)(NLOS) |
|---|---|---|---|---|
| 0cm | 3.56e-4 | 30 | 1.68e-5 | 1.7 |
| 2.5cm | 1.96e-4 | 18 | 9.2e-6 | 0.94 |
| 5cm | 8.4e-6 | 0.85 | 3.8e-6 | 0.4 |
| 7.5cm | 1.3e-4 | 12 | 2.3e-05 | 2.3 |
| 10cm | 5.6 e-06 | 0.57 | 1.22e-05 | 1.24 |

TABLE E.4 Spatial correlation coefficient of the two patch antennas, one placed in vertical orientation and one in horizontal orientation.

| Antenna Spacing | 2.5cm | 5cm | 7.5cm | 10cm |
|---|---|---|---|---|
| Middle and Right Ant with LOS | 0.2923 | 0.0187 | 0.2365 | 0.3617 |
| Middle and Right Ant with NLOS | 0.2457 | 0.2729 | 0.1472 | 0.2447 |

### E.2 Two Antennas, One Monopole and One Patch Antenna

In this section, a vertically placed monopole and a horizontally placed patch antenna are considered as shown Figure E.7. The monopole antenna is designed for UWB band 1 frequency range from 3.168-4.752 GHz. Figure E.8 and E.9 show the BER results for different antenna spacing in LOS and NLOS. The results show a gain of 6dB in the NLOS environment and 4dB in the LOS environment. The increase in the performance is better than the BER results shown in Figure E.5, where two patch antennas are used. The two antenna used here have different pattern which resulted to having smaller spatial correlation. This suggests using different

antenna patterns could improve the performance of the system. The PER and spatial correlation results are given in Table E.5 and Table E.6 respectively. The correlation coefficient values are 0.35 and 0.5 for LOS and NLOS scenarios respectively. Hence, high diversity gain is achieved.

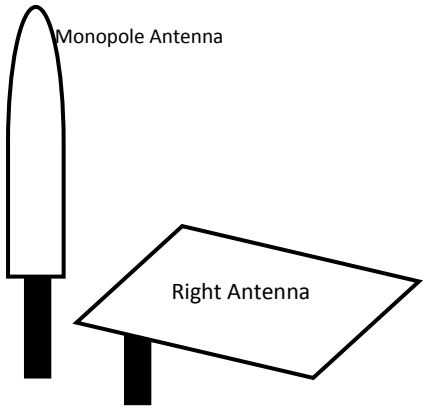


Figure E.7 Simulation of two antennas, one monopole antenna placed in vertical orientation and one patch in horizontal orientation

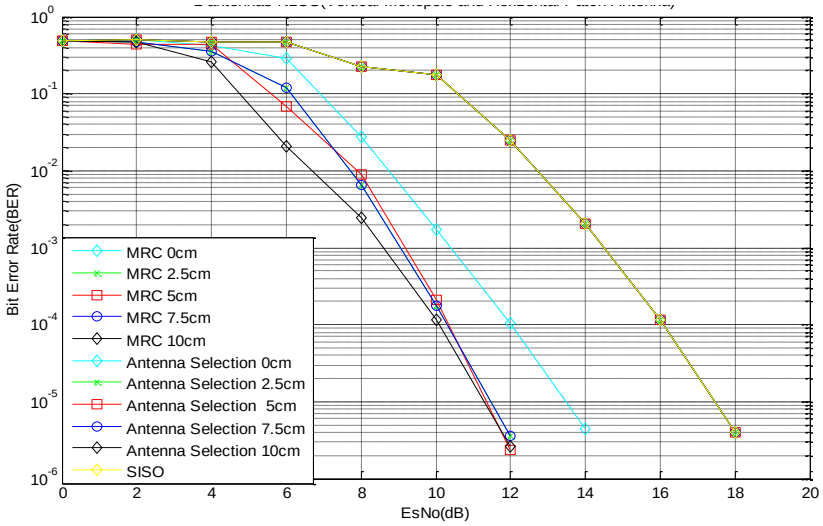


Figure E.8 BER performance of the SIMO UWB system in a LOS environment

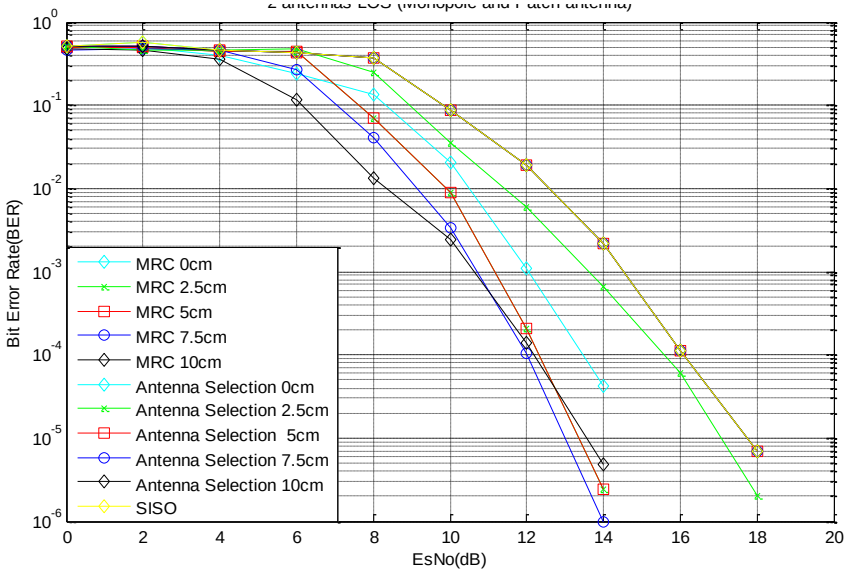


Figure E.9 BER performance of the SIMO UWB system in a LOS environment

TABLE E.5 PER of the simulated result using a payload size of 1kb with MRC

| **Antenna spacing (cm)** | **BER with 2 antennas (LOS) at 12 dB** | **Packet Error Rate (%)(LOS)** | **BER with 2 antennas (NLOS) at 14dB** | **Packet Error Rate (%)(NLOS)** |
|---|---|---|---|---|
| 0cm | 4.19e-5 | 4.1 | 4.4e-6 | 0.45 |
| 2.5cm | 2.46e-6 | 0.25 | 3.6e-6 | 0.4 |
| 5cm | 2.46e-6 | 0.25 | 2.4e-6 | 0.3 |
| 7.5cm | 1.0e-6 | 0.1 | 3.6e-6 | 0.4 |
| 10cm | 4.8e-6 | 0.5 | 2.6e-6 | 0.3 |

TABLE E.6 Spatial correlation coefficient of two antennas (monopole and patch)

| Antenna Spacing | 2.5cm | 5cm | 7.5cm | 10cm |
|---|---|---|---|---|
| Middle and Right Ant with LOS | 0.0025 | 0.1724 | 0.1670 | 0.3539 |
| Middle and Right Ant with NLOS | 0.1213 | 0.0198 | 0.1069 | 0.0181 |

# APPENDIX F

**BILL OF MATERIALS, CIRCUIT AND PCB LAYOUT**

**F.1 Antenna Selection Circuit**

Table F.1 shows the list of the all the component used in the circuit design. Figure F.1 shows the complete schematic of the antenna selection and Figure F.2 shows the complete layout of the selection circuit in Ultiboard which contains both digital and analogue parts, while figures F.3 and Figure F.4 From the figure F. 1, the green copper layer is the top layer of the PCB while the red copper layer is the bottom layer of the PCB. This is a 2 layer PCB design approach. Figure F.2 show the 3D dimensional image of the layout of the complete circuit.

Table F.1 List of Parts that are used in the antenna selection circuit design

| VALUE | FOOTPRINT | QTY | REFDES | DESCRIPTION |
|---|---|---|---|---|
| 0.01uF, 10nF | 805 | 2 | C34,C36 | |
| 0.1uF 2% | 805 | 6 | C20,C25,C30,C33,C39,C49 | CAPACITOR,MLCC, 0805, 50V, 100NF |
| LED | LEDC1608X80N | 3 | DS1,DS2,DS3 | LED SUPER RED CLEAR 0805 SMD |
| DEA453960BT-3002B1 | 1812(4532 Metric), 8 PC Pad | 6 | U35,U36,U37,U38,U43,U46 | FLTR BANDPASS 3.1-4.9GHZ UWB SMD |
| coupler | 603 | 3 | Coupler2,Coupler3, Coupler4 | AVX CP0603AXXXXA COUPLER, HIGH DIRECTIVITY, 0603 |
| 1KOhm | 805 | 1 | R19 | RESISTOR, 0805, 1K, 0.1%, 0.125W |
| 1M | 805 | 6 | R3,R6,R8,R10,R12,R16 | RESISTOR, 0805, 1M, 0.1%, 0.125W |
| 1nF | 805 | 6 | C44,C45,C69,C70,C72,C73 | CAPACITOR, 0805, C0G, 50V, 1nF |
| 1uF | 805 | 1 | C35 | CAP CER 1UF 10V 5% X7R 0805 |
| 3.3K | 805 | 3 | R4,R9,R13 | RES 3.30K OHM 1/8W 1% 0805 SMD |
| 7M | 805 | 1 | R20 | RES 6.98M OHM 1/8W 1% 0805 SMD |
| 47pF | 805 | 4 | C28,C29,C37,C38 | CAPACITOR, 0805, C0G, 50V, 47PF |
| 51Ohm | 805 | 3 | R15,R17,R21 | RES 51 OHM 1/8W .1% 0805 SMD |
| 52.3Ohm | 805 | 3 | R24,R25,R26 | RES 52.3 OHM 1/8W 1% 0805 SMD |

| VALUE | SHAPE | QTY | REFDES | Description |
|---|---|---|---|---|
| 74HC164N_6V | SOIC127P600X175-14N | 3 | U6,U18,U28 | IC REGISTER SER/PAR I/O 14SOIC |
| 100pF 2% | 805 | 6 | C21,C24,C25,C30,C31,C32,C40,C46 | CAPACITOR, 0805, C0G, 100V, 100PF |
| 215K | 805 | 1 | R18 | RES 215K OHM 1/8W 1% 0805 SMD |
| 4023BT_10V | SOIC127P600X175-14N | 1 | U25 | IC TRIPLE 3-IN NAND GATE 14-SOIC |
| 4042BT_5V | SOIC127P1032X265-16N | 1 | U20 | IC QUAD CLOCKED D LATCH 16SOP |
| 4075BT_5V | SOIC127P600X175-14N | 1 | U24 | IC 3IN OR GATE TRIPLE 14SOIC |
| AD8318 | QFN65P400X400X100 | 3 | U30,U34,U39 | IC LOG DETECTOR/CTRLR 16-LFCSP |
| DIODE | 805 | 1 | D1 | DIODE SCHOTTKY 500MA 20V 1005 |
| LM555CM | SOIC127P600X175-8N | 1 | U32 | IC OSC MONO TIMING |
| LMV331M5 | SOT95P284X122-5N | 3 | U5,U21,U26 | IC COMPARATOR TINY LV SOT23-5 |
| MGA-85563-TRIG | SC70 | 6 | U61,U63,U66,U70,U85,U87 | AMP RFIC LNA GAAS 3V SOT-363 |
| NC7S04_5V | SOT95P280X140-5N | 3 | U12,U13,U31 | IC INVERTER HS SINGLE SC70-5 |
| NC7S08_5V | SOT95P280X140-5N | 6 | U7,U9,U17,U19,U27,U29 | IC GATE AND SINGLE 2 INPUT SC70 |
| NC7S32_4V | SOT95P280X140-5N | 1 | U22 | IC GATE OR 2-INPUT SINGLE SOT-23 |
| NC7ST00_5V | SOT95P280X140-5N | 1 | U11 | IC GATE NAND 2-INPUT SGL SOT-23 |
| MULTICOMP 19-70-4-TGG | SMA | 4 | J3,J4,J5,J8 | JACK SMA, END LAUNCH |
| SKY13317-373LF | 8-XFDFN Exposed Pad | 1 | U33 | IC SWITCH RF SPDT 8-MLP |
| 22nH | 805 | 6 | R27,R28,R29,R30,R35,R36 | INDUCTOR, 0805 CASE, 5N6, 5% |
| 52.3Ohm | 805 | 6 | U60,U62,U65,U68,U86,U88 | RES 52.3 OHM 1/8W 1% 0805 SMD -(R-BIAS-) |
| 56pF | 805 | 6 | U59,U64,U67,U69,U71,U72, | CAPACITOR, 0805, C0G, 50V, 56PF |
| 56pF | 805 | 18 | C41,C42,C43,C47,C51,C52,C53,C54,C55,C56,C57,C58,C71,C74,C75,C76,C77,C78 | CAPACITOR, 0805, C0G, 50V, 56PF |

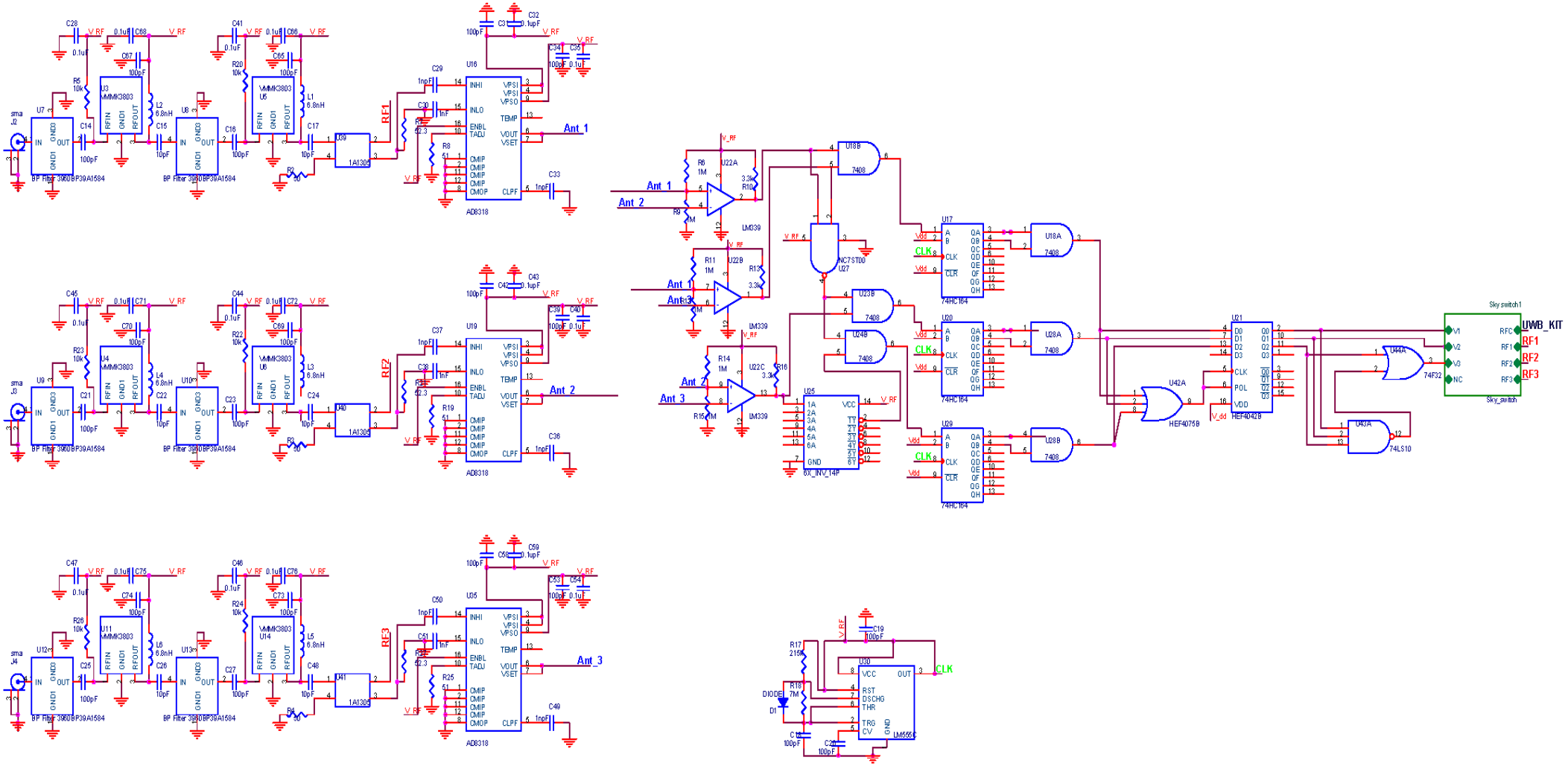


Figure F.1 Antenna Selection Circuit

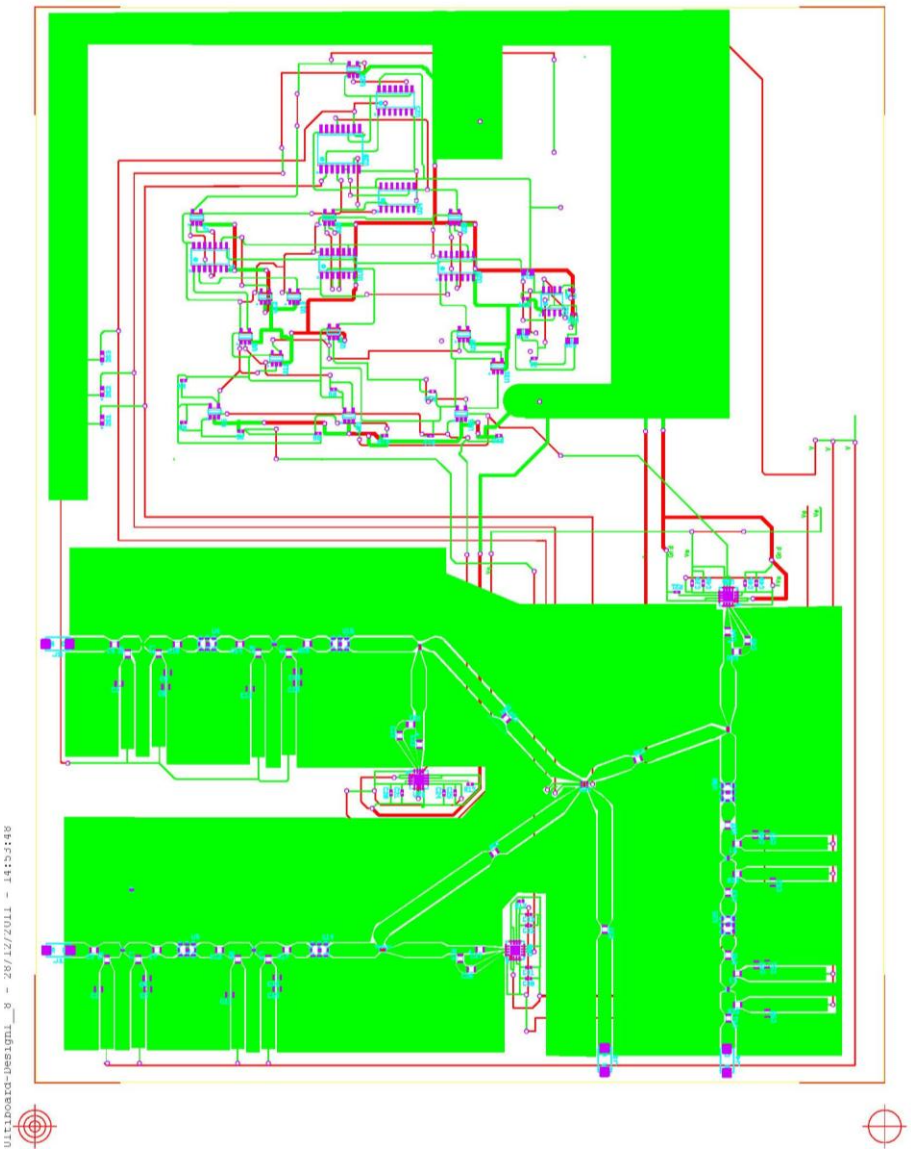

Figure F.2 Complete layout of the selection circuit which contains both digital and analogue

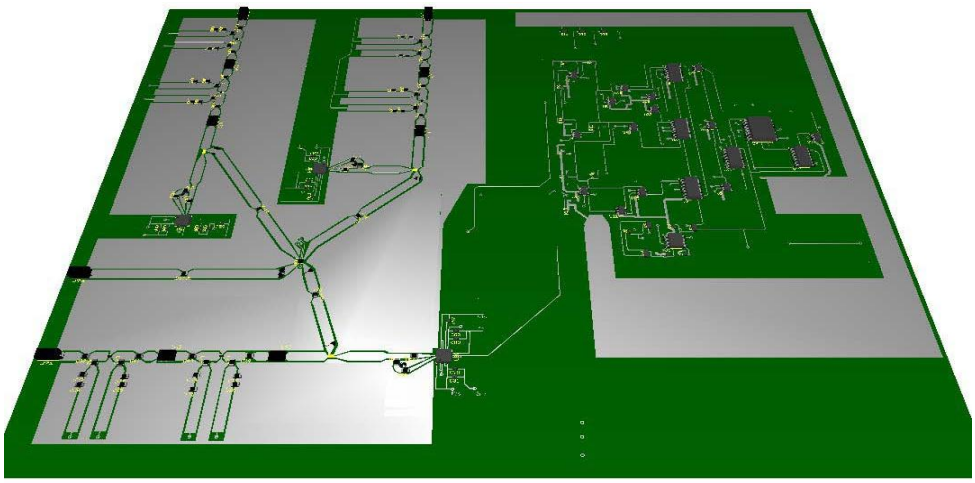

Figure F.3 3D dimensional image of the complete layout- top layer

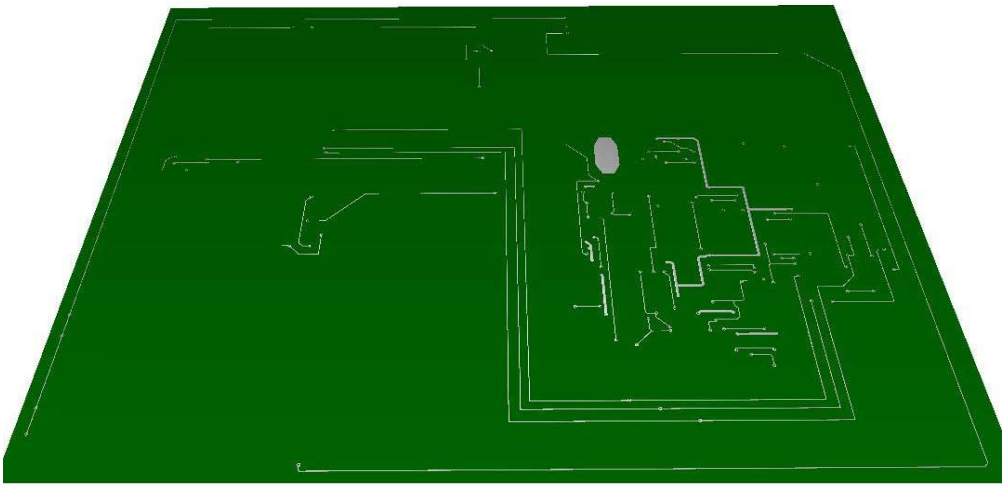

Figure F.4 3D dimensional image of the complete layout- Bottom layer

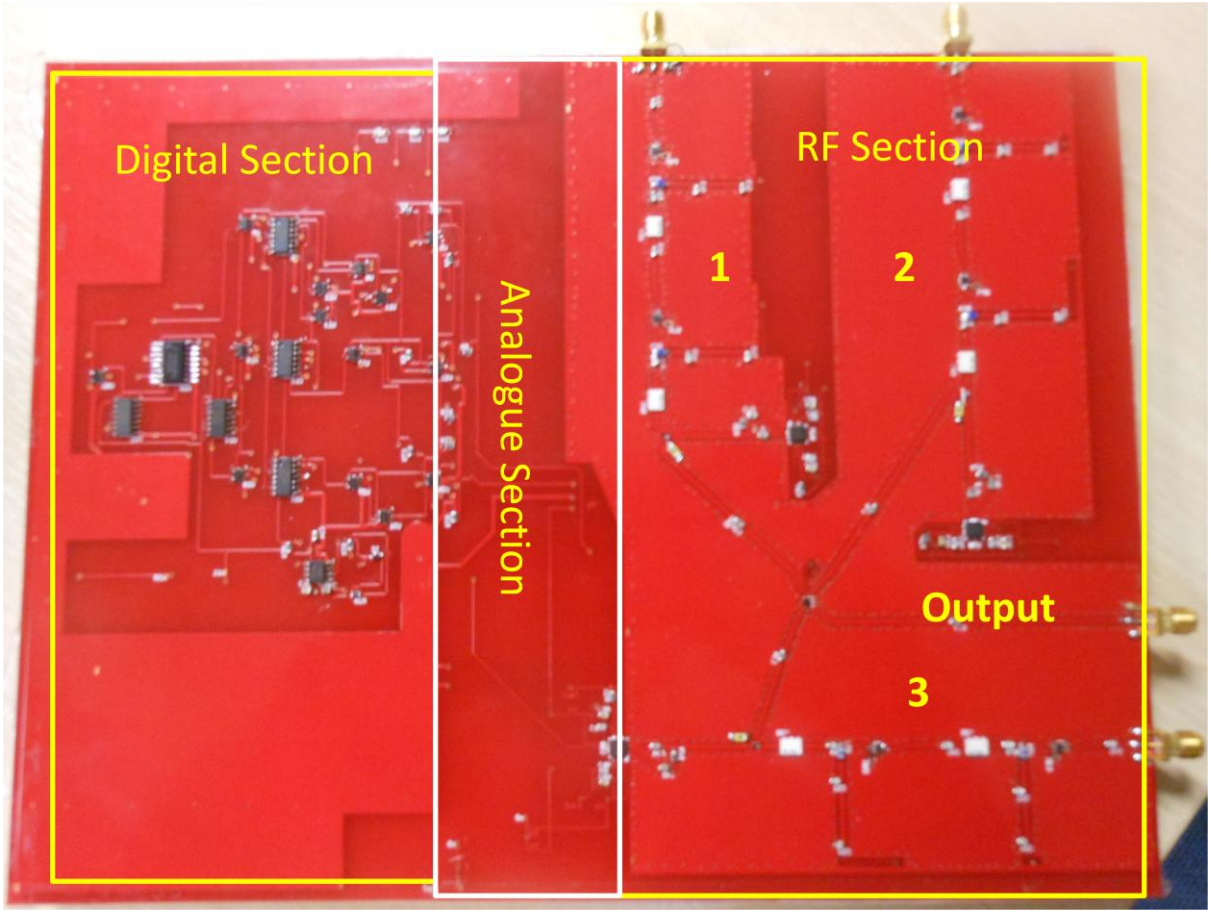


Figure F.5 Printed and assembled board

**F.2 Design consideration on PCB**

For best practice from references [6-9] the following where taken into consideration while designing the circuit.

**F.2.1 CPW Case**

1) The distance between the grounds in the RF section should be less than λ/2 for best performance.
2) Ground must extend greater than five times the distance between the grounds on either side of the trace.
3) Coplanar waveguide allows variation of trace width or spacing to ground. This is used to match the characteristics impedance with components that have different pin sizes.

**F.2.2 General Case**

1) Low level analogue , RF / Microwave and digital section must be separated
2) Inductors have large magnetic field around them. They should not be placed together when in parallel, except where the intent is to have the magnetic field couple. They should be separated by at least one times the body height or placed perpendicular to each other.
3) RF lines must be kept away from each other to prevent unintended coupling and crosstalk.
4) Have more copper in your ground path. This is highly desirable for many electrical reasons.
5) Track Impedance must be maintain to match ( SMA, RF components)

**F.3 Signal Attenuation**

In RF design, losses can be grouped into four main components. This are

1. Dielectric Loss – This is contributed due to the type of material. Materials with low dissipation factor or loss tangent will help in reducing the effect of this component. The dissipation factor is the inverse of the quality factor (Q factor). Though the component is important, attending to the loss of other component can make a material of higher dissipation factor be acceptable. Loss tangent is the loss of signal energy into the dielectric of material. It is the measure of how much the signal propagation will be lost in the dielectric region. The lower the loss tangent means more of the output signal

gets to its destination. The amount of signal loss is not only on the type of the material but also a function of frequency and line length on PCB.[9]

2. Conductive Loss – This is due to the skin effect properties. Different metals and their finishing either smooth or rough will result in different degree of losses. In high frequency transmission, signal moving in the trace is forced to the outer perimeter. This effect is known as skin depth because majority of the energy is forced to the outer skin of the trace. The degree of penetration of signal into the trace is measured in skin depth with approximately 66%of the energy penetrating in to one skin depth and approximately 97% of the energy penetrating to three skin depths. [9]
3. Radiation Loss – This depends on the type of transmission line. Transmission lines on the outer layer such as CPW and micro strip line have more radiation loss. Strip line types have the minimal loss. [8]
4. Design induced Loss – These are losses introduce to the design due to discontinuities in the signal paths. These could be impedance mismatch between transmission lines and components due to different pad size, transition between transmission lines etc.[8]

Table F.2 shows comparison between different transmission lines and their properties. Factoring these properties while designing the layout could improve the performance of the system.

Table F.2 Comparison of various transmission-line types [10]

| Transmission line | Q factor | Radiation | Dispersion | Impedance range |
|---|---|---|---|---|
| Microstrip(dielectric)<br>(GaAs, Si) | 250<br>100 -150 | Low<br>High | Low | 20 to 120 |
| Stripline | 400 | Low | None | 35 to 250 |
| Suspended stripline | 500 | Low | None | 40 to 150 |
| Slotline | 100 | Medium | High | 60 to 200 |
| Coplanar waveguide | 150 | Medium | Low | 20 to 250 |
| Finline | 500 | None | Low | 10 to 400 |

**References (Appendices A-F)**


1. A Batra , "*Design of a Multiband OFDM System for realistic UWB Channel Environments"* , IEEE Transaction on Microwave Theory and Techniques Vol 52, No 9 September 2004
2. Phy Specification: Final Deliverable 1.5 Multiband OFDM Physical Layer Specification , WiMedia Alliance, Inc ,2009
3. Embedded Design Handbook, Altera Co, San Jose, CA, 2001
4. AT91CAP9 UWB-EK Evaluation kit, User guide and technical documents 6457B–CAP–19-Jan-10
5. A Batra, "*Design of a Multiband OFDM System for realistic UWB Channel Environments"*, IEEE Trans on Microwave Theory and Techniques Vol 52, No 9 Sept 2004
6. David L. Jones, "PCB design Tutorial", Rev A- 29th June 2004
7. Sean Mercer, Minimizing RF PCB electromagnetic emissions, RF Design Magazine January 1999
8. Judy Warner "Signal Loss: A Big Picture Approach to RF/MW PCB Design" Accessed from: http://mwexpert.typepad.com/rfmw_pcb_design/2011/10/signal-loss-a-big-picture-approach-to-rfmw-pcb-design.html
9. Rick Hartley, "Base Materials for High Speed, High Frequency PC Boards". March 2002, Published in PCB & A
10. L.G. Maloratsky, "Reviewing the Basics of Microstrip Lines," Microwaves & RF, March 2000, pp. 79-88.